Development of a new tyre tread by using silanized pre-treated silica nanofiller

By

Saeed Ostad Movahed

Submitted in partial fulfillment of the requirements of the award of Doctor of Philosophy

Acknowledgement

I am grateful to my project supervisors Dr. Ali Ansarifar and Dr. Mo Song for their continuous support and encouragement.

I am thankful to Mr. Ray Owen and Mr. Andy Woolley for training and helping me with the experimental work of my project.

I would like to express my sincere gratitude to all the administrative and secretarial staff at the Department of Materials for their friendly attitude and continuous support during the course of my stay at Loughborough University.

Synopsis

The tyre tread compound for passenger car tyres is a blend of natural rubber (NR), styrene butadiene rubber (SBR), polybutadiene rubber (BR) and synthetic polyisoprene (IR). It is designed to have high abrasion resistance and traction, low rolling resistance and long durability in service. To achieve these requirements, reinforcing fillers such as colloidal carbon blacks and synthetic silicas are added to raw rubbers. Reinforcing fillers helps to increase the properties mentioned above and also hardness, tensile properties and tear strength. In recent years, silica has been replacing carbon black in industrial rubber articles, for example passenger car tyres, offering significant benefits. Some studies have shown that using silicas in rubber compounds can reduce the excessive use of the curing chemicals without compromising the mechanical properties of rubber vulcanisates, which are essential for long service life.

In this study, effects of 60 parts per hundred rubber by weight (phr) precipitated amorphous white silica nanofiller on the viscosity, curing, mechanical and dynamic properties of NR, SBR, BR and IR rubber compounds were investigated. The silica surfaces were pre-treated with bis(3-triethoxysilylpropyl)tetrasulphane (TESPT) bifunctional organosilane, known also as Si69 coupling agent, to chemically bond silica to rubber. The rubbers were primarily cured by using sulphur in TESPT, and the cure was optimised by the addition of accelerator and activator, which helped to form stable covalent sulphur chemical bonds between the rubber and filler. Different amounts of accelerator and activator were needed to fully crosslink the filled rubbers. The mechanical properties of the NR, SBR, BR and IR vulcanisates improved substantially by the incorporation of the filler. This was due to high levels of rubber-filler adhesion and formation of sulphur chemical bonds between the rubber and filler via TESPT.

The unfilled and silanized silica filled NR, SBR and BR rubbers were subsequently mixed together to produce SBR/BR and NR/BR blends. Using the modulated temperature differential scanning calorimetry (MTDSC) technique, the composition and mass fraction of the interphase in the blends were determined. The rubbers were mixed together for different times, temperatures and rotor speeds to produce the blends. The mass fraction of the SBR with respect to BR in the blend was increased to measure its effects on the composition and mass fraction of the interphase in the blend. The effect of silica nanofiller on the composition and mass fraction of the interphase in the blends was also investigated. The viscosity, cure properties, hardness, tensile strength, elongation at break, stored energy density at break, tear strength, Young's modulus, tensile modulus at different strain amplitudes, abrasion resistance, heat build up, and tan δ of the blends were measured.

This study showed that long mixing times up to 30 minutes, high mixing temperatures up to 105°C, and incorporation of silica in the rubbers increased the mass fraction of the interphase and altered its composition in the blend. However, increasing the rotor speed and the mass fraction of SBR with respect to BR did not benefit the mass fraction of the interphase in the blend. Properties related to fracture such as elongation at break, stored energy density at break, tearing energy and resistance to abrasion benefited significantly from an increase in the mass fraction and changes in the composition of the interphase in the blend. Furthermore, MTDSC was a useful technique for studying the interphases in the blends of SBR/BR and SBR/NR rubbers.

The dynamic properties of the silanized silica filled SBR, NR, BR and IR rubbers and SBR/BR (75:25 by mass) blend were measured as a function of oscillation amplitude, test frequency and temperature. The blends were prepared by mixing the filled SBR and BR rubbers for 1, 7 and 20 min. This study showed that these parameters had a profound effect on the tan δ, loss and storage modulus of the rubbers. There were a few blends, which were ideal for tyre tread applications because of their high tan δ at low temperatures (good for high skid resistance) and low tan δ at high temperatures (good for low rolling resistance).

Symbols and Abbreviations

$\tan\delta$	Tangent delta , the ratio of loss modulus to storage modulus
G''	Loss modulus (MPa)
G'	Storage modulus (MPa)
SBR	Poly styrene-butadiene co-polymer rubber
BR	Poly butadiene rubber
NR	Natural rubber
IR	Synthetic poly isoprene
TESPT	bis [3-triethoxysilylpropyl] tetrasulphane
ODR	Oscillation disc rheometer cure meter
TBBS	N-t-butyl-2-benzothiazole sulphenamide
Santoflex 13	N-(1, 3-dimethylbutyl)-N'-phenyl-p-phenylenediamine
Enterflex 74	Process oil
$\Delta Torque$	Delta torque (dN.m)
CRI	Cure rate index (min^{-1})

t_{s1}	Scorch time (min.)
t_{90}	Cure time (min.)
ZnO	zinc oxide
Coupsil 8113	TESPT pre treated precipitated silica nanofiller
MTDSC	Modulated temperature differential scanning calorimetry
Phr	Part per hundred by mass
μm	Micrometre
σ	Standard deviation
DMA	Dynamic measurement Analyser

List of Tables

List of Figures

Contents

CHAPTER 1

General Introduction

1.1 Introduction

The wheel is one of the greatest inventions in human history due to its wide range of applications for example transporting people, materials, or equipment.

Charles Goodyear [1] invented the first rubber tyres in 1839 when he accidently discovered that when natural rubber was mixed with sulphur and then heated on a hot stove, it hardened and its mechanical properties improved. This was called vulcanisation. He subsequently used this discovery to develop rubber tyres. In 1886, R. William Thomson [2] introduced the idea of first pneumatic tyre.
With the discovery of sulphur vulcanization, and the beginning of the industrial revolution in both Europe & North America, the tyre evolved from a rubberised canvas protecting a rubber tube to a more complex structure containing fabric, steel and elastomers.

A tyre consists of several components including tread, sidewall, carcass, beads and inner liner. The tread is probably the most critical component of a tyre determining its durability, performance and service life. It is also the thickest part of the tyre structure, which contributes to energy losses and increases in running temperature or heat build up and fuel consumption of vehicle. Tread is also responsible for the safety of a tyre and hence a car and its surface is designed to provide good grip in contact with the road surface in normal driving condition such as dry, wet, ice or snow, but with minimum noise generation. In fact trying to achieve good wear resistance, high wet- and ice- grip and low rolling resistance, as well as many other essential properties such as good resistance to crack

growth, has lead to the development of a wide range of tread formulations made from several natural and synthetic rubbers and different types and amounts of reinforcing fillers [3-19]. Raw rubbers possess poor mechanical properties even after vulcanization and therefore there is a need to add reinforcing materials to achieve improvement in their mechanical properties. Traditionally, there have been two major materials used in rubber reinforcement, they are carbon blacks and silicas [20-36] .

The introduction of carbon blacks in rubber compounds as a reinforcing agent goes back to 1904, which lead to a substantial increase in tread wear resistance. Carbon blacks are used to reinforce rubber compounds and provide enhanced physical properties of the cured rubber. Since 1912, carbon blacks have replaced zinc oxide in rubber compounds as a reinfrocing filler to provide adequate mechanical and physical properties, while a small amount of zinc oxide, up to 5 phr, is still added to rubber compounds to assist with the curing reaction and formation of sulphur crosslinks in the rubber.

Since early 1940s, carbon blacks have been complemented by a group of highly active silica fillers because they significantly improve wear as well as performance of tyre tread. However, technological reasons, e.g. the fact that silicas retard sulphur curing reaction in rubber compounds and have a tendency to form aggregates and agglomerates in the rubber matrix, prevented the use of silicas in tyre tread compounds until recently. Conventionally, carbon blacks are considered to be a more effective reinforcing agent for tyre treads than silicas, if the latter is used without a coupling agent. In fact, good dispersion of reinforcing fillers in polymer matrix is a key factor in achieving good mechanical and physical properties, which before using coupling agents restricted the use of silicas in rubber compounds.

Bifunctional organosilanes or coupling agents modify silica surfaces chemically by reacting with the silanol or hydroxyl groups, which make the filler acidic and

hydrophobic, and either destroy these groups or make them inaccessible to the rubber chains [37-47]. In addition, bifunctional coupling agents which contain sulphur can chemically react with chemically active double bonds or unsaturated sites along the rubber chains and form strong covalent sulphur crosslinks between the filler and rubber.

Since the introduction of green tyres [48], the use of silicas in rubber compounds for tyre applications has been increasing. Use of silicas in green tyre compounds has reduced rolling resistance up to 20% and consequently lowered fuel consumption by about 5% [49]. In addition, silicas enhance wearing resistance including abrasion resistance, hardness and modulus as well as wet- or ice- grip, which prevent car from skidding on road surfaces in winter [50-52].

Tyres comprise of chemicals, which are potentially harmful to the human body and the environment. For example, when tyres are disposed of in landfills at the end of their useful service life, rubber chemicals can leach out and get into underground water resources polluting the drinking water. Moreover, handling rubber chemicals can cause danger to the safety and well-being of workers in the rubber industry. Therefore, it is essential to reduce the number and amount of these chemicals in rubber formulations [53]. For instance, it is customary to use up to 5 phr zinc oxide (ZnO) and 2 phr stearic acid in the sulphur cure systems of tyres. High concentration of zinc in water is known to be toxic to aquatic organisms, in particular many species of algae, crustaceans and salmonids [53]. The rubber dust produced from worn tyres that becomes airborne or is collected along the road- sides and highways is of major concern due to high surface area of the dust particles and its ready access to drainage and runoff streams. Hence, reducing or eliminating ZnO and stearic acid in rubber compounds must be a priority [53]. This project will offer a novel technique for reducing ZnO and eliminating stearic acid altogether from rubber formulations.

1.2 Aims and objectives

The overall aim of this project is to develop new blends of SBR/BR rubbers filled with precipitated amorphous white silica nanofiller pre-treated with bis(3-triethoxysilylpropyl)tetrasulphane (TESPT) for use in green tyre tread. Equally, to develop and test a novel technique for reducing or eliminating the excessive use of the curing chemicals in rubber compounds using silanized silica nanofiller, and to promote a safer, more efficient and environmental-friendly method for preparing rubber compounds.

The specific objectives are:

1. To prepare natural rubber, styrene-butadiene rubber, polybutadiene rubber and synthetic polyisoprene compounds filled with 60 phr silanized silica nanofiller. The filler particles will be dispersed well in the rubber matrix by increasing the mixing time.

2. To crosslink or cure, the rubbers primarily by using sulphur in TESPT, and optimise the cure by the addition of accelerator and activator, which will form strong covalent sulphur chemical bonds between the rubber and filler via TESPT. To measure the viscosity and cure properties of the rubber compounds in order to assess effects of the filler, accelerator and activator on the processing properties of the rubber compounds.

3. To fully cure the unfilled and silanized silica filled NR, SBR, BR and IR rubber compounds to produce suitable test pieces for measuring the Mooney viscosity, cure properties, hardness, tensile strength, elongation at break, stored energy density at break, tearing energy and tensile modulus at different strain amplitudes. In addition, to measure the dynamic properties such as $\tan\delta$, loss and storage modulus as a function of the oscillation amplitude, test frequency and test temperature. The bound

rubber content and crosslink density of the rubber vulcanisates will be determined by swelling in toluene in order to understand the mechanism of reinforcement of the filler in the rubbers by filler-filler and rubber-filler interactions.

4. To mix the unfilled and silanized silica filled NR, SBR and BR rubber compounds together for different mixing times, e.g. 10 and 30 min, mixing temperatures, e.g. 23 to 100°C, and rotor speeds, 45 and 90 r.p.m. to produce NR/SBR and NR/BR blends, and determine the mass fraction of the interphase and its composition in these blends, using modulated temperature differential scanning calorimetry (MTDSC). The idea will be to identify the mixing condition/conditions where the interphase properties in these blends can be optimised.

5. To measure the viscosity and cure properties of the SBR/BR blends, and fully cure the blends to produce suitable test pieces to measure the hardness, tensile strength, stored energy density at break, elongation at break, tearing energy, tensile modulus at different strain amplitudes, abrasion resistance, heat build up and dynamic properties such as $\tan\delta$, loss and storage modulus of the cured blends at different oscillation amplitude, test frequency and test temperature. The bound rubber and crosslink density of the cured blends will be determined in toluene in order to understand the extent of filler-filler and filler-rubber interaction in these blends.

6. To collect results and findings from all the tests performed in objective 5 to identify the blend or blends with the lowest rolling resistance and highest skid resistance which may be suitable for green tyre tread applications.

1.3 Structure of the thesis

Chapter 1 – Background to the aims and objectives of the project

This chapter will include a brief introduction to the development of early tyres; important tyre properties such as wear, wet- and ice-grip and rolling resistance and the importance of tyre tread in tyre performance will be mentioned. The need to use reinforcing colloidal carbon blacks, synthetic silicas and coupling agents to improve the mechanical properties of rubber compounds for use in tyre manufacture will be emphasised. In addition, the hazards, which rubber chemicals cause to health, safety and the environment will be mentioned briefly. Finally, the overall aim and objectives of the project will be listed.

Chapter 2 – Reinforcement of rubbers with silanized silica nanofiller

This chapter will include a brief mention of the previous work done on the use of silanized silica and carbon black in rubbers and compares the effects of these fillers on the rubber properties. The mechanism of sulphur curing in hydrocarbon rubbers and the use of accelerators and activators to increase the cure efficiency will be discussed. There will be a brief mention of other ingredients such as antidegradants and processing aids. Differences between the surface chemistry of synthetic silica and carbon black fillers will be examined, and the reaction mechanism of bifunctional organosilanes or coupling agents with the functional groups on the silica surfaces and hydrocarbon rubbers will be discussed.

Chapter 3 – Mechanical and dynamic properties of rubbers

This chapter will discuss a wider range of rubber properties measured with standard laboratory procedures. These properties are of significant importance to tyre rubbers. These include cure or vulcanization characterisation with oscillating disc rheometers, hardness, abrasion resistance, tear resistance, tensile properties and Mooney viscosity. To understand the mechanism of reinforcement in cured rubbers, crosslink density and bound rubber content will be calculated

using appropriate expressions after swelling the rubber samples in toluene. Principles behind measuring tanδ, storage modulus and loss modulus and their dependence on temperature for rubbers filled with surface pre-treated silica will be discussed too. There will be a review of some of the work reported on the effect of silane-treated silica on the dynamic properties of rubber vulcanisates such as NR and SBR.

Chapter 4 – Use of modulated temperature differential scanning calorimetry (MTDSC) to measure the mass fraction and composition of interphases in rubber blends

This chapter will review several techniques for measuring interphases in rubber blends including MTDSC. The principles and basic equations for MTDSC will be discussed and its merits and advantages over the more traditional techniques will be highlighted.

Chapter 5 – Employed standard procedures for measuring the mechanical and dynamic properties of cured rubbers

This chapter will mention the raw rubbers, chemicals, antidegradant and processing oil used for this study. It will also describe briefly the British Standard test procedures for preparing rubber samples and measuring the rubber properties such as Mooney viscosity, cure properties using oscillating disc rheometer, hardness, abrasion resistance, tear strength, tensile properties and tensile modulus at different strain amplitudes. The methods for measuring glass transition temperature, tanδ, loss and storage modulus and the equations for calculating crosslink density and bound rubber content will be mentioned too.

Chapter 6 – Effects of silanized silica nanofiller on the crossking and mechanical properties of NR

This chapter will discuss the mixing procedure for the NR compounds, optimisation of cure or chemical bonding between the filler and rubber via TESPT with accelerators, activators and elemental sulphur. Crosslink density and bound

rubber measurements of the cured NR rubber compounds will be included. The hardness, mass and volume losses in the abrasion tests, bound rubber content, tearing energy, tensile strength, elongation at break, stored energy density at break, tensile modulus at different amplitudes and hysteresis results of the cured NR rubbers will be presented.

Chapter 7 - Assessing effects of several processing parameters on the mass fraction and composition of interphases in the unfilled and uncured SBR/BR and NR/BR blends using MTDSC

This chapter will discuss the mathematical principles behind the use of MTDSC technique for calculating the mass fraction and composition of interphases in the SBR/BR and NR/BR rubber blends, and will summarise effects of mixing temperature, mixing time, rotor speed, and different weight ratios of SBR to BR rubbers in the SBR/BR blend on the interphase properties.

Chapter 8 - Measuring the mass fraction and composition of interphases in SBR/BR rubber blends filled with silanized silica nanofiller prepared at different mixing temperatures and mixing times using MTDSC

This chapter will discuss the procedures for preparing the SBR/BR rubber blends at different mixing temperatures and mixing times. The mass fraction of the interphase and its composition in the SBR/BR blends will be measured and the results will be examined to determine how the processing parameters aforementioned affected the interphase properties in the blend. The aim will be to optimise the interphase properties in order to achieve the best possible mechanical and dynamic properties for the blend.

Chapter 9 – Evaluating effects of silanized silica nanofiller on the mechanical properties of the SBR and BR rubbers and SBR/BR blend

This chapter will evaluate effects of silanized silica nanofiller on the Mooney viscosity, cure characteristics and mechanical properties of the SBR and BR rubbers. The silanized silica filled SBR and BR rubbers will be mixed together for

different times and at different temperatures to produce SBR/BR blends. The mass fraction and composition of the interphase in the blends will be determined using MTDSC. The Mooney viscosity of the SBR/BR compounds (blends) will be measured, and after the blends are cured, the hardness, tensile strength, elongation at break, stored energy at break, tearing energy, tensile modulus at different strain amplitudes and bound rubber content will be measured.

Chapter 10 – Measuring dynamic properties of the SBR, BR, NR and IR rubber vulcanisates filled with silanized silica nanofiller at different test temperatures, test frequencies and oscillation amplitudes

This chapters reports the $\tan\delta$, loss modulus and storage modulus test results for the cured SBR, BR, NR and IR rubbers filled with 60 phr silanized silica nanofiller at test frequencies 1-100 Hz, test temperatures -50 to 100°C and oscillation amplitudes 15-1000 μm. The overall aim is to evaluate how these parameters will affect the dynamic properties of these rubbers before they are mixed together to produce blends for further work. In addition, effect of elemental sulphur on these properties will be examined too.

Chapter 11 – Evaluating the dynamic properties of the silanized silica-filled SBR/BR rubber blends

This chapter reports the $\tan\delta$, loss modulus and storage modulus test results for the SBR/BR (75/25 weight ratio) rubber blends which will be measured at 256-1000 μm oscillation amplitudes, -50 to 85°C temperatures, and 1 and 20Hz test frequencies. Initially, the SBR and BR rubbers filled with 60 phr silanized silica nanofiller will be prepared and mixed together for 1, 7 and 20 min and then tested at different temperatures, i.e. -50 to 85°C. The idea is to identify the blends or blend, which will have the highest $\tan\delta$ at low temperatures (good skid resistance) and the lowest $\tan\delta$ at high temperatures (low rolling resistance). Such as blends or blend will be idea for trye tread applications.

Chapter 12 – Measuring effects of an increasing loading of silanized silica nanofiller on the viscosity, green strength and adhesion strength of SBR, BR, NR and SBR/BR rubber blend

This chapter reports the effects of up to 75 phr silanized silica nanofiller on the viscosity, green strength and tack or adhesion of the SBR, BR, NR rubbers and SBR/BR (75/25) blend. The tack of the rubbers was measured as a function of the intimate contact time for up to 32 min by means of the peel test method at 180° and at ambient temperature. The aim was to assess effect of the filler on the strength of the interfacial adhesion, since when the two rubbers are mixed to produce blend, the mechanical properties of the blend will depend on good adhesion forming at the interface between the two rubbers.

Chapter 13 – Conclusions and suggestions for future work

In this chapter, all the important conclusions from this study will be summarized. In addition, the viscosity, cure, mechanical and dynamic properties of some SBR/BR blends, which are currently used to manufacture treads for green tyres will be compared with the results from this study to show the advantages of the new blends developed. Results for tyre treads containing carbon black/silica combination will also be included in this chapter.

Finally, some suggestions for further work and continuation of this project work in the future will be put forward.

References:

1) Internet website:
http://www.eng.buffalo.edu/Courses/ce435/2001ZGu/Firestone_Tires/FirestoneTiresReport.htm

2) Eric Tompkins, "The history of the pneumatic tyre", Dunlop archive project (1981).

3) Zhang P,Wang M J,Kutsovsky Y,Presented at a meeting of the rubber division, American Chem. Soc.,Ohio(Oct. 16-19,2001).

4) Wang MJ.,Zhang P, Mahmud K, Presented at a meeting of the rubber division, American Chem. Soc.,Texas(April 4-6,2000).

5) De D,Das A,Kumar P,Dey B, *J. Appl. Polym. Sci.* **99**:957(2006).

6) Agrawal S L,Mandot S K,Mandal S K,Malik A S, *J. Mat. Sci.* **41**:(**17**)5657 (2006).

7) US Patent 6482884, Pirelli pneumatical S.p.A (Milan, It) 2002-11-19.

8) US Patent 6686408, Bridgestone corporation (Tokyo, Jp.) 2004-02-03.

9) Weydert M , Kaes C, *Patent Application no.* 20060060285, Goodtear tyre & rubber company, Intellectual depart. US, 03/23/2006.

!0) *US Patent* 6201054, Sumitomo rubber industries,13/03/2001

11)The Yokohama rubber co.,*Tyre Sci. Technol* **34**:(**4**)237(2006).

12) Zheng D, Tyre Sci. Technol. **31**:(**3**)189(2003).

13) Knisley S, *Tyre Sci. Technol.* **30**:(2)83(2002).

14) Rattanasom N, Poonsuk A, Makmoon T, *Polymer testing* **24**:728(2005).

15) Hao P T, Ismail H, Hashim A S, *Polymer testing* **20**:539(2001).

16) Rios S, Chicurel R., Castillo L, *Materials & Design* **22**:369(2001).

17) *US Patent* 6469101, Pirelli coo. Pneumatic (Milan, IT) 22/10/2002

18) *US Patent* 6737466, Pirelli Pneumatic (Milan, It)18/05/2004.

19) *US Patent* 5886086, The Goodyear tyre & rubber co. 23/03/1999.

20) Poh B T, Ismail H , Tan K S, *Polymer testing* **21**:801(2002).

21) Baccaro S, Cataldo F, Cecilia A, *NIMB* **208**:191(2003).

22) Heinrich G, Kluppel M, Vilgis T A,*Current option in solid state and material sci.* **6**:195(2002).

23) Gauthier C, Reynaud E, Vassoille R, *Polymer* **45**:2761(2004).

24) Hu H., Zheng O, *J. Material Sci.* **40**:249(2005).

25) Hussain S, Hoofatt M S, *Tyre Sci. Technol.* **3**:(**2**)119(2006).

26) Kueseng K, Jacob K I , *European Polym. J.* **42**:220(2006).

27) Shanmugharaj A M Bae,Yong K,*Composites Sci. Technol.*, Article at press (2006).

28) Rattanansom N, Saowapark T, *Polymer testing*, article in press(2006).

29) Stenenson I., David L, *Polymer* **42**:9287(2001).

30) Bokobza L, Chauvin J, *Polymer* **46**:4144(2005).

31) Vilgis T A., *Polymer* **46**:4223(2005).

32) Choi S S., Nah C, Wook B , *Polym Int.* **52**:1382 (2003).

33) Choi S S, *J. Appl. Polym. Sci.* **99**:691(2006).

34) Suzuki N, Ito M., *Polymer* **46**:(**1**)193(2005).

35) Frohlich J , Niedermeier W, Luginsland H D,*Composites* **PartA 36**:449(2005).

36) Frogley M., Ravich D, *Composites Sci. Technol.* **63**:1647(2003).

37) Seen Chao S, Choi S J, *Bull. Korean Chem. Soc.* **27**:9(2006).

38) Silane coupling agent, Sin young cheong Co. report, Malaysia(1999).

39) Thammathadanukul et al, *J.Appl Polym. Sci.***59**:1741(1996).

40) Sae-oui P , Thepsuwan U, Hatthapanit K, *Polymer testing* **23**:397(2004).

41) Ten J W,Debnath S C, Reuvekamp L.,*Composite Sci. Technol.*63:(8)1165 (2003).

42) Castellano M., Conzatti L., Costa G., *Polym.* **46**:(**3**)695(2005).

43) Jea Kim K., Vanderkooi J, *Composite Interfaces* **11**:(**7**)471(2004).

44) Wolff S.,"Silanes in tyre compounding after ten years-a review",*Tyre sci. Technol.* **15**:(**4**)276(1987).

45) Jea Kim K.,Vanderkooi J, A paper presented in rubber division, American Chemical Soc. (Oct. 16-19,2001).

46) Notch consulting group, a market research published on August (2006).

47) Jin Park S., Sook K. Cho, *J. of Colloid and Interface Sci.* **267**:86(2003).

48) *Natural rubber newsletter* 29:1st quarter(2003).

49) Internet website: www.tyres-online.co.uk

50)http://www.negevsilica.com/products/rd_services/green_tyre/defa%20%20%20ult.asp

51) Internet website: www.viamicheline.com

52) Internet website: www.specialchem4polymers.com

53) Byers J, *Rubber world* **236**:(**5**)6(2007)

LITERATURE SURVEY

CHAPTER 2

Reinforcement of rubbers with silanized silica nanofiller

2.1 Introduction

Ansarifar and co-workers [1-7] studied effects of precipitated silica nanofiller pre-treated with TESPT on the processing, mechanical and dynamic properties of BR, NR and SBR rubbers and reported significant improvements in these properties. According to their findings, silanized silica filler was a more efficient reinforcing material than some fine grades of carbon black. For example, when the mechanical properties of SBR vulcanisates containing the same amount of precipitated silica and high abrasion furnace carbon black of roughly the same average particle size were compared, the rubber with silica had superior elongation at break, tensile strength, stored energy density at break and tearing energy [8]. The minimum fatigue life of the silica-filled rubber was noticeably longer than that of the carbon black filled one. In addition, the use of TESPT pre-treated silica offered major advantages over the more traditional silica/liquid silane mixture [8]. Previous studies [9,10] have shown that when a large amount of liquid TESPT was mixed with precipitated silica and then added to NR, the filler dispersion was poor and there were large aggregates formed in the rubber matrix. Moreover, there was evidence that the silica surfaces were not properly treated with the liquid silane, which could have caused retardation of the curing reaction in the rubber compound. Use of the TESPT pre-treated silica was more efficient and easier to handle and mix with the rubber.

2.2 Curing systems for rubber compounds

Crosslinking or curing where covalent sulphur or hydrogen bonds are formed between polymer chains, is a widely used technique for improving the polymer properties such as hardness, tensile strength and fracture properties [11].

As mentioned earlier, the first method of curing or crosslinking rubber was developed by Charles Goodyear in 1839 [12] when he cured NR with elemental sulphur at a high temperature. It took longer than 5 hours to achieve a reasonably full cure. Since then, the vulcanization process has been massively improved, and in addition to elemental sulphur, a huge number of new curing chemicals have been manufactured and marketed, which are being used successfully by the rubber industry to crosslink a wide range of natural and synthetic rubbers. Cure systems often consist of several ingredients such as accelerators, activators and curing agents. In addition to the curing chemicals, antidegradants, processing aids, fillers and special purpose materials, e.g. flame retardants and blowing agents, are also added to raw rubbers. However, reinforcing fillers and curing chemicals are by far the most important ingredients added to raw rubbers to improve their physical and mechanical properties.

2.2.1 Elemental sulphur

Initially, vulcanization was accomplished by heating elemental sulphur at a concentration of 8 phr in the rubber for 5 hours at 140°C. The addition of ZnO reduced the cure time to 3 hours. Accelerators in concentrations as low as 0.5 phr helped to reduce the vulcanization time to 1-3 minutes. As a result, the vulcanization process with sulphur and without accelerator is no longer of commercial significance [13]. An exception is the use of about 30 phr of elemental sulphur, with little or no accelerator, to produce moulded products of a hard rubber called ebonite.

Figure 2-1 shows typical sulphur bridge formed between two polymer molecules [13]. As can be seen in this figure, double bonds or un saturation sites along the back- bone of rubber chains contribute to the formation of crosslinks by

enhancing the activity of the allylic hydrogen, at which the crosslinking takes place.

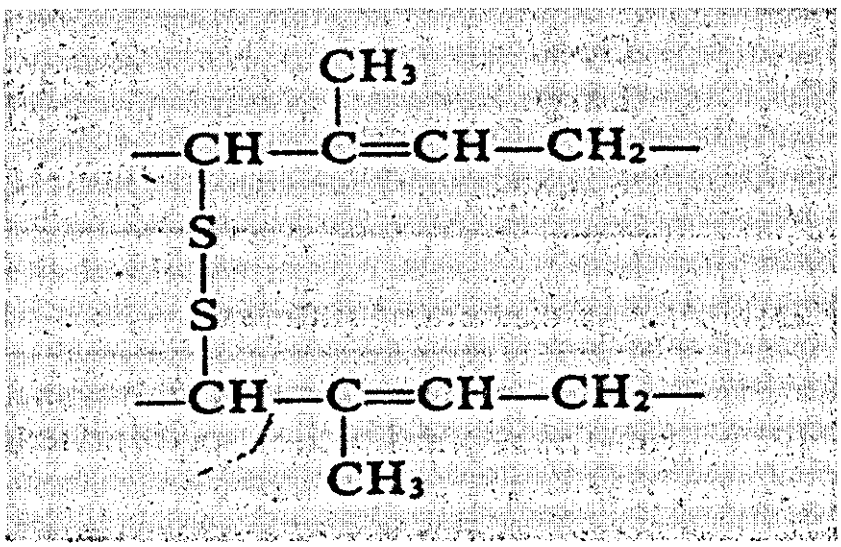

Figure 2-1: Typical sulphur-bridge between rubber chains[13].

The mechanisms of sulphur curing is not fully understood, but it is believed that the accelerator reacts with sulphur to give sulfide of the type:

$Ac-S_x-Ac$

where Ac is a free radical derived from an accelerator. These polysulfides then interact with the rubber to give intermediates of the type:

$rubber-S-Ac$

This reacts further with the final crosslinks being of the general type shown in Figure 2-1. Over the years, three different cure systems have been developed. They are efficient vulcanization (EV), Semi-efficient vulcanization (SEV) and Conventional vulcanization (CV) systems.

In EV system, there is a low level of sulphur and a correspondingly high level of accelerator or sulphurless curing to produce a vulcanisate. This is suitable when

an extremely high heat and reversion resistance is required. In the conventional curing system, the sulphur dosage is high and correspondingly the accelerator level is low. The CV systems provide better flex and dynamic properties but poorer thermal and reversion resistance. For optimum mechanical and dynamic properties with intermediate heat, reversion, flex and dynamic properties, the so-called SEV system with an intermediate level of accelerator and sulphur are employed. The levels of accelerator and sulphur in CV, SEV and EV systems as shown in Table 2-1.

Table 2-1: Levels of accelerator and sulphur in CV, SEV and EV systems

Type	Sulphur (phr)	Accelerator (phr)	Accelerator/sulphur ratio
CV	2-3.5	0.4-1.2	0.1-0.6
SEV	1.0-1.7	1.2-2.4	0.7-2.5
EV	0.4-0.8	2.0-5.0	2.5-12

In addition to elemental sulphur, sulphur- bearing compounds that donate sulphur at the vulcanization temperature can be used as curing agent [11]. Some compounds like DTDM (4,4'-dithiodimorpholine), can directly substitute with elemental sulphur and some may use directly as accelerator, like TMTD(Tetramethyl Thiuram Disulfide). Sulphur donors may use when there is not need to high amount of sulphur as they use in EV or SEV systems.

2.2.2 Accelerators

Although vulcanization or crosslinking can take place by heating sulphur in rubber, the process is relatively slow. It can be speeded up quite considerably by adding small amounts of organic or inorganic compounds known as accelerators. Organic accelerators were not used until 1906. Sixty five years after Goodyear and Hancock developed un accelerated vulcanization, the effect of aniline on sulphur vulcanization was discovered by Oenslayer [13].

Aniline, however, is too toxic for use in rubber products. Further developments led to the introduction of guanidine accelerators [14]. Reaction products formed between carbon disulfide and aliphatic amines (dithiocarbamates) were first used

as accelerators in 1919 [15] .However, most dithiocarbamate accelerators give little or no scorch resistance and therefore, can not be used in all applications. The first delayed action accelerators were introduced in 1925 with the development of 2-mercaptobenzothiazole (MBT) and 2-mercaptobenzothiazoledisulfide (MBTS) [16-18]. Even more delayed action and yet faster-curing vulcanization became possible in 1937 with the introduction of the first commercial benzothiazole sulfenamide accelerators [19, 20]. Further progress was made in 1968 [21] with the introduction of pre-vulcanization inhibitor (PVI), N-cyclohexylthiophthalimide (CTP), which can be used in small concentrations together with benzothiazolesulfenamide accelerators. Figure 2-2 shows the cure behaviour of several accelerators used in NR at 140°C [11].

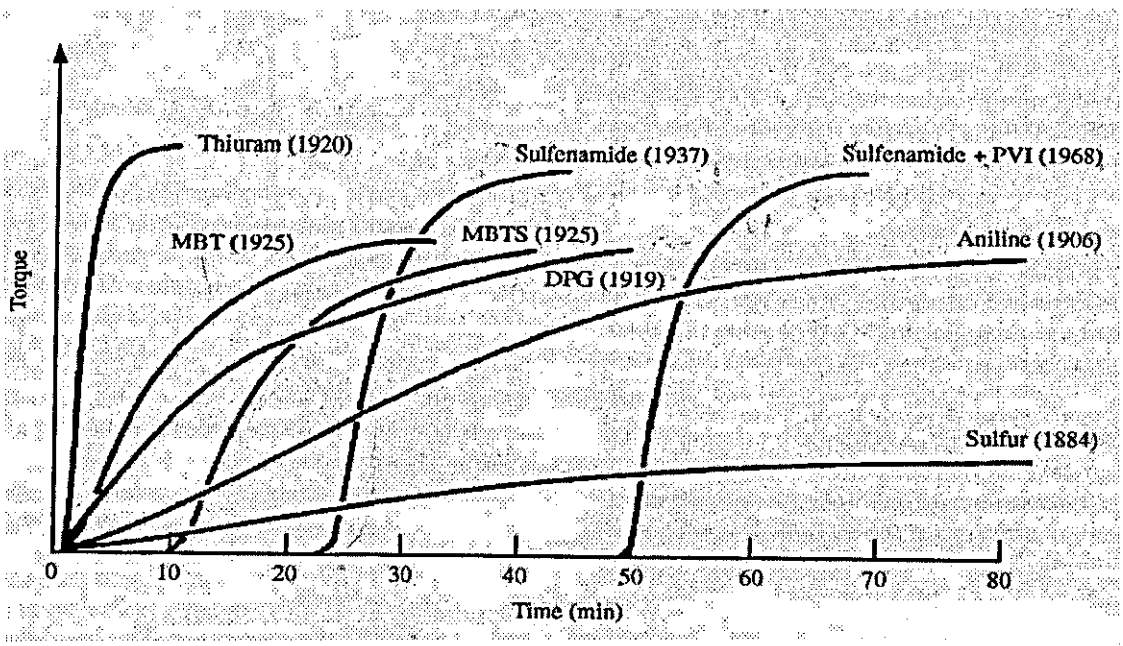

Figure2-2 : Cure behaviour of several accelerators in NR at 140 $^{\circ}C$ [11].

Accelerators can be divided into two major groups: primary and secondary. Primary accelerators are generally efficient and have good processing safety in rubber compounds and exhibit a broad vulcanization plateau with relatively low crosslink density. Secondary accelerators may be used in combination with

primary accelerators in rubber compounds. These combinations produce much faster rate of vulcanization than each product separately and therefore, are more efficient for general properties of industrial rubber products. Figure 2-3 represents these categories in brief [11].

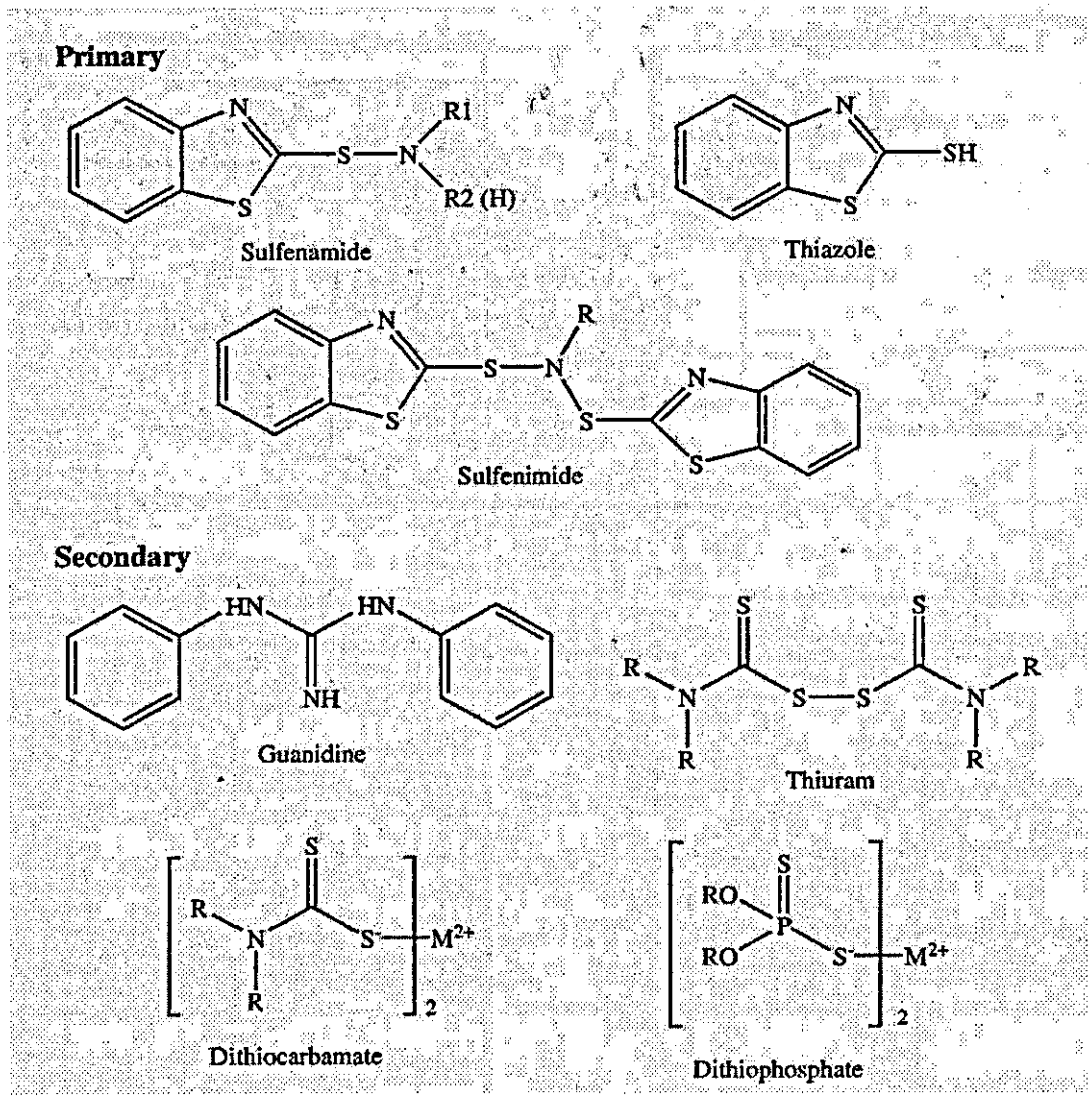

Figure2-3: Some examples of primary and secondary accelerators

2.2.3 Other ingredients in cure systems

In addition to reinforcement agents or fillers, which will be discussed fully in section 2-3, elemental sulphur and accelerators, there are many other

ingredients that are added to raw elastomers. They are: activators, antidegradants, processing aids such as processing oils (to reduce viscosity) and special purpose materials for example, flame retardants and colouring agents. Activators are added to improve the efficiency of accelerators in sulphur-cure systems.

The most widely used activators for sulphur cure systems are zinc oxide (ZnO) and stearic acid. Stearic acid is a fatty acid, which is added to improve the solubility of ZnO in the rubber. The role of zinc oxide, which produces zinc ions in the presence of stearic acid, is to form chelates with the accelerator and sulfides. This helps to increase the efficiency of the vulcanization process.

Rubbers that possess chemically active double bonds or un saturation sites along their backbones and in their side groups such as NR, SBR, nitrile rubber (NBR) and ethylene-butadiene diene rubber (EPDM), are sensitive to heat, light and particularly oxygen. Unless protected with antidegradants such as antioxidants and antiozonants (e.g. α and β-naphtylamines), the rubber will age by an autocatalytic process accompanied by an increase in oxygen content. The consequences of aging may be either softening or embrittlement depending on the elastomer type, suggesting competing processes of degradation and crosslinking of polymer chains. The first step in the ageing process is presumed to be the same as that in the oxidation of any olefin, that is, the formation by free radical attack of a peroxide at a carbon atom next to a double bond [11].

$$-CH_2CH=CH- \rightarrow -\overset{\circ}{C}H-CH=CH-+H^\circ$$

$$H^\circ + -\overset{\circ}{C}H-CH=CH-+O_2 \rightarrow HO-O-\overset{/}{C}H-CH=CH-$$

Subsequent steps may include crosslinking or chain cleavage or involvement of the double bonds, probably initially through an epoxide group. Many of the steps in the reaction process resemble closely those of certain types of vulcanization.

Many unsaturated rubbers when subjected to a minimum 5-6% applied strain are sensitive to attack by ozone, and therefore require protection by antiozonants. These are often derivatives of *p*-phenylenediamine and are thought to react with the ozone before it can undergo reaction with the rubber surface.

2.3 Reinforcement mechanism of fillers in rubber

2.3.1 Reinforcing agents for rubbers

For many applications, even vulcanized rubbers may not exhibit satisfactory mechanical properties including tensile strength, stiffness (hardness), abrasion resistance, and tear resistance. These properties can be enhanced by the addition of certain types of fillers to the rubber before curing. Fillers for rubber are divided into two distinct groups, inert or extender fillers, such as clay, whiting and barites, which make the rubber mixture easy to process before vulcanization but have little effect on the mechanical properties of rubber vulcanisates; and reinforcing fillers, which do improve the mechanical properties of rubber vulcanisates. Carbon blacks and silicas are in the latter group. In fact, vulcanization offers a partial improvement to the rubber properties for example rubber becomes stiffer and its hardness and tensile strength improve because of crosslinks between the rubber chains. However, this still leaves significant local chain segmental mobility in the rubber. High reinforcement stiffens the rubber mass and improves its toughness by restricting chain mobility and freedom of movement to a much larger extent.

2.3.2 Comparison of carbon black with silica in hydrocarbon rubbers

Precipitated amorphous white silica has been used in the rubber industry for a long time and in some applications for instance in shoe soles, it has replaced carbon black entirely. However, its use in tyre compounds had been limited to two types of compounds: off–the-road tread compound to improve chipping and chunking resistance, and textile and steel cord bonding compound for increasing adhesion between the cord surface and rubber materials [22] . Even in these two

applications, silica had to be blended with up to 15 phr carbon black. The reason that silica could not completely replace carbon black as the main filler in tyre compounds was because it caused processing difficulties and exceedingly long cure times of the rubber compounds. The reason for poor processability was its weak polymer-filler interaction and strong filler-filler interaction, which increased the compound viscosity and made it difficult to disperse the silica particles well in the rubber matrix. Both of these problems were associated with the surface chemistry of the filler.

The surfaces of carbon blacks consist of a certain number of unorganized carbons and are made mainly of graphitic basal planes with some functional groups and mostly oxygen containing groups, which are located on the edges and crystal defects. The silica surfaces are made of siloxane and silanol or hydroxyl groups. Based on the adsorption investigation of different chemicals by means of inverse gas chromatography (I.G.C), it has been found that carbon blacks possess a high dispersive component of surface energy, γ_s^d, whereas silicas have low γ_s^d . By contrast, the specific or polar component of the surface free energy, γ_s^p, estimated from the specific interaction between the filler surfaces and polar chemicals, is much higher for silicas than it is for carbon blacks [23, 24]

.

With regard to polymer-filler and filler–filler interactions, Wang et al [23] were able to differentiate between carbon blacks and silicas by means of measuring the adsorption energies of model compounds, which were associated with different components of their corresponding surface free energies. In principle, as cited earlier, while silica fillers have polar surfaces, hydrocarbon rubbers are generally non-polar, or have very low polarity. The higher adsorption energy of non-polar chemicals such as heptane, resulting from higher γ_s^d of the filler surface, indicated a greater ability for the filler to interact with hydrocarbon rubbers. However, the higher adsorption energy of a more highly polar chemical

such as acetonitile (MeCN), resulting from a higher, γ_s^p, was representative of filler aggregate- aggregate interaction in hydrocarbon rubbers. The existence of silanol or hydroxyl groups on the silica surfaces led to strong hydrogen bonding between silica aggregates and formation of a stronger filler network in comparison with its carbon black counterpart. In addition, the lower filler-polymer interaction of silica with hydrocarbon rubber also resulted in low bound rubber content in the compound [25,26], which facilitated filler flocculation. Consequently, the filler network of silica was more developed and much stronger in hydrocarbon rubbers. In fact, with silica and carbon black having similar surface areas and structures, Wolf et al [25, 27] demonstrated that the Payne effect of the silica filled NR compound was much higher than that of a carbon black filled compound.

2.3.3 Coupling agents

Apart from difficulties encountered in mixing silica with rubber and dispersing it well in the rubber matrix, silica is also an acidic material because of silanol or hydroxyl groups on its surfaces. The presence of these groups interfere with the reaction mechanism of sulphur cure in the rubber, which often requires alkaline condition [28]. This cure retarding effect and the difficulties experienced in mixing and dispersing hydrophilic silica particles are often remedied with bifunctional organosilanes known also as coupling agents.

Bifunctional organosilanes perform two functions in rubber. They react with the rubber to form strong bonds, which increases the rubber/filler adhesion. They also react with the silanol groups on the surfaces of silicas to form stable filler/TESPT bonds. The use of silane coupling agent also improves the dispersion of silica particles in the rubber matrix and prevents formation of aggregates and agglomerates in the rubber [29].

(silica reactive part) $(RO)_3 - Si - (CH_2)_3 - SH$ (rubber reactive part)

The formation of strong filler-rubber linkages via organosilanes has a major influence on the properties of rubber compounds [30]. 3-mercaptopropyltrimethoxysilane was one of the first coupling agents for rubber applications [31] . Addition of this silane to a silica filled NR compound increased the tensile strength, tear strength and modulus, and improved hysteresis and lowered permanent set of the rubber vulcanisate [30]. However, two properties of this silane were disadvantageous. It emanated an unpleasant odor during mixing, especially at elevated temperatures and caused scorch problems and therefore its use remains limited [28].

Using trichlorosilane as a starting point, more than one hundred different organosilanes were synthesised by Wolff and co-workers [32, 33]. These compounds were subsequently tested for their utility in silica-filled rubber compounds. Only two silanes were found to be suitable as coupling agents namely, 3-thiocyanatopropyltriethoxy) (TCPTS), $(C_2H_5O)_3-Si-(CH_2)_3-SCN)$ and bis(3-triethoxysilylpropyl)tetrasulphane (TESPT). The latter is shown in Figure 2-4.

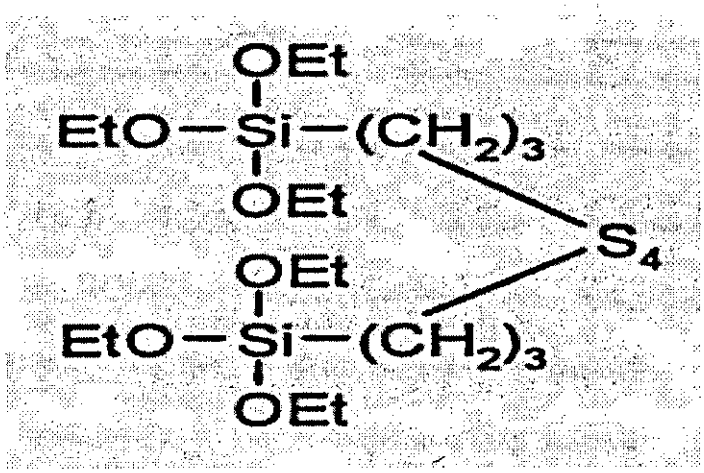

Figure 2-4: TESPT chemical structure[32].

The remaining silanes had drawbacks regarding handling, odor, ease of transport, storage stability, kinetics of the modification and/or curing reactions,

toxicological safety and their reaction products. TESPT is used in the Michelin's green tyre formulation [34]. Wolff [35] assumed that the reaction mechanism of TESPT with silica surfaces and the rubber would be as following (Figure 2-5):

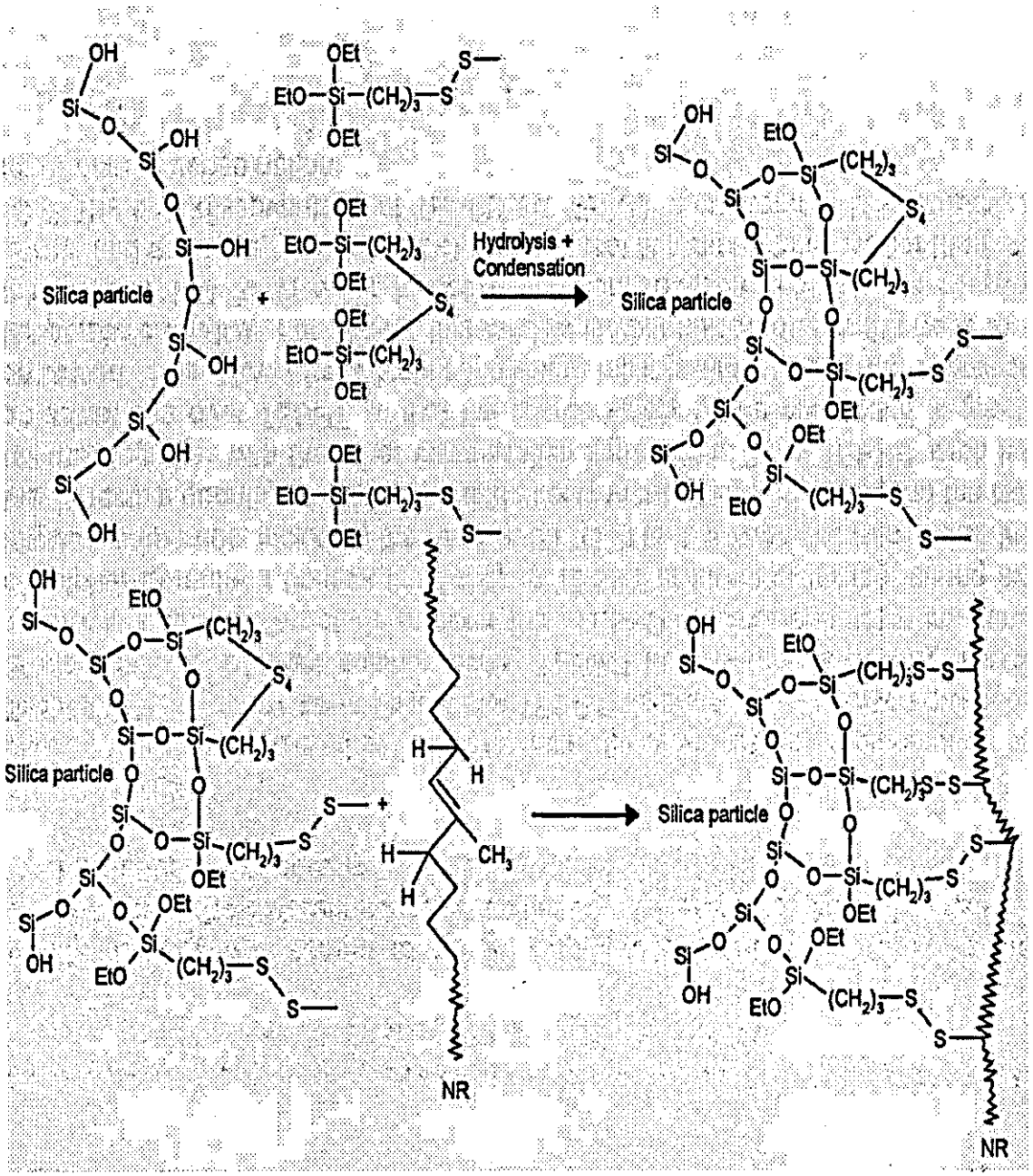

Figure 2-5: Mechanism of TESPT reaction with silica and rubber (NR)

As shown in figure 2-5, the ethoxy groups react with the silanol groups on the surfaces of silica particles to form stable filler/TESPT bonds. This reduces the number of silanol groups after reaction with TESPT, and the remaining groups

become less accessible to the rubber because of steric hindrance. This weakens the strong interaction between silica particles, which reduces the viscosity of rubber compounds, and improves cure properties by preventing acidic silicas from interfering with the curing reaction in sulphur-cured rubbers. The tetrasulphane groups react with the rubber in the presence of accelerators at elevated temperatures, i.e. 140-240°C, with or without elemental sulphur being present to form crosslinks in unsaturated rubbers. In order to obtain optimum effect in rubber properties, it is essential to ensure that both reactions take place under strict temperature control.

2.3.4 Precipitated amorphous white silica nanofiller pre-treated with TESPT

In this work, a precipitated amourphous white silica nanofiller pre-treated with TESPT was used. Using pre-treated silica nanofiller in rubber compounds has major advantages over silica/liquid silane mixture. There are several disadvantages in using silica/liquid silane mixtures in rubber compounds [36]. For example, the reaction that takes place between silica, silane and rubber takes place at elevated temperatures, often greater than 140°C, and this releases a considerable amount of alcohol, which must be ventilated. In this regard, the use of TESPT pre-treated silica is safer and much cleaner. This also places the responsibility for the silanisation process onto the producers of silica and not users such as the tyre industry.

Owing to the fact that for a silanized silica, the reaction between silica and silane had already taken place fully, the filler can then be stored for a period of at least one year before its use in rubber with no or very little adverse effect on the rubber properties. TESPT pre-treated silica was stored for a period of one year at 50°C and then used in SBR at regular intervals to determine whether storage had any adverse effect on the rubber properties. The tests showed no adverse effects at all and therefore it was concluded that the filler had retained its original properties and integrity after a year in storage[36].

As a result of silanisation, the filler will have less tendency to adsorb moisture and when it is added to rubber, the curing reaction will be more efficient as a result of a drier filler. Moreover, the filler particles will disperse a lot better in the rubber matrix, which will be greatly beneficial to the rubber properties.

Let us now consider the reaction kinetic of TESPT with silica. Udo Goerl proposed a reaction kinetic for silica and TESPT [37], but, this may not be the full story, since side reactions in one form or another may also take place. According to his view, 1 mol of TESPT reacts to produce 2 mols of EtOH. This means that the primary reaction completes according to equation 2.1 without any secondary reaction proceeding.

$$TESPT \rightarrow Z1 + 2EtOH \tag{2.1}$$

where Z1 is the primary reaction product and is described by the following first order rate law:

$$-\frac{d[TESPT]}{dt} = k_a[TESPT] = \frac{1}{2}\frac{d[EtOH]}{dt} \tag{2.2}$$

where $[TESPT]$ is the concentration of TESPT in mol/kg, $[EtOH]$ is the concentration of ethanol in mol/kg, t is time in minute and k_a is the rate constant in minute^{-1}.

Based on the assumption that 1 mol of TESPT reacts to form 2 mols of ethanol, the concentration of TESPT at any time is determined from the amount of ethanol evolved. This amount is determined experimentally [37] and consequently the values of k_a is determined at several temperatures.

In secondary reactions, three sequential reaction steps of the first order follow:

$Z1 \xrightarrow{k_b} Z2 + EtOH$ Secondary reactions (2.3)

$Z2 \xrightarrow{k_b} Z3 + EtOH$ (2.4)

$Z3 \xrightarrow{k_b} P + EtOH$ (2.5)

where k_b is the rate constant in minute^{-1}, $Z1, Z2, Z3$ are intermediate products, and p is the final product of the reaction between silica and TESPT.

In summary, it seems carbon black should be replaced with silica in tyre industry. This replacement makes several benefits for this industry, including improvement of tyre mechanical and dynamic properties.

So far, tyre manufacturers hadn't enough tendency toward silica due to processing difficulties.

In this study, author tries to introduce silanized pre-treated silica nanofiller as a strong reinforcement filler which has enough eligibility to discard carbon black completely.

References

1) Ansarifar A., Wang L., Ellis R., Kirtley S P, Riyazuddin, *J. Appl. Polym. Sci.***105**:322 (2007).

2) Ansarifar A., Nijhawan R., Nanapoolsin T, Song M, *Rubber Chem. Technol.***76**:(**5**) 1290 (2003).

3) Ansarifar A., Wang l., Ellis R., Kirtley S P., *The fifth international conference*, Munich, Germany (Dec. 5-6,2006).

4) Ansarifar A., Ibrahim N., Bennett M., *Rubber Chem. Technol.***78**:(**5**)793 (2005).

5) Ansarifar A., Azhar A., Ibrahim N, Shiah F, Lawton D, *International J. Adhesion and Adhesives* **25**:77(2005).

6) Ansarifar A., Shiah S F, Bennett M., *International J. Adhesion and Adhesives* **26**:454 (2006).

7) Ansarifar A., Wang L., Ellis J., Kirtley S, *Rubber Chem. Technol.***79**:39(2006).

8) Hashim A.S, Azahari B, Ikeda Y, Kohjiya S, *Rubber Chem. Technol.* **71**:289(1998).

9) Rattanason N, Saowapark T, *Polymer testing* **26**:369(2007).

10) Sung-Seen Choi, *J. Appl. Polym. Sci.***99**:691(2006).

11) R.N.Datta,"Rubber curing systems" 12, Rapra report (2002).

12) Goodyear C, Inventor, *US patent* 3633 (1844).

13) Bateman L, Moore CG., .Porter M.,"The chemistry and physics of rubber like substances" 19 (1963).

14) Weiss M.L., Dovan chemical co., *US patent* 1,411,231(1922).

15) Molony S B., Michigan chemical co., *UDpatent* 1, 343, 224 (1920).

16) Bedford C W , Goodyear tyre co., *US patent* 1, 371, 662 (1921).

17) Sebrell L B, Goodyear tyre co., *US patent* 1, 544, 687 (1925).

18) Bruni G, Romani E, *Indian Rrubber Journal* **62**:63(1921).

19) Zaucker E, Orthner L, *US patent* 1, 942, 790 (1934).

20) Harman M W, Monsanto Chemical co., *US patent* 2, 100, 692 (1937).

21) Coran A Y, Kerwood J E, Monsanto co., *US patent* 3, 546, 185 (1970).

22) Wolff S, Wang M J, *Eur. Rubber J.* **76**:(**11**)16 (Jan.,1994).

23) Wang M J, Wolff S, Donnet, *Rubber Chem. Technol.***64**:714(1991).

24) Wang M J, Wolff S, Donnet, *Rubber Chem. Technol.* **64**:559(1991).

25) Wolff S, Wang M J, *Rubber Chem.Technol.* **65**:329(1992).

26) Wolff S, Wang M J, *Proc. Int. conf. carbon black*, Mulhouse, France 133-145 (Sep. 27-30, 1993).

27) Wolff S ,Wang M J , *Kautsch Gummi Kunstst* **47**:873(1994).

28) Brinke A.ten, *Ph.D thesis*, Twente university, the Netherland (2002).

29) Dannenberg E M., *Elastomerics* 30 (1981).

30) Evans L.R, Waddell W H, *Kautsch. Gummi Kunstst* **48**:718(1995).

31) Ziemansky L P, *Rubber World* **163**:53(1970).

32) Thurn F, Burmester K, Wolff S (to degussa), *US patant* 3, 873, 489 (1975).

33) Thurn F, Wolff S, *Kautsch Gummi Kunstst* **28**:733(1975).

34) Rauline R (to compagnie generale des etablissements Michelin –Micheline and cie), *E.Pat.* 0501 227 A1 (12-02-1992).

35) Wolff S , *Tyre Sci. Technol.* **15**:276(1987).

36) Technical infotmation, silanized silica (COUPSIL), No. 6030.1, Degussa AG, Germany (1994).

37) Goerl Udo, Hunsche A., Mueller A, Kaban H.G., *Rubber Chem. Technol.***70**:608 (1997).

CHAPTER 3

Test procedures for measuring the mechanical and dynamic properties of rubber compounds and rubber vulcanisates

The testing procedures described in this chapter are based on the British standards for measuring rubber properties [1 -4].

3.1 Measuring vulcanization or cure characteristics of rubber compounds

According to the British standard [5], the curemeter is designed to measure increases in the stiffness of a vulcanizable rubber compound during heating. The curemeter, or rheometer as it is known, is used to determine the time needed to cure or vulcanise a rubber compound at a given temperature, i.e. somewhere between 140 and 240°C, which industrial rubber articles are cured and also to assess the scorch time or onset of cure in rubber compounds at elevated curing temperatures [6].

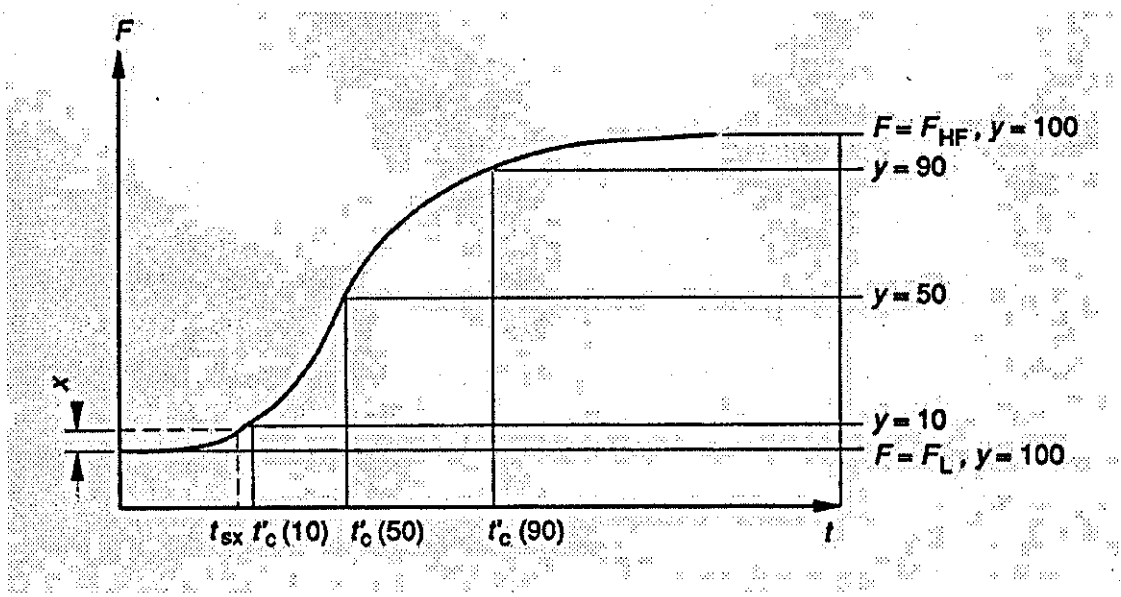

Figure 3-1: Typical vulcanization curve (ODR results)

Figure 3-1 represents a typical vulcanization curve[6].

where F is shear force or torque, F_L minimum force or torque, F_t force or torque at a specified time t, t_{sx} scorch time (time to incipient curve), $t_c'(y)$ time to a percentage y of the full curve from minimum force or torque, F_{HF} plateau force or torque.

The minimum force or torque F_L characterises the stiffness of the unvulcanized compound at the curing temperature. The scorch time, t_{sx}, is a measure of the processing safety of the compound and start of the crosslinking process. The time $t_c'(y)$ and the corresponding force or torque value give information on the progress of cure. The optimum cure is often shown as $t_c'(90)$ or $t_c'(95)$. The highest force or torque is a measure of the stiffness of the vulcanized rubber at the curing temperature.

Three types of curemeter have found widespread use in the rubber industry. They are oscillating-disc rheometer (ODR) (Figure 3-2), reciprocating-paddle, which was popular but is now hardly used, and rotor less curemeter [5] .

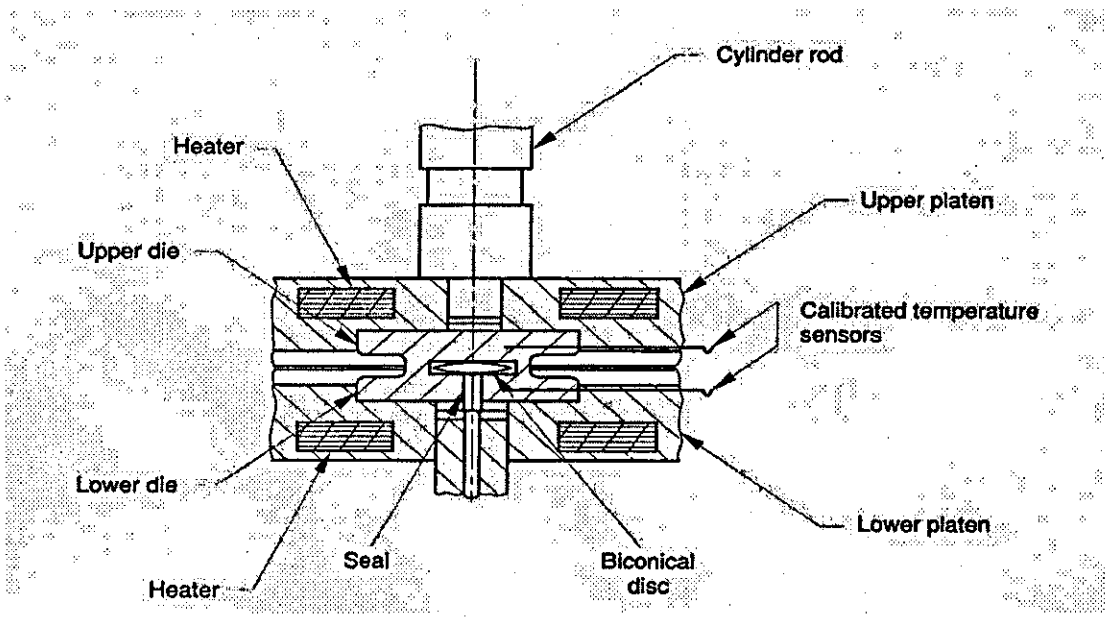

Figure 3-2: ODR rheometer

The ODR curemeter has for many years been the most widely used machines, but more recently, the rotor less curemeter has been used too. The principal advantages of the latter is that specified temperatures are reached in a shorter time after insertion of the rubber sample into the die cavity and moreover, there is better temperature distribution in the test piece.

3.2 Measurement of the mechanical properties of rubber vulcanisates

3.2.1 Hardness

Unlike other hardness test methods, which measure resistance to permanent deformation, in rubber, the hardness measurement is the indication of rubber stiffness [7]. Hardness is determined from the depth of indentation of a spherical indentor, under a specified force, into a rubber sample. An empirical relationship between depth of indentation and Young's modulus for a perfectly elastic isotropic material is used to derive a hardness scale, which may conveniently be used for most rubbers.

A hardness scale [7] chosen so that 0 represents the hardness of a material having a Young's modulus of zero, and 100 represents the hardness of a material of infinite Young's modulus, with the following conditions being fulfilled over most of the normal range of hardness:

a) One international rubber hardness degree (IRHD) always represents approximately the same proportionate difference in the Young's modulus

b) For highly elastic rubbers, the scales of IRHD and the Shore A durometer are comparable.

The indenting force is applied in three ways [8] as follow:

a) A constant force is applied and the resulting indentation is measured

b) A force required to produce a constant indentation is measured

c) A spring loading is used, which results in variation of the indenting force with the depth of indentation

The principle of a hardness tester is a load, which is applied by a weight or a spring, acting on the rubber through an indentor of defined geometry. The resulting indentation is measured with a displacement transducer (traditionally a dial gauge) relative to the test piece surface and, in order to define this, an annular foot of specified dimensions exerting a specified load surrounds the indentor.

Equation 3.1 represents the empirical relation between hardness and other parameters for example Young's modulus [7].

$$D = 61.5R^{-.48}[(\frac{F}{E})^{0.74} - (\frac{f}{E})^{0.74}] \qquad (3.1)$$

where D is indentation in hundredths of a millimetre, R radius of the ball, E Young's modulus, F total indenting force in Newton and f contact force.

3.2.2 Abrasion resistance

Abrasion is the loss of material (mass loss or wear) resulting from frictional action upon a surface [9]. The resistance of rubbers to abrasion is one of their most important mechanical properties. However, the analysis of the processes of abrasion and its measurement under laboratory conditions and in service, have proved to be very challenging.

In performing laboratory abrasion tests, it is generally necessary to obtain a significant amount of abrasion in a short time in order to have measurable mass losses. This has led to tests based on the use of sharp abrasive surfaces of corundum, high loads, and high slip velocities, though these conditions are not

characteristic of abrasion in service. Wear in service, for example, can take place not only on surfaces with sharp asperities but also on mechanically smooth surfaces such as glass or polished metal. In the case of asperities, the predominant action is that of cutting or tearing of the surface, and loss of material which occurs as asperities plough through the surface. The mass loss is directly related to the sliding distance and to the applied load. It is also very dependent upon the sharpness of the edges of the asperities and upon the hardness of the rubber. With smooth surfaces, abrasion is due to different processes and is considered to arise from stress concentrations in the surface associated with the mechanism of friction of polymers. However, abrasion by frictional forces between relatively smooth surfaces is not of sufficient interest to justify the preparation of a standard method at the present time. No close and meaningful relationship between the results of an abrasion test and service performance can be inferred at this stage.

3.2.3 Tear properties

In a tear test, the force is concentrated on a deliberate flaw or sharp discontinuity and the force to continuously produce a new surface in the rubber is measured. The force needed to start or maintain tearing will depend in rather a complex manner on the geometry of the test piece and on the nature of the discontinuity. Hence, it would be expected that different tear methods, using different geometries, will yield different tear strengths. However, there is evidence that, for at least a number of rubbers, the ranking of compounds is the same regardless of which tear method is used [10-12]. What is certain is that the initiation and propagation of a tear is a real and very important factor in the failure of rubber products, being involved in fatigue and abrasion processes as well as the catastrophic growth of a cut on the application of a stress. There is, therefore, considerable interest in the tearing resistance of rubbers.

The British standard [13] suggests three test methods for the determination of the tear strength of vulcanised rubbers, namely:
Method A, using a trouser test piece (this method will be used in this study)
Method B, using an angle test piece, with or without a nick of specified depth
Method C, using a crescent test piece with a nick
The value of tear strength obtained depends on the shape of the test piece, speed of stretching and test temperature. It may also be susceptible to grain effects in vulcanized rubber.

Method A is preferred because it is not sensitive to the length of the cut, unlike the other two test piece geometries in which the nick has to be very closely controlled. In addition, the results obtained are more easily related to the fundamental tear properties of the material and are less sensitive to modulus effects, provided that the leg extension is negligible, and the rate of propagation of the tear is directly related to the rate of grip separation. With some rubbers, the propagation of tear is not smooth, and analysis of the tests results may be difficult.
The grips should separate at a rate of 50mm/min until the test piece fractures. The tear strength, T_s will be expressed in kiloNewton per metre of thickness, and is given by equation 3.2:

$$T_s = \frac{2F}{d} \qquad (3.2)$$

where F is median or mean force in Newton, and d median thickness of the test pieces in mm.

Method B for measuring tear strength, is a combination of tear initiation and propagation. Stress is built up at the point of the angle until it is sufficient to initiate a tear and then, further stresses propagate the tear. However, it is only

possible to measure the overall force required to rupture the test piece, and, therefore, the force cannot be resolved into two components.

Method C, also measures the force required to propagate a nick already produced in the test piece though the rate of propagation is not related to the jaw speed.

3.2.4 Tensile properties

After indentation hardness measurement, the most common type of stress strain measurement is that made in tension. The ability of a rubber to stretch to several times its original length is one of its chief characteristics and it is worth mentioning that at least as many rubber products are used in compression or shear as are used in tension. Besides being of relevance to products strained in tension, tensile stress/ strain properties have been taken, since the beginning of the industry, as a general guide to the quality of a rubber, being sensitive to filler or plasticizer content as well as to mixing and curing efficiently.

Two shapes of test pieces are generally used, ring and dumb-bell and both are covered by international standard, ISO-37 [14] and ASTM D412 [15].
The advantages of rings are that there are no gripping problems, as the ring may be mounted on two pulleys, and that the elongation is easily measured by monitoring the distance between the pulleys. Their principal disadvantage is that the strain distribution in the ring is not uniform.
Dumb-bells, on the other hand, are rather more difficult to grip and the measurement of elongation cannot be taken from grip separation as the strain along the whole test piece is not uniform. However, the stress and strain is uniform throughout the central parallel portion of the dumb-bell and, hence, the problem of non-uniform strain in ring test pieces is avoided. In addition, by cutting dumb-bells in different directions, grain effects can be studied which is not possible with ring-shaped test pieces. Largely because of the uneven strain

problem, but perhaps also because most laboratories consider ring-shaped test pieces to be more difficult to cut from cured sheets of rubber, dumb-bells are the most commonly used of the two test pieces.

Considerable effort has been put into selecting the best dumb-bell shape and size, particularly by ISO committee TC45 (Figure 3-3). Type 1 dumb-bell shape of ISO 37 with a 6 mm wide centre portion and preferably cut from 2 mm thick sheet is widely used but type 2 has gained in popularity simply because it is smaller and uses less material.

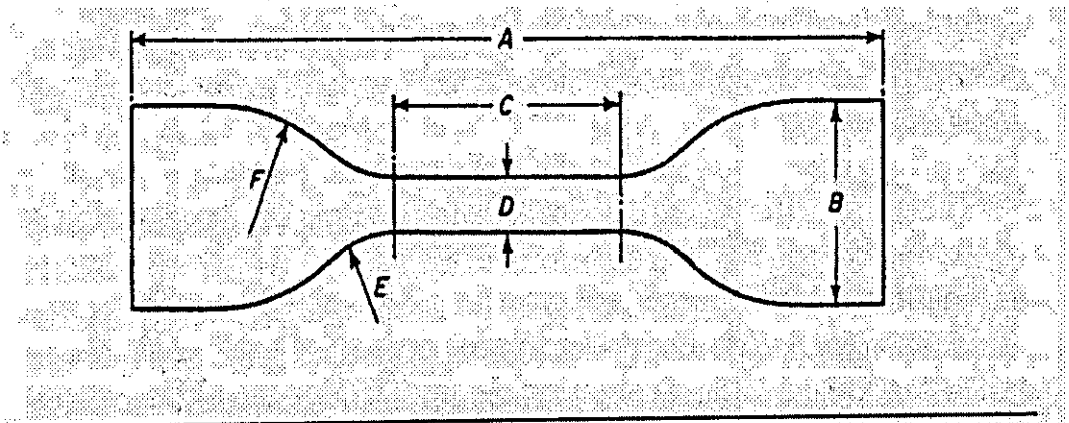

Dimension	Type 1	Type 1A	Type 2	Type 3	Type 4
A Overall length (min)	115	100	75	50	35
B Width of ends	25 ± 1.0	25 ± 0.5	12.5 ± 1	8.5 ± 0.5	6 ± 0.5
C Length of narrow portion	33 ± 2	20 + 2/-0	25 ± 1	16 ± 1	12 ± 0.5
D Width of narrow portion	6 + 0.4/-0	5 ± 0.1	4 ± 0.1	4 ± 0.1	2 ± 0.1
E Transition radius outside	14 ± 1	11 ± 1	8 ± 0.5	7.5 ± 0.5	3 ± 0.1
F Transition radius inside	25 ± 2	25 ± 2	12.5 ± 1	10 ± 0.5	3 ± 0.1
Gauge length	25 ± 0.5	20 ± 0.5	20 ± 0.5	10 ± 0.5	10 ± 0.5

Figure 3-3: Standard dumb- bell dimensions for tensile properties measurement

3.2.5 Mooney viscosity

The torque necessary to rotate a metal disc in a cylindrical chamber filled with un compounded or compounded rubber is measured by this method using a

Mooney viscometer. The Mooney viscosity number (MU) is proportional to the value of the torque [16, 17]. The Mooney viscometer has a single speed rotor, two half dies which form a cylindrical cavity and can be heated and maintained at constant temperature and pressure. The method measures the torque needed to flow the rubber in the die cavity and is ideal for measuring the flow properties of rubber compounds. The results from this method are expressed as ML(1+4, 100°C), where, M, means Mooney, L, large rotor, 1 minute preheat time, 4 minutes run time and the tests are performed at 100°C.

3.3 Crosslinking and bound rubber

Bound rubber, sometimes termed filler gel, has been recognized as an important factor in the mechanism of rubber reinforcement, and is often considered to be a measure of surface activity of reinforcing fillers [18, 19]. The first description of the bound rubber phenomenon was by Twiss in 1925, who observed that the resistance of carbon black filled NR mixes to solvents was related to improved mechanical properties. Boiry studied many of the factors influencing the insolubilization of NR by fillers including type, amount of fillers, mixing and testing variables. In 1937 J. H. Fielding of Goodyear developed a so-called "bound rubber" test because of his interest in the possibility of chemical bond formation between fillers and rubber. During the start of the U.S. synthetic rubber program In 1945, Baker and Walker reported insolubilization of SBR when mixed with carbon black significantly greater than the amount of normal gel in the unfilled elastomer. They were also the first to report that the amount of gel increased with increasing molecular weight and that a selective adsorption of high molecular weight material occurred. Since that time, many investigations have confirmed these findings with many other elastomers, and theories of bound rubber formation have been based on these observations. The early concept that bound rubber is a gel of carbon black particles held together in a three-dimensional lattice by longer inter particle polymer molecules is still valid.

The nature of the segmental attachments of the polymer molecules to the filler surfaces now appears to be both physical and chemical, depending upon filler surface activity and chemical functionality, and the chemical composition and functionality of the elastomer. Regardless of the type of interaction, the bonding is essentially permanent and can only be disrupted by extraction with good solvents at high temperatures.

The relationship of bound rubber to reinforcement was shown by Sperberg who correlated the amount and tightness of the gel to abrasion resistance encountered in actual road tests. Switzer who coined the term "carbon gel complex " agreed with Sperberg and concluded that the carbon gel complex was basic to reinforcement because it was affected not only by particle size and structure but also by surface activity. There is now general agreement that bound rubber is an important factor in rubber reinforcement [20].

Bound rubber is determined by immersing small pieces of cured or uncured mix in a large excess of a good solvent such as toluene for three to four days at room temperature. Soluble rubber is extracted from the sample by the solvent, but a small amount of soluble rubber must remain within the swollen gel. The pieces swell to as much as 40 times their original volume, forming a weak coherent gel containing all of the carbon black and from 5 to 60 wt% of the original rubber content, depending on factors such as the amount and type of filler. In order to minimise extraneous mixing and storage factors and approach more stable values, some investigators preheat the samples for one hour at $145°C$.

3.4 Dynamic properties

3.4.1 Introduction

Although static mechanical properties such as tear strength and abrasion resistance have a great role to play in the service life of tyres, attention must also be given to the dynamic properties of rubber vulcanisates. In fact wearing

properties of a tyre as well as it's performance in service are two sides of the same coin.

When fillers are added to polymer systems, they are known to cause a considerable change in dynamic properties, not only the viscous (loss) modulus and elastic (storage) modulus, but also their ratio, $\tan\delta$, which is related to the portion of the energy dissipated during dynamic deformation [20]. In practice, the energy loss in rubber products during dynamic straining is of great importance, as for example, in vibration mounts and automotive tyres where it affects the service performance of these products with regard to heat generation and fatigue life for the former, and rolling resistance, traction and skid resistance for the latter. In fact, with regard to tyre applications, it is well known that repeated straining of the compound due to rotation and braking can be approximated to a process of constant energy input involving different temperature and frequencies [21-23].

Rolling resistance is related to the movement of the whole tyre corresponding to deformation at a frequency of 10-100Hz and a temperature of 50-80$^{\circ}C$ [20]. In the case of skid- or wet- grip, the stress is generated by resistance from the road surface and movement of the rubber at the surface, or, near the surface of the tyre tread at frequencies around 10^4 to 10^7 Hz at room temperature [22-23]. It is therefore obvious that any change in the dynamic hysteresis of rubber compound at different frequencies and temperatures will alter the performance of the tyre.

Since certain tyre properties involve frequencies, which are too high to be measured, these frequencies are reduced to a measurable level (1Hz) at lower temperatures by applying the time-temperature equivalence principle even though in the case of filled vulcanisates the shift factors for building the elastic modulus master curve are not exactly the same as those for the master curve of viscous modulus, hence of $\tan\delta$ [24]. However, the master curve for each property can be constructed experimentally according to the temperature-frequency principle. Figure 3-4 [25] shows $\tan\delta$ versus temperature for a SBR-1500 rubber compound. As can be seen, several distinct features are present as

temperature rises from transition zone or near glass transition temperature, T_g to ambient and higher temperatures. From the viscoelastic property point of view, an ideal compound which is able to meet the requirements of a high-performance tyre should give a low $\tan\delta$ value at a temperature of 50-80 $°C$ in order to reduce rolling resistance and save energy [20]. The ideal compound should also demonstrate high hysteresis at low temperatures, e.g. -20 to 0 $°C$, in order to obtain high skid resistance and wet grip. However, the factors involved in skid resistance are recognized to be more complex than a single compound property. Dynamic properties of compounds as well as their temperature dependent bahaviour can be influenced by filler parameters. The effect of filler morphology, namely, its fineness related to surface area and particle size and particle size distribution, and its structure related to its aggregate irregularity of shapes and their distribution, has been investigated and reviewed by Medalia [21] . A large change in dynamic properties, both storage and loss modulus, can also be achieved via chemical modification of filler surfaces [26]. The silanized silica nanofiller used in this project is a filler the surfaces of which had been chemically treated by a silane coupling agent and therefore, was significantly different from untreated silica.

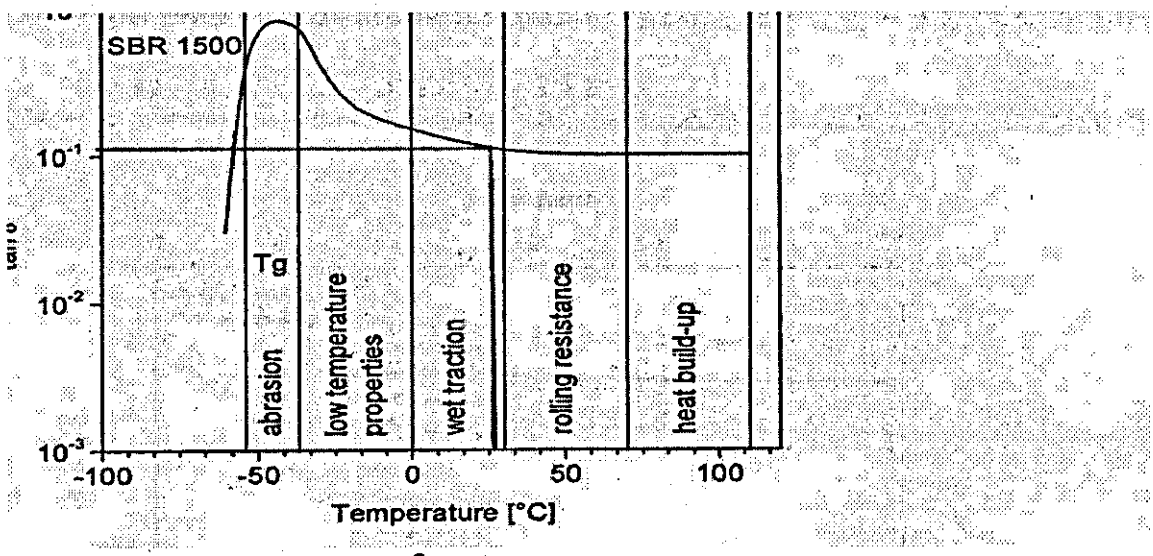

Figure 3-4: Typical tan δ versus temperature for a SBR-1500 rubber compound.

3.4.2 Principal equations

When a shear stress is imposed periodically with a sinusoidal alternation at a frequency of ω on a viscoelastic rubber, the strain will also alternate sinusoidally, but will be out of phase, the strain will lag the stress (Figure 3-5).

$$\gamma = \gamma_0 \sin \omega t \qquad (3.3)$$

where γ is shear strain, γ_0 is maximum amplitude of strain, ω is oscillation frequency and t is time.

$$\sigma = \sigma_0 \sin(\omega t + \delta) \qquad (3.4)$$

where σ is shear stress, σ_0 is maximum shear stress amplitude and δ is the phase angle between stress and strain.

Alternatively, equation 3.4 can be written as:

$$\sigma = \sigma_0 \sin\omega t \cos\delta + \sigma_0 \cos\omega t \sin\delta \qquad (3.5)$$

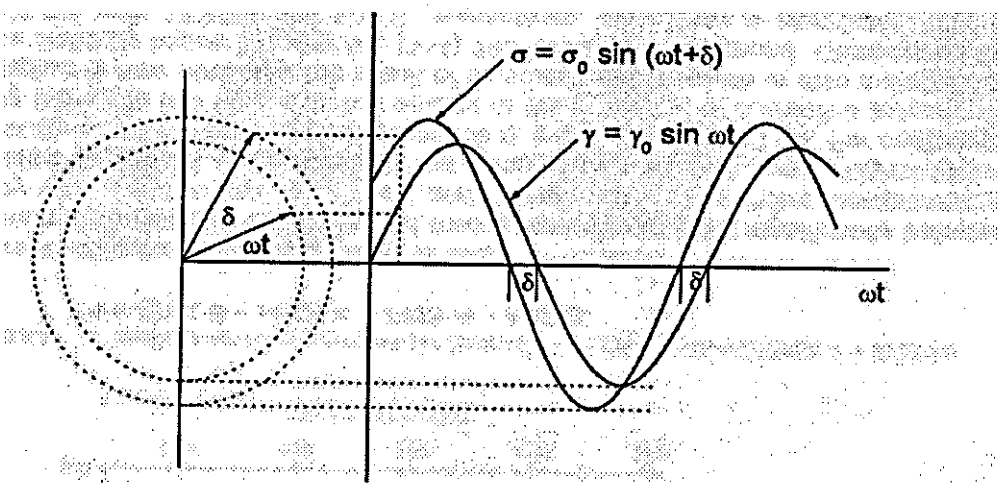

Figure 3-5: Shear stress and strain versus ωt

Accordingly, the dynamic stress-strain behaviour of a rubber can be expressed by a modulus $G^{'}$, which is in phase with strain (elastic or storage modulus), and a modulus $G^{''}$, which is 90° out of phase (viscous or loss modulus). Hence equation 3.5 can be re written as:

$$\sigma = \gamma_0 G^{'} \sin \omega t + \gamma_0 G^{''} \cos \omega t \qquad (3.6)$$

where $G^{'} = (\sigma_0 / \gamma_0)\cos\delta$ (3.7)

$$G^{''} = (\sigma_0 / \gamma_0)\sin\delta \qquad (3.8)$$

Hence

$$\tan\delta = \frac{G^{''}}{G^{'}} \qquad (3.9)$$

Alternatively, the complex, G^{*} can express the global modulus as:

$$G^{*} = (\sigma_0 / \gamma_0) = G^{'} + iG^{''} \qquad (3.10)$$

The energy loss during one cycle of strain, ΔE is given by:

$$\Delta E = \int \sigma d\gamma = \int_0^{2\pi\omega} \frac{\sigma d\gamma}{dt} dt \qquad (3.11)$$

Substitute the relevant values from equations 3.3 and 3.6 in equation 3.11:

$$\Delta E = \omega {\gamma_0}^2 \int_0^{2\pi\omega} (G^{'} \sin \omega t \cos \omega t + G^{''} \cos^2 \omega t) dt = \pi {\gamma_0}^2 G^{''} \qquad (3.12)$$

By substituting equation 3.8 in equation 3.12, ΔE can be written as:

$$\Delta E = \pi \sigma_0 \gamma_0 \sin\delta \approx \pi \sigma_0 \gamma_0 \tan\delta \qquad (3.13)$$

If the stress is plotted against strain for a single deformation cycle, a hysteresis loop is obtained. The area within this closed loop is the amount of mechanical energy converted to heat during this cycle, which is termed hysteresis or H. H is given approximately by the following equation [27].

$$H=(\pi/4)(DSA/100)^2 G' \tan\delta \qquad (3.14)$$

where DSA is the double or peak to peak strain amplitude as a percentage of the undeformed sample dimension.

3.4.3 Measurement of dynamic properties of cured rubbers

Many types of instruments have been developed over the years for measuring the dynamic properties, energy losses or heat generation of rubber products [27]. The most versatile and the costliest are the servo-hydraulic machines. These can be used for testing rubber articles, as well as special test specimens, under arbitrary conditions of strain or (with some limitations) stress. Data can be obtained after only a few cycles, or, if desired, during prolonged cycling. Commercially available electromagnetic test equipments are useful for testing small specimens but lack the power to test most rubber products. Of the other devices, special mention should be made of the rebound tester, which permits rapid precise measurement of the loss tangent at very low equipment cost.

The Goodrich Flexometer is widely used for measuring the heat build-up and flexing fatigue of rubbers in compression [28]. While a static load is applied to maintain a constant static compression, the cycling is carried out at a definite strain amplitude (typically 17.5% DSA). The temperature is monitored and recorded in a platen at the end of a cylindrical specimen. Since the specimen temperature changes considerably during a test run, especially at the centre of the specimen where the temperature rise can be much greater than the

measured temperature rise, this instrument is not generally suitable for basic studies. This instrument is especially valuable for detecting the irreversible changes, which take place during cycling at elevated temperatures. However, the results should be interpreted with caution in view of the difference in heat transfer, ambient temperature, strain cycle, and oxygen diffusion between the flexometer and the actual service conditions of a given rubber article.

3.4.4 Temperature dependence of G', G" and tan δ for unfilled rubbers

Generally, for unfilled rubbers, storage modulus, loss modulus and tan δ are highly affected by temperature changes (Figure 3-4). At sufficiently low temperatures, the tan δ values are very low because the viscosity of the rubber is high and the free volume in the polymer is so small that the movement of the polymer segments and adjustment of their relative positions can hardly take place in the time scale involved in the normal dynamic experiment. This results in low energy dissipation in the rubber, hence low hysteresis. Under this condition, the polymer falls in the glassy state with a very high storage or elastic modulus.

With increasing rubber temperature, the movement of the polymer segments increases. When the temperature reaches a certain level, the free volume of the polymer increases more rapidly than the volume expansion of the molecules, facilitating segmental motion. From this point on, which is known as the glass transition temperature, T_g the viscosity of the polymer decreases very rapidly and the molecular adjustment takes place more easily. Therefore, the storage modulus decreases and the energy dissipation in the polymer will increase with temperature, resulting in high hysteresis. Moreover, at high temperatures, the Brownian motion is very rapid and the viscosity is very low in the polymer. The thermal energy is comparable to the potential energy barriers to segmental motion, hence, the molecular adjustment will be quick enough to be able to follow

the dynamic straining. In this case, long range contour changes of polymer molecules may take place and low resistance to strain. In fact, the material falls in a so-called rubbery region with low modulus and low energy dissipation during dynamic deformation.

From the above discussion, it is concluded that the dynamic properties of rubbers depend on the time scale of the experiment. This is a fair conclusion, since the loss and storage modulus as well as tan δ are dependent on the test frequency [29-30].

3.4.5 Temperature dependence of G', G" and tanδ for filled rubbers

Carbon black

Carbon blacks are the most widely used reinforcing filler in rubber. When added to rubber, they increase mechanical properties such as wear or abrasion resistance, hardness, tear strength and tensile strength. Moreover, the filler absorbs ultraviolet light and consequently prevents the rubber from degradation.

The effect of carbon black on the dynamic properties of rubbers has been studied by several workers [20, 27, 31-34]. The results showed that the addition of carbon black increased the loss and storage modulus with temperature changes in comparison with the unfilled rubber. The values of tanδ at low temperatures, were lower and at high temperatures higher than those measured for the unfilled rubbers.

In rubber compounds with reinforcing fillers, the filler makes a major contribution to heat generation [21]. Carbon black forms aggregates in rubber. At normal loading, aggregates form networks, which extend throughout the rubber compound. The existence of the networks is proved unequivocally by the sharp rise in electrical conductivity as the loading of carbon black is increased beyond a threshold value of about 20-25 phr, depending on the grade of black.

When rubber is subjected to strain cycling of moderate magnitude for example, 1- 20% in compression or approximately three times this in shear, a continuous process of network breakdown and re-formation takes place. During each cycle, the increasing strain breaks down inter-aggregate bonds, starting with the weakest bonds (or those which are least affected by the strain) and progressing to the breakdown of stronger bonds. As the specimen is deformed, the aggregates form new bonds in new positions, which are again broken down and then re-formed in new positions. The breakage and re-formation of inter-aggregate bonds is a hysteresis process which, in typical reinforced rubber compounds, is responsible for the major share of the heat generation. At very low strain amplitudes, deformation of rubber causes very little network breakdown and thus the contribution of the carbon black to hysteresis is negligible. Under these conditions, the filler network makes a major contribution to the stiffness or modulus of the compound.

The effect of carbon black on storage modulus and $\tan\delta$ is essentially added to the effect produced by crosslink density in the rubber, as shown by Payne and co-workers [35]. Similarly, Kraus and Rollmann [36] have found good correlation between the loss compliance of gum and black-filled polybutadiene rubbers containing different amounts of untrapped entanglements, though with some deviation. This was attributed to the adsorption of polymer chain segments onto the carbon black surfaces.

Wang [37] studied effect of different amounts of carbon black on the storage modulus, loss modulus and $\tan\delta$ of some SBR compounds at a test frequency of 10 Hz and DSA 5%. He concluded that simply by reducing the filler loading, it was possible to satisfy the dynamic properties of the rubbers for tyre applications at least from the point of view of hysteresis. In fact, while the gum rubber gave lower hysteresis at relatively high temperatures, its friction coefficient remained higher [38]. Enough filler should be loaded in tyre compounds to meet the

requirements for stiffness, wear resistance and tensile strength. These properties influence not only the service life of the tyre but can also affect driving safety as hysteresis may not be the only factor to govern skid resistance and cornering performance. Wang concluded that the loading effects at different temperature regions, were governed by different mechanisms. It seemed that at temperatures near the $\tan\delta$ peak in the transition zone, the presence of carbon black gave a lower hysteresis for a given energy input. This was understood in terms of a reduction in polymer fraction in the composite as the polymer in situ was responsible for the high portion of energy dissipation, and individual solid filler particles in the polymer matrix did not absorb energy significantly. While this interpretation was reasonable for hysteresis in the transition zone, it was not true at high temperatures where the hysteresis increased by the introduction of the filler. In fact at high temperatures, another mechanism governed the hysteresis behaviour of the rubber. That was break down and re-formation of the filler-filler and/or polymer-filler network, which was responsible for heat dissipation rather than the polymer matrix.

The number and strength of inter aggregate bonds are largely affected by the dispersion of carbon black particles in the rubber. The mixing process can thus have a considerable influence on the heat generation of the compound. During mixing, the pellets are crushed and the fragments are progressively swollen and broken down into agglomerates of micrometre or sub-micrometre dimensions, which form a network with high conductivity and $\tan\delta$. Continued mixing breaks down these fragments and agglomerates, and pulls apart the individual aggregates and separates them from one another. The increased inter-aggregate separation or separation dispersion, gives reduced values for $\tan\delta$ and electrical conductivity [27].

Precipitated silica

The second most important filler for reinforcing rubber is precipitated white silica [39]. Like carbon black, silica is composed of fused aggregates, but the aggregates tend to be larger and more tightly clustered than those of carbon black.

The silica surfaces have a high population of hydroxyl or silanol groups, which affect the rate and state of cure in sulphur-accelerator cure systems. The interaction of hydrocarbon chains with silica is weaker than with carbon black as shown by the lower heat of adsorption of hexane, 32 kJ/mol for the former and 62 kJ/mol for the latter. Conversely, the inter-aggregate interaction of silica is stronger, as shown by the tendency of silica-filled stocks to stiffen up on standing. Probably owing to this strong inter-aggregate interaction, silica gives higher hysteresis than carbon black in rubber compounds adjusted to be comparable in other respects. Because of its surface chemistry, silica is particularly amenable to treatment by coupling agents. With suitable coupling agent for example TESPT, silica gives lower hysteresis than carbon black in otherwise comparable compounds. The reduction in hysteresis due to the addition of coupling agent could be attributed to improved dispersion of the filler or to an increase in the effective crosslink density or both. It is difficult to determine the state of dispersion of silica, especially the separation dispersion, which is important for hysteresis. Wagner [40] studied the effect of coupling agent on the hysteresis of NR compounds.

The formation of crosslinks contributed by coupling agents such as TESPT where polymer chains bond to the surfaces of silica via sulphur in the coupling agent, have the same effect as crosslinks formed by using larger amounts of cross linking agent such as elemental sulphur. Thus, the main effect of the coupling agent on hysteresis was due to the formation of greater number of effective crosslinks between the filler and rubber. Wagner reported results with dicumylperoxide, methacryloxysilane (MAS), and a sulphur-accelerator cure system with a mercaptosilane coupling agent in a SBR rubber compound. With

carbon black, MAS gave little or no coupling, and therefore there was no distinction between different amounts of MAS [40]. Interestingly, at the same crosslink density, silica gave slightly higher hysteresis than carbon black (N285). Although in many systems, which were adjusted to give comparable physical properties, the combination of silica with a coupling agent gave lower hysteresis than carbon black [39]. It is also interesting that higher crosslink density reduced the initial rate of temperature rise, despite increasing the stiffness and storage modulus of the rubber, which in itself should have increased the hysteresis.

3.4.6 Temperature dependence of G' , G" and tan δ for compounds filled with surface pre-treated silica nanofiller

Physical surface modification

When certain chemicals are added to a silica-filled compound, they may be strongly adsorbed on the silica surfaces via dispersive interaction, polar interaction, hydrogen bonding, and acid-basic interaction. Examples include glycols, glycerol, triethanolamine, secondary amines, as well as diphenyl guanidine (DPG) or di-o- tolylguanidine (DOTG) [41].

Generally, the polar or basic groups of these chemicals are directed towards the silica surfaces, and the less polar or alkylene groups, towards the polymer matrix, thereby increasing affinity with the hydrocarbon polymer. Consequently, the tendency of the filler particles to network substantially retards, resulting in better dispersion of the filler particles in the polymer matrix, lower viscosity of the compound.

With respect to dynamic properties, this modification results in a lower dynamic modulus. Tan [42] measured the effect of increasing dosages of diethylene glycol (DEG) on $E'(G')$ of peroxide-cured NR vulcanisates containing 50 phr silica and no oil. The measurements were carried out at low strain amplitudes (less than

2% DSA) and at room temperature. Whereas effect of DEG on the $E^{'}(G^{'})$ of the gum compounds was insignificant, increasing the concentration of DEG lead to a drastic decrease in the $E^{'}(G^{'})$ of the silica-filled vulcanisates. However, as DEG physically bound onto the surfaces of silica, it readily extracted from the vulcanisates in a good solvent. In fact, the $E^{'}(G^{'})$ of the silica-filled rubber was substantially restored after extraction with ethanol. This phenomenon attributed to the restoration of the filler network upon removal of the DEG. In addition, the increase in $E^{'}(G^{'})$ by extraction was so great that it provided some information about the filler network structure. If the high modulus of the extracted vulcanisates was related to the reconstruction of the filler network, either the silica aggregates were very close to each other, or, there was little or no rubber between the aggregates, since in a crosslinked polymer the aggregates are only able to move very short distances to form filler networks following extraction. Another possible interpretation was associated with very low polymer-filler interaction as DEG served as a lubricant like material at the polymer-filler interface, thereby reducing the modulus. However, if this was the case, it was not the main cause of the low $E^{'}(G^{'})$ because at this very low strain amplitude, significant slippage of the polymer molecules over the filler surfaces could not have occurred. Nevertheless, surface modification by the physical adsorption of the chemicals was not preferred, as the solvent could have extracted the chemicals, or, evaporated at high temperatures. In addition, such an approach rarely applied in highly reinforced compounds because of the relatively poor polymer-filler interaction.

Chemical surface modification

With chemical treatment, the filler surfaces can be modified in such a way that the filler is tailored to new applications such as for use in rubber compounds. The filler surfaces can be chemically treated to perform two functions: chemical groups can be grafted on the filler surfaces to change the surface characteristics

of the filler, and at the same time, the chemical groups can react with polymer chains to form strong stable covalent bonds. These chemicals are frequently called coupling agent or bifunctional organosilane as they provide chemical linkages between the filler surfaces and polymer molecules via the coupling agent. There are also monofunctional coupling agents that do not react chemically with polymer chains but modify the filler surfaces.

Surface chemical modification to change the surface chemistry of silicas has been investigated [43], and chemically treated silica fillers have been found to have many applications in different fields. According to the thermodynamic analysis of filler networking, one would expect that formation of linkage or crosslinks between polymer chains and filler surfaces would result in significant changes in the nature and intensity of the surface energy of the filler, providing a surface similar to that of the polymer, thus eliminating the driving force behind the filler networking. Although more work will be needed to understand this phenomenon, surface modification of silica has demonstrated the importance of the effect of surface energy on the flocculation of filler particles in a polymer.

By esterification of fumed silica (Aerosil 130- surface area of $130 m^2/g$) with methanol and hexadecanol, Donnet et al. [44-45] have shown a drastic reduction in the filler surface energy, both the dispersive and specific components. In the case of hexadecanol modified silica, the polarity of the filler surfaces was eliminated, producing very hydrophobic filler. The effect of surface modification on the filler networking was investigated by measuring the rheological bahaviour of suspensions, which gave some information about the formation of a particulate network or a flocculated structure [46-47].

Wang and co-workers [48] found that grafting monofunctional silanes for example, octadecyltrimethoxy or hexadecyltrimethoxy, with a long alkyl chain on silica surfaces, produced non–polar and low-energy filler that was more compatible and had more affinity with hydrocarbon polymer chains. When such

modified silica was incorporated in NR, a compound with low-filler networking was produced and characterized by a substantially lower Payne effect as shown by Wolff [49].

Although modification of silica surfaces by monofunctional chemicals may greatly improve the micro-dispersion of the filler particles and provide low hysteresis materials, the absence of polymer-filler interaction would result in a lower static modulus and consequently poorer mechanical properties particularly abrasion or wear resistance. The bifunctional chemicals referred to here are a group of chemicals that are able to form molecular bridges between the filler surfaces and polymer matrix. These chemicals are generally referred to as coupling agent and they enhance the degree of polymer-filler interaction, hence, impart improved mechanical properties to the filled materials.

The chemicals belonging to this group are numerous and include titanate-based coupling agents [50], zirconate-based coupling agents [51] and other metal complex coupling agents [50, 52], which have found application in inorganic filler reinforced polymer composites. The most important coupling agents for inorganic filler modification for example silica, is the group of bifunctional organosilanes with the general formula as:

$$X_{3-m} - R_m - Si - (CH_2)_n - Y$$

where X is a hydrolysable group such as halogen, alkoxyl or acetoxyl groups, and Y is a functional group, which itself is able to react chemically with the polymer chain either directly or through other chemicals. It may also be a chemical group, which is able to develop a strong physical interaction with polymer chains. For the Y groups, important silane coupling agents include amino, epoxy, acrylate, vinyl, and sulphur-containing groups such as mercapto, thiocyanate, and polysulfide [53-57].

The bifunctional silane coupling agents most often contain three (m=0) X groups and a functional group Y is generally in the γ position (n=3). Practically, when silica is incorporated in a hydrocarbon rubber, the most popular and effective coupling agents are γ-mercaptopropyltrimethoxy silane and bis(3-triethoxysilylpropyl)tetrasulphane (TESPT) known as Si 69 coupling agent.
In fact, as far as the commercialized coupling agents are concerned, TESPT is the most widely used silane, enabling silica to be used in tyre tread compounds. The hysteresis at higher temperatures for rubbers with silica and coupling agent is significantly lower than those with carbon black [58].

At low temperatures, rubbers filled silica and coupling agent showed higher hysteresis. These findings showed the eligibility of silica and coupling agent (TESPT) for better dynamic properties compared with carbon black in rubber compounds. Hashim and co-workers [59] studied the reinforcing effects of silica on the dynamic properties of SBR with and without TESPT. They compared the $\tan\delta$ and G' of the compound with silica and no TESPT with those of the compound with silica and TESPT. They found that the formation of crosslinks between rubber and filler via TESPT significantly decreased the damping and heat build-up properties of the rubber vulcanisates.

Summary

To conclude, for a given polymer filler system, filler networking is the dominant factor in the determination of the hysteresis of the filled vulcanisates. Its roles are:

- To the extent that the filler network cannot be broken down under the applied deformation, the formation of filler network substantially increases the effective volume fraction of the filler due to the rubber trapped in the agglomerates.

- The breakdown and reformation of the filler network would cause additional energy dissipation, hence higher hysteresis during cyclic strain in the rubbery state.

- Alternatively, in the transition zone at low temperatures, where the main portion of the composite for energy dissipation is polymer matrix and the filler network may not be easily broken down, the hysteresis may be significantly attenuated by the filler networking due to the reduction of the effective volume of the polymer.

- Also in the transition zone, once the filler network can be broken down and reformed under a cyclic deformation, the hysteresis can be substantially augmented through release of polymer to participate in energy dissipation and change in the network structure.

- Accordingly, besides the hydrodynamic effect, the necessary conditions for high hysteresis of filled rubber, among others, are presence of filler network and breakdown and reformation of the network under dynamic strain.

References

1) British standard institution, Physical testing of rubber, Introduction BS 903:0(1990).

2) British standard institution ,Physical testing of rubber, General BS 903(2003).

3) British standard institution,Physical testing of rubber, Methods for the determination of dimensions of test pieces and products for test purposes BS 903:A38(1991).

4) British standard institution ,Physical testing of rubber BS903:A64 (1995).

5) British standard institution ,Physical testing of rubber BS903:A60.1 (1996).

6) British standard institution ,Physical testing of rubber BS903:A60.1(2000).

7) British standard institution,Physical testing of rubber, Method for determination of hardness BS 903:A26(1995).

8) Brown R. *Physical testing of rubber*, Springer edition, Hardness(2006).

9) British standard institution ,Method of testing vulcanized rubber BS 903:A9(1988).

10) Clamroth R,Kempermann Th, *Polym. Test.* **5**:6(1985).

11) Warhurst D M, Slade J C, Ochiltree B C,*Polym. Test.* **6**:(**6**)463 (1986).

12) Brezik R, *Int. Polym. Sci.Tech.* **9**:4(1982).

13) British standard institution,Physical testing of rubber, Method for determination of tear strength BS 903:A3(1995).

14) British standard institution,Determination of tensile stress-strain properties BS ISO 37(2005).

15) ASTM D412, Tension (2002).

16) British standard institution,Physical testing of rubber, Method using the Mooney viscometerBS 903:A58(1990).

17) British standard institution,Physical testing of rubber,Methods using the Mooney viscometer BS 903:A58.1(2001).

18) Wolff S, Wang M J, *Rubber Chem. Technol.* **66**:163(1993).

19) Dannenberg E M, *Rubber Chem. Technol.* **59**:512(1986).

20) Wang M J., *Rubber Chem. Technol.* **71**:521(1998).

21) Medalia A I, *Rubber Chem. Technol.* **51**:437(1978).

22) Buigin, Hubbard D G,Walters M H., *Proc. Rubber Technol. Conf.,* London, 173(1962).

23) Saito Y, *Kautsch Gummi Kunstst* **39**:30(1986).

24) Duperray B, Leblanc J L, K*autsch. Gummi. Kunstst* **35**:298(1982).

25) Nordsiek K H., *Kautsch .Gummi Kunstst* **38**:178(1985).

26) Wolff S , Wang M J, Tan E H., *Kautsch Gummi Kunstst* **47**:102(1994).

27) Medalia A I, *Rubber Chem. Technol.* **64**:481(1991).

28) ASTM test D623, Method A.

29) Williams M L., *J. Phy. Chem.***59**:95(1955).

30) Williams M L., Landel R F, Ferry J P , *Am J. Chem. Soc.* 77:3701(1955).

31) Roelig H, *Rubber Chem. Technol.* **12**:384(1939).

32) Naunton W S J, Waring J R S, *Trans. Inst. Rubber Ind.* **14**:340(1939).

33) Gehman S D, Woodford D E, Embaugh S, *Ind Eng. Chem.* **33**:1032(1941).

34) Stambaugh RB, *Ind. Eng. Chem.***34**:1358(1942).

35) Payne A R, Whittaker R E.,Smith J F, *J. Appl. Pol.Sci.***16**:1191(1972).

36) Kraus G, Rollmann K, *J. Pol. Sci., poly. Symp.* **N.48**:87(1974).

37) Wang M J, Presented at a workshop *"Praxis und theorie der verstarkung von elastomeren"*, Hanover, Germany (June 27-28,1996).

38) Grosch K G, *Rubber Chem., Technol.* **69**:459(1996).

39) Wagner M P, *Rubber Chem. Technol.* **49**:703(1976).

40) Wagner M P, *Rubber Chem. Technol.* **47**:697(1974).

41) Hofmann W."*Rubber technology handbook*", Hanser publication, Munich Ch. 4(1989).

42) Tan E H., *Ph.D thesis*, Universite de Haute Alsace, Mulhouse,France(1992).

43) Iler P K, "*The chemistry of silica*", Interscience, New york (1979).

44) Vidal A, Papirer E, Wang M J, Donnet J B, *Chromatographia* **23**:121(1987).

45) Papirer E., Vidal A, Wang M J, Donnet J B, *Chromatographia* **23**:279(1987).

46) Iler R K, *J.Colloid Interface Sci.***37**:354(1971).

47) Ribio, Kitchener A J , *J. Colloid Interface Sci.* **57**:132(1976).

48) Wang M J, Wolff S, *Rubber Chem. Technol.* **65**:715(1992).

49) Wolff S, Wang M J,Tan E H., *Kuutsch. Gummi Kunstat* **47**:102(1994).

50) Monte J, Sugerman G, Presented at a meeting of rubber division, ACS, Chicago, Illinoise, oct.5(1982), *Abstract in Rubber Chem.. Technol.***56**:493(1983).

51) Monte J, "ken-react preference manual Titanate, Zirconate and Aluminate coupling agent", second revised edition, Kenritch Petrochemicals, Inc(1993).

52) "Metal-Acid estate-Chelates", Huls AG (1992).

53) Plueddemann E P , "Silane coupling agents" Plenum press, New york (1982).

54) Mittal K L, "Silanes and other coupling agents" vs. P, Utrecht (1992).

55) Donald G W., *Rubber Age* **102**:(**4**)66(1970).

56) Grillo T A., *Rubber Age* **103**:(**8**)37(1971).

57) Ranney M W., Pageno C A.,Ziemiansky L P, *Rubber World* **163**:54(1970).

58) Wang M J, Mahmud K, Murphy L,Patterson W J, P.No.24, Presented at a meeting of rubber division, ACS, Anaheim, California, May6-9(1997), *Abstract in Rubber Chem. Technol.* **70**:687(1997).

59) Hashim A S,Azahari B ., Ikeda Y, Kohjiya S, *Rubber Chem. Technol.* **71**:289(1998).

CHAPTER 4

Modulated temperature differential scanning calorimetry (MTDSC) technique for measuring the mass fraction and composition of interphases in rubber blends

4.1 Introduction

In the last three decades, the precision and resolution of calorimetric methods have increased significantly by the application of improved non-adiabatic and/or dynamical methods[1-3], which are called temperature-modulated calorimetry (TMC), differential scanning calorimetry (DSC) [4,5], heat-pulse (or relaxation-time) calorimetry [6,7] , continuous heating calorimetry [8,9] and the revived 3ω method [10], which was introduced by Corbino in 1910 [11]. The recent application of temperature modulation principles to differential scanning calorimetry (DSC), resulted in the construction of what is known as temperature-modulated differential scanning calorimeter (TMDSC) [12]. This had a profound impact on the technical development of both DSC and TMC equipment, on the underlying theoretical background of these dynamic instruments as well as on the physics and chemistry of the measured values, e.g. dynamic heat capacity and related kinetic mechanisms.

Modulation calorimetry, better known to physicists as AC calorimetry, was introduced in 1968 by Sullivan and Seidel [1, 13, 14] and Handler et al. [2], simultaneously. Today, it is a well-established, reliable and widely used classical calorimetric method particularly suited for the investigation of small samples and good resolution at all temperatures. The method is theoretically well understood[1,5,15-22]. It has been set up in widely different types of experimental arrangements and used at very low and very high temperatures (up to 3600 K) as well, including linear temperature scanning, measurement of

frequency-dependent heat capacities [5, 10, 16, 21-30] and time dependence of specific heat [10, 31-34]. However, in most experiments, the information from the phase of the temperature signal was not utilized. The frequency dependence of the heat capacity was scarcely studied over more than one and a half decades and the frequency range remained usually restricted to the (1-10)Hz range. On the other hand, differential scanning calorimetry was widely used in physics, chemistry and material science in the temperature range from 100 to 2000 K. It is accepted as a useful tool for the investigation of chemical reactions, phase transition, a source of thermodynamic data and for establishing phase diagrams. Since they are commercially available, these instruments are widely used in industrial research and production control. In recent years, the theory of DSC and its applications progressed considerably [35-39], and some shortcomings, which were identified with the technique at the early stages, were corrected for [36-39].

The combination of DSC and TMC techniques, however, caused some confusion and misunderstanding in recent years with respect to the interpretation of data produced with MTDSC. Although data from TMC and DSC by themselves are understood rather well in most details of heat flow and internal thermal relaxation times, it turned out that the simultaneous effects of temperature scanning and periodic heating /cooling were not described sufficiently by the present models. The essential implication of MTDSC originates from the fact that, besides the temperature-dependent heat capacity, the frequency dependence of heat capacity becomes involved. Hence, any type of relaxation phenomena, being intrinsic to the sample studied and/or characteristics of the calorimetric cell used, i.e. heat resistance, influences the experimental results.

Strictly speaking, MTDSC should be called spectrometry. It enables the measurement of the dynamic heat capacity C(T, ω) that is as a function of temperature and frequency. This feature, at a first glance, appears surprising, since heat capacity is in general considered to be a statistical thermodynamic quantity. More drastically, it can be expressed as follows: thermodynamically

non-equilibrium properties can be studied with temperature scanning methods at various scanning rates. This situation necessitates recalling the concept of dynamic heat capacity and considering how the heat capacity depends on the time scale of the experiment. Similar to the concept of treating real and imaginary parts of physical parameters, e.g. impedance, susceptibility, dielectric constant, sound velocity or optical absorption, the specific heat displays real and imaginary contributions. Indeed, the mathematical fundamentals of dynamic / complex heat capacity have already been described in the literature [40, 41]. It is referred, in analogy to the mechanical modulus (stress / strain ratio), to the general response theory in order to extend the definition of the static specific heat to a dynamic one. There is, however, an essential difference between the imaginary part of heat capacity and the imaginary part of other physical properties. The latter are normally related to dissipation processes. That is generally not true for heat capacity because heat is not converted to other forms of energy. Whenever, an imaginary term exists, the entropy increases. However, for the heat capacity phenomena, the phonon system acts usually as a thermodynamic heat reservoir, and during storage and loss of heat by samples, the intrinsic relaxation phenomena remains in most cases reversible when averaged over a sufficiently long time, i.e. chemical reaction are excluded. The reader may find more details on that tricky problem in the contributions by Donth et al. [46], Jeong [47], Schawe [48] and Wunderlich et al. [45].

4.2 Basic equations [49]

Heat capacity can be defined as the amount of energy required to increase the temperature of a material by 1 degree Kelvin or Celsius. Thus:

$$Cp = Q / \Delta T \qquad (4.1)$$

where Cp is heat capacity, ΔT, is change in temperature and Q is amount of heat required to achieve ΔT.

Often, it is considered that this is the heat stored in the molecular motion available to the material that is the vibrational and translational motions, and is stored reversibly. Thus, the heat given out by the sample when it is cooled down by $1°C$ is the same as that required to heat it up by the same amount. This type of heat capacity is often called vibrational heat capacity. When temperature changes, the rate of heat flow required to achieve it, is given by

$$dQ/dt = CpdT/dt \qquad (4.2)$$

where t is time.

This is intuitively obvious. Clearly, if one wishes to increase the temperature of the material twice as fast, twice the amount of energy per unit time must be supplied. If the sample has twice the heat capacity, this also doubles the amount of heat required per unit time for a given rate of temperature rise.

Considering a linear temperature program, such as is usually employed in scanning calorimetry:

$$T = To + \beta t \qquad (4.3)$$

where T is temperature, To is starting temperature and β is heating rate, dT/dt. This leads to

$$dQ/dt = \beta Cp \qquad (4.4)$$

Or

$$Cp = (dQ/dt)/\beta \qquad (4.5)$$

This provides one way of measuring heat capacity in a linear rising temperature experiment. One simply divides the heat flow by the heating rate.

If the temperature program is replaced by one comprising of a linear temperature ramp modulated by a sine wave, this can be expressed as

$$T = To + \beta t + B\sin\omega t \qquad (4.6)$$

Where B is the amplitude of modulation, ω the angular frequency of modulation.

The derivative with respect to time of this is

$$dT/dt = \beta + \omega B\cos\omega t \qquad (4.7)$$

Thus, it follows:

$$dQ/dt = Cp(\beta + \omega B\cos\omega t) \qquad (4.8)$$

For the special case where β is zero, this yields:

$$dQ/dT = Cp\,\omega B\cos\omega t \qquad (4.9)$$

For the simplest possible case, from equation (4.2), the resultant heat flow must also be a cosine wave. Thus,

$$Ahf\cos\omega t = Cp\,\omega B\cos\omega t \qquad (4.10)$$

where Ahf is the amplitude of heat flow modulation.

It follows that ωB is the amplitude of the modulation in the heating rate.

Thus,

$$Cp = Ahf / Ahr \qquad (4.11)$$

where Ahr is the amplitude of modulation in the heating rate.

This provides a second method for measuring the heat capacity by looking at the amplitude of modulation. The same relationship applies even if there is an underlying heating ramp.

In essence, MTDSC is based on simultaneously measuring the heat capacity of the sample using both methods, the response to the linear ramp and the response to the modulation, and comparing them. When the sample is inert and there are no significant temperature gradients between the sample temperature sensor and the centre of the sample, both methods should give the same value. The interest lies in the fact that during transitions, these two methods give different values [49].

References

1) Sullivan P F,Seidel G, *Phys. Rev.* **173**:679(1968).

2) Handler P , Mapother D E, Rayl M,*Phys. Rev. Lett.***19**:356(1967).

3) Kraftmakher Y A, Prikl Zh., *Mekh. and Tekh. Fiz.* **5**:176(1962).

4) Hemminger W,Höhne G,*Grundlagen der Kalorimetrie.*,Verlag Chemie, Weinheim (1979).

5) Kraftmakher Y A., *Modulation Calorimetry.* In: K.D. Maglic, A. Cezairliyan and V.E. Peletsky, Editors, Compendium of Thermophysical Property Measurement Methods 1, Plenum Press, New York 591,1(1984).

6) Bachmann R, DiSalvo F J, Geballe T H , Greene R L , Howard R E, King C N., Kirsh H C, Lee K N., Schwall R E., Thomas H U, Zubeck R B., *Rev. Sci. Instrum.***43**:205 (1972).

7) Rahm U, Gmelin E, *J. Therm. Anal.* **38**:335(1992).

8)Junod A., Bonjour E., Calemzuczuk R., Henry J Y, Muller J , Triscone G,Vallier J C., *Physica C* **211**:304(1993).

9) Schnelle W, Gmelin E, *Thermochim. Acta.* **269/270**:27(1995).

10) Jeong Y H., Bae D J, Kwon T W ,Moon I K , *J. Appl. Phys.* **70**:6166(1991).

11) Corbino O M., *Phys.* **Z.12**:292(1911).

12)Reading M.,Elliott D,Hill.V L,*J.Therm.Anal 40*:949(1993).

13) Sullivan P F,Seidel G, *Phys. Lett.* **25A**:229(1967).

14) Sullivan P F, Seidel G, Ann. *Acad. Sci. Fennicae* **210**:58(1966).

15) Velichkov I V, *Cryogenics* **32**:285(1992).

16) Kraftmakher Ya A., Tonaevskii. V L, *Phys. Stat. Sol.* **(a) 9**:573(1972).

17) Manuel P, Niedoba H,Veyssié J J, *Rev. Physique Appliquée* **7**:8(1972).

18) Eichler A,Gey W, *Rev. Sci. Instrum.* **50**:1445(1979).

19) Graebner J E., *Rev. Sci. Instrum.* **60**:1123(1989).

20) Hatta I., Yao H., Kato R, Maesono A, *Jpn. J. Appl. Phys.* 29:2851(1990).

21) Hatta I, Ikushima. A, *J. Phys. Chem. Solids* **34**:57(1973).

22) Gast T H, Jakobs H, *Thermochim. Acta* **72**:71(1984).

23) Birge N O, Nagel S R, *Rev. Sci. Instrum.* **58**:1964(1987).

24) Birge N O, *Phys. Rev.* B **34**:1631 (1986).

25) Dixon P K, *Phys. Rev.* **B 42**:8179(1990).

26) Hatta I ,Ikushima. A , *Phys. Lett.* **37A**:207(1971).

27) Yao H, Nagano H, Kawase Y, Ema. K , *Biochimica et Biophysica Acta* **1212:** 73(1974).

28) Phelps R B ,Brimingham J T , Richards P L, *J. Low Temp. Phys.* **92**:107(1993).

29) Saruyama.Y, *J. Therm. Anal.* **38:**1827(1992).

30) Schowalter L J, Salamon M B, Tsuei C C, CravenR A, *Solid State Commun.* **24:** 525(1977).

31) Tietje H., Schickfus M V., Gmelin E, *Z. Phys. B - Condensed Matter.* 64 (1986).

32) Zimmermann J.*Cryogenics* **24**:27(1984).

33)Loponen M T, Dynes R C, Narayanamurti V,Garno J, *Phys. Rev.* **B 25**:1161(1982).

34) Meissner M, Spitzmann K, *Phys. Rev. Lett.* **46**:265 (1981).

35) Wunderlich B , *Thermal Analysis* , Academic Press, San Diego (1990).

36) Höhne G W H., Hemminger W, Flammersheim H J, *Differential Scanning Calorimetry.*, Springer, Berlin (1996).

37) Höhne G W H., Schawe J E K , *Thermochim. Acta* **229**:27(1993).

38) Gmelin E, Sarge St.M, *J. Appl. Chem.* **67**:8179(1995).

39) Richardson M J, *The application of differential scanning calorimetry to the measurement of specific heat.,* Maglic K.D., Cezairliyan A, Peletsky V.E., Editors, Compendium of Thermophysical Property Measurement Methods Vol. 2, Plenum Press, New York **518**:18(1984) .

40) Ferell R A., Bhattacharjee J K, *Phys. Rev.* **A 31**:1788(1985).

41) Herzfeld K F, Rice F O , *Phys Rev.* **31**:691(1928).

42) Schawe J, *Thermochim Acta* **261**:1(1995).

43) Schawe J, *Thermochim. Acta* **271**:127(1996).

44) Wunderlich B, *Thermochim. Acta* **304/305**:125 (1997).

45) Wunderlich B, Yin Y, Boller A, *Thermochim. Acta* **238**:277 (1994).

46) Donth H. et al., *Thermochim. Acta* **304/305**:239 (1997).

47) Jeong Y H, *Thermochim. Acta* **304/305**:67(1997).

48) Schawe J, *Thermochim. Acta* **304/305**:111 (1997).

49) Reading M., Hourston D J,"*Modulated-temperature differential scanning calorimetry",* Springer edition, 2 (2006).

EXPERIMENTAL

CHAPTER 5

Materials and methods for measuring curing properties, crosslink density, bound rubber, glass transition temperature, mechanical and dynamic properties of rubber vulcanisates

5.1 Materials

5.1.1 Rubbers and filler

The raw rubbers used were standard Malaysian natural rubber grade L (SMRL) containing 98 wt % cis 1,4 polyisoprene, polybutadiene rubber (Buna CB 24, Bayer; not oil-extended) containing 96 wt % 1,4 cis, styrene-butadiene copolymer (23.5 wt % styrene; Intol 1712, Polimeri Europa) and IR (synthetic polyIsoprene minimum 96 wt % cis-1-4content; Kraton IR-307) (Table 5-1).

The reinforcing filler was Coupsil 8113 (Evonik Industries AG, Germany). Coupsil 8113 is precipitated amorphous white silica-type Ultrasil VN3 surfaces of which had been pre-treated with TESPT. It has 11.3 % by weight TESPT, 2.5 % by weight sulphur (included in TESPT), 175 m^2/g surface area (measured by N_2 adsorption), and a 20-54 nm particle size.

Table 5-1: Raw rubber specification

Rubber	Specific gravity	Mooney viscosity, ML(1+4) at 100 °C	T_g (°C)
NR (SMRL)	0.92	96.71	-64
SBR-1712	0.94	51.30	-50
High cis-BR	0.91	49.00	-107
IR	0.91	69.00	-61

The glass transition temperatures of the raw rubbers were measured by the MTDSC technique.

The specific gravity was determined using 2 g of each pure rubber and by measuring the liquid displacement in a calibrated cylindrical column of water (Table 5-1).

5.1.2 Curing chemicals, antidegradants and processing oil

In addition to the raw rubbers and filler, the other ingredients were *N*-t-butyl-2-benzothiazole sulfenamide (Santocure TBBS, Flexsys, USA; a safe-processing delayed action accelerator), zinc oxide (ZnO, Harcros Durham Chemicals, UK; activator), stearic acid (Anchor Chemical ltd, UK; activator), elemental sulphur (Solvay Barium Strontium, Hannover, Germany; curing agent), N-(1,3-dimethylbutyl)-N′-phenyl-*p*-phenylenediamine (Santoflex 13, Brussels, Germany; antidegradant) and heavy paraffinic distillate solvent extract aromatic processing oil (Enerflex 74, Milton Keynes, UK). The cure system consisted of TBBS, ZnO, stearic acid, and elemental sulphur, which were added to optimize the chemical bonding or crosslinks between the rubber and filler.

Accelerators are ingredients used to control the onset and rate of cure and the crosslink density in rubber. Activators are chemicals used to enhance the effectiveness of the accelerators during the curing reaction in rubber. Elemental sulphur is a curing agent used to crosslink rubbers with unsaturation sites or chemically active double bonds such as NR. Processing oils such as Enerflex 74 are added to modify viscosity.

5.2 Measuring cure properties of the rubber compounds

An oscillating disc rheometer curemeter (ODR) (Monsanto, Swindon, UK) was used to measure the cure properties of the rubber compounds. These included scorch time, t_{s1} or t_{s2}, which is the time for the onset of cure, and the optimum cure time, t_{90} or t_{95}, which is the time for the completion of cure. These properties were measured from cure traces generated at 140°C by the ODR at an angular displacement of $\pm$ 3° and a test frequency of 1.7 Hz [1]. The cure rate index,

which is a measure of the rate of cure in the rubber, was calculated using one of the following equations [2]:

$$CRI = 100/(t_{95} - t_{s1}) \text{ or } CRI = 100/(t_{90} - t_{s1}) \quad (5.1)$$

The rheometer tests ran for up to 2 h. Δtorque, which is the difference between the maximum and minimum torque values on the cure traces of the rubbers tested and is an indication of crosslink density changes in the rubber [3] was subsequently plotted against the loading of TBBS, ZnO, stearic acid, and elemental sulphur.

5.3 Compound curing procedure

An electrically heated hydraulic press was used to cure the rubber compounds under a nominal atmosphere pressure of 110 (40000 kg. on an 20 cm diameter disc). The curing temperature was 140°C and the curing times for the rubber compounds were taken from the ODR traces. About 150 gr. of the uncured rubber compound was placed in the centre of a square-shaped mould, 2.5 mm thick, 22.5 cm long and 22.5 cm wide, to enable it to flow in all directions when pressure was applied. To prevent the rubber from sticking to the mold surfaces, the uncured rubber compound was placed between two thin sheets of polymer. After the rubber was cured, the mold was removed from the press and the cured rubber was taken out of the mold. The protecting polymer sheets were removed and the rubber was allowed to cool down at ambient temperature. Since the fresh rubber surfaces were sticky, talc powder was used to minimize its stickiness. Finally, the cured rubber was placed in some clean plastic bags and stored for at least 48 h at ambient temperature. The hardness, tensile properties, tear strength, Young's modulus, tensile modulus, abrasion resistance, heat buildup and dynamic properties were subsequently measured.

For measuring the hardness, abrasion resistance, and bound rubber content, cylindrical samples 9 mm in height, 16 mm in diameter, or, 13 mm in high and 29 mm in diameter were cured.

5.4 Crosslink density and Bound rubber measurement

Bound rubber is a measure of the percentage of polymer bounded by filler. The solvent used for bound-rubber and crosslink density determination was toluene (Merck-Germany). For the determination, cylindrical samples, 9 mm in high and 16 mm in diameter, were placed individually in 60 ml of the solvent in labeled bottles and allowed to swell. The weight of the samples was measured every day until they reached equilibrium. The solvent was subsequently removed and the samples were dried in air for 9 h. The samples were then dried in a vacuum oven at 85 $°C$ for 24 hours, and allowed to stand for an extra 24 hours at ambient temperature (23°C) before they were re-weighed. The bound rubber and crosslink density were calculated using the following equations [4]:

$$R_b = \frac{W_f - W[m_f/(m_f+m_p)}{W[m_p/(m_p+m_f)]} X100 \qquad (5.2)$$

where R_b is the bound rubber content, W_f is the final weight of the sample after reaching equilibrium in the solvent (g), W is the initial weight of the sample before swelling, m_f is the amount of filler in the sample (g), and m_p is the amount of polymer in the sample.

For measuring the crosslink density of the rubbers, the Flory-Rehner equation was used [5]:

$$\rho_c = -\frac{1}{2V_s}\frac{Ln(1-\upsilon_r^0)+\upsilon_r^0+x(\upsilon_r^0)^2}{(\upsilon_r^0)^{1/3}-\upsilon_r^0/2} \qquad (5.3)$$

where ρ_c is the crosslink density (mol/m^3), V_s= is the molar volume of toluene ($1.069 \times 10^{-4}\ m^3$/mol at $25°C$), υ_r^0 is the fraction of rubber (polymer) in the swollen gel, χ is the interaction parameter.

5.5 Measurement of the rubber viscosity

The viscosity of the rubber compounds was measured at $100°C$ in a single-speed rotational Mooney viscometer (Wallace Instruments, Surry, UK) according to British Standard 1673 [6].

5.6 Measurement of hardness

For measurement the hardness of the rubbers, cylindrical samples 13 mm in height and 29 mm in diameter were used. The samples were placed in a Shore A durometer hardness tester (The Shore Instrument & MFG, Co., New York), and the hardness of the rubber was measured at ambient temperature (~ 23 °C) over a 20 s interval, after which a reading was taken. This was repeated at four different positions on the sample, and the median of the four reading was calculated [7].

5.7 Measurement of abrasion resistance

For determining the abrasion resistance of the rubbers, molded cylindrical test pieces 8 mm thick and 16 mm in diameter were cured. The tests were performed at 23°C in accordance with BS 903:Part A9:1995 with method A.1 (Zwick abrasion tester 6102, Croydon, UK and abrasion standard rubber S1) [8]. The abrasion resistance of the blends was measured by applying a similar procedure and using standard rubber S2, a typical tyre compound formulation [8]. The abrasion resistance was expressed as an abrasion resistance index (ARI). An index value of greater that 100% indicated that the test compound was more resistance to abrasion than the standard rubber under the conditions of the test.

For each rubber, three samples were tested to calculate relative volume loss.

5.8 Measurement of tear strength

Rectangular strips, 114mm long and 30 mm wide, were cut from the cured sheets of rubber and a sharp crack, approximately 40 mm in length, was introduced into the strips half way along the width and parallel to the length of the strip, to form the trouser test pieces for the tear experiments (Scheme 5-1). The tear tests were performed at an angle of 180°, ambient temperature, and a constant crosshead speed of 50 mm/min [9] in a Lloyd mechanical testing machine (Hampshire, UK). The tears produced in the rubber after the test pieces were fractured were up to 80 mm in length. In each experiment, the tearing force was recorded as a function of crosshead separation to produce traces from which an average force was measured. The peaks on the trace were used for calculating the average tearing force for the rubber. In some cases involving the filled rubbers, the test produced only one peak, from which a tearing force was calculated. For each rubber, five test pieces were used. After these measurements were completed and following the procedure described previously [10], the force values were placed in equation 5.4 to calculate tearing energies for the rubbers.

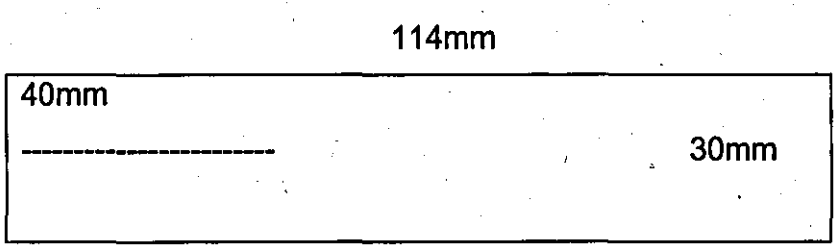

Scheme 5-1: Dimension of tear test sample

$$T=2F/t \qquad (5.4)$$

where T is the tearing energy (kJ/m^2), F is the tearing force, and t is the thickness of the test piece (mm)

5.9 Measurement of tensile properties

The tensile stress, elongation at break, and stored energy density at break were determined in uniaxial tension in a Lloyd mechanical testing machine with dumb bell test pieces, 3.6 mm wide, gauge, with a central neck 25 mm long, and an overall length of 75 mm. The samples were die-stamped from slabs of cured rubber. The tests were performed at ambient temperature (approximately 23°C) and at a crosshead speed of 50 mm/min [11]. Lloyd DAPMAT computer software was used to store and process the data. For each rubber, three test pieces were used. The thickness of the samples were 2.3 -2.7 mm. The strain on the sample was calculated as (final length-original length)/original length.

5.10 Measurement of tensile modulus at different strain amplitudes

The tensile modulus of the vulcanized rubbers was measured at 50%, 100%, 200%, 300%, 400%, 500% strain amplitudes in uniaxial tension in a Hounsfield mechanical testing machine, using dumb-bell test pieces. The tests were performed at 23°C at a crosshead speed of 50 mm/min [11]. Hounsfield DAPMAT computer software was used for storing and processing the data.
To calculate tensile modulus, the following equation was used:

Modulus (N/mm^2) = Slope of tensile stress (N/mm^2)-strain curve (5.5)

where tensile stress = Force (N)/(width X thickness of sample)

5.11 Measurement of Hysteresis in the rubber vulcanisates

To measure the energy losses in the rubber, a single stress versus strain loop was produced for each rubber using dumb-bell test pieces in the mechanical testing and by stretching the rubber sample to 100% strain amplitude. The area between extension and retraction curves was used to calculate the energy losses in the sample. The tests were performed at ambient temperature at a crosshead speed of 50 mm/min [11]. RCONTROL computer software was used to store and process the data.

5.12 Measurement of glass transition temperature, mass fraction and composition of interphases in rubbers

An MTDSC calorimeter model 2920 (TA Instruments, USA) was used to measure mass fraction and composition of interphases in rubber blends and glass transition temperature of the rubbers and rubber blends. Figure 5-1 shows a schematic representation of a heat flux MTDSC cell [12]. The oscillation amplitude was 1°C and period of 60 s were used throughout the investigations, which were conducted at a heating rate of 3°C/min. The calorimeter was calibrated with an Indium standard. Both temperature and baseline were calibrated as for conventional DSC. Standard aluminium pan and lid were used, and samples of rubber approximately 10-15 mg in weight were placed in the pan at ambient temperature, and the lid was subsequently closed under some nominal pressure. The assembly was placed in the chamber of the calorimeter and the temperature was lowered to -140°C with the flow of liquid nitrogen at a rate of 35 ml/min, which was used as the heat transfer gas. The temperature was allowed to modulate back to ambient as described above. The T_g of the pure rubbers and the mass fraction of the interphase and its composition were subsequently calculated. The TA Instrument Graphware software (TA Instrument, USA) was used to measure the heat flow, the heat capacity and the differential of heat capacity.

A TA-analysis software was also used to smoothen and process the data. All data were smoothened at $3°C$, $6°C$ or $9°C$, depending upon the degree of curve resolution in each case.

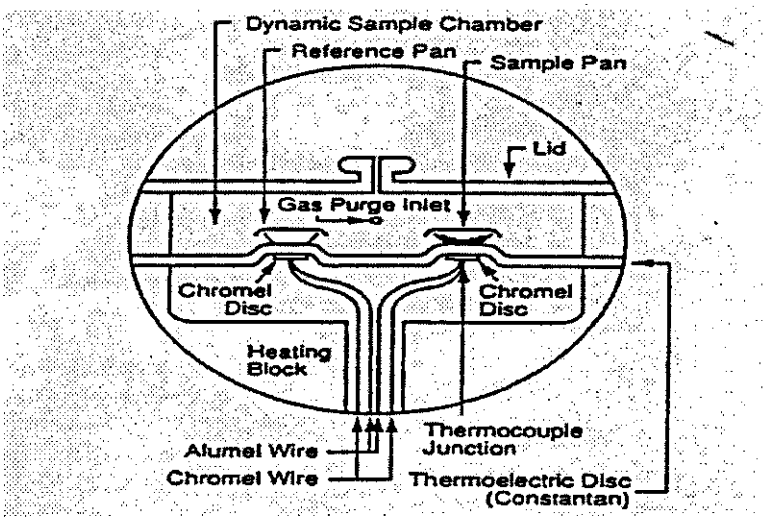

Figure 5-1: Typical heat flux MTDSC cell [12].

5.13 Measurement of G', G"and tan δ of the rubbers

Tanδ is the ratio between the loss modulus and storage modulus. The loss modulus represents the viscous component of the modulus and includes all the energy dissipation processes during dynamic strain. The tanδ was measured in a dynamic mechanical thermal analyser (DMAQ800) model CFL-50 (TA Instruments, USA), using Universal Analysis 2000 Software Version 4.3A. Figure 5-2 shows a schematic view of the DMA head [13].

Test pieces 35 mm long, 13 mm wide and approximately 2.40 mm thick were used. The tests were performed at, 1, 20 and 100 Hz frequencies and the

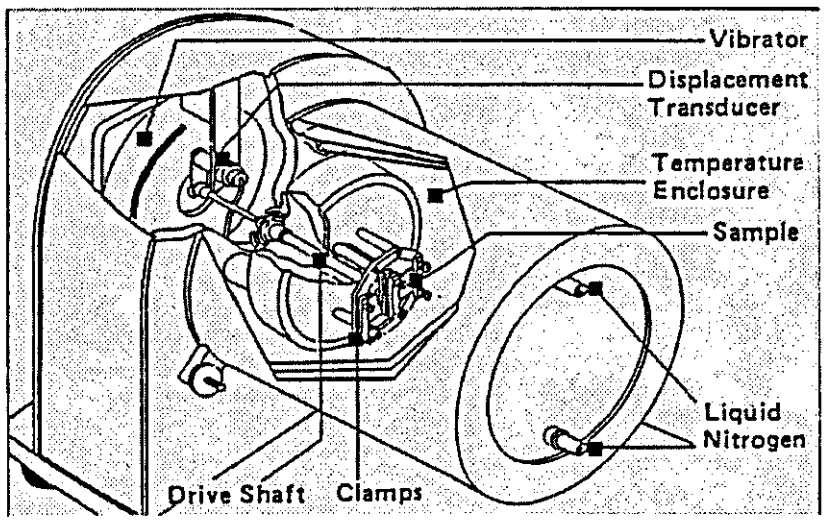

Figure 5-2: Typical view of the DMA head [13].

samples were deflected by 15, 256, 500 and 1000 μm (nominal peak-to-peak displacement) during the test. The sample temperature was raised from -130°C to 100°C at 5°C/min steps. Figure 5-3 shows a sample clamped in the DMA head prior to measurement [13].

In addition to measuring tan δ, loss modulus and storage modulus of the rubbers were also measured using the DMA.

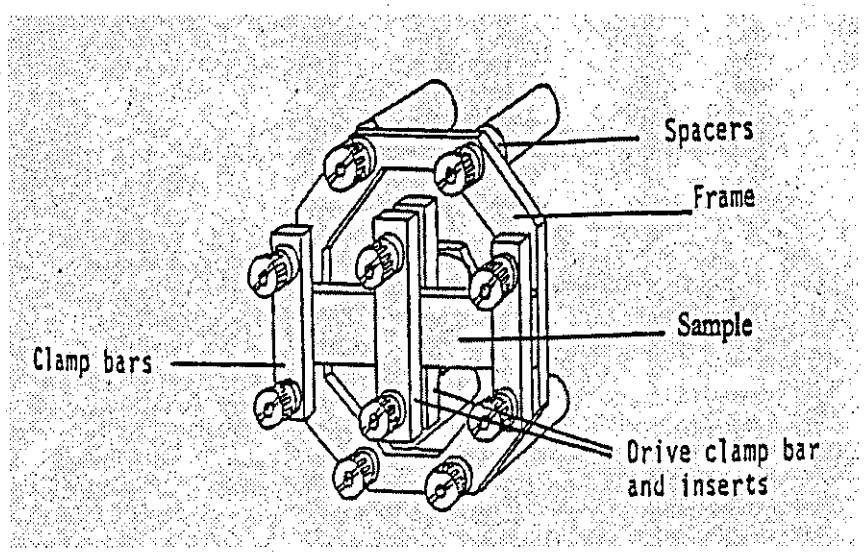

Figure 5-3: Sample clamped apparatus in the DMA prior to measurement [13].

5.14 Measurement of heat buildup in the rubber vulcanisates

The heat build up of the blends was determined in accordance with BS903 Part A50. The load applied during testing was equivalent to 1 MPa. The samples were tested at ambient temperature (23°C). The test duration was 30 minutes in total: 5 minutes static and 25 minutes dynamic flexing. The height of the test pieces was measured, having been allowed to cool to ambient temperature testing in accordance with the standard, and the permanent set calculated. The test pieces were cut opened and the internal structure of the test pieces was examined for evidence of porosity. A porous structure would have indicated that some breakdown of the rubber had occurred on testing. The test pieces would be reported as showing signs of 'onset of failure' [14].

5.15 Assessment of the silica dispersion in the rubbers

Dispersion of the silica particles in the rubber was assessed by a LEO 1530 VP Field emission gun scanning electron microscope (SEM). Small pieces of the uncured rubber were placed in liquid nitrogen for 3 min, and then fractured to create two fresh surfaces. The samples, 60 mm^2 in area and 5 mm thick, were coated with gold, and then examined and photographed in the SEM. The degree of dispersion of the silica particles in the rubber was subsequently studied from SEM photographs. After the SEM photos were examined, suitable mixing times were used for adding the filler to the rubbers.

References

1) British standard institution, Methods of test for raw rubber and unvulcanised compounded rubber 1673,10, London, UK (1977).

2) British standard institution, Physical testing of rubber- Curemetering –BS 903-A60.1 (2000).

3)Wolff S, *Rubber Chem. Technol.* **48**:795(1975).

4) Hamed G R, Rattanasom N, *Rubber Chem. Technol.***75**:323(2001).

5) Wolff, Rubber Chem. Technol. 66, 163 (1993).

6) British standard institution, Physical testing of rubber: Methods using the Mooney viscometer-BS 903-A58.1 (2001), BS 903-A58 (1990).

7) British standards institution, Physical testing of rubber: Method for determination of hardness, BS 903, A26, London, UK (1995).

8) British standards institutions, Determination of resistance to abrasion, BS 903, A9:MethodA.1, London, UK (1995).

9) British standard institution, Method for determination of tear strength trousers, BS 903, A3, London, UK (1995).

10) Greensmith H V, Thomas A G , *J. Polym. Sci.* **43**:189(1955).

11) British standards institution, Method for determination of tensile stress strain properties, BS 903, A2, UK (1995).

12) *The TA Hotline* **2**:1(1992).

13) DMTA Mk II user manual, *Rheometric scientific* (1995).

14) British Standard Institution, Methods of testing vulcanized rubber. Determination of temperature rise and resistance to fatigue in flexometer testing (compression flexometer). Br Standard 903: London, UK,Part A50(1984).

Chapter 6

Effects of silanized silica nanofiller on the curing and mechanical properties of NR

6.1 Introduction

On tapping the Hevea brasiliensis tree, natural rubber latex exudes, which has a rubber content between 25 to 40 percent by weight. The solid rubber or cis-1-4 polyisoprene is extracted from the latex. The useful properties of NR include high gum and tear strength, high abrasion resistance, long flex life and high resilience. Because of these excellent properties, NR is used in many industrial applications for example, tyres, belting, anti-vibration mountings, and bridge bearings. Synthetic polyisoprene (IR) is the synthetic analogue of NR, and is chemically and structurally similar to it. IR has been used in the same applications as NR such as in blends with styrene-butadiene rubber and polybutadiene rubber to improve their processibility, and also mineral filled IR is used in footwear, sponge, and sporting goods [1] . Raw rubbers often possess weak mechanical properties, and must be reinforced with fillers. Reinforcement increases properties for example hardness, abrasion resistance, and tensile strength. Carbon blacks, synthetic silicas, quartz, and metal oxides, which have large surface areas ranging from 150 to 400 m^2/g are very effective in improving the rubber properties [2]. The major disadvantage of silicas (scheme 6-1) is their acidity [3] and polarity [4], which is caused by the presence of silanol groups on the silica surfaces. This causes unacceptably long cure times and slow cure rates [5] and also loss of crosslink density in sulphur-cured rubbers [6]. Moreover, processing becomes more difficult when a large amount of silica is added because the viscosity increases significantly [7-8]. The availability of the coupling agent (TESPT) has provided a better opportunity for using synthetic silicas to crosslink and reinforce rubbers. TESPT possesses tertrasulphane and ethoxy reactive groups (Scheme 6-2).

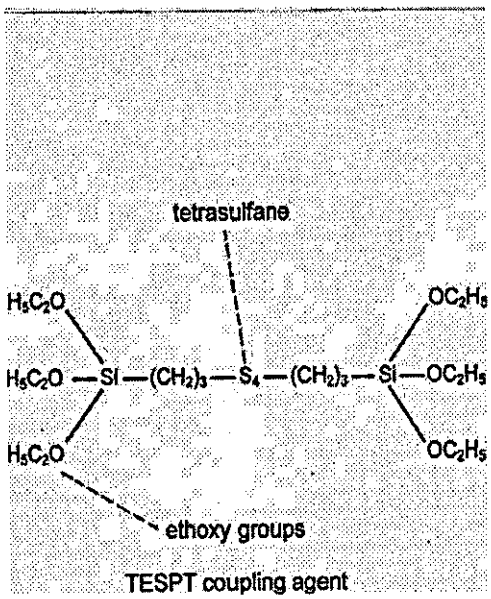

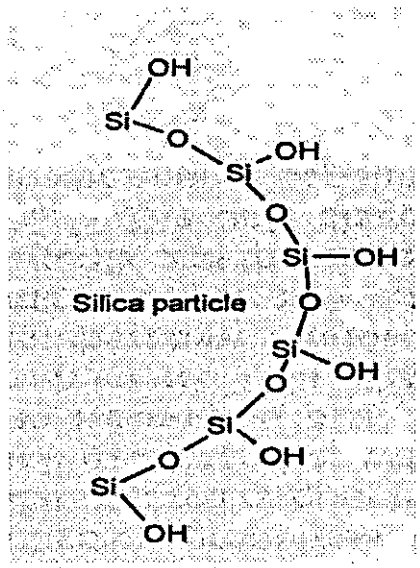

Scheme 6-1: TESPT **Scheme 6-2: silica surface**

The tetrasulphane groups react with the rubber in the presence of accelerators at elevated temperatures, i.e. 140-240°C, with or without elemental sulphur being present, to form crosslinks in unsaturated rubbers. The ethoxy groups react with the silanol groups on the surfaces of silicas to form stable filler/TESPT bonds. Moreover, the number of silanol groups decreases after reaction with TESPT, and the remaining groups become less accessible to the rubber because of steric hindrance [5]. This weakens the strong interaction between silica particles [5], which reduces the viscosity of rubber compounds, and also improves cure properties by preventing acidic silicas from interfering with the curing reactions in sulphur-cured rubbers. It has been reported [9] that TESPT is a satisfactory property promoter in silica/NR composites through C-S bonding with rubber molecules.

Precipitated silica pre-treated with TESPT is classified as a crosslinking filler. Parker and Koenic [10] evaluated effects of silane pre-treated silica, and silica and liquid silane mixture on the crosslink density of a sulphur-cured rubber and

concluded that the rubber with silane pre-treated silica had a higher crosslink density and increased filler-rubber adhesion. Ansarifar and co-workers [11-12] carried out a similar study and reached to the same conclusion. They also found that the mechanical properties of rubber improved more substantially with TESPT pre-treated silica.

The aim of this study was to crosslink and reinforce the mechanical properties of NR with 60 phr silanized silica nanofiller pre-treated with TESPT, and to determine whether this compound was suitable for use in tyre tread or not. The bound rubber content and crosslink density of the rubber compound were also measured to assess the extent of rubber-filler adhesion and chemical bonding between the rubber and filler, respectively.

6.2 Mixing

The compounds were prepared in a Haake Rheocord 90 (Berlin, Germany), a small laboratory mixer with counter rotating rotors. In these experiments, the Banbury rotors and the mixing chamber were maintained at 50 $°C$ and the rotor speed was 45 rpm. The above temperature was nominal and the exact temperature of the rubber compound in some cases rose to 74 $°C$ due to heat generation by frictional forces during mixing process.

50 wt% of the filler was first placed in the mixing chamber and the raw rubber was added and then the rotors started. The remaining mass of the filler was added within 30 seconds. This was due to the small size of the mixing chamber, which make it difficult to add full mass of the filler in a single stage. During mixing, the ram was lowered to keep the rubber and filler in the mixing chamber under pressure. The volume of mixing chamber was 78 cm^3 and it was 60% full. Haake sofrware version 1.9.1 was used to control the mixing condition and store the mixing data. The rubber and filler were mixed together for 13 minutes as recommended by Ansarifar and co-workers [13]. After 13 minutes elapsed, the

rotors stopped and the ram was raised to cool down the rubber compound before the curing chemicals were added. After the curing chemicals were added, mixing continued for an extra 3 minutes until it stopped and the rubber compound was removed from the mixer. The compound was subsequently stored at ambient temperature for at least 24 hours before its viscosity and cure properties were measured. 48 h after the cure properties were measured, the rubber was cured to make samples for measuring its mechanical properties. All the tests were carried out according to the British Standard [14]. Table 6-1 represents typical temperature and torque variation versus time in the Haake mixer during the first 13 minutes mixing of the rubber and filler.

Table 6-1: Typical compound temperature as a function of time in the mixer. The torque values are also shown.

Time (min.)	Temperature ($^{\circ}C$)	Torque (N.m)
0	50	2.3
1	52	25.3
2	57	27.6
3	64	35.5
4	74	30.6
5	75	25.3
6	76	21.4
7	74	21.8
8	75	19.7
10	73	18.8
11	72	19.3
12	72	21.1
13	71	18.4

6.3 Measurement of the optimum loading of TBBS for crosslinking the rubber

To activate the rubber reactive tetrasulphane groups of TESPT, TBBS was added. The loading of TBBS in the rubber was increased progressively to 10 phr to measure the amount needed to optimize the chemical bonding between the rubber and TESPT, and to increase the crosslink density in the rubber (compounds 1-11; Tables 6-2 and 6-3).

Table 6-2: Formulation: 100 phr NR, 60 phr silica and an increasing loading of TBBS.

Compound No.	1	2	3	4	5	6	7	8	9	10	11
TBBS(phr)	1	2	3	4	5	6	7	7.5	8	9	10

Table 6-3: Formulation: 30 g NR, 18 g silica and an increasing loading of TBBS.

Compound No.	1	2	3	4	5	6	7	8	9	10	11
TBBS(g)	0.3	0.6	0.9	1.2	1.5	1.8	2.1	2.25	2.4	2.7	3.0

6.4 Measurement of the optimum loading of ZnO for optimizing the efficiency of TBBS and cure in the rubber

The loading of zinc oxide in the filled rubbers with 6 phr TBBS was raised to 2 phr to determine the amount needed to maximize the efficiency of TBBS and cure (compounds 12-19 ; Tables 6-4 and 6-5).

Table 6-4: Formulation: 100 phr NR, 60 phr silica, 6 phr TBBS and an increasing loading of ZnO.

Compound No.	12	13	14	15	16	17	18	19
ZnO (phr)	0.1	0.2	0.3	0.5	0.8	1.0	1.5	2.0

Table 6-5: Formulation: 30 g NR, 18 g silica, 1.8 g TBBS, and an increasing loading of ZnO.

Compound No.	12	13	14	15	16	17	18	19
ZnO (g)	0.03	0.06	0.09	0.15	0.24	0.30	0.45	0.60

6.5 Measurement of the effect of stearic acid on the cure properties of the rubber with silica, TBBS, and ZnO

Stearic acid is a fatty acid, which is added to improve the solubility of ZnO in rubber. The loading of stearic acid in the filled rubbers with TBBS and ZnO was increased to 2 phr to measure the amount needed to optimize the efficiency of ZnO and cure in the rubber (compounds 20-23 ; Table 6-6 and 6-7).

Table 6-6: Formulation: 100 phr NR, 60 phr silica, 6 phr TBBS, 0.3 phr ZnO and an increasing loading of stearic acid.

Compound No.	20	21	22	23
Stearic acid (phr)	0.5	1	1.5	2

Table 6-7: Formulation: 30 g NR, 18 g silica, 1.8 g TBBS, 0.09 g ZnO and an increasing loading of stearic acid.

Compound No.	20	21	22	23
Stearic acid (g)	.15	.30	.45	.60

6.6 Measurement of the effect of elemental sulphur on the cure properties of the rubber with silica, TBBS, and ZnO

To evaluate the effect of elemental sulphur on the cure properties of the filled

NR compound with TBBS and zinc oxide, four compounds were prepared. The loading of sulphur in the rubber was increased to 2 phr (compounds 24-27; Table 6-8 and 6-9).

Table 6-8: Formulation: 100 phr NR, 60 phr silica, 6 phr TBBS, 0.3 phr ZnO and an increasing loading of elemental sulphur.

Compound No.	24	25	26	27
Elemental sulphur (phr)	0.5	1	1.5	2

Table 6-9: Formulation: 30 g NR, 18 g silica, 1.8 g TBBS, 0.09 g ZnO and an increasing loading of elemental sulphur.

Compound No.	24	25	26	27
Elemental sulphur(g)	.15	.30	.45	.60

6.7 Assessing effect of an increasing loading of ZnO on the cure properties of the filled rubber with 7 phr TBBS

To evaluate effect of an increasing loading of ZnO on the cure properties or crosslinking of the filled rubber with 7 phr TBBS, eight compounds were prepared (compounds 28-35, Table 6-10 and 6-11). To optomise the reaction between the rubber and TESPT, 6 phr TBBS was sufficient. However, it was of interest to find out what optimum loading of ZnO was needed if the loading of TBBS was raised to 7 phr.

Table 6-10: Formulation: 100 phr NR, 60 phr silica, 7 phr TBBS and with an increasing loading of ZnO.

Compound No.	28	29	30	31	32	33	34	35
ZnO (phr)	0.3	0.5	0.8	1.0	1.3	1.5	2.0	2.5

Table 6-11: Formulation: 30 g NR, 18 g silica, 2.1 g TBBS and with an increasing loading of ZnO.

Compound No.	28	29	30	31	32	33	34	35
ZnO (g)	0.09	0.15	0.24	0.30	0.39	0.45	0.60	0.75

6.8 Rubber formulations and cure properties of the rubber compounds

After the optimum curing chemicals, i.e TBBS and ZnO, were measured in the filled rubber, three formulations were selected for further studies. These were control compound, filled rubber with no elemental sulphur, and filled rubber with 1.5 phr elemental sulphur (Table 6-12). The viscosity and cure properties of these compounds were measured and then the compounds were cured. The amount of elemental sulphur in the control compound was the same as the 2.5 wt % sulphur concentration in silanized silica (Compound 36; Table 6-12), which was equivalent to 1.5 phr elemental sulphur [15]. 1 phr antidegradant was also added to the compounds to protect against environmental ageing. Table 6-12 shows the rubber formulations, viscosity and cure properties of the rubber compounds.

6.9 Bound rubber and crosslink density measurements

The Bound rubber content is the percentage of polymer attached or bound to the filler. The solvent used for Bound rubber and crosslink density determination was Toluene (Merck-Germany). For determination, 2.11 and 2.23 g for the filled rubbers, and 1.65 g for the control rubber, respectively, were cured to produce cylindrical samples with the following dimensions (Table 6-13):

Table 6-12: Formulations and the ODR test results for the three compounds.

Compound No.	36*	37	38
NR(phr)	100	100	100
Coupsil (phr)	---	60	60
TBBS (phr)	6	6	6
ZnO (phr)	0.3	0.3	0.3
Sulphur (phr)	1.5	----	1.5
Santoflex 13	1	1	1
Min. Torque (dN m)	12.2	25.8	26.8
Max.Torque (dN m)	71.1	106.9	135.1
$\Delta torque$ (dN m)	58.9	81.1	108.3
t_{s1} (min)	21	8.1	5.5
t_{90} (min)	32.5	23.5	9.1
t_{95} (min)	34.3	26.6	9.2
CRI(min^{-1})	8.7	6.52	28.33

*Compound 36 is the control compound.

Table 6-13: Dimensions of samples for Bound rubber measurement

Compound No.	Sample diameter (mm)	Sample height (mm)	Sample weight (g)
36 (control)	15.42	9.01	1.65
37	15.57	9.45	2.11
38	15.96	9.42	2.23

6.10 Results and Discussion

6.10.1 Optimising the loading of TBBS in the filled rubber

A typical ODR trace from which scorch time and optimum cure time were measured from is shown in Figure 6-1.

Table 6-14 and Figure 6-2 show the ODR test results and ODR traces produced for compounds 1-11.

To measure the optimum amount of TBBS needed to cure the rubber, the Δtorque values from Table 6-14 were plotted against the loading of TBBS in Figure 6-3. The aim was to measure the minimum amount of TBBS to produce the maximum Δtorque value. Δtorque increased from 9 to 54 dN m as the loading

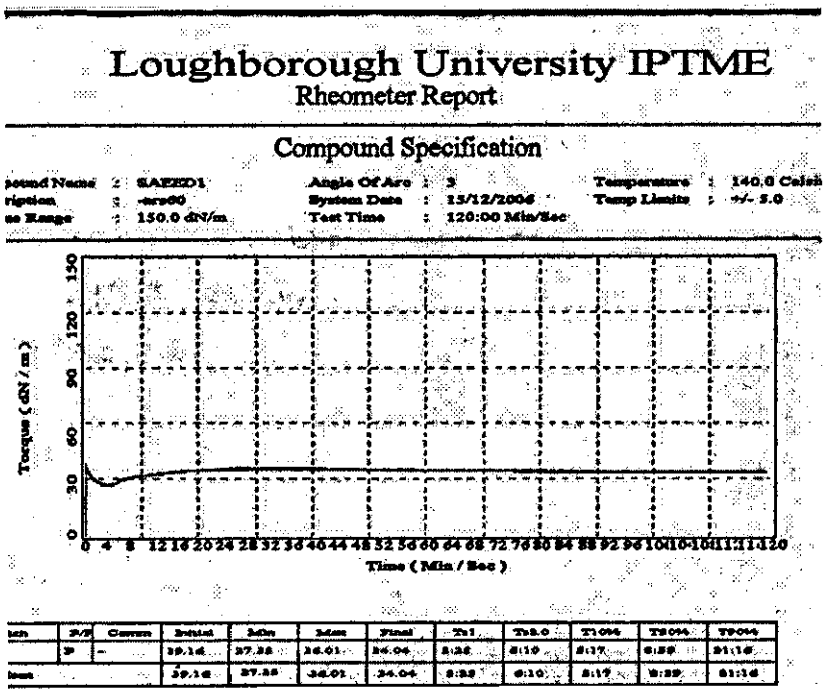

Figure 6-1: ***Typical ODR trace for compound 1***

Table 6-14: ODR test results for compounds 1-11. Formulation: 100 phr NR, 60 phr silica, and an increasing loafing of TBBS.

Compound No.	1	2	3	4	5	6	7	8	9	10	11
Min. Torque (dN.m)	27	29	28	26	26	27	24	21	21	21	18
Max. Torque (dN.m)	36	47	60	69	72	81	81	77	76	77	79
Δtorque (dN.m)	9	18	32	43	46	54	57	56	55	56	61
t_{s1} (min)	5.3	5.6	6.6	8.1	8.1	9.0	11.0	11.0	10.4	12.0	11.5
t_{s2} (min)	6.1	6.3	7.4	9.1	9.2	10.1	12.2	12.1	11.5	13.1	13.1
t_{90} (min)	21	24	26	31	30	31	37	36	37	39	40
CRI(1/min)	6.3	5.6	5.1	4.5	4.6	4.5	3.8	4.0	3.8	3.7	3.5

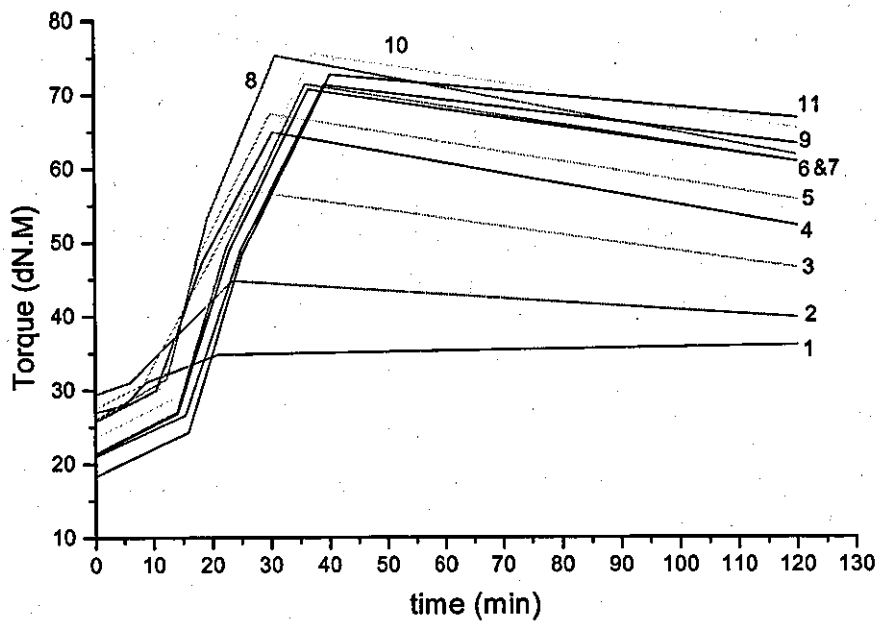

Figure 6-2: ODR traces for compounds 1-11

of TBBS was raised to 6 phr, and then it continued rising at a much slower rate to about 61 dN.m when the loading of TBBS reached 10 phr. Evidently, the addition of 6 phr TBBS to the filled NR compound was sufficient to react the rubber reactive tetrasulphane groups of TESPT with the rubber chains to form crosslinks, and to optimize the chemical bonding between the two. Note that further increase in the loading of TBBS has little or no effect on Δtorque.

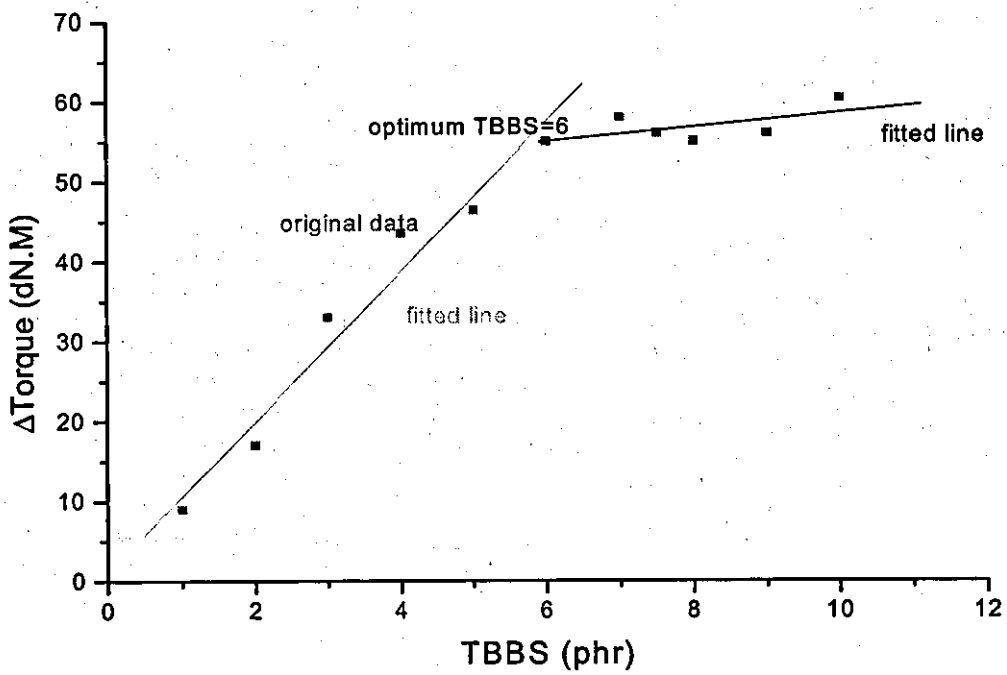

Figure 6-3: Δtorque as a function of TBBS loading for compounds 1-11 (Table 6-14)

6.10.2 Optimising the loading of ZnO in the filled rubber with 6 phr TBBS.

ZnO was added to optimise the efficiency of TBBS in the filled rubber. The loading of ZnO in the filled rubber with 6 phr TBBS was increased progressively. Δtorque increased from 78 to 91 dN m when 0.3 phr ZnO was added, and it continued rising at a much slower rate to 112 dN m when the loading of zinc oxide reached 2 phr (Figures 6-4 and 6-5 and Table 6-15).

Table 6-15: ODR test results for compounds 12-19. Formulation: 100 phr NR, 60 phr silica, 6 phr TBBS, and an increasing loading of ZnO

Compound no.	12	13	14	15	16	17	18	19
Min. Torque (dN.m)	24	23	23	24	22	24	24	24
Max. Torque (dN.m)	102	107	114	120	120	125	134	136
Δtorque (dN.m)	78	84	91	96	98	101	110	112
t_{s1} (min)	8.2	8.1	8	7.5	7.3	8.1	8.1	7.5
t_{s2} (min)	9	8.5	8.4	8.3	8.2	8.5	8.5	8.3
t_{90} (min)	24.3	22.4	22.4	22.2	25.3	25.2	29.2	31.3
CRI(1/min)	6.2	7	6.9	6.8	5.6	5.9	4.7	4.2

It emerged that the addition of 0.3 phr ZnO was sufficient to maximize the efficiency of TBBS in the filled NR, and consequently optimised the chemical bonding between the rubber and filler.

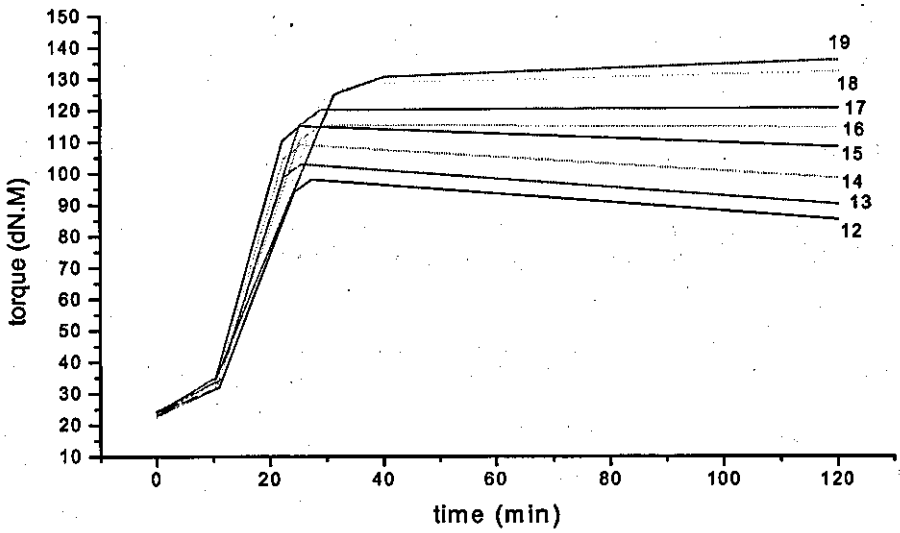

Figure 6-4: ODR traces for compounds 12-19

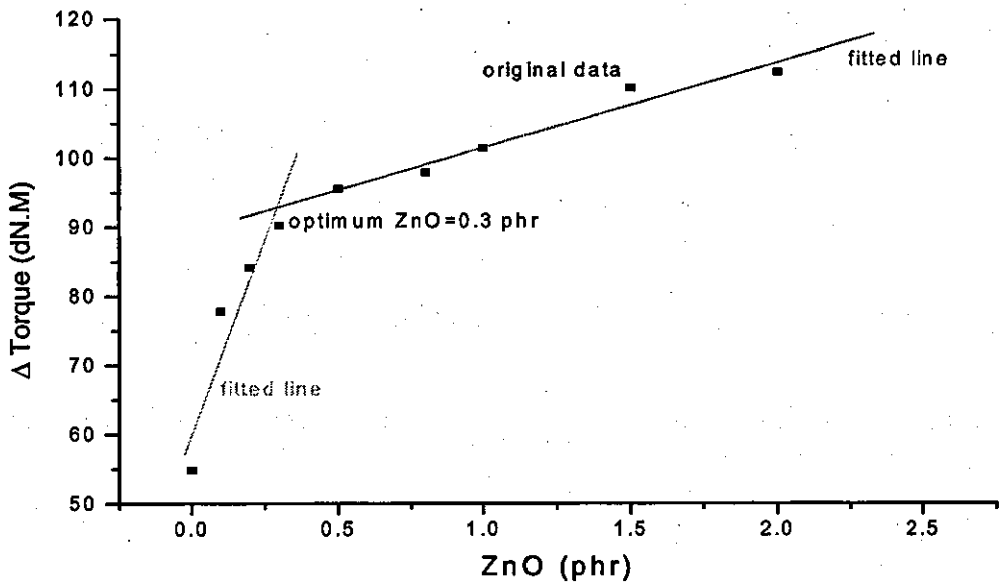

Figure 6-5: Δtorque as a function of ZnO loading for compounds 12-19 (Table 6-15)

6.10.3 Optimising the loading of stearic acid in the filled rubber with TBBS, ZnO and an increasing loading of stearic acid

Table 6-16 and Figure 6-6 represent the ODR test results for compounds 20-23 where the loading of stearic acid was increased.

Table 6-16: ODR test results for compounds 20-23. Formulation: 100 phr NR, 60 phr silica, 6 phr TBBS, 0.3 phr ZnO, and an increasing loading of stearic acid.

Compound No.	20	21	22	23
Min. Torque (dN.m)	22	21	20	21
Max. Torque (dN.m)	103	107	103	104
$\Delta Torque$ (dN.m)	81	86	83	84
t_{s1} (min	9.1	9.1	9.6	9.4
t_{s2} (min)	9.5	9.6	10.4	10.3
t_{90} (min)	25.3	24.2	25.1	25.3
CRI(1/min)	6.2	6.6	6.4	6.3

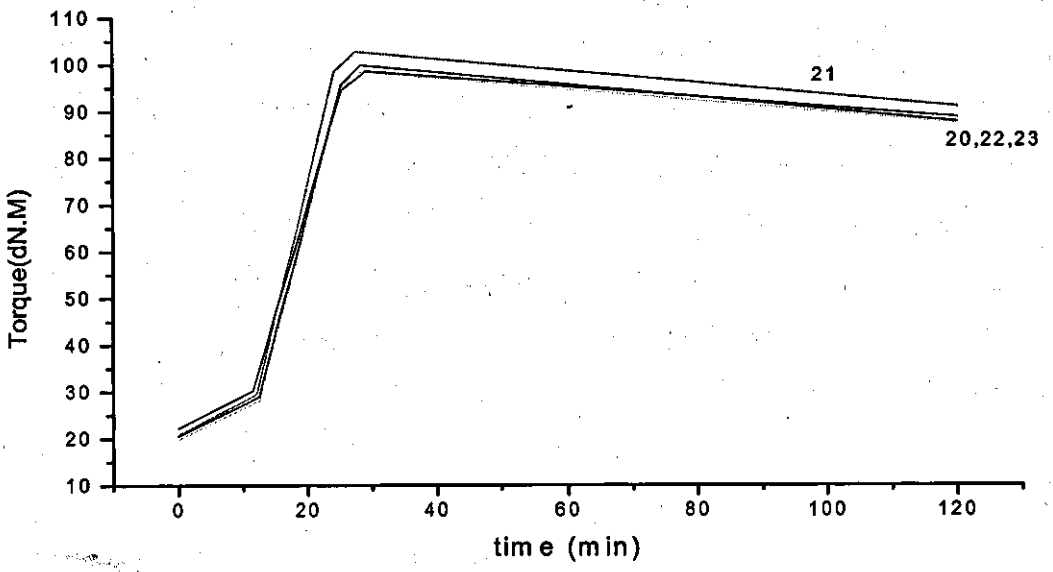

Figure 6-6: ODR test results for compounds 20-23

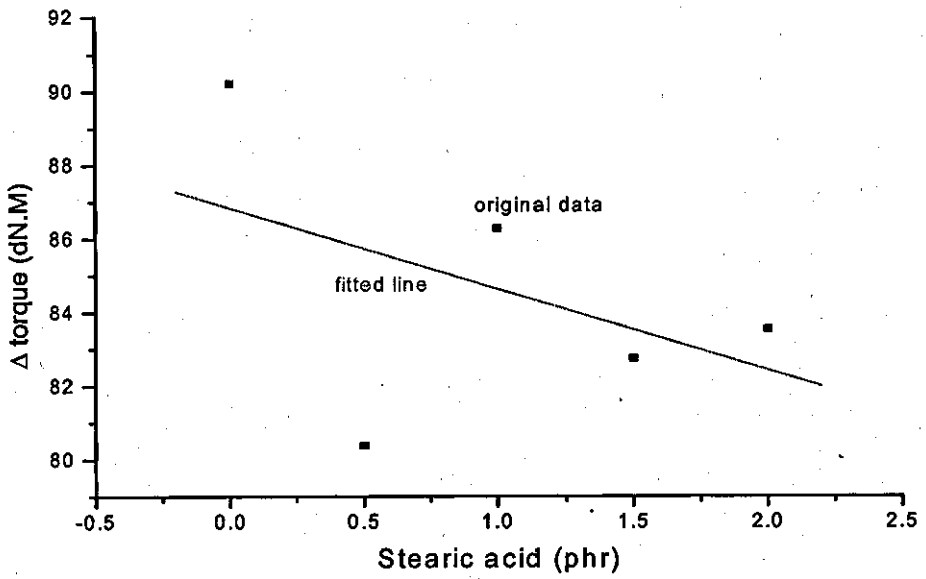

Figure 6-7: Δtorque as a function of stearic acid loading for compounds 20-23 (Table 6-16)

From Figure 6-7, it is evident that when up to 2 phr stearic acid was incorporated in the filled NR with 6 phr TBBS and 0.3 phr zinc oxide, the Δtorque value decreased from 91 to about 83 dN m. It was concluded that the addition of

stearic acid had no potential benefit for the cure of the rubber and did not help to increase chemical bonding between the rubber and filler.

6.10.4 Effect of elemental sulphur on the curing properties of the filled rubber with 6 phr TBBS and 0.3 phr ZnO

Table 6-17 and Figure 6-8 show the ODR test results and traces, respectively, for compounds 24-27. Figure 6-9 shows Δtorque as a function of elemental sulphur loading. The addition of elemental sulphur to the filled NR compound affected its cure characteristics. t_{s1} and t_{90} shortened from 8.2 to 6.5 min and 16.2 to 10.4 min, respectively. The rate of cure increased, with the cure rate index rising from 12.6 to 26 min^{-1}. Δtorque also increased from 93 to 105 dN m. This suggested a large increase in the crosslink density of the rubber. When elemental sulphur was added to NR, its cure properties improved substantially. These results are in line with the previous findings [16].

Table 6 -17: ODR test results for compounds 24- 27. Formulation: 100 phr NR, 60 phr silica, 6 phr TBBS, 0.3 phr ZnO, and an increasing loading of elemental sulphur.

Compound No.	24	25	26	27
Min. Torque (dN.m)	26	26	25	25
Max. Torque (dN.m)	119	124	134	130
Δtorque (dN m)	93	98	109	105
t_{s1} (min	8.2	7.4	6.1	6.5
t_{s2} (min)	9.1	8.1	6.4	7.3
t_{90} (min)	16.2	11.5	9.4	10.4
CRI(1/min)	12.6	24	30.2	26

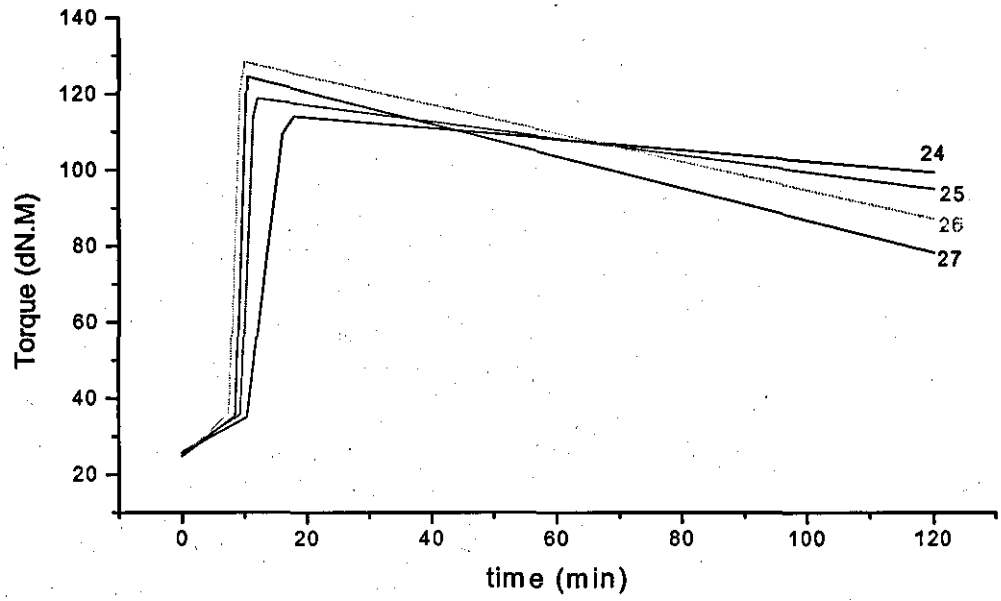

Figure 6- 8: ODR test results for compounds 24-27

It is clear from Figure 6-9 that adding elemental sulphur to the filled rubber with TBBS and ZnO increases Δtorque quite considerably and hence the crosslink density in the rubber. Often when the torque value increases beyond 100 dN m, the rubber becomes too brittle and may loose its elasticity. Therefore, the addition of too much elemental sulphur to the filled rubber, which is cured with the tetrasulphane groups of TESPT may not be desirable for the rubber properties.

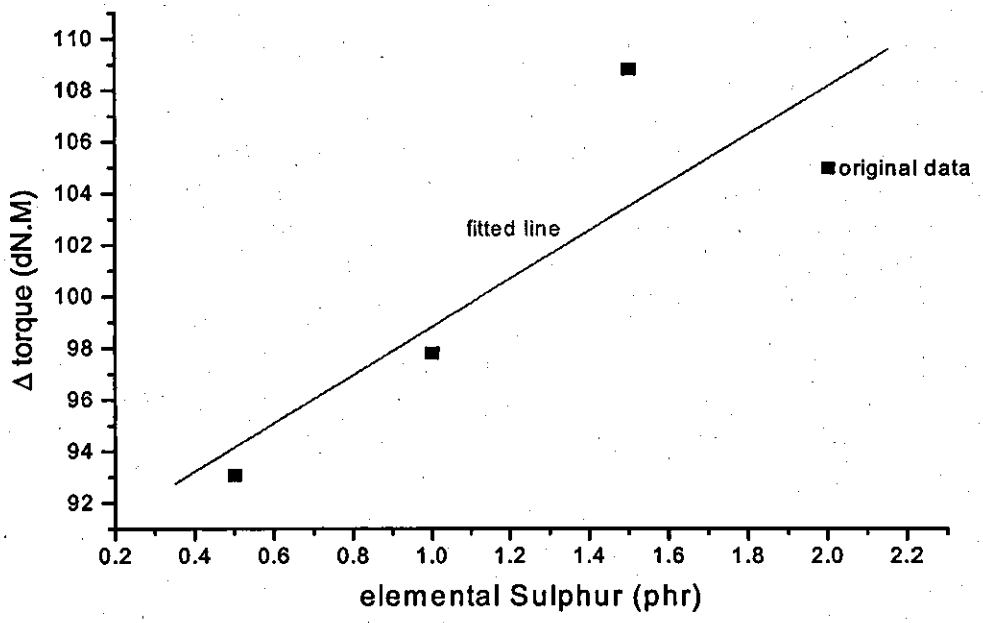

Figure 6-9: Δtorque as a function of elemental sulphur loading for compounds 24-27 (Table 6-17)

6.10.5 Assessing effects of an increasing loading of ZnO on the cure properties of a filled rubber with 7 phr TBBS.

As shown in section 6.10.1, 6 phr TBBS was sufficient to optimise the Δtorque of the filled rubber. To assess the effect of an increasing loading of ZnO on the cure properties of the filled rubber with 7 phr TBBS, some rubber compounds were prepared and tested in the ODR (compounds 28-35). Table 6-18 and Figure 6-10 show the ODR test results and the cure traces of these compounds, respectively. Figure 6-11 shows the Δtorque values as a function of the loading of ZnO for the compounds.

Figure 6-11 shows the optimum amount of ZnO in the filled compound with 7 phr TBBS to be 1.3 phr. It is worth mentioning that the filled rubber with 6 phr TBBS,

Table 6-18: ODR test results for compounds 28-35. Formulation: 100 phr NR, 60 phr silica, 7 phr TBBS, and an increasing loading of ZnO

Compound No.	28	29	30	31	32	33	34	35
Min. Torque (dN.m)	22	24	22	23	23	23	23	24
Max. Torque (dN.m)	99	111	123	127	135	136	138	140
$\Delta Torque$ (dN.m)	77	87	101	104	112	113	115	116
t_{s1} (min)	8	8	7.5	8	9	8.4	9	9.1
t_{s2} (min)	8.4	8.3	8.2	8.4	10.1	9.2	9.5	10.1
t_{90} (min)	24.3	24.5	24.6	26.1	32.3	31.3	35.1	38.1
CRI(1/min)	6.1	5.9	5.9	5.5	4.3	4.4	3.8	3.5

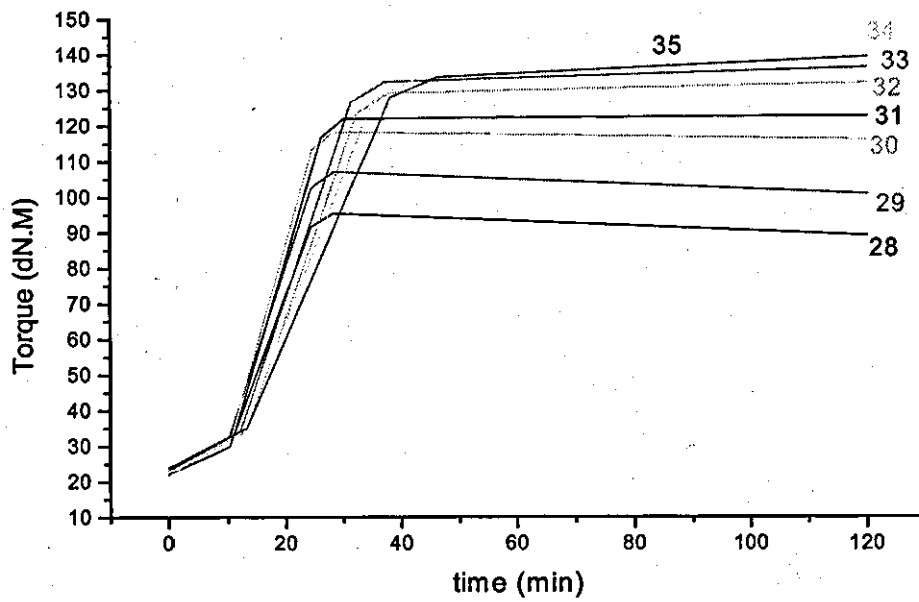

Figure 6-10: ODR test results for compounds 28-35.

needed 0.3 phr ZnO to optimise Δtorque. The former, needed 1 phr extra ZnO to optimize Δtorque. Therefore, optimising the amount of TBBS in the filled rubber helped to reduce the need for ZnO at the same time.

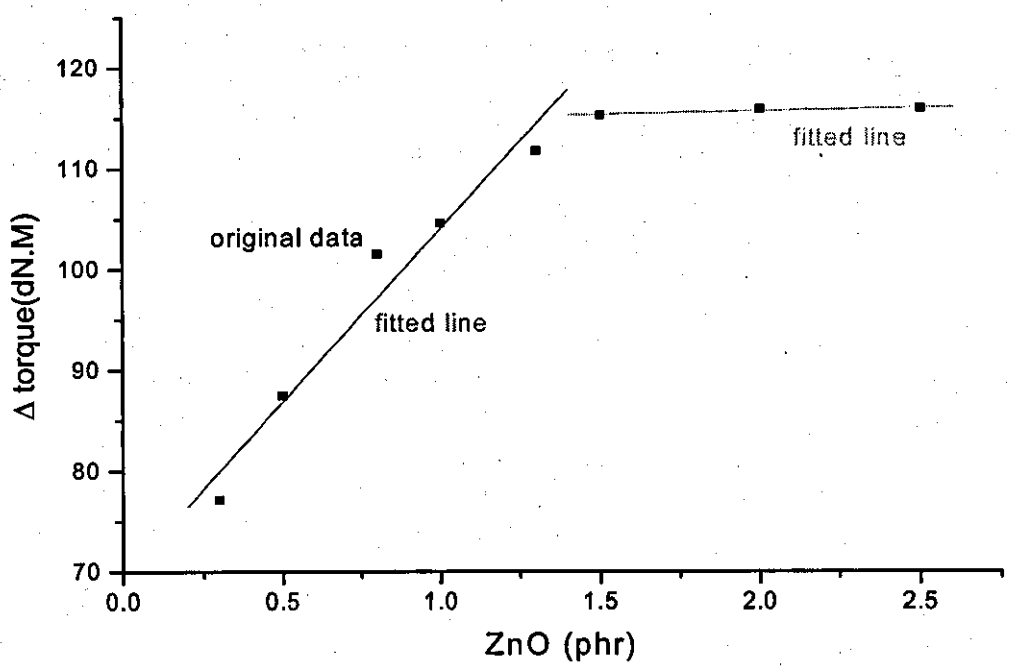

Figure 6-11: Δtorque as a function of zinc oxide loading for compounds 28-35 (Table 6-18)

6.10.6 Effect of silanized silica nanofiller on the viscosity, cure and mechanical properties of the NR compound

When silanized silica was added to the NR compound (comparing compounds 36 and 37; Table 6-12), the cure time, t_{95} decreased from 34.3 to 26.6 min, and the rate of cure slowed down, with the cure rate index decreasing from 8.7 to 6.52 min^{-1}. In addition, the scorch time, t_{s1} shortened from 21 to 8.1 min, and Δtorque rose from 59 to 81 dN m. Clearly, the incorporation of the filler was greatly beneficial to the cure properties of the rubber. This was attributed to the sulphur content of TESPT, which was 2.5 wt% [5, 17].

Mooney viscosity

192 h after the compounds were mixed, the Mooney viscosity of the rubber compounds were measured (Table 6-19).

Table 6-19: Mooney viscosity of compounds 36-38. (36) Control compound, (37) filled rubber with no elemental sulphur, (38) filled rubber with elemental sulphur.

Compound No.	36	37	38
Mooney viscosity (MU)	49	106	111

The Mooney viscosity of the filled rubbers (compounds 37 and 38) was more than twice the viscosity of the unfilled rubber (compound 36). This was due to the reinforcing effect of the filler in the rubber. It was also interesting that the filled rubber with elemental sulphur had a slightly higher viscosity of 111 MU than the filled one with no elemental sulphur, which was 106 MU. Figure 6-12 shows Mooney viscosity versus storage time. These measurements were taken after the rubber compound was kept in storage at the ambient temperature for different lengths of time before its viscosity was measured. It is clear that the viscosity increased as a function of storage time and this was due to the formation of bound rubber.

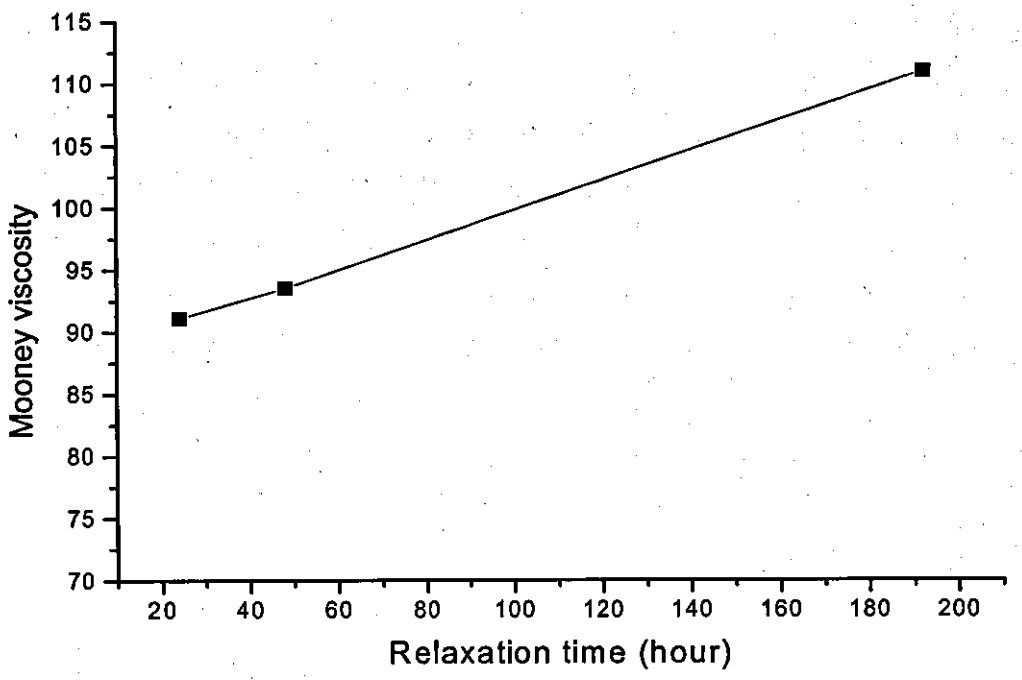

Figure 6-12: Mooney viscosity as a function of storage time at the ambient temperature. Data for compound 38.

Hardness

Table 6-20 shows results of hardness tests on the cured rubbers. The control rubber had a hardness of about 54 Shore A, the filled rubber with no elemental sulphur 75 Shore A, and the filled rubber with elemental sulphur 78 Shore A. Clearly, adding the filler had increased the rubber hardness. It was also interesting that the hardness of the filled rubber was higher because of the elemental sulphur which produced more crosslinks in the rubber and hence hardening it further.

Table 6-20: Hardness of the cured rubbers. (36) control compound, (37) filled rubber with no elemental sulphur, (38) filled rubber with elemental sulphur

Rubber	Number of reading					
	1	2	3	4	Mean	σ
37-1	75.2	77.3	75.4	76		
37-2	75	72.9	73.5	75.4	75.1	1.29
36-1	55	50.6	54.5	55.3		
36-2	54.5	54	55	56	54.36	1.53
38-1	78	79.6	80.8	79.4		
38-2	78.6	76.9	75.8	76.3	78.18	1.64

Abrasion resistance

Table 6-21shows the abrasion resistance test results for compounds 36-38. Abrasion resistance or resistance to weight or mass loss when rubber is in contact with a hard surface, is one of the most important properties for tyre tread compounds. Results in Table 6-21 clearly show that this property improved when the reinforcing filler was added to the rubber (compounds 37 and 38). For the control compound (compound 36), 470.7 mm^3 was lost during the abrasion test. However, for the filled rubber with no elemental sulphur, the volume loss was 76 mm^3 and for the filled rubber with elemental sulphur, it was 126.8 mm^3, which was slightly higher than the former. It seemed that the addition of elemental sulphur, which produced extra crosslinks and hardened the rubber, was not beneficial to the abrasion resistance of the filled rubber.

Table 6-21: Abrasion resistance test results for compounds 36-38. (36) control compound, (37), filled rubber, (38) filled rubber with elemental sulphur.

Compound No.	Initial weight(gr.)	Final weight(gr.)	Weight loss(gr.)	DIN standard	Volume loss mm^3
36-1	1.7244	1.1650	0.5594	208	538
36-2	1.626	1.2006	0.4254	208	409
36-3	1.6314	1.1474	0.484	208	465
Mean value = 470.7			σ = 52.82		
37-1	2.1567	2.0548	0.1019	208	86
37-2	2.0718	1.9776	0.0942	208	79
37-3	2.0873	1.9981	0.0892	208	75
37-4	2.1249	2.0489	0.076	208	64
Mean value = 76			σ =7.97		
38-1	2.136	1.9816	0.1544	208	128
38-2	2.1588	2.01105	0.1483	208	123
38-3	2.119	1.9551	0.1639	208	136
38-4	2.1028	1.9578	0.145	208	120
Mean value = 126.8			σ =6.06		

Bound rubber and crosslink density of the cured rubbers

Table 6-22 and Figure 6-13 show the percentage increases in the weight of the rubber samples after immersion in toluene.

Table 6-23 shows that the rubber samples had taken up different amounts of toluene with time. For example, the amount of toluene absorbed by the control compound was 5.16 g, and by compounds 37 and 38, 3.27 and 3.20 g, respectively. The weight of the samples after drying were, 1.55 g for the control compound, 2.03 and 2.15 g for compounds 37 and 38, respectively.

Table 6-22: Increase in the weight of the rubber samples in toluene as a function of time. (36) control compound, (37) filled rubber with no elemental sulphur, (38) filled rubber with elemental sulphur.

	Increase in weight of the rubber sample(%)		
Time in toluene (h)	37	36	38
0	0	0	0
23.5	126.5	246.7	------
24.5	-----	-----	113.9
47.5	146.9	293.3	-----
65.5	-----	-----	136.3
71	151.2	309.7	-----
90.25	-----	-----	139
96	152.6	312.7	-----
114.75	-----	------	140.4
120.5	153.5	312.7	------
138.25	-----	-----	140.8
144	153.6	312.7	------
161.75	-----	-----	141.3
168.5	153.9	312.7	-----
186.25	-----	-----	143.5
193	154.97	312.7	-----
210.25	------	-----	143.5
217	154.97	312.7	----

These values were subsequently used to calculate the bound rubber content and crosslink density of the cured rubbers.

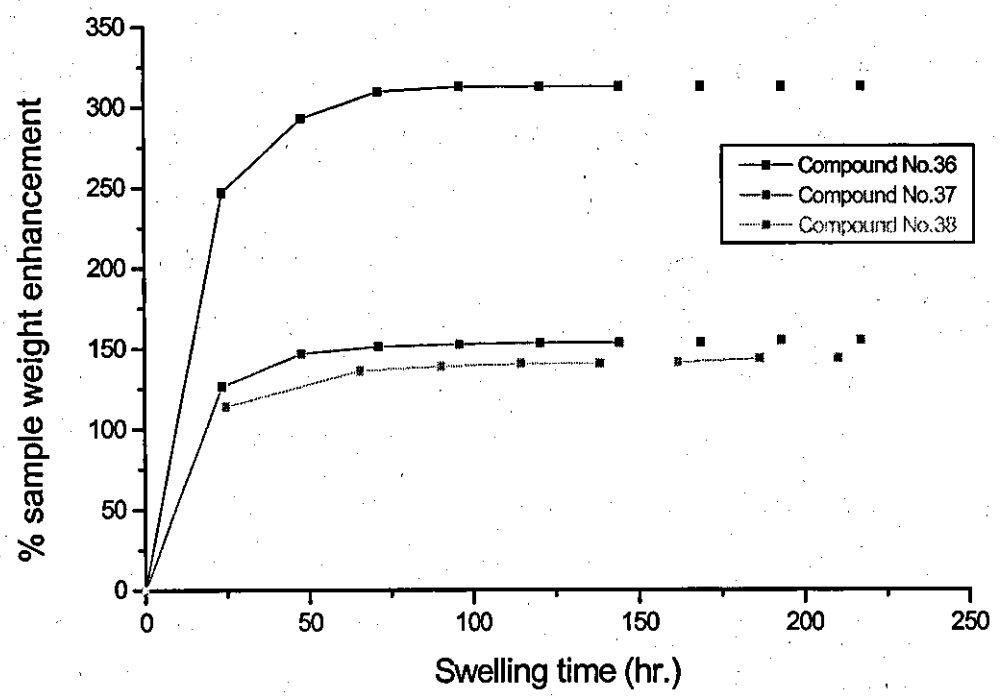

Figure 6-13: Increase in the weight of the rubber samples as a function of immersion time in toluene.

Table 6-23: Initial weight, equilibrium weight in toluene, weight after drying, crosslink density and Bound rubber measurements for compounds 36-38. (36) control compound, (37) filled rubber with no elemental sulphur, (38) filled rubber with elemental sulphur.

Compound No.	36	37	38
Initial weight (g)	1.65	2.11	2.23
Equilibrium weight (g)	6.81	5.38	5.43
Final weight (g)	1.55	2.03	2.15
Bound rubber, R_b (%)	----	94	94.3
Crosslink density (mol/m^3)	85	153	168

The bound rubber content for compounds 37 and 38 were almost the same, 94% and 94.3%, respectively, which indicated strong rubber/ filler interaction. It seems that the addition of elemental sulphur did not affect the bound rubber content.

The crosslink density of the filled rubbers (compounds 37 and 38) were 153 and 168 mol/m^3, which were twice as high as that of the control compound, which was 85 mol/m^3. It is worth remembering that the control compound had 1.5 phr elemental sulphur, which was equivalent to the 2.5 wt % sulphur in silanized silica. It is clear from these results that the filled rubbers had a lot more crosslinks in them than the control compound.

Tear properties

Figure 6-14 shows typical tearing force versus crosshead separation from the tear tests.

Table 6-24 shows the tearing force and their mean values which were calculated for the rubbers tested. For these tests, up to five test pieces were used.

Table 6-25 shows the tear energies, T, for the rubbers tested. The tear energy of the control compound was 15 kJ/m^2, whereas, the filled rubbers had tearing energies up to 62 kJ/m^2. It was interesting that the filled rubber with elemental sulphur (compound 38) had a lower tearing energy than compound 37. Clearly the addition of elemental sulphur was not beneficial to the tear strength of the filled rubber.

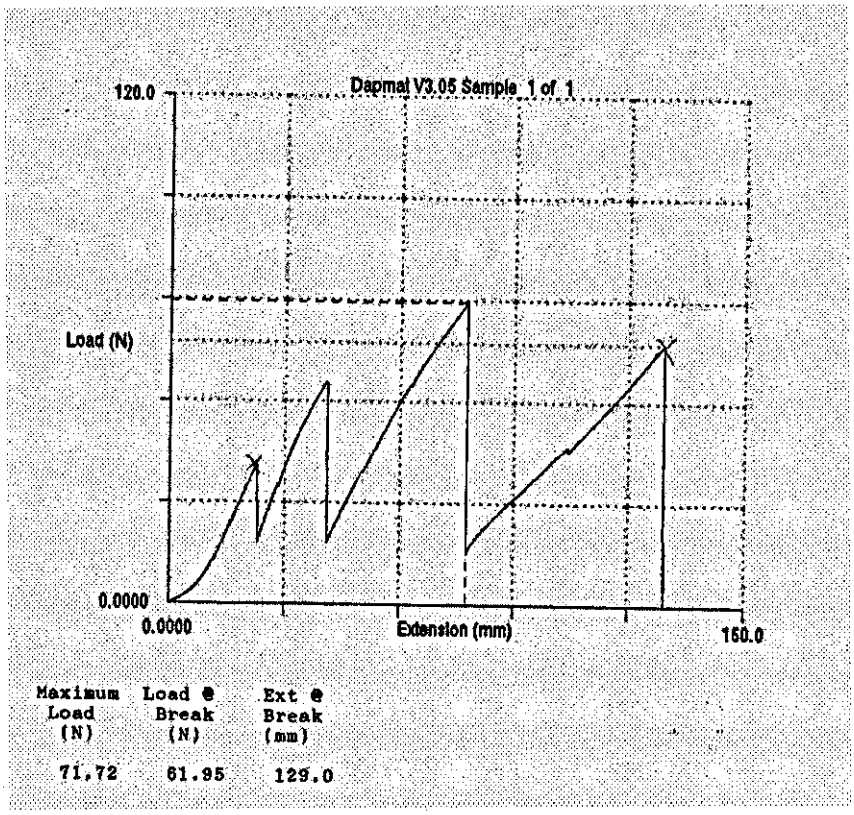

Figure 6-14: Typical tearing force versus crosshead separation from the tear test. Data for compound 37

Tensile properties of the cured rubbers

The tensile strength, elongation at break, and stored energy density at break of the rubbers are summarized in Table 6-26. Three dumb-bell test pieces were used for each compound. The tensile strength of the control compound was 17.4 MPa and increased to up to 37 MPa when the filler was added. Similarly, the stored energy density at break increased from 56 to 137 mJ/m^3 when silica was incorporated in the rubber. However, strain at break decreased from 11 for the control compound, to 7 for the filled rubbers. It must be noted that elemental sulphur had a detrimental effect on the tensile properties of the filled rubber. For example, tensile strength decreased by 7%, strain at break by 15% and stored energy density at break by 20 % because of the elemental sulphur in the filled

rubber. It is evident that the filler had significantly improved the tensile properties of the rubber.

Table 6-24: Tearing forces and their mean values from the tear tests. (36) control compound, (37) filled rubber with no elemental sulphur, (38) filled rubber with elemental sulphur.

Sample No.	$F_1(N)$	$F_2(N)$	$F_3(N)$	$F_4 - F_5(N)$	Mean(N)	σ
37-1	------	51.90	61.95	-------	56.93	5.03
37-2	------	53.57	------	-------	53.57	
37-3	84.19	------	------	-------	84.19	
37-4	109.6	------	------	-------	109.6	
37-5	------	51.90	64.81	-------	58.35	6.46
36-1	12.00	12.28	13.95	15.62	13.46	1.3
36-2	------	20.46	25.11	28.38	24.65	2.8
36-3	17.67	16.74	18.60	20.98	18.50	1.41
36-4	10.23	23.27	22.32	15.81	17.91	5.26
36-5	18.60	23.16	16.74	13.95 & 20.46	18.58	3.14
38-1	34.60	39.06	------	---------	36.83	2.23
38-2	------	75.26	------	-----	75.26	
38-3	82.59	------	------	-----	82.59	
38-4	------	58.59	------	-----	58.59	
38-5	------	88.50	------	-----	88.50	

Table 6-25: Tear energies of the rubber compounds. (36) control compound, (37) filled rubber with no elemental sulphur, (38) filled rubber with elemental sulphur.

Sample No.	Thickness (mm)	Mean thickness (mm)	Max. force (N)	Mean Force (N)	T=2F/d (kJ/m^2)	Mean	σ
37-1	2.32-2.36	2.34	71.72	56.93	48.65		
37-2	2.31-2.33	2.32	81.33	53.57	46.18		
37-3	2.33-2.35	2.34	84.19	84.19	71.96	62.38	18.6
37-4	2.30-2.33	2.315	109.6	109.6	94.68		
37-5	2.30-2.33	2.315	64.81	58.35	50.42		
36-1	2.46	2.46	15.62	13.46	10.94		
36-2	2.46	2.46	28.38	24.65	20.04	15.14	2.9
36-3	2.46	2.46	20.98	18.50	15.04		
36-4	2.46	2.46	23.27	17.91	14.56		
36-5	2.46	2.46	23.16	18.58	15.11		
38-1	2.50-2.55	2.53	42.30	36.83	29.11		
38-2	2.50-2.56	2.53	75.26	75.26	59.49	53.72	14.5
38-3	2.50-2.56	2.53	82.59	82.59	65.29		
38-4	2.44-2.55	2.50	70.30	58.59	46.87		
38-5	2.44-2.55	2.50	88.50	88.50	70.80		

Table 6-26: Tensile strength, elongation at break and stored energy density at break of the rubbers tested. (36) control compound, (37) filled rubber with no elemental sulphur, (38) filled rubber with elemental sulphur.

Sample No.	Width (mm)	Thickness(mm)	Extension at break (mm)	Strain at break	Max. load at break (N)	Tensile stress at break N/mm^2	Stored energy at break MJ/m^3
36-1	3.6	2.45	248	9.92	108	12.24	39.02
36-2	3.6	2.45	272.9	10.92	183.8	20.84	61.68
36-3	3.6	2.45	309.4	12.37	168.3	19.08	66.15
Mean values for compound 36			**276.8**	**11.07**	**153.4**	**17.38**	**55.62**
σ			**25.2**	**1**	**32.7**	**3.7**	**11.9**
37-1	3.6	2.3	209.3	8.372	308.5	37.26	142.3
37-2	3.6	2.3	215.0	8.602	306.6	37.03	140.89
37-3	3.6	2.3	201.0	8.041	295.0	35.63	130.52
Mean values for compound 37			**208.4**	**8.338**	**303.4**	**36.64**	**137.87**
σ			**5.7**	**0.23**	**6**	**0.72**	**5.3**
38-1	3.6	2.6	170.7	6.83	315.7	33.73	107.00
38-2	3.6	2.7	175.2	7.01	328.6	33.81	105.96
38-3	3.6	2.7	184.4	7.37	333.3	34.29	119.16
Mean values for compound 38			**176.8**	**7.07**	**325.9**	**33.94**	**110.71**
σ			**5.7**	**0.22**	**7.44**	**0.25**	**6**

Modulus at different strain amplitudes

Table 6-27 and Figure 6-15 show the tensile modulus at 50 % , 100 % , 200 %, 300 %, 400 %, and 500 % strain amplitudes for the three compounds. For each compound, three dumb-bell pieces were tested. The modulus is a measure of the rubber stiffness. The modulus of the control compound was 0.69 MPa and decreased to 0.62 MPa at 400 % strain amplitude. However, at 500 % strain amplitude, it reached 0.82 MPa. The modulus of the filled rubbers were significantly higher. For example, the filled rubber with no elemental sulphur, had a modulus of 2.03 at 50 % strain amplitude. This increased to 5.32 MPa when the strain amplitude reached 500 %. Similarly, the modulus of the filled rubber with elemental sulphur, increased from 2.95 to 5.44 MPa as the strain amplitude was increased to 500 %. The higher modulus of the filled rubber with elemental sulphur was due to a higher crosslink density, which made the rubber harder and stiffer.

Table 6-27: Modulus at different strains for compounds 36-38 (36=control, 37=without elemental sulphur, 38=with elemental sulphur)

Sample No.	Modulus at 50 % elongation	100 %	200 %	300 %	400 %	500 %	Modulus at break (MPa)
37-1	2.115	2.224	3.530	4.529	5.02	5.32	5.32
37-2	1.816	2.177	3.370	4.02	4.57	5.22	5.29
37-3	2.166	2.07	3.42	4.40	5.22	5.41	5.41
Mean	2.032	2.157	3.44	4.32	4.94	5.32	5.34
σ	0.15	0.6	0.07	0.22	0.27	0.08	0.05
36-1	0.722	0.49	0.48	0.54	0.58	0.77	4.00
36-2	0.722	0.56	0.48	0.56	0.67	0.93	7.82
36-3	0.640	0.53	0.45	0.52	0.62	0.76	5.31
Mean	0.69	0.53	0.47	0.54	0.62	0.82	5.71
σ	0.04	0.03	0.01	0.02	0.04	0.08	1.6
38-1	3.10	3.45	4.45	5.24	5.62	5.62	5.62
38-2	2.81	3.21	4.64	5.10	5.56	5.56	5.56
38-3	2.93	3.13	4.32	4.83	5.14	5.14	5.14
Mean	2.95	3.26	4.47	5.06	5.44	5.44	5.44
σ	0.12	0.14	0.13	0.17	0.21	0.21	0.21

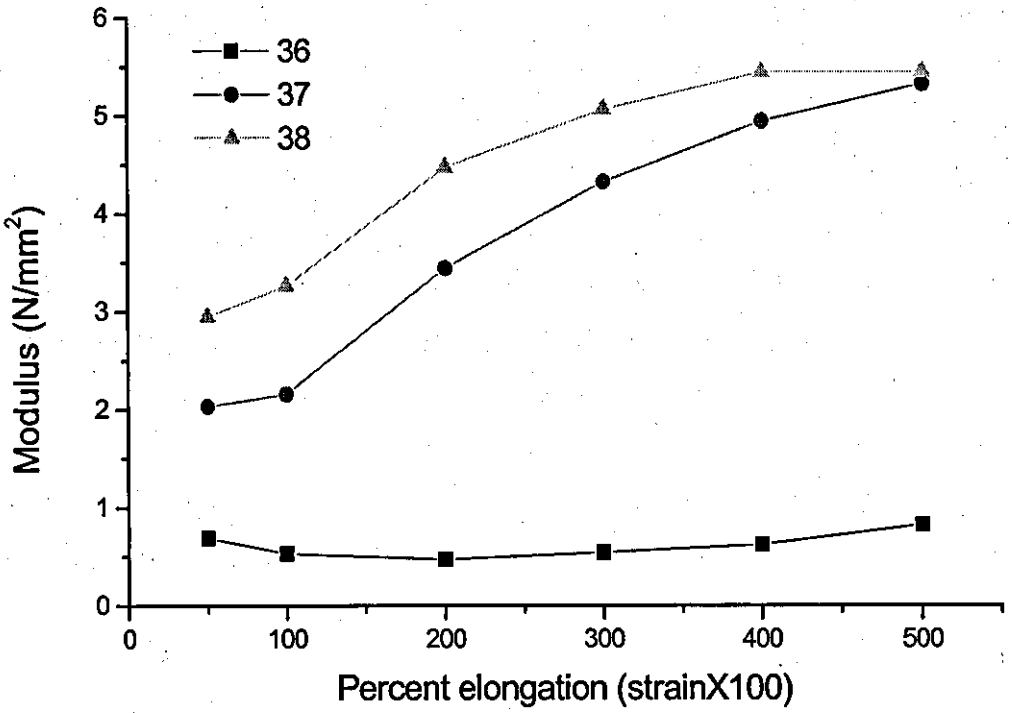

Figure 6-15: Tensile modulus at different strain amplitudes for compounds 36-38

Calculation of energy losses in the rubber

To calculate the energy losses in the rubber, dumb-bell test pieces were extended to 100 % of their original lengths and then returned to zero load to produce a load versus deflection trace. The load versus deflection data was changed into stress versus strain data, and the area between the extension and retraction curves was calculated. This was the total energy loss in the rubber at that maximum strain. To calculate the energy losses as a percentage of the total energy input in the rubber, this value was divided by the total energy stored in the rubber, calculated from the area under the extension curve. Figure 6-16 shows typical tensile stress versus strain data from which energy losses in the rubber were calculated.

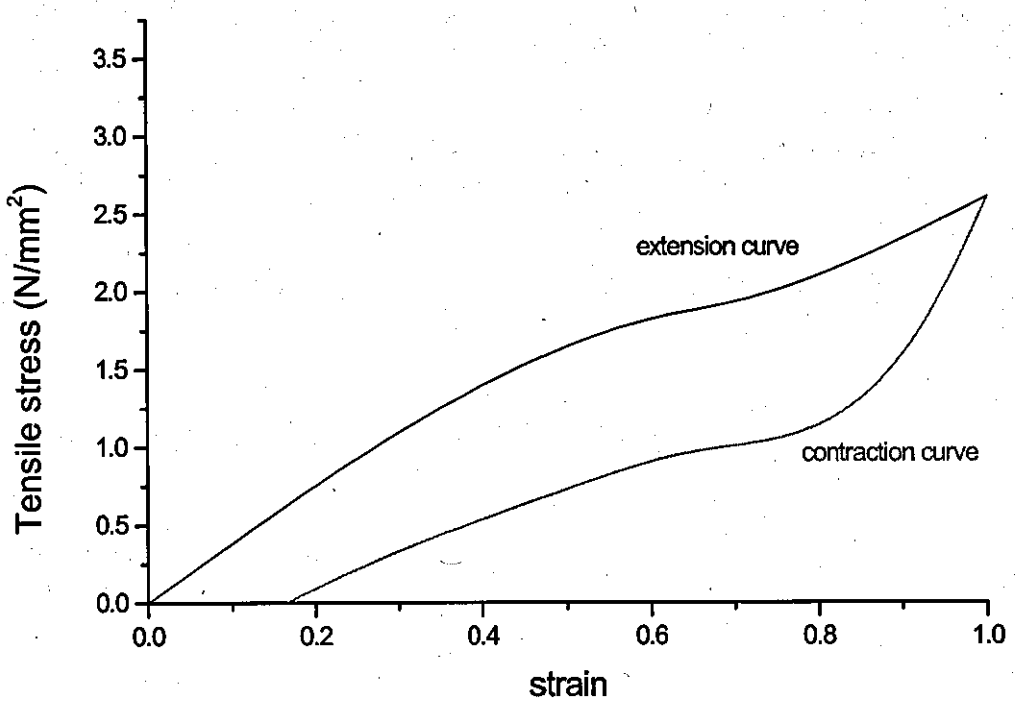

Figure 6-16: Tensile stress versus strain showing the hysteresis loop between the extension and retraction curves from which energy losses in the rubber were calculated. Data for compound 37.

Table 6-28 summarises all the results for the three rubber compounds. The largest energy loss, i.e. 52% was recorded for the filled rubber with no elemental sulphur. This was significantly higher that the value measured for the filled rubber with elemental sulphur, which was 38%. Clearly, adding elemental sulphur reduced the energy dissipation processes in the filled rubber. The energy losses in the control compound was almost 0.

Table 6-28: Energy losses in the rubber calculated as a percentage of total stored energy. (36) control compound, (37) filled compound with no elemental sulphur, (38) filled compound with elemental sulphur

Compound No.	Energy calculated from the area between the extension/retraction curves MJ/m^3	Total input energy calculated from the area under the extension curve MJ/m^3	Energy losses in the rubber as a percentage of the total input energy (%)
36	0.0	----	----
37	0.827	1.585	52
38	0.737	1.965	37.5

It is clear that measuring the area between the extension and retraction curves provides a useful method for calculating the energy losses in the rubber. However, other techniques such as tan δ measurements are by far more accurate and representative of the energy dissipation processes in the rubber and therefore, will be considered in the subsequent work.

Conclusions

- The filled NR rubber containing 60 phr silanized silica nanofiller needed 6 phr TBBS and 0.3 phr ZnO to optimize the reaction between the rubber reactive tetrasulphane groups of TESPT and the rubber.

- The incorporation of stearic acid in the filled rubber with TBBS and ZnO offered no benefit to Δtorque and the chemical bonding between the rubber and filler.

- The addition of elemental sulphur to the filled rubber with 6 phr TBBS and 0.3 phr ZnO increased the Δtorque value, which indicated benefit for the crosslink density of the rubber.

- The viscosity, hardness, tensile strength, elongation at break, stored energy at break, T, tensile modulus, and abrasion resistance of the rubber vulcanisate increased substantially when the filler was added. The improvement in the mechanical properties of the rubber was mainly due to high level of rubber-filler adhesion and high crosslink density that was produced by the chemical bonding between the rubber and TESPT. The bound rubber measurement also confirmed a strong rubber-filler adhesion.

- The tensile modulus of the three rubber vulcanisates increased as a function of the strain amplitude.

- When elemental sulphur was added to the filled rubber with 6 phr TBBS and 0.3 phr ZnO, the mechanical properties aforementioned, with the exception of the tensile modulus, deteriorated.

In summary, this novel technique for crosslinking and reinforcing NR with a silanized silica nanofiller has numerous advantages. It helps to optimize the reaction between the rubber and filler via TESPT by using the minimum amounts of TBBS and ZnO and eliminating stearic acid altogether. In addition, small amounts of elemental sulphur can be used to reduce the scorch and cure times of the rubber compound and shorten the cure cycle.

References

1) Hoffman W., *Rubber Technology Handbook*, Carl Hanser Verlag, Munich, Germany (1989).

2) Warrick E L, Pierce O R, Polmanteer K E, Saam J C,*Rubber Chem. Technol.***52**:437 (1979).

3) Hair M L., Hertl W, *J Phys. Chem.***74**:91 (1970).

4) Hockley J A, Pethica B A,*Trans Faraday Soc.* **57**:2247(1961).

5) Wolff S,GÖrl U, Wang M J, Wolff W, *Eur. Rubber J.* **16**:16(1994).

6) Wolff S, *Rubber Chem.Technol* **69**:325(1996).

7) Tan E H., Wolff S, Haddeman S M., Gretwatta H P, Wang M.,*Rubber Chem. Technol.* **66**:594(1993).

8) Dannenberg E M, *Rubber Chem. Technol.* **48**:410(1975).

9) Thongsang S, Sombatsompop N, *Polymer Composites* **27**:30(2006).

10) Parker D D, Koenic J L, *J. Adhesion* **73**:299(2000).

11) Ansarifar A, Nijhawan R, Nanapoolsin T, Song Mo, *Rubber Chem.Technol.* **76**:1290 (2003).

12) Ansarifar A, Azhar A, Song Mo, *J. Rubber Research* **6**:129(2003).

13) Ansarifar A, Azhar A, Ibrahim N, *International J. Adhesion and Adhesives* **25**:77 (2005).

14) British Standard,'Physical testing of rubber', part A64, BS 903-A64(1995).

15) Technical information, Degussa AG, D-60287, Frankfurt-Germany 6030.1(1994).

16) Brown P S., Porter M, Thomas A G, *Gummi Kunststoffe* **40**:17(1987).

17) Ansarifar A., Jain A, Nanapoolsin T J, *J. Rubber Res.* **5**:11(2002).

CHAPTER 7

Assessing effects of mixing parameters, silanized silica nanofiller, and different mass fractions of pure rubbers on the composition and mass fraction of interphases in blends of SBR/BR and NR/BR using MTDSC

7.1 Introduction

The formation of any heterogeneous system is accompanied by the formation of an interface (interphase) or boundary layer, which determines important properties of the systems, mainly the polymeric one [1]. Thermal diffusion between two miscible or partially miscible polymers results an interfacial phase developing. With increasing of the diffusion time, in most cases, the thickness of the interface will increase, and the concentration profile will change [2]. The interface is characterized by a two–dimensional array of atoms and molecules, which are impossible to measure, while the interfacial layer or interphase has a large enough assembly of atoms or molecules to have its own properties such as modulus, strength, heat capacity, density, etc [1].

According to Sharpe [3], interphase is a region intermediate for two phases in contact, the composition and/or structure and/or properties of which may be variable across the region, and which may differ from the composition and/or structure and/or properties of either of the two contacting phases. It is obvious that interphase is the result of molecular diffusion between pure phases.

The blends have a significant role in the tyre industry, which tries continuously to achieve a better compromise between wearing, rolling resistance and ice- and wet-grip (named magic triangle) properties of the tyre tread. Studying the interphase characteristics is essential to understand the rubber blend performance and durability.

Currently used instrumental techniques for the analysis of interfacial structures are Fourier transform-infrared spectroscopy(FT-IR), differential scanning calorimetry (DSC), dynamic mechanical spectroscopy (DMS), nuclear magnetic resonance (NMR), transmission electron microscopy (TEM), scanning electron microscopy (SEM), X-ray photoelectron spectroscopy (XPS), and gel permeation chromatography [4]. However, because the chemical structure of tyre tread rubbers are relatively similar, it is difficult to analyse their blend morphologies using some of above techniques including small-angle X-ray scattering technique [5]. Figure 7-1 shows typical optical microscopy sections of a SBR/BR blend (75/25 by weight ratio) filled with 60phr silanized silica nanofiller. As can be seen, it is almost impossible to distinguish phases and it is even more difficult to see interphases in the blend.

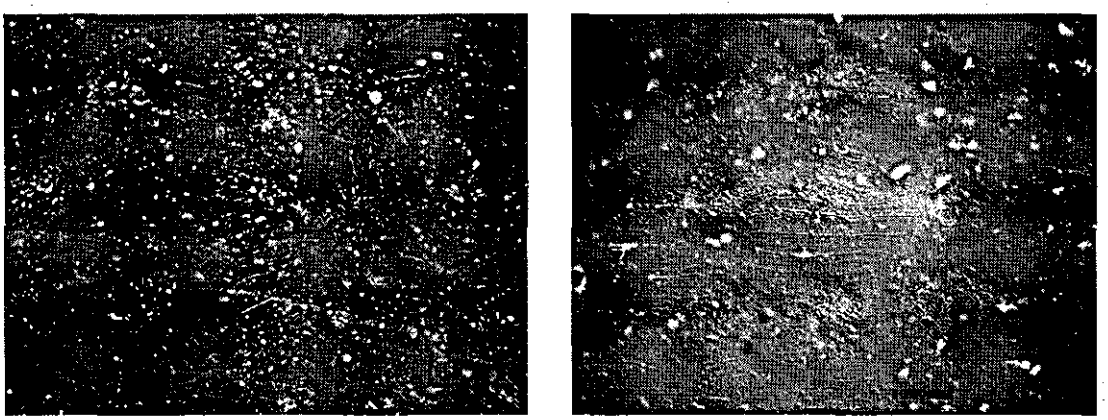

Figure 7-1: Typical optical microscopy sections of a SBR/BR blend (75:25 by mass) filled with 60phr silanized silica nanofiller

As mentioned earlier, a newly developed MTDSC technique has several advantages in comparison with conventional DSC[5]. For example, it is sufficiently sensitive and has good enough resolution to separate overlapping thermal events such as T_g and signals from interphases developing from partially miscible rubbers during blending [6]. This technique will be used to determine the mass fraction and composition of interphases in some SBR/BR and NR/BR blends.

7.2 Preparation of SBR/BR and NR/BR blends

SBR/BR and NR/BR blends were prepared in a Haake Rheocord 90 (Berlin-Germany), a small laboratory mixer with counter-rotating rotors. In these experiments, the Banbury rotors and the mixing chamber were maintained at the ambient temperature (~25°C), 50 and 100°C, and the rotor speed were 45 and 90 rpm. The volume of the mixing chamber was 78 cm^3 and it was 60 % full. The pure SBR and BR, and NR and BR rubbers, were mixed together for 10 and 30 minutes to produce blends. Haake software version 1.9.1 was used for controlling the mixing conditions and storing data. During mixing, the compound temperature rose above the temperature of the mixing chamber (Table 7-1). This was due to the mechanical work done on the rubber, which resulted in heat dissipation and temperature rises.

Table 7-1: Deviation from nominal rubber blending temperatures*

Rubber	Pure rubbers	NR-BR blends	SBR-BR blends
Deviation from nominal temperature ($^{\circ}C$)	10-13	11-15	11-16

** Nominal temperatures, 25, 50 and 100 $^{\circ}C$.*

7.3 Background of the analysis

Figure 7-2 shows dC_p/dT versus temperature for the physical mixture of the two pure SBR and BR rubbers (75/25 wt %) which was smoothened at 3 $^{\circ}C$.

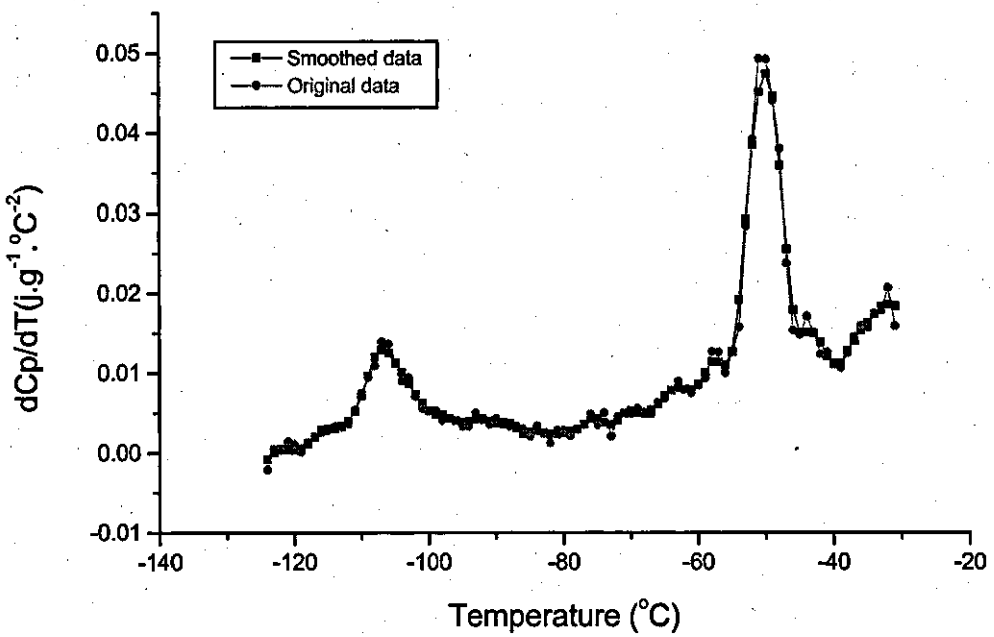

Figure7-2: Original and smoothened data at 3°C for the physical mixture of pure SBR and BR rubbers (75:25 by mass)

The change of heat capacity, Cp, vs. temperature, and dCp/dT vs. temperature for the NR/BR (50:50) blend and for a physical mixture of the two samples of NR and BR (50:50) are shown in Figures 7-3 and 7-4, respectively. The increase of increment of heat capacity, ΔCp, at the glass transition temperature of both rubbers can be seen in Figure 7-3. The value of ΔCp for a component is proportional to its mass fraction in the system under investigation. The heat capacity vs. temperature can not provide information about the interphase glass transition temperature and its composition distribution but the dCp/dT vs. temperature data (Figure 7-4) can provide that information [6].

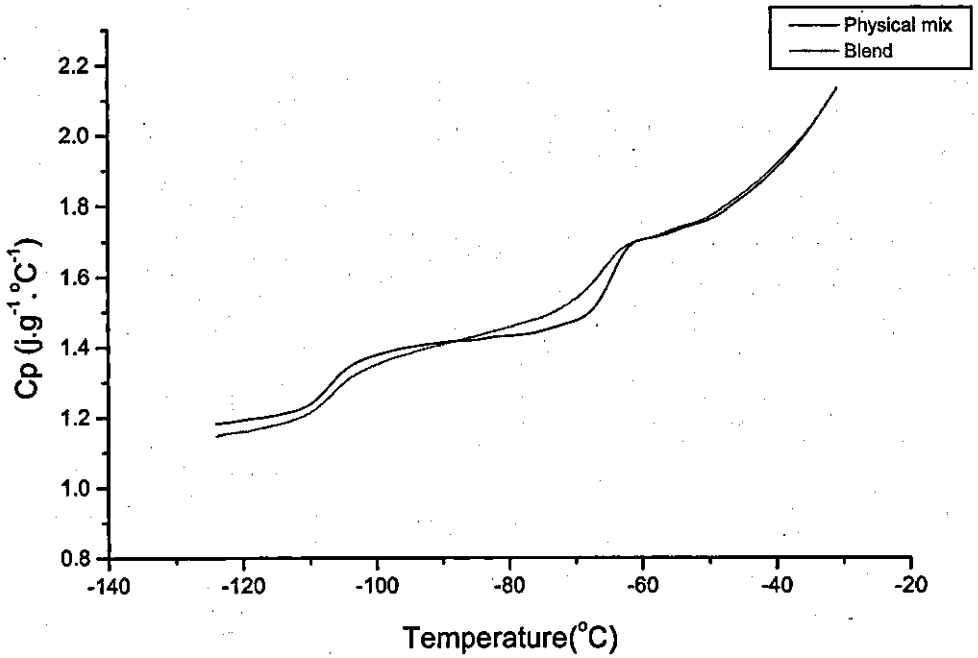

Figure 7-3: C_p versus temperature for NR/BR (50:50 by mass) blend and NR/BR (50:50 by mass) physical mixture. Samples prepared at 50°C for 30 min.

Figure 7-4 shows dCp/dT vs. temperature for a diffuse interphase in the NR/BR (50:50) blend prepared at 50°C for 30 minutes, and for a physical mixture of the two pure NR and BR samples (50:50) prepared in the same way, respectively. The data in this figure shows that the value of the dCp/dT vs. temperature for the NR/BR blend is larger than that for the pure NR and BR samples (physical mixture) between the glass transition temperatures of NR and BR. The NR/BR blend has a single interphase, and this interphase does not exhibit a separate glass transition temperature, but occurs continually between the glass transition temperatures of the constituent rubbers.

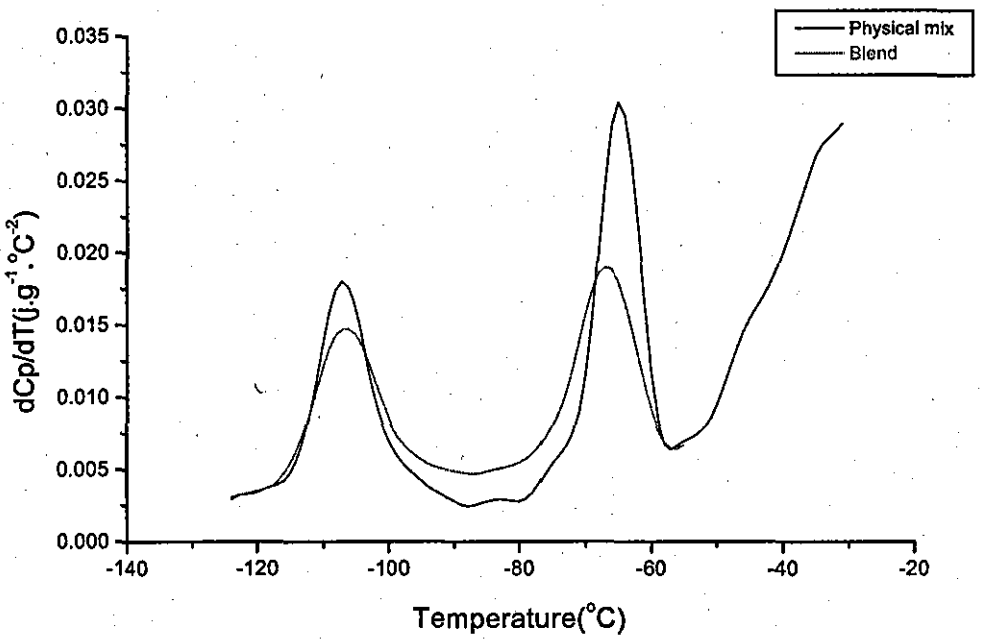

Figure 7-4: dCp/dT versus temperature for NR/BR (50:50 by mass) blend and NR/BR (50:50 by mass) physical mixture. Samples prepared at 50°C and for 30 min.

The dCp/dT vs. temperature signal can be described by a Gaussian function for polymers and miscible polymer blends. However, the dCp/dT vs. temperature signals for the rubber 1 + rubber 2 physical mixture can not be described well by the sum of two Gaussian functions because of the shift of the baseline between the glass transition temperatures. Thus, the dCp/dT vs. temperature signal includes a non baseline for multi-phase systems, e.g. see Figure 7-5. Because a Gaussian function was used for the quantitative analysis of interphase in these multi-phase systems, the non-constant baseline had to be corrected.

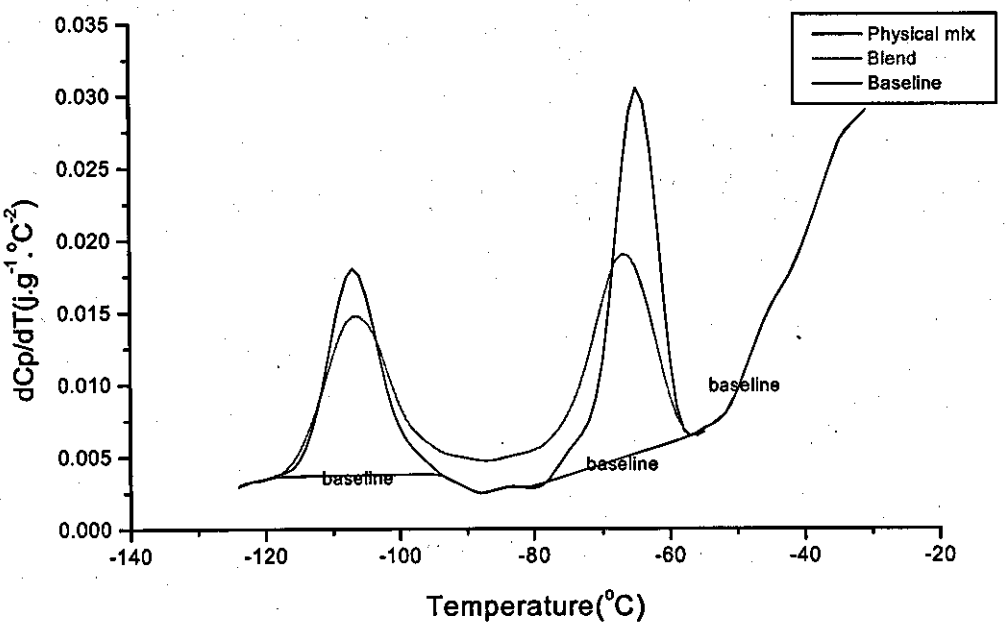

Figure7-5: dCp/dT versus temperature for NR/BR (50:50 by mass) blend and NR/BR (50:50 by mass) physical mixture, showing a baseline. Samples prepared at 50°C for 30 min.

The values of the dCp/dT vs. temperature signal for rubbers 1 and 2 physical mixtures above and below the two glass transition temperatures are considered as the baseline for the dCp/dT signal of these multi-phase systems. For the glass transitions, baselines which were linear with temperature from the starting and end points of the glass transition temperature peaks were chosen. An example is given in Figure 7-5 for the NR/BR (50:50) blend. When the dCp/dT vs. temperature signal is analysed using a multi-Gaussian function for multi-phase systems, this baseline must be subtracted from the raw dCp/dT vs. temperature signal.

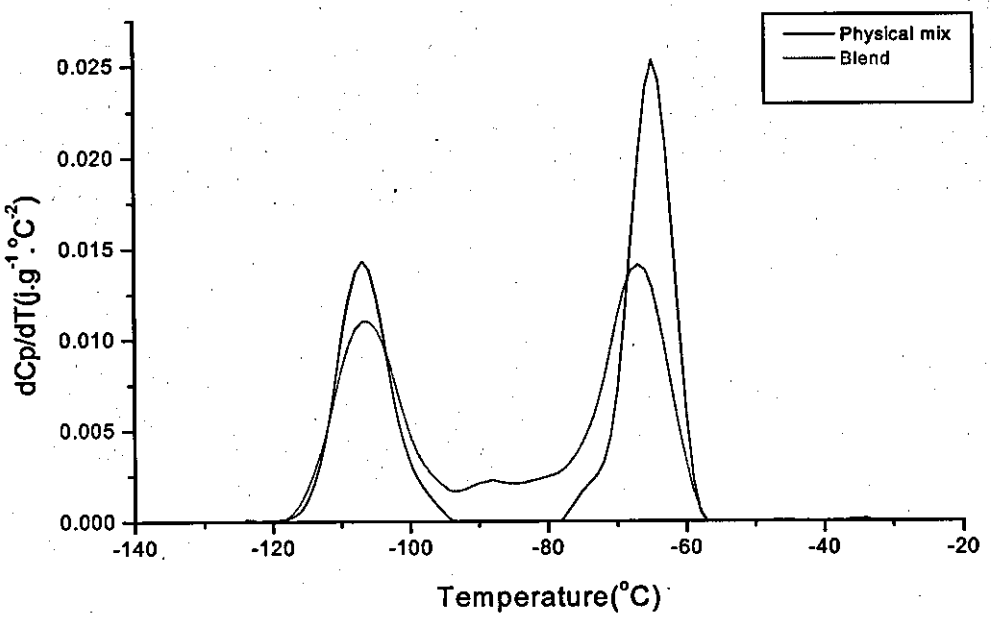

Figure7-6-a: dCp/dT versus temperature for NR/BR (50:50 by mass) blend and NR/BR (50:50 by mass) physical mixture after baseline correction in Figure 7-5. Samples prepared at 50 ^0C for 30 min.

Figure 7-6-a shows the corrected differential of heat capacity, dCp/dT, vs. temperature signal for the NR/BR (50:50) blend and the NR/BR (50:50) physical mixture after 30 minutes at 50°C. For an interphase, the differential of heat capacity with temperature, dCp/dT, may be considered as the sum of "i" sub systems with individual glass transition temperature for each sub-system, as follows:

$$\sum [dCp/dT]_{\text{interphase}} = \sum [dCp/dT]_i = \sum_{i=1}^{N} \frac{\Delta Cp_i}{[\omega_{di}(\pi/2)^{0.5}]\exp[\frac{-2(T-T_{gi})^2}{(\omega_{di})^2}]} \quad (7\text{-}1)$$

where N is less than 10, ΔC_{pi} is the increment of heat capacity, T_{gi} is the glass transition temperature, and ω_{di} is the half width of the ith sub-system in interphase [6].Using Eq. (7-1), the interphase can be analysed quantitatively. Figure 7-6-b shows typical interphase region after baseline correction and peak resolution. Finally, an interphase curve was obtained (Figure 7-7) by subtracting the blend curve from a Gaussian simulation of the same blend curve shown in Figure 7-6.

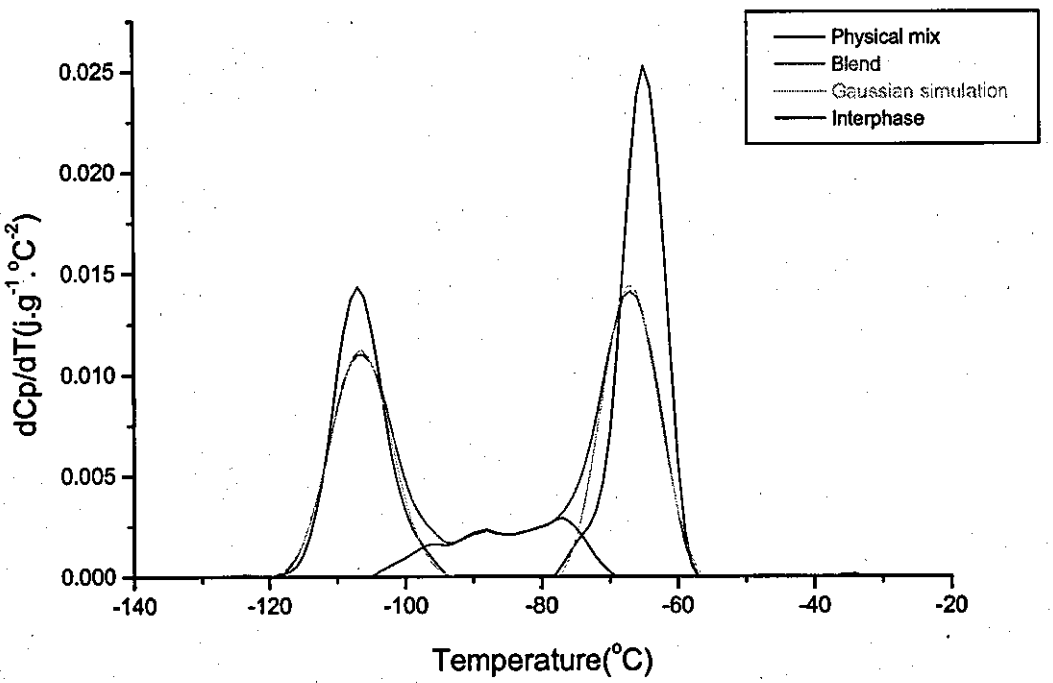

Figure 7-6-b: dCp/dT versus temperature for NR/BR (50:50 by mass) blend after peak resolution in Figure 7-5 showing the interphase region.

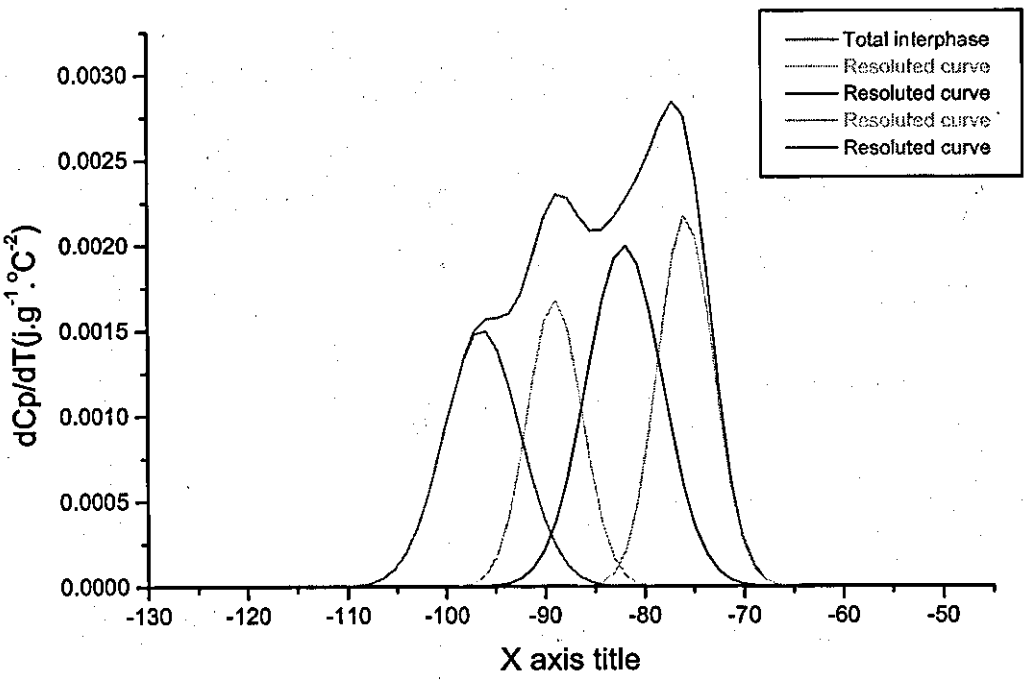

Figure 7-7 : dCp/dT versus temperature for interphase of NR-BR (50-50 phr) for blending temperature and time, 50 $^{\circ}C$ and 30 min. respectively.

After determining the area under the curve of physical mixture for individual peaks as well as simulated Gaussian one, the following equations may be used to determine the mass fraction of interphase and it's composition [2].

$$\delta_1 = \omega_{10}(1-\frac{\Delta Cp_1}{\Delta Cp_{10}}) \qquad (7\text{-}2)$$

$$\delta_2 = \omega_{20}(1-\frac{\Delta Cp_2}{\Delta Cp_{20}}) \qquad (7\text{-}3)$$

where δ_1 and δ_2 are the mass fractions in the interphase of rubbers 1 and 2,

respectively, ω_{10} and ω_{20} are the mass fraction of the rubbers before mixing, ΔCp_1 and ΔCp_2 are increments of dC_p/dT at glass transition temperatures of pure rubbers in blend (area under curve of Gaussian simulation curve), ΔCp_{10} and ΔCp_{20} are increments of dC_p/dT at glass transition temperatures of pure rubbers (area under curve of physical mixture).The amount of interphase in a blend is given as follows:

$$\text{Percent of interphase} = \frac{\text{Amount of interphase}}{\text{Total amount of blend}} \times 100 = (\delta_1 + \delta_2) \times 100 \qquad (7\text{-}4)$$

It is important to get the ΔCp value accurately. The quantity ΔCp is defined as follows:

$$\Delta Cp = \int_{T_i}^{T_e} [dC_p / dT]\, dT \qquad (7\text{-}5)$$

where Ti and Te are the initial and final values of the temperature in the glass transition region (see Figure 7-6-b). Thus, according to equation 7-5, it is possible to obtain accurate ΔCp values experimentally [7].
This method of analysis was justified by Hourston and Mo song [5-7].

7.4 Results and Discussion

7.4.1. Effect of different mixing times and temperatures on the mass fraction and composition of the interphase in the SBR/BR and NR/BR blends

Understanding how increases in mixing time and temperature affect the mass fraction of interphase and its composition in blends of dissimilar and partially

miscible rubbers is of significant importance in optimising adhesion development at rubber-rubber interfaces and ultimately the final properties of rubber blends [8-9].

Table 7-2 shows the effect of temperature changes on the mass fraction of the interphase in the NR/BR (50:50) and SBR/BR (50:50) blends after 10 minutes mixing.

Table 7-2: Composition and mass fraction of interphases in NR/BR and SBR/BR blends prepared at different temperatures for 10 min.

System	NR/BR (50:50)	NR/BR (50:50)	SBR/BR (50:50)	SBR/BR (50:50)
Temperature ($°C$)	25	100	25	100
I* (%)	0	22.9	0	39
I**		(NR=49%,BR=51%)		(SBR=%88, BR=12%)
I***		0.96		7.33

I* Mass fraction of the interphase
I** Composition of the interphase
I*** Mass fraction of NR to BR and SBR to BR in the blends
The mass fraction of the rubbers in the interphase was calculated as follows:
For NR/BR, 49/51=0.96, and for SBR/BR, 88/12=7.33

For these blends, the mass fraction of the interphase was 0% at 25°C and then increased to approximately 23% and 39%, respectively at 100°C. The mass fraction of NR to BR and SBR to BR in the interphase were 0.96 and 7.33, respectively at this temperature. Clearly an increase in mixing temperature was beneficial to the formation of an interphase in each blend.

Figure 7-8 shows the mass fraction of interphase in the SBR/BR and NR/BR blends as a function of nominal temperature. It is clear that the SBR/BR blend benefited more from increases in temperature.

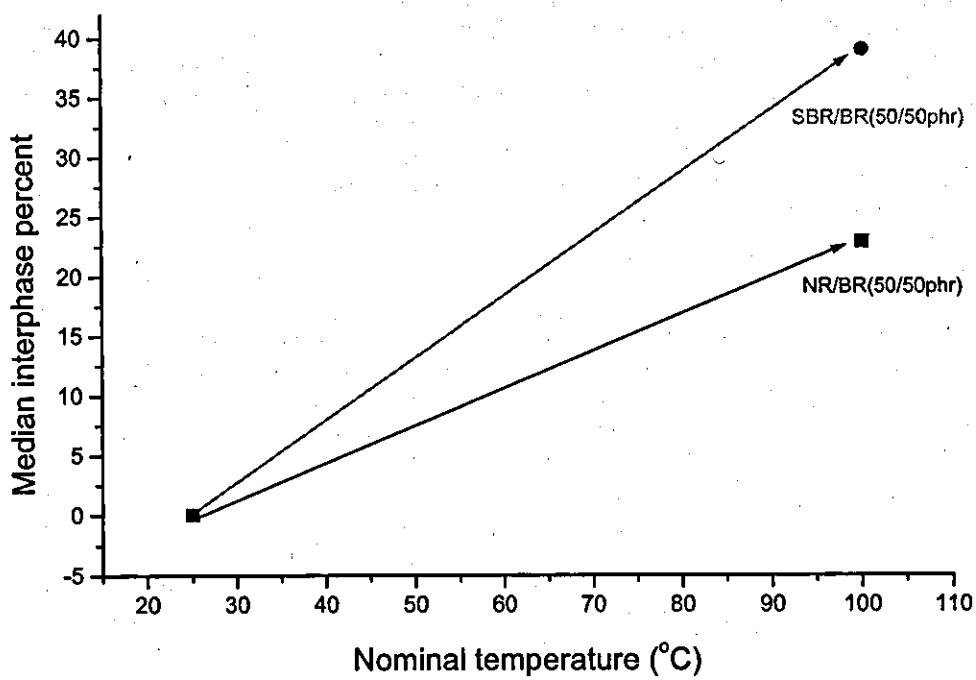

Figure 7-8: Mass fraction of the interphase in SBR/BR (50:50) and NR/BR (50:50) blends prepared at different temperatures for 10 min.

A similar trend was also seen when the temperature was increased from 50 to 100°C at 30 minutes mixing time. For the NR/BR (50:50) blend, the mass fraction of the interphase was 16.5% at 50 °C, and approximately 24% at 100°C, respectively. The mass fraction of NR to BR in the interphase also increased from 3.76 to 6.69, respectively. Evidently, a longer mixing time and a higher mixing temperature increased the mass fraction of the interphase and altered its composition in these blends (Table 7-3).

Table 7-3: Composition and mass fraction of interphases in NR/BR and SBR/BR blends prepared at different temperatures for 30 min

Blend	Temperature (°C)	I*(%)	I**	I***
NR-BR	50	16.5	(NR=79%, BR=21%)	3.76
NR-BR	100	23.4	(NR=80%7, BR=13%)	6.69
SBR-BR	50	49	(SBR=83.5%, BR=16.5%)	5.06
SBR-BR	100	44	(SBR=79%, BR=21%)	3.76

I* Mass fraction of the interphase
I** Composition of the interphase
I*** Mass fraction of NR to BR and SBR to BR in the blends

Figure 7-9 shows the mass fraction of interphase as a function of temperature. As can be seen, the mass fraction of the interphase in the SBR/BR blend did not benefit from increases in temperature whereas, that of the NR/BR blend did.

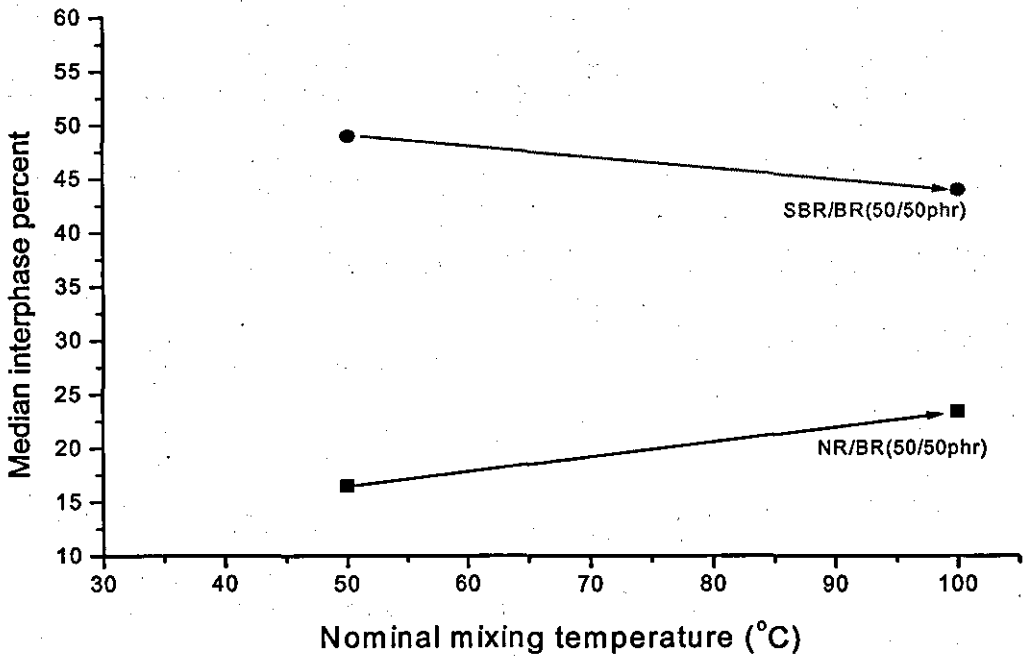

Figure 7-9: Mass fraction of the interphase in SBR/BR (50:50) and NR/BR (50:50) blends prepared at different temperatures for 30 min.

When mixing time was increased from 10 to 30 minutes at 100°C, the mass fraction of the interphase for the SBR/BR (50:50) blend rose from 39% to 44%. However, the increase for the NR/BR (50:50) blend was only 0.5% (Table 7-4). Interestingly, the effect of temperature rise on the composition of the interphase was even more significant. For the NR/BR blend, the mass fraction of NR to BR in the interphase rose from 0.96 to 6.69, as the temperature was raised, whereas for the SBR/BR blend, the mass fraction of SBR to BR in the interphase decreased from 7.33 to 3.76, indicating a substantial change in the make up of the interphase layers.

Table 7-4: Composition and mass fraction of interphases in NR/BR and SBR/BR blends prepared at different mixing times and at 100°C.

Blend	Mixing time (min)	I*(%)	I**	I***
NR-BR	10	22.9	NR=49%, BR=51%	0.96
NR-BR	30	23.4	NR=87%, BR=13%	6.69
SBR-BR	10	39	SBR=88%, BR=12%	7.33
SBR-BR	30	44	SBR=79%, BR=21%	3.76

I* Mass fraction of the interphase
I** Composition of the interphase
I*** Mass fraction of NR to BR and SBR to BR in the blends

7.4.2. Effect of rotor speed on the mass fraction and composition of the interphase in the SBR/BR and NR/BR blends

One important factor in optimising filler dispersion and improving rubber blend properties is rotor speed, which helps to control the level of shear stresses in rubber compounds during mixing. Two rotor speeds were used in these experiments, i.e. 45 and 90 r.p.m. The mixing temperature and mixing time were 100 °C, and 30 minutes, respectively. For the SBR/BR (50:50) blend, the mass fraction of the interphase was 44% at 45 r.p.m., and subsequently decreased to approximately 39% at 90 r.p.m. The mass fraction of SBR to BR in the interphase also reduced from 3.76 to 0.96 as the rotor speed was increased. Similarly, for the NR/BR (50:50) blend, the mass fraction of the interphase decreased from 23% to 20% as a function of rotor speed, and there was no change at all in the mass fraction of NR to BR in the interphase, which remained essentially unchanged at 6.69, irrespective of the rotor speed (Table 7-5). An increase in the rotor speed was detrimental to the mass fraction of the interphase and altered its composition, at least for the SBR/BR blend.

Table 7-5: Composition and mass fraction of the interphase in the SBR/BR and NR/BR blends as a function of the rotor speed. Blends were prepared at 100°C for 30 min.

Blend	Rotor speed (rpm)	I* (%)	I**	I***
NR/BR(50:50)	45	23.4	NR=87%, BR=13%	6.69
NR/BR(50:50)	90	20	NR=87%, BR=13%	6.69
SBR/BR(50:50)	45	44	SBR=79%, BR=21%	3.76
SBR/BR(50:50)	90	38.7	SBR=49%, BR=51%	0.96

I* Mass fraction of the interphase
I** Composition of the interphase
I*** Mass fraction of NR to BR and SBR to BR in the blends

Figure 7-10 shows the mass fraction of interphase as a function of rotor speed. Increasing the rotor speed has had an adverse effect on the mass fraction of the interphase in both blends.

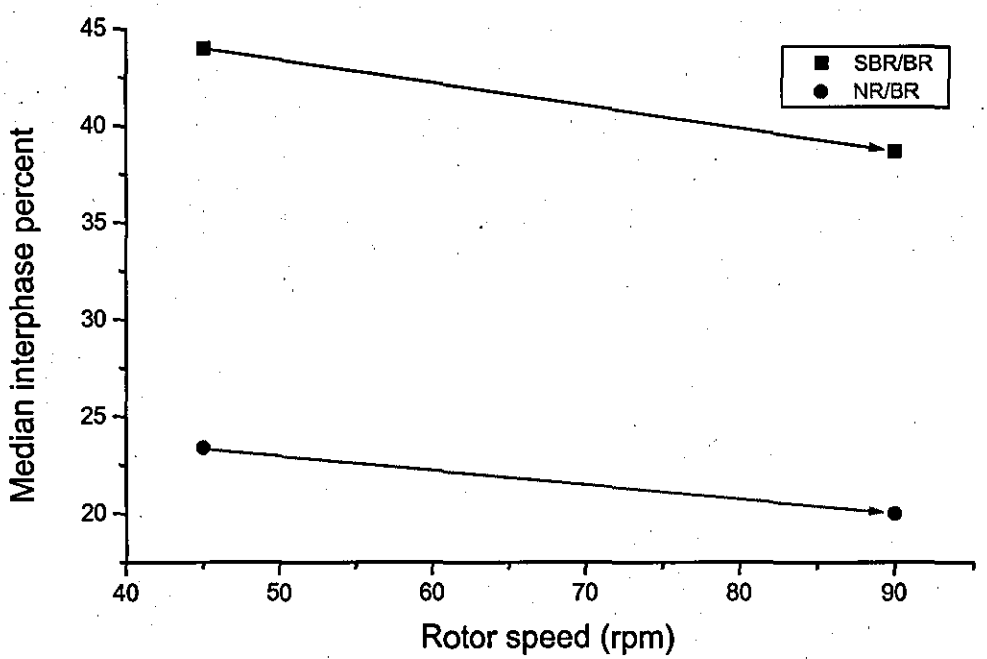

Figure 7-10 Mass fraction of the interphase in the SBR/BR and NR/BR blends as a function of the rotor speed. Blends were prepared at 100^{0}C for 30 min.

7.4.3. Effect of different mass fractions of pure SBR and BR rubbers on the mass fraction and composition of the interphase in the SBR/BR blend

Altering the mass fraction of pure rubbers in blending may affect the mass fraction and composition of the interphase in the blend. Five SBR/BR (50:50, 60:40, 75:25) blends were prepared at 50 and 100°C mixing temperatures and 30 minutes mixing time. For the SBR/BR (50:50) blend at 100°C (Table 7-6), the mass fraction of the interphase was 44%. However, when the mass fraction of pure SBR and BR in the blend was increased to 60:40 and 75:25, the mass fraction of the interphase decreased to 41 and 31.2%, respectively. Evidently, an increase in the mass fraction of pure SBR was not beneficial to the mass fraction of the interphase in the blend. Moreover, the mass fraction of SBR to BR in the interphase also decreased from 3.76 to 1.56, in spite of using a significantly larger mass of SBR in the blending process.

When the SBR/BR (50:50) and (75:25) blends were prepared at 50°C for 30 minutes, the mass fraction of the interphase and its composition were substantially affected. For the SBR/BR (50:50) blend, the mass fraction of the interphase was 49%, and for the SBR/BR (75:25) blend, it was 22.2%. The mass fraction of SBR to BR in the interphase also reduced from 5.06 to 1.40 (Table 7-6).

Figure 7-11 shows mass fraction of the interphase in the SBR/BR blend as a function of the mass fraction of pure SBR to pure BR. Evidently, when the mass fraction of pure SBR to pure BR increases, this adversely affects the mass fraction of the interphase in the blend.

Table 7-6: Composition and mass fraction of interphase in the SBR/BR blend as a function of mass frcation of pure SBR and BR rubbers in the belnds. Blends were prepared at 50 and 100°C for 30 min.

Blend	Temperature (°C)	I* (%)	I**	I***
SBR/BR (50:50)	50	49	SBR=84%, BR=16%	5.25
SBR/BR (75:25)	50	22.2	SBR=58%, BR=42%	1.38
SBR/BR (50:50)	100	44	SBR=79%, BR=21%	3.76
SBR/BR (60:40)	100	41	SBR=77%, BR=23%	3.35
SBR/BR (75:25)	100	31.2	SBR=61%, BR=39%	1.56

I* Mass fraction of the interphase
I** Composition of the interphase
I*** Mass fraction of NR to BR and SBR to BR in the blends

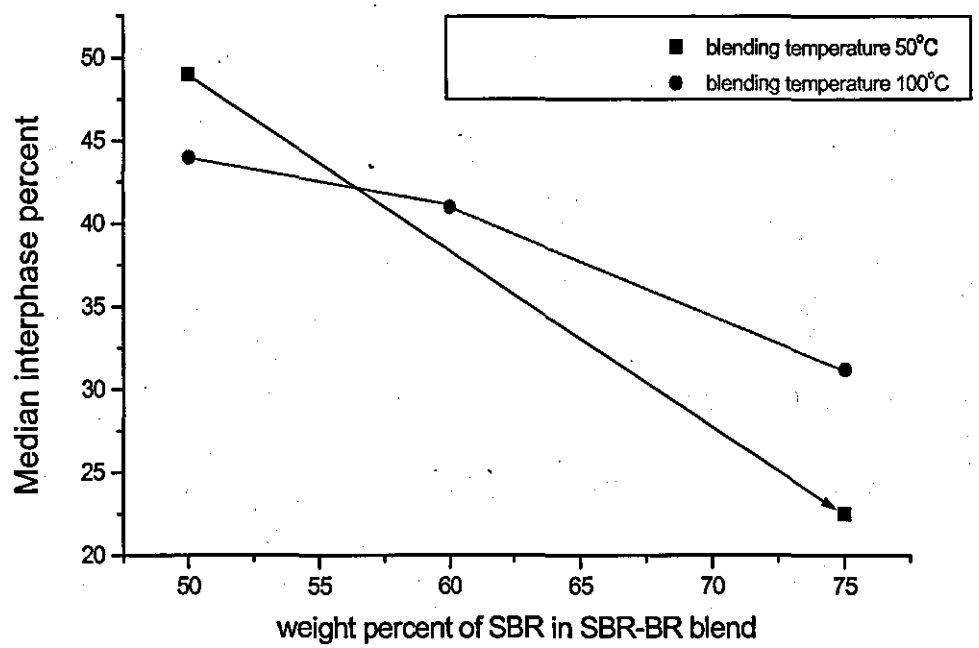

Figure 7-11: Mass fraction of the interphase in the SBR/BR blend as a function of mass fraction of pure SBR to pure BR. Blends were prepared at 50 and 100°C for 30 min.

7.4.4. Effect of silanized silica nanofiller on the mass fraction and composition of the interphase in the SBR/BR blend

Silanized silica nanofiller is used extensively in green tyres where SBR and BR rubbers are blended [10]. To investigate the effect of this filler on the mass fraction of the interphase and its composition in the SBR/BR blend, raw SBR and BR rubbers and 60 phr silica were mixed for 30 minutes at 100°C to produce SBR/BR (60:40) and SBR/BR (75:25) blends (Table 7-7). In addition to these blends, SBR/BR (60:40) and SBR/BR (75:25) blends with no silica filler were also made. For the SBR/BR (60:40) blend, the mass fraction of the interphase increased from 41 to 60% when silica was added. However, the mass fraction of SBR to BR in the interphase decreased from 3.35 to 2.57, which indicated a change in the composition of the interphase. Similarly, for the SBR/BR (75:25) blend, the mass fraction of the interphase also increased from 31.2 to 50%, and the mass fraction of SBR to BR in the interphase increased from 1.56 to 3.17 as a result of incorporating silica in the rubbers. It appeared that for both blends the mass fraction of the interphase benefited from the filler and at the same time its composition changed.

7.4.5. Empirical equations for the prediction of mass fraction of interphases in the rubber blends

From the results, it may be assumed that the dependence of the mass fraction of interphase upon mixing time and temperature for the NR/BR (50:50) blends could be expressed as following:

Table 7-7: Composition and mass fraction of interphase in the SBR/BR blends filled with 60 phr silica nanofiller. Blends were prepared at 100°C for 30 min.

Blend	Mixing time (min)	Temperature ($°C$)	I*	I**	I***
SBR-BR (75:25)	30	100	31.2	SBR=%61, BR=%39	1.56
SBR/BR (75:25) with 60phr silica	30	100	50	SBR=%76, BR=%24	3.17
SBR/BR(60:40)	30	100	41	SBR=%77, BR=%23	3.35
SBR/BR (60:40) with 60 phr silica	30	100	60	SBR=%72,BR=%28	2.57

I* Mass fraction of the interphase
I** Composition of the interphase
I*** Mass fraction of NR to BR and SBR to BR in the blends

$$I_f = At^a T^b + C \qquad (7\text{-}6)$$

where I_f is the mass fraction of the interphase in the blend, t is the mixing time, and T is the mixing temperature. A, a, b, and C are constant coefficients for a given blend.

After substituting the experimental results in equation 7-6 and finding the best possible graphical fit to the data, an empirical equation (7-7) for the NR/BR is found:

$$I_f = 0.0215 t^{0.02} T^{0.504} \qquad (7\text{-}7)$$

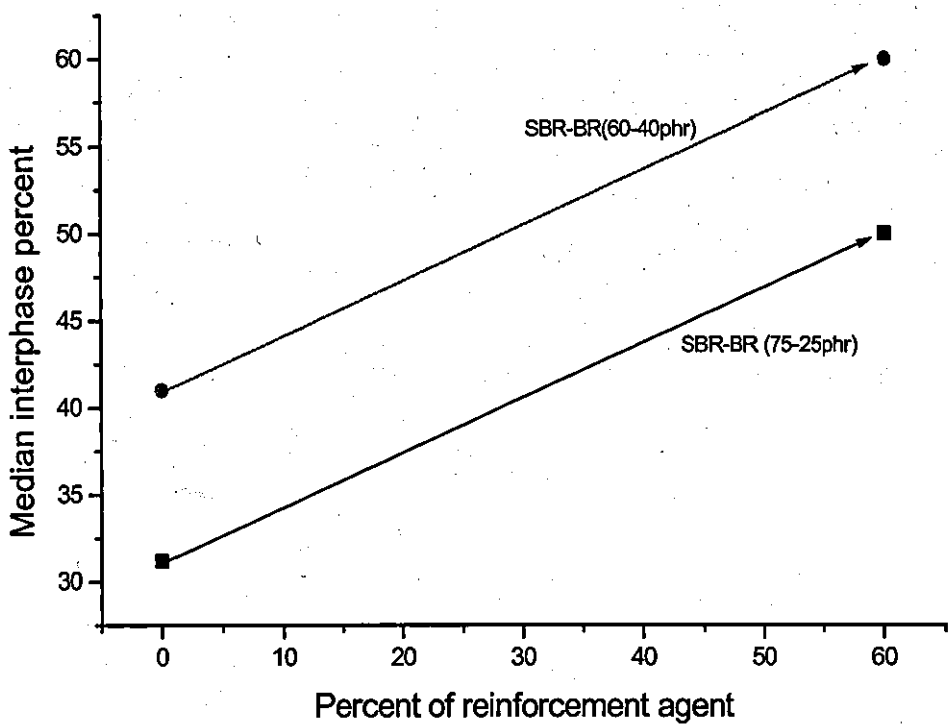

Figure 7-12: Composition and mass fraction of interphases in the SBR/BR blends filled with 60 phr silica nanofiller. Blends were prepared at 100 ^{0}C for 30 min.

This equation is valid for the NR/BR (50:50) blend, for mixing times 10-30 min and mixing temperatures 50-100 °C and, therefore, may be used to calculate the mass fraction of the interphases in these blends.

Finally, it is worth mentioning that the SBR and BR rubbers had similar viscosities, i.e. 51 and 49 MU, respectively, whereas NR, had a much higher viscosity of 97 MU (Table 5-1). Since the rubber viscosities were different, this might have affected the dispersion of the NR/BR blend components and formation of the interphase between the two rubbers [11]. A future study will examine the effect of rubber viscosity on the formation of interphases between these rubbers.

Conclusions

From this work, it is concluded that for the NR/BR (50:50) and SBR/BR (50:50) blends:

- At 10 minutes mixing time, a rise in temperature from 25 to 100 °C increased the mass fraction of the interphase in the NR/BR (50:50) and SBR/BR (50:50) blends.

- At 30 minutes mixing time, a rise in temperature from 50 to 100 °C increased the mass fraction of the interphase in the NR/BR (50:50) blend, and reduced it in the SBR/BR (50:50) blend.

- At 100°C mixing temperature, an increase in mixing time from 10 to 30 minutes, increased the mass fraction of the interphase in the NR/BR (50:50) and SBR/BR (50:50) blends. The increase for the latter was more significant.

The rotor speed also influenced the mass fraction and composition of the interphase in the blends. For the SBR/BR (50:50) and NR/BR (50:50) blends:

- At 100°C mixing temperature and 30 minutes mixing time, the mass fraction of the interphase decreased for both blends as the rotor speed was increased from 45 to 90 r.p.m.

When the mass fraction of pure SBR to BR rubbers changed in the SBR/BR blend, the mass fraction and composition of the interphase were significantly affected. It emerged that:

• At 50 and 100°C mixing temperatures and 30 minutes mixing time, the mass fraction of the interphase decreased progressively as the mass fraction of SBR to BR in the SBR/BR blend increased from 50:50 to 75:25.

When 60 phr silanized silica nanofiller was incorporated in the raw SBR/BR blend at 100°C for 30 minutes, the mass fraction of the interphase changed. It was concluded that:

• For the SBR/BR (60:40) and SBR/BR (75:25) blends, the mass fraction of the interphase increased. Note that in all cases, the composition of the interphase in the blends also changed.

In summary, MTDSC was found to be a useful technique for measuring the mass fraction of the interphase and estimating its composition in the SBR/BR and NR/BR blends.

References

1) Vasile C, Kulshreshtha k., *Hand book of polymer blends and composites*, rapra technol. **3A**:103(2003).

2) Hourston D J, Song M., Hammiche A, Pollack H.M., Reading M., *Polym.***38**:(**1**) 1(1997).

3) Sharpe L., In *"The interfacial interactions in polymeric composites"*, Akovali Ei. G.Kluwer Academic publishers, Dordrecht, The Netherlands **1**(1993).

4) Ishida H, Jang J, *Die Makromolekulare chemie, Macromolecular symposia* **22**:191(1998).

5) Hourston D J., Song Mo, *J. Appl. Polym. Sci.* **76**:1791(2000).

6) Song M, Hourston D J., Reading M., .Pollock H M, Hammiche A., *J. Thermal analysis and calorimetry* **56**:991(1999).

7) Song Mo, Hourston D J, Schafer F U , *Polym* **40**:5773(1999).

8) Voyutskii S S, Vakula V L, *J. Appl. Polym. Sci.*7:475(1963).

9) Jabbari E, Peppas N A, *Polym* **36**(**3**):575(1995.

10) Okel T A, Waddell W H, *Rubber Chem. Technol.* **67**:217(1994).

11) Mangaraj D, *Rubber Chem. Technol.* **75**:365(2002).

CHAPTER 8

Measuring the composition and mass fraction of interphases in blends of SBR/BR rubbers filled with silanized silica nanofiller using MTDSC

8.1 Introduction

The main objective of blending two or more dissimilar polymers together is to reduce cost and to improve the physical and mechanical properties of the rubbers. Elastomers are often blended to reduce hysteresis losses [1]. In some cases, rubber blends are used to improve air retention, pre-selectivity (membranes), and resistance to vapor ingress [2]. Keller used a blend of chlorobutyl (CR), nitrile (NBR) and polybutadiene (BR) rubbers in tyre tread compound to reduce rolling resistance [3]. Hirakawa [4] used a blend of NR with SBR and BR to improve poor tack (auto-adhesion) of the SBR and BR rubbers. Silicone elastomers are blended with other elastomers for enhanced bio-compatibility [5]. Both NR and synthetic polysioprene (IR) suffer from deficiencies such as poor resistance to ozone and heat aging and poor corrosion resistance. Rankin [6] has shown that these deficiencies can be overcome by using a blend of chlorinated ethyelene-propylene diene rubber (EPDM) with NR or IR.

From a blending point of view, polymers can be divided into three categories: miscible, immiscible, and partially miscible. Miscible blends lead to a homogeneous rubbery phase with single glass transition temperature. For example, blends of NBR rubber and poly vinyl chloride (PVC) are in this category [7]. Unfortunately, most of polymers are immiscible with two or more glass transition temperatures (depending upon the individual polymers in the blend), or partially miscible, with a range of glass transition temperatures [8]. In addition, there is limited information available on the effect of fillers such as silica on the properties of interphases in SBR/BR blends.

In this chapter, the composition and mass fraction of interphases in some blends of SBR and BR rubbers filled with silanized silica nanofiller were measured using MTDSC. The silica filled SBR and BR rubbers were prepared individually and then mixed together to produce the SBR/BR blends. Effects of mixing time and mixing temperature on the interphases properties were investigated.

8.2 Experimental

8.2.1 Materials - Rubbers, nanofiller, and curing chemicals

The raw rubbers used, nanofiller, and curing chemicals were described in sections 5.1.1 and 5.1.2.

The oil was added to reduce the rubber viscosity, and the antidegradant to protect the rubbers against environmental ageing. The cure system consisted of TBBS, zinc oxide, and elemental sulphur, which were added to fully crosslink the rubbers.

Two SBR and BR rubber compounds filled with 60 parts per hundred rubber by weight (phr) silica were prepared and then mixed together to produce SBR/BR (75:25 by mass) blends for his study (Tables 8-3, 8-4 and 8-6). The mass fraction of SBR to BR in typical SBR/BR tire tread blend compounds is 75 to 25 [9]. The BR rubber needed 7.5 phr TBBS and 0.3 phr elemental sulphur, and the SBR, 3 phr TBBS and 0.5 phr ZnO to fully cure. The procedures for preparation of individual rubbers and measuring TBBS, zinc oxide, and elemental sulphur in these compounds were described previously [10,11].

8.2.2 Mixing

The compounds were prepared in a Haake Rheocord 90 (Berlin, Germany), a small size laboratory mixer with counter rotating rotors. The rotor speed was 45 r.p.m., and the volume of the mixing chamber was 78 cm^3, and it was 60% full.

Haake Software Version 1.9.1. was used for controlling the mixing condition and storing data.

To prepare the SBR compounds, TBBS, zinc oxide, elemental sulphur, and antidegradant were added 4 min after the filler and rubber were mixed together, and mixing continued subsequently for an extra 6 min before the rubber compound was removed from the mixer. To mix the BR compounds, the filler was placed in the mixing chamber, and then the raw rubber was added. TBBS, elemental sulphur, and the antidegradant were added together 10 min after the filler and rubber were mixed together, and the mixing continued subsequently for an extra 6 min before the rubber was removed from the mixer.

Finally, when mixing ended, the rubber compound was recovered from the mixer and milled to a thickness of about 6 mm for further work. The compounds were kept at ambient temperature (~23°C) for at least 24 h before their viscosity and cure properties were measured.

8.2.3 Assessment of the silica dispersion in the rubbers

In order to select a suitable mixing time for incorporating the filler in the rubbers, the rubber and filler were mixed together for different times. The filler was introduced first in the mixer, and then the raw rubber was added. The filler was added when the viscosity of the rubber was still relatively high, which lead to an improved dispersion[12]. The mixing time was increased to 16 min to disperse the silica particles fully in the rubber. The temperature of the rubber compounds during mixing increased from 23 (ambient) to 105°C. Twenty four hours after mixing ended, the rubbers were examined in an scanning electron microscope (SEM) to assess the filler dispersion as described in section 5.15.

8.2.4 Mooney viscosity, specific gravity, and cure properties of the rubber compounds

The viscosity of the rubber compounds was measured at 100 °C in a single-speed rotational Mooney viscometer as described in section 5.5 and in accordance with the British Standard[13]. The scorch time, which is the time for the onset of cure, and the optimum cure time, which is the time for the completion of cure, were determined from the cure traces generated at 140 ± 2°C by an oscillating disc rheometer curemeter (ODR) at an angular displacement of ± 3° and a test frequency of 1.7 Hz [14]. The cure rate index, which is a measure of the rate of cure in the rubber, was calculated using the method described previously [15]. The rheometer tests ran for up to 2 h.

8.2.5 Glass transition temperature and mass fraction of the interphase in the blends

The procedure was described in section 5.12.

The T_g of the pure rubbers (Table 5.1) and the mass fraction of the interphase and its composition for the SBR/BR blends were subsequently calculated for different mixing times and temperatures.

8.3 Effect of an increasing loading of elemental sulphur on the cure properties of BR and SBR rubbers filled with silica nanofiller, TBBS and ZnO

When the cure properties of the SBR and BR compounds were measured, the optimum cure times were different [10,11]. Before the two compounds were mixed together to produce SBR/BR blends, the optimum cure times had to be the same. To prepare SBR and BR compounds with the same optimum cure times, five BR compounds (Table 8-1) and three SBR compounds (Table 8-2) were prepared with the loading of elemental sulphur increasing from 0.1 to 0.7 phr in the former, and from 0 to 0.2 in the latter.

Table 8-1: Formulations and ODR test results for the BR rubbers with 60 phr silica, 7.5 phr TBBS and an increasing loading of elemental sulphur

Compound No.	1	2	3	4	5
Elemental sulphur (phr)	0.1	0.2	0.3	0.4	0.7
ODR Results					
Minimum torque (dN m)	44	42	45	44	43
Maximum torque (dN m)	139	130	133	130	171
Δtorque (dN m)	94	88	88	87	129
Scorch time, t_{s1} (min)	5.4	5.4	5.1	5.3	5.1
Optimum cure time, t_{90} (min)	52	57	49	46	50
Cure rate index (min^{-1})	2.1	1.9	2.3	2.5	2.2

Table 8-2 shows the formulations of the three compounds (compounds 6-8), which were prepared to assess effect of an increasing loading of elemental sulphur on the cure properties of the SBR compound.

After the ODR test results were examined, 0.3 phr elemental sulphur was sufficient to produce a BR compound (compound 3; Table 8-1) with the similar optimum cure time as the SBR compound with 0 elemental sulphur (compound 6; Table 8-2). These compounds were subsequently mixed together to produce SBR/BR blends, and the composition and mass fraction of interphases in these blends were measured.

Table 8-2: Formulations, Mooney viscosity and ODR results: SBR with 60phr silica, 3 phr TBBS, 0.5 phr ZnO, 1 phr Santoflex 13, 5 phr processing oil and an increasing loading of elemental sulphur. Compound 6 had a viscosity of 109 MU.

Compound No.	6	7	8
Elemental sulphur (phr)	0	0.1	0.2
ODR Results			
Minimum torque (dN m)	23	23	21
Maximum torque (dN m)	66	69	70
Δtorque (dN m)	43	46	49
Scorch time, t_{s1} (min)	12	12	11
Optimum cure time, t_{90} (min)	49	43	37
Cure rate index (min^{-1})	2.7	3.2	3.8

8.4 Silica dispersion in the rubbers

To disperse the silica particles fully in the rubbers, the mixing time was increased to 16 min. Large silica aggregates approximately 144 nm were seen in the rubber matrix after short mixing times, e.g. 4 min (Fig. 8-1), and the aggregate size decreased to about 74 nm in size as mixing time was increased to 16 min (Fig. 8-2). The size of the particles in Figure 8-2 was fairly similar to the actual particle size of the filler (20-54 nm). It was concluded that maximum mixing times of 10 and 16 minutes were sufficient to fully disperse the silica particles in the SBR and BR rubbers, respectively.

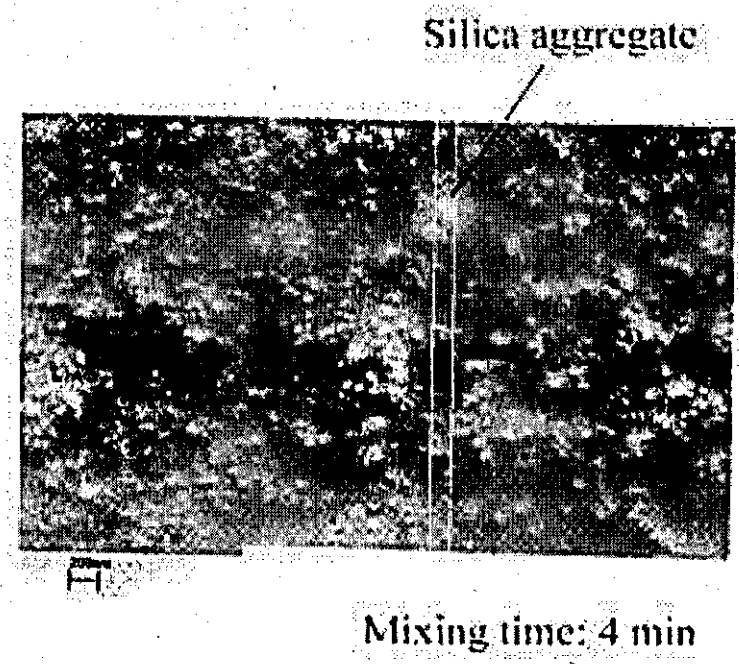

Figure 8-1: SEM photograph showing a typical poor dispersion of the silica particles in the rubber (mixing time = 4 min). Data for the BR rubber are shown.

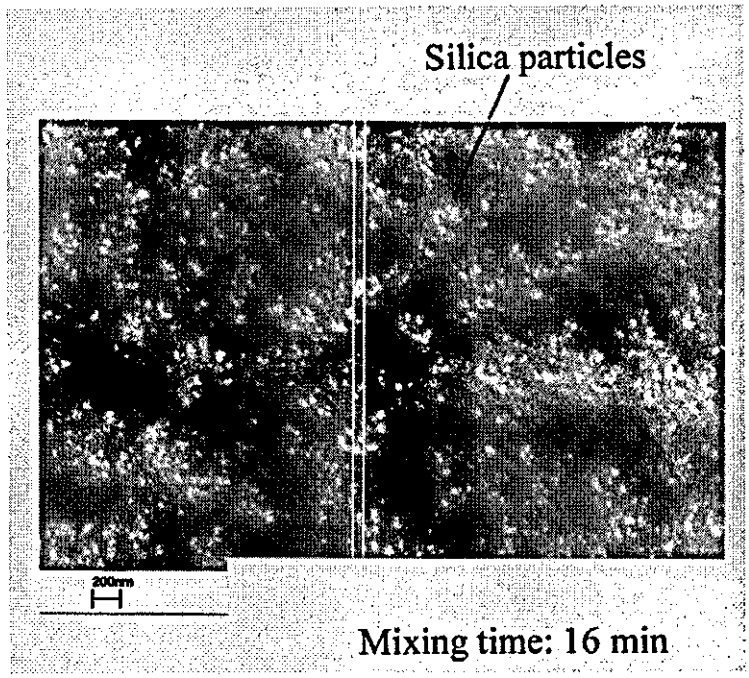

Figure 8-2: SEM photograph showing a typical good dispersion of the silica particles in the rubber (mixing time = 16 min). Data for the BR rubber are shown.

8.5 Results and discussion

The differential of heat capacity with temperature, dCp/dT, vs. temperature data for the SBR/BR blend and for a physical mixture (samples of pure SBR and BR rubbers placed in physical contact) of the two samples of SBR and BR is shown in Figure 8-3. The increase of increment of heat capacity, ΔCp, at the glass transition temperature of both rubbers for a component is proportional to its mass fraction in the system under investigation. The heat capacity, Cp, vs. temperature can not provide information about the interphase, glass transition temperature and its composition distribution, but the dCp/dT vs. temperature data (Fig. 8-3) can provide that information [16].

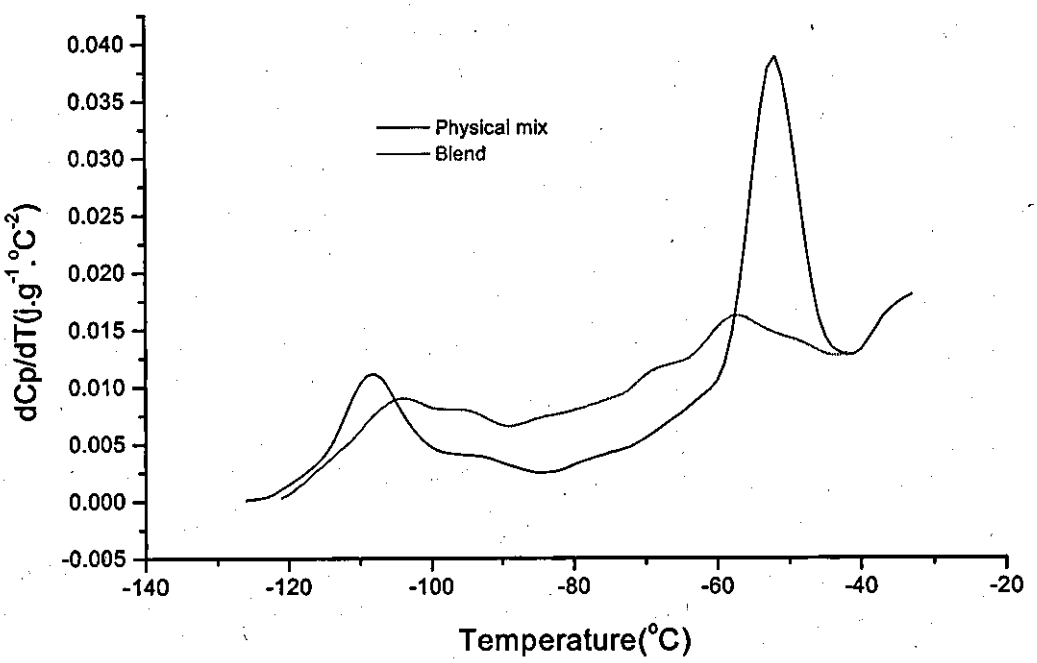

Figure 8-3: Typical dCp/dT versus temperature for SBR/BR blend and SBR/BR physical mixture. Samples were mixed at 60-65 ^{0}C for 5 min.

Figure 8-3 shows dCp/dT versus temperature for a diffuse interphase in the SBR/BR blend prepared at 60-65°C for 5 minutes, and for a physical mixture of the two pure SBR and BR samples (75:25) prepared in the same way, respectively. The data in this figure shows that the value of dCp/dT vs. temperature for the SBR/BR blend is larger than that for the pure SBR and BR samples (physical mixture) between the glass transition temperatures of SBR and BR. The SBR/BR blend has a single interphase and this interphase does not exhibit a separate glass transition temperature, but occurs continually between the glass transition temperatures of the constituent rubbers.

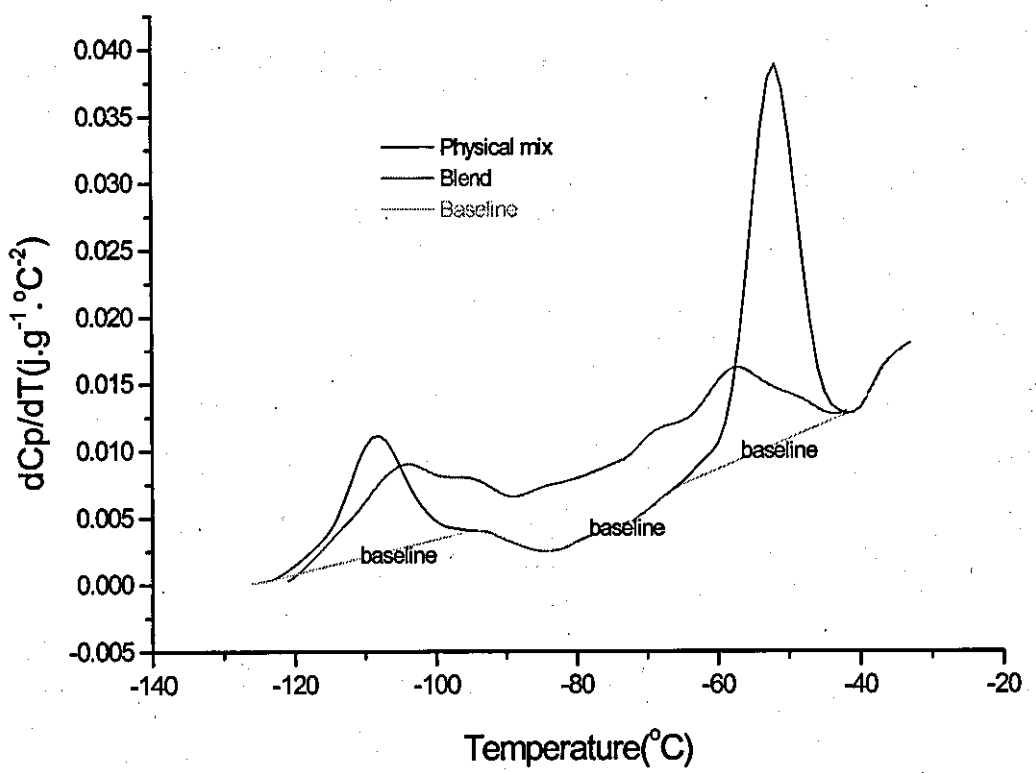

Figure 8-4: Typical dCp/dT versus temperature for SBR/BR blend and SBR/BR physical mixture and correspondent baseline. Samples were mixed at 60- 65 ^{0}C for 5 min.

As It was described in section 7.4, the dCp/dT, vs. temperature signal can be described by a Gaussian function for pure polymers and miscible polymer blends. However, the dCp/dT vs. temperature signals for the rubber 1 + rubber 2 physical mixture can not be described well by the sum of two Gaussian functions because of the shift of the baseline between the glass transition temperatures. Thus, the dCp/dT vs. temperature signal includes a non baseline for multi-phase systems (Fig. 8-3). Because a Gaussian function was used for the quantitative analysis of interphase in these multi-phase systems, the non-constant baseline had to be corrected.

The values of the dCp/dT vs. temperature signal for rubbers 1 and 2 physical mixtures above and below the two glass transition temperatures are considered as the baseline for the dCp/dT signal of these multi-phase systems. For the glass transitions, baselines which are linear with temperature from the starting and end points of the glass transition temperature were chosen. An example is given in Figure 8-4 for the blend. When the dCp/dT vs. temperature signal is analysed using a multi-Gaussian function for multi-phase systems, this baseline must be subtracted from the raw dCp/dT vs. temperature signal. Figure 8-5 shows the baseline corrected dCp/dT, vs. temperature signal for the blend and the physical mixture after 5 minutes at 60-65°C.

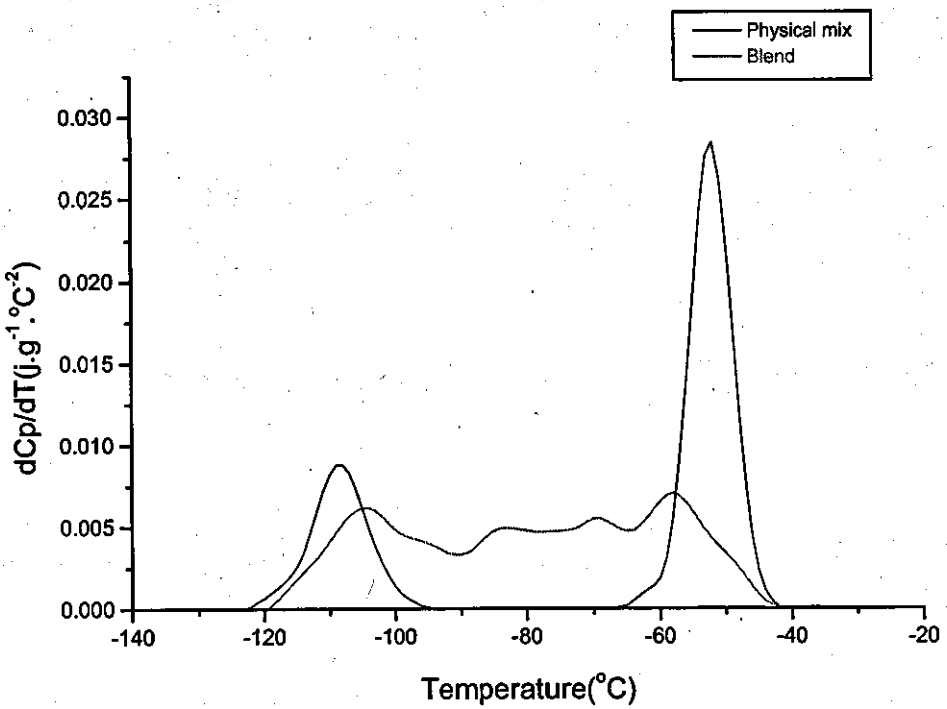

Figure 8-5 : Typical dCp/dT versus temperature for SBR/BR blend and SBR/BR physical mixture after baseline correction in Figure 8-4. Samples were mixed at 60- 65°C for 5 min.

Figure 8-6 shows typical interphase region after baseline correction and peak resolution. Finally, an interphase curve was obtained by subtracting the blend curve from a Gaussian simulation of the same curve (Fig. 8-7).

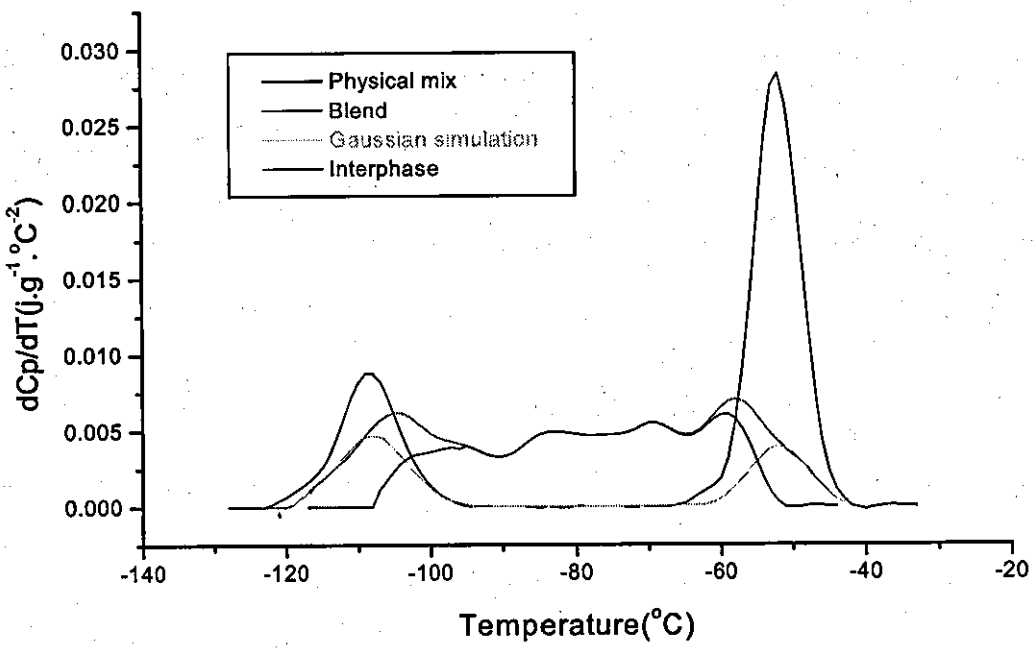

Figure 8-6 :Typical dCp/dT versus temperature for SBR/BR blend after peak resolution in Figure 8-5 showing the interphase region

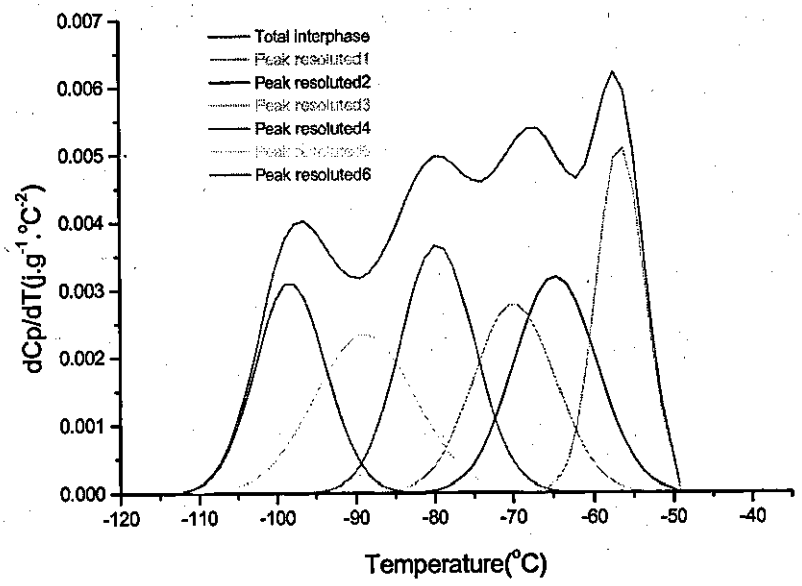

Figure 8-7: Typical dCp/dt versus temperature for SBR/BR blend showing typical interphase obtained by subtracting the blend curve from Gaussian simulation of the same curve. The area under the curve is a measure of the mass fraction of the interphase.

Sample was prepared at 60-65 ^{0}C for 5 min.

After determining the area under the curve of physical mixture for individual peaks as well as simulated Gaussian one, the mass fraction of interphases and their composition were calculated as it was described in section 7.3.

8.5.1 Effect of the mixing time of the SBR and BR compounds on the cure properties, mass fraction and composition of the interphase in the SBR/BR blend

The ODR test results of the two SBR and BR compounds and the SBR/BR blend, and the composition and mass fraction of the interphase in the blend as a function of mixing time are shown in Tables 8-1, 8-2 and 8-3, respectively. The minimum and maximum torque values, which corresponded to the viscosity of the uncured blend and extent of cure in the blend, were 23-25 dN m and 94-99 dN m, respectively (Table 8-3). It appeared that when the SBR and BR compounds were mixed together for longer times, the torque values of the blend were not affected. Δtorque, which is an indication of crosslink density changes in the blend [17] increased from 70 to 75 dN m after 10 minutes mixing time, and then decreased slightly to 73 dN m. The scorch and optimum cure times of the blend were not affected by increases in the mixing time of the two compounds and remained at 10 and 28-30 minutes, respectively. The cure rate index rose from 5 to 5.6 min^{-1} as a function of mixing time up to 10 min, though it subsequently decreased to 5 min^{-1} after the mixing time was increased to 20 min.

The mass fraction of the interphase in the blend increased from 72 to 88% after the two compounds were mixed together for 10 min. It then decreased to 63% when the mixing time was increased to 20 min. The composition of the interphase also changed. At prolong mixing times, the mass fraction of BR to SBR in the interphase increased from approximately 0.16 to 0.47. Longer mixing times also replaced SBR with BR in the interphase (Table 8-3). Figure 8-8 shows the mass fraction of BR in the interphase as a function of mixing time.

8.5.2 Effect of the mixing temperature of the BR and SBR compounds on the Mooney viscosity, cure properties, mass fraction and composition of the interphase in the SBR/BR blend

As expected, a higher mixing temperature reduced the viscosity of the blend from 108 to 96 MU (Table 8-4). The rubber breaks down during mixing, which causes reduction in its molecular weight and viscosity [12,18,19]. The reduction is due to chain scission [20] or, the mechanical rupture of the primary carbon-carbon bonds that are present along the back-bone of the rubber chains. This is often compensated by the reinforcing effect of the filler.

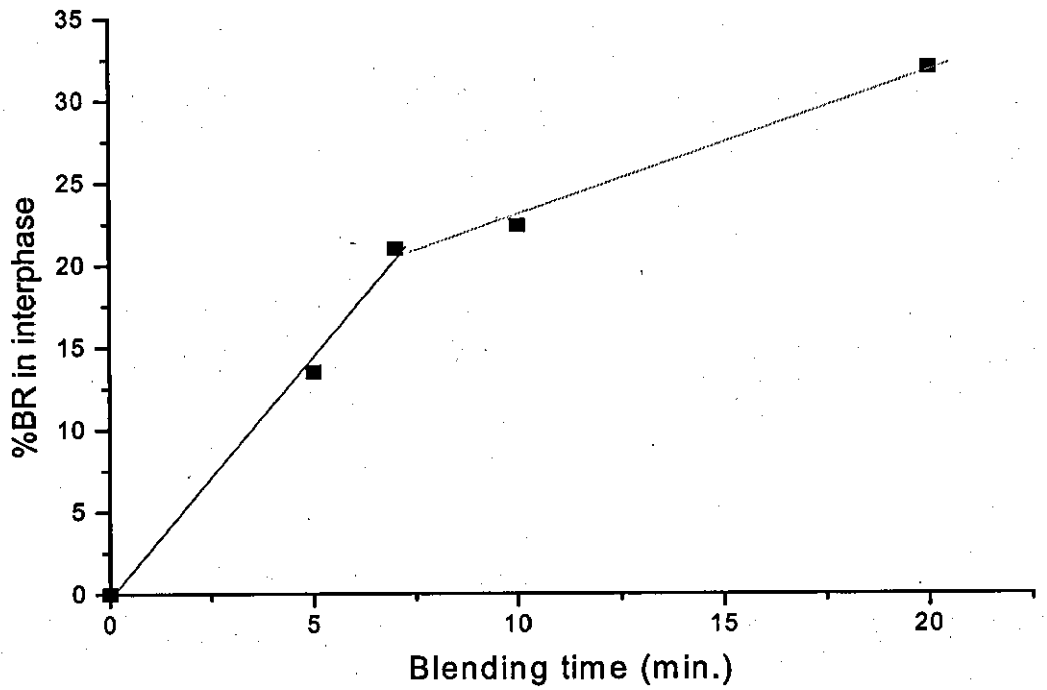

Figure 8-8: Mass fraction of BR in the interphase as a function of mixing time

Table 8-3: Mixing condition, cure Properties, mass fraction and composition of the interphase in the SBR/BR Blends. The SBR and BR compounds were mixed together for different times.

Compound No.	9	10	11	12
Mixing temperature (°C)	60-65	60-65	60-66	60-65
Mixing time (min)	5	7	10	20
ODR Results				
Minimum torque (dN m)	24	25	24	23
Maximum torque(dN m)	94	97	99	96
Δtorque (dN m)	70	72	75	73
Scorch time, t_{s1} (min)	10	10	10	10
Optimum cure time, t_{90} (min)	30	29	28	30
Cure rate index (min^{-1})	5	5.3	5.6	5
Mass fraction of the interphase (%)	72	82	88	63
Mass fraction of BR in the interphase (%)	13.5	21	22.4	32
Mass fraction of SBR in the interphase (%)	86.5	79	77.6	68
Mass fraction of BR to SBR in the interphase	0.16	0.27	0.29	0.47

Note that the mass fraction of BR to SBR in the interphase was calculated as follows: For example for compound 9, BR/SBR = 13.5/86.5 = 0.16

The scorch time of the blend was unaffected and remained at 10-11 min, but its optimum cure time increased from 29 to 43 min as the mixing temperature of the two compounds was increased from 60 to 105 °C. As a result, the cure rate index decreased from 5.3 to 3 min^{-1}, which indicated a slowing down of the curing rate in the rubber. The Δtorque of the blend did not change and stayed at approximately 72 dN m. Similarly, the minimum and maximum torque values stayed at about 23-25 and 94-97 dN m, respectively. This suggested that increases in the mixing temperature of the two compounds had no obvious effect on the viscosity of the uncured blend as indicated by the minimum torque value, and the extent of crosslinking in the blend as indicated by the maximum torque value. The optimum cure time was the only property that was affected by increases in the mixing temperature of the two compounds.

The mass fraction of the interphase in the blend increased from 82 to 85% because of a higher mixing temperature of the two compounds. The mass fraction of BR to SBR in the interphase also increased from 0.27 to 0.33 when the mixing temperature was increased from 60 to 105°C. Clearly, higher temperatures during the mixing of the two compounds were beneficial to the formation of the interphase in the blend and increased the BR component of the interphase.

8.5.3 Effect of pre-scorch time on the mass fraction and composition of the interphase in the SBR/BR blend

As shown in Table 8-5, the scorch times of the BR and SBR compounds were 5 and 12 minutes, respectively. When the two compounds were mixed together for 1 min at 34-54°C and then tested in the ODR at 140°C, the scorch time of the blend was 10 min (Table 8-6). 170 g of the blend was subsequently placed in a

Table 8-4: Mooney viscosity, cure properties, mass fraction and composition of the interphase in the SBR/BR blends. The SBR and BR compounds were mixed together for 7 min at different temperatures to produce the blends.

Compound No.	13	14	15
Mooney viscosity (MU)	108	104	96
Mixing temperature (°C)	60-65	80-90	90-105
ODR Results			
Minimum torque (dN m)	25	23	24
Maximum torque (dN m)	97	94	96
Δtorque (dN m)	72	71	72
Scorch time, t_{s1} (min)	10	11	10
Optimum cure time, t_{90} (min)	29	40	43
Cure rate index (min^{-1})	5.3	3.5	3.0
Interphase properties			
Mass fraction of the interphase (%)	82	81	85
Mass fraction of BR in the interphase (%)	21	23.5	24.6
Mass fraction of the SBR in the interphase (%)	79	76.5	75.4
Mass fraction of BR to SBR in the interphase	0.27	0.31	0.33

hydraulic press at 140°C for 8 min (pre-scorch time) under a pressure of 11MPa, to produce sheets 2.5 mm thick. The rubber was then removed from the press and left at ambient temperature to cool down. The mass fraction and composition of the interphase in the blend were determined to evaluate the effect of the heat treatment on the interphase properties (Table 8-7).

Table 8-5 : Mooney viscosity and cure properties of the BR and SBR rubbers

	Compound	
	3	6
Mooney viscosity (MU)	162	109
Minimum torque (dN m)	45	23
Maximum torque (dN m)	133	66
Δ torque (dN m)	88	43
Scorch time, t_{s1} (min)	5	12
Optimum cure time, t_{90} (min)	**49**	**49**
Cure rate index (min^{-1})	2.3	2.7

For the blend prepared by mixing the two compounds for 1 min at 34-54°C, the mass fraction of the interphase was 59%, and the mass fraction of BR to SBR in the interphase was approximately 0.27. However, when the same blend was kept at 140°C for 8 min, the mass fraction of the interphase increased to 62%, and the mass fraction of BR to SBR in the interphase rose to 0.63. A strong interphase was formed in the blend during the pre-scorch stage of the cure cycle at elevated temperature, and the BR component of the interphase also increased.

The diffusion theory of adhesion, is also known as autohesion in the case of rubbers, states that adhesion of two macromolecules in intimate contact results from the interdiffusion of the molecules of the superficial layers [21,22]. This interdiffusion allows the formation of an interphase between the two rubbers. In the case of polymer autohesion corresponding to the mutual diffusion of identical molecules, adhesion under a constant assembly pressure, is a function of temperature and contact time, following Fick's classical law [23]. Therefore, the average interpenetration depth, χ, of one phase into another is given as:

$$\chi = \exp(-E/2RT)\, t^{1/2} \qquad \ldots 8\text{-}1$$

where, E, is the diffusion activation energy, t, the contact time, R, the molar gas constant, and T, the temperature.

Table 8-6: Mooney viscosity, cure properties, mass fraction and composition of the interphase in the SBR/BR blends. The SBR and BR compounds were mixed together for 1 min at 34-54°C to produce the blend.

Compound No.	16
Mooney viscosity (MU)	108
t_{s1} (min)	10
t_{90} (min)	35
Cure rate index (min^{-1})	4
Minimum torque (dN m)	26
Maximum torque (dN m)	96
Δtorque (dN m)	70
Mass fraction of the interphase (%)	59
Mass fraction of BR in the interphase (%)	21
Mass fraction of SBR in the interphase (%)	79
Mass fraction of BR to SBR in the interphase	0.27

Table 8-7 : Mass fraction and composition of the interphase in the SBR/BR blend after 8 minutes scorch at 140°C. The SBR and BR compounds were mixed together for 1 min at 34-54°C to produce the blend.

Blend	Mass fraction of the interphase (%)	Composition of the interphase (%)	Mass fraction of BR to SBR
SBR/BR	62	(BR=38.5, SBR=61.5)	0.63

The mass fraction of BR to SBR in the interphase was calculated as described in Table 8-3.

Polymer interdiffusion has been the subject of numerous studies. For example, Skewis [24] measured the rate of interdiffusion of butyl and SBR rubber chains when samples of the two rubbers were pressed against each other. He also showed that the diffusion of polymer chains across the interface did occur when the two samples of uncured rubbers were brought into intimate contact, and that this interdiffusion enhanced the adhesion between the two rubbers.

There are two fundamental requirements, which must be met in order to obtain adhesion by interdiffusion [23,25] the substrates must be mutually soluble or compatible, and, the macromolecules must be very mobile, thus at a sufficient temperature. For pure SBR and BR rubbers, solubility parameters 8.30 and 8.41 $(cal/cc)^{1/2}$ have been reported, respectively [26,27]. The small difference in the solubility parameters of the rubbers suggests that they were, at least, partially miscible, and therefore adhesion by interdiffusion could have occurred. Please note, the presence of a large amount of reinforcing filler did not change the solubility parameters of the rubbers [27]. The glass transition temperatures of the SBR and BR rubbers were -50 and -107^0C, respectively (Table 5-1), which indicated a high degree of mobility for the macromolecules at ambient temperature. However, temperature during the mixing of the SBR and BR compounds rose from 34 to 105^oC, and this increased the mobility of the chain segments further, facilitating a more extensive interdiffusion between the rubbers. In addition, the mixing time of the two compounds was increased to 20 min, allowing sufficient time for the mutual diffusion of the SBR and BR macromolecules to take place [24] and formation of interphases in the blends.

As mentioned earlier [28], interphase formation is the result of molecular diffusion between pure phases. The large mass fraction of the interphases in the blends (Tables 8-3 and 8-4) indicated that significant molecular diffusion had taken place between the BR and SBR rubbers, which improved the adhesion between the two.

Conclusions

From this study, it is concluded that:

1 - When the mixing time of the SBR and BR compounds was increased progressively from 5 to 10 min, the mass fraction of the interphase in the SBR/BR blend increased from 72 to 88%. However, as the mixing time of the two compounds was increased to 20 min, this had a detrimental effect on the mass fraction of the interphase in the blend. The mass fraction of BR to SBR in the interphase also rose from 0.16 to 0.47 as the mixing time of the two compounds was increased to 20 min.

2 - When the mixing temperature of the two compounds was increased from 60 to 105°C, the mass fraction of the interphase in the blend rose from approximately 82 to 85%. Similarly, the mass fraction of BR to SBR in the interphase increased from 0.27 to 0.33.

3 - The mass fraction of the interphase in the blend was 59% when the two compounds were mixed together for 1 min at 34-54 °C, for 8 min (pre-scorch time), the mass fraction of the interphase was 62% and the mass fraction of BR to SBR in the interphase about 0.63.

In summary, increasing the mixing time and mixing temperature of the two compounds helped to increase the mass fraction of the interphase in the SBR/BR blend, and alter the composition of the interphase. A similar trend was also observed when the blend was kept at elevated temperature for 8 min (pre-scorch time) during its cure cycle. The results suggested that strong interphases could be formed in the blend during the pre-scorch time of the rubber, without a need for the two compounds to be mixed together for long times and at high temperatures prior to curing.

References

1) Hirshfield S M., *U.S Patent* 3:(280)876 (1966).

2) Nielson L E.,"*Predicting the properties of mixtures*", Marcel Dekker, NY (1978).

3) Keller C, *Tyre Sci. Technol.* 1:190(1973).

4) Hirakawa M, Ahagon A, *Tyre Sci. Technol.***10**:16(1982).

5) Gregen W, Lutz R, Davison S, Holden G, " *Thermoplastic elastomers*", N.R. Legge, Ed., Hanser publishers, NY,507(1987).

6) Rankin G M., *Rubber world* **219**:(1)52(1998).

7) Kresge E N., *Rubber world* **216**:(3)30(1997).

8) Vasile C., Kulshreshtha A K., *Hand book of polymer blends and composites*, rapra technology **3A**,103(2003).

9) Datta R.N, Hondeveld M. G, *Kautschuk Gummi Kunststoffe* **6**:54(2001).

10 – Ansarifar A., Wang L, Ellis R J, Kirtley S P, Riyazuddin N, *J Apply Polym Sci* **105**:322(2007).

11 – Ansarifar A, Wang L, Ellis R J, Haile-Meskel Y, *J Apply Polym Sci* **106**:1135(2007).

12 – Fries H., Pandit R P, *Rubber Chem Technol* **55**:309(1982).

13 - British Standards Institution, Methods of testing raw rubber and unvulcanised compounded rubber: Methods of physical testing. British Standard 1673: Part 3; London, UK(1969).

14 - British Standards Institution, Methods of testing raw rubber and unvulcanized compounded rubber: Measurement of pre-vulcanizing and curing characteristics by means of curemeter. British Standard 1673: Part 10; London, UK(1977).

15 - British Standards Institution, Methods of testing raw rubber and unvulcanized compounded rubber: Measurement of pre-vulcanizing and curing characteristics by means of curemeter. British Standard 903: Part A60: Section 60.1; London, UK(1996).

16 – Song M, Hourston D J, Reading M, Pollock H M, Hammiche A, *J*

Thermal Analysis and Calorimetry **56**:991(1999).

17) Wolff S, *Rubber Chem Technol* 69:325(1996).

18) Harmon D J, Jacobs H L, *J Appl Polym Sci* **10**: 253(1966).

19) Ansarifar A, Shiah S F, Bennett M,. *Int J Adhes Adhes* **26**:454(2006).

20) Ahagon A, *Rubber Chem Technol* **69**:742(1996).

21) Voyutskii S S, Margolina Y L, *Rubber Chem Technol* **30**:531(1957).

22) Voyutskii S S, Margonila Y L, *Uspekhi Khimi* **18**: 449(1949).

23) Vasenin R M, *In Adhesion: Fundamentals and practices*, Part 1. Ch. 4. Ministry of Technology (UK). Elsevier, New York (1970).

24) Skewis J D, *Rubber Chem Technol* **39**:217(1966).

25) Fourche G, *Poly Eng Sci* **32**:(**12**)957(1995).

2 6) Ansarifar M A., Fuller K N G, Lake G J, *Int J Adhes Adhes* **13**:(**2**)105(1993).

27) Ansarifar M A., Fuller K N G.,Lake G J, Raveendran B, *J Rubb Res* **3**:1(2003).

28) Sharp, L. *The interfacial interactions in polymer composites.* Dordrecht, The Netherlands: Kluwer Academic Publishers (1993).

CHAPTER 9

Measuring effects of silanized silica nanofiller on the mechanical properties of styrene-butadiene (SBR) and poly butadiene (BR) rubbers and SBR/BR blends

9.1 Introduction

Mixing dissimilar elastomers to produce blends is often carried out to achieve specific properties for industrial rubber articles such as tire tread. It is therefore important to understand how properties of blends are affected by the properties of individual rubbers in the blend. For example, the viscosity of rubber blends can differ from the viscosity of the individual rubbers in the blend [1].

For example, the hardness and modulus of rubber compounds are important properties in product development [2]. Dissimilar elastomers are often mixed together to produce blends, which possess better tear strength, cut growth resistance, fatigue life and resistance to ozone cracking than the individual elastomers. In rubber blends, property enhancement is, to a large extend, due to the formation of strong interfacial bonding between dissimilar elastomers, which facilitates stress transfer from one phase to the other [3-7]. The properties of the continuous phase often determines the strength properties of a blend [8-9]. It has been shown that the modulus of a blend is generally intermediate, when measurements were carried out between the glass transition temperatures of the two rubbers. A similar behaviour has been shown by the blends of an elastomer of high and low molecular weights [10]. Hess and Chirico have shown that modulus increases when the continuous phase contains filler [8]. A non-uniform distribution of filler in NR/BR and NR/SBR blends provided high cut growth resistance in some rubber vulcanisates [11]. Roger and Waddel [12] have reviewed the previous work on the use of blends of butyl, chlorobutyl, bromobutyl and brominated methyl styrene-isobutylene co-polymer with NR and SBR in

many tyre and non tyre applications. Addition of chlorobutyl rubber to NR/BR blend increased their tearing strength and reduced cut growth rate. Rattanasom and co-workers [13] showed that the addition of reclaimed rubber into virgin NR increased the hardness and modulus but decreased the tensile strength, tear strength and abrasion resistance. Pham Thi Hao and co-workers [14] found that the mechanical properties of SBR/BR blend varied with the mass fraction of SBR with respect to BR in the blend. For the NR filled rubber, the addition of silica gave reasonable mechanical properties [15]. Effect of filler loading on the tensile strength and tear strength of NR/SBR and NR/ENR (epoxied NR) blends was studied [16], which found that the aforementioned properties increased with filler loading.

In this chapter, effects of a silanized silica nonofiller on the mechanical properties of styrene-butadiene rubber (SBR), polybutadiene rubber (BR) and SBR/BR blends will be investigated. SBR/BR rubber blends (75/25 by mass) are used in the manufacture of tyre treads.

9.2 Experimental

9.2.1. Materials- Rubbers, filler, curing chemicals, antidegradants, and processing oil

The used raw rubbers, nanofiller, and curing chemicals were described in sections 5.1.1 and 5.1.2.

The procedures for measuring these curing chemicals for the BR and SBR rubber compounds were described previously [17,18].Table 9-2 shows the rubber formulations used for making the SBR/BR blends. Note that the two compounds had the same optimum cure times 49 minute.

9.2.2 Mixing

The compounds were prepared in a Haake Rheocord 90 (Berlin, Germany), a small size laboratory mixer with counter rotating rotors. In these experiments, the Banbury rotors and the mixing chamber were maintained at 23 °C (ambient temperature) during mixing. The rotor speed was 45 r.p.m. The volume of the mixing chamber was 78 cm^3, and it was 60% full during mixing. Haake Software Version 1.9.1. was used for controlling the mixing condition and storing data.

Two SBR and BR rubber compounds filled with 60 parts per hundred rubber by weight (phr) silanized silica nanofiller were prepared and then mixed together to produce SBR/BR (75:25 by mass) blends for this study (Table 9-3). The mass fraction of SBR to BR in typical SBR/BR tyre tread blend compounds is 75 to 25 [18]. To prepare the SBR compound, the filler was placed in the mixing chamber and then the raw rubber and processing oil were added. TBBS, ZnO and antidegradant were added 4 min after the filler, rubber and processing oil were mixed together, and mixing continued subsequently for an extra 6 min before the rubber compound was removed from the mixer. To mix the BR compound, the filler and rubber were mixed together for 10 min and then TBBS, elemental sulphur and antidegradant were added together. Mixing continued subsequently for an extra 6 min before the rubber was removed from the mixer. Elemental sulphur was added to the BR compound to achieve the same optimum cure time as the SBR compound before the two rubbers were mixed together to produce the blend. Note that before the curing chemicals were added, the rotors were stopped and the rubber compounds were cooled down to 40-50°C to avoid pre-scorch in the compounds during the subsequent mixing.

Finally, when mixing ended, the rubber compounds were stored at ambient temperature (~23°C) for at least 24 h before their viscosity and cure properties were measured. The SBR and BR rubber compounds were then mixed together for 1, 7 and 20 min to produce SBR/BR blends. The viscosity and cure properties of the blends were measured 12 h after mixing ended.

9.2.3 Mooney viscosity and cure properties of the rubber compounds and the blends

The viscosity of the rubber compounds was measured at 100°C in a single-speed rotational Mooney viscometer (Wallace Instruments, Surrey, UK) as described in section 5.5 and in accordance with the British Standard [20]. The scorch time, which is the time for the onset of cure, and the optimum cure time, which is the time for the completion of cure, were determined from the cure traces generated at 140 ± 2°C by an oscillating disc rheometer curemeter (ODR, Monsanto, Swindon, UK) at an angular displacement of ± 3° and a test frequency of 1.7 Hz [21]. The cure rate index, which is a measure of the rate of cure in the rubber, was calculated using the method described in the British Standard [22]. The rheometer tests ran for up to 2 h.

9.2.4 Specific gravity and glass transition temperature of the SBR and BR rubbers, and mass fraction of the interphase in the SBR/BR blends

Specific gravity, glass transition temperature of the SBR and BR rubbers, and mass fraction of the interphase in the SBR/BR blends were measured and calculated as it was described in sections 5.1.1 and 5.12.
The results are shown in Tables 9-1 to 9-3.

Table 9-1: Specific gravity, Mooney viscosity and glass transition temperature of the raw rubbers

Compound	Specific gravity	Mooney viscosity (MU)	Tg (°C)
SBR	0.94	51	-50
BR	0.91	49	-107

Table 9-2: Formulations, Cure properties and viscosity of the SBR and BR rubber compounds

Formulation (phr)	Compound no. 1	Compound no. 2
BR	100	-
SBR	-	100
Silanized silica	60	60
TBBS	7.5	3
Santoflex 13	1	1
Enerflex 74	0	5
ZnO	0	0.5
Elemental sulphur	0.3	0
Mooney viscosity (MU)	162	109
	ODR Results	
Minimum torque (dN m)	45	23
Maximum torque (dN m)	133	66
Δtorque (dN m)	88	43
t_{s1} (min)	5	12
t_{90} (min)	**49**	**49**
Cure rate index (min^{-1})	2.3	2.7

Total mixing times for compounds 1 and 2 were 16 and 10 min, respectively.

9.2.5 Compounds curing

After these measurements were completed, the rubber compounds were cured in a compression mould as was described in section 5.3.

9.2.6 Swelling tests and bound rubber measurements

Swelling tests and bound rubber measurements were performed in accordance with descriptions in section 5.4.

Fig. 9-1 shows Increase in weight in percentage versus time of immersion in toluene for compounds 1 and 2 and blends 3-5 (Table 9-4).

Table 9-3: Mixing condition, Mooney viscosity, cure properties, mass fraction and composition of interphase in the SBR/BR (75:25 by mass) blends.

	Blend		
	3	4	5
	Mixing conditions of the SBR and BR compounds		
Mixing time (min)	1	7	20
Mixing temperature (°C)	34-54	90-105	80-94
Mooney viscosity (MU)	108	96	78
Minimum torque (dN m)	27	24	21
Maximum torque (dN m)	96	96	93
Δtorque (dN m)	69	72	72
t_{s1} (min)	10	10	9
t_{90} (min)	35	43	45
Cure rate index (min^{-1})	4	3	2.8
	Interphase properties in the uncured blends		
Mass fraction of the interphase (%)	59	85	90
Mass fraction of BR in the interphase (%)	21	24.5	18
Mass fraction of SBR in the interphase (%)	79	75.4	82
Mass fraction of BR to SBR in the interphase	0.27	0.33	0.22
	Interphase properties at 8 minutes pre-scorch at 140°C		
Mass fraction of the interphase (%)	62	86	81
Mass fraction of BR in the interphase (%)	38.5	27	27
Mass fraction of SBR in the interphase (%)	61.5	73	73
Mass fraction of BR to SBR in the interphase	0.63	0.37	0.37

Note, the mass fraction of BR to SBR in the interphase was calculated as follows: for example, the mass fraction of BR to SBR in the interphase of the uncured blend 3 was BR/SBR = 21/79 = 0.27.

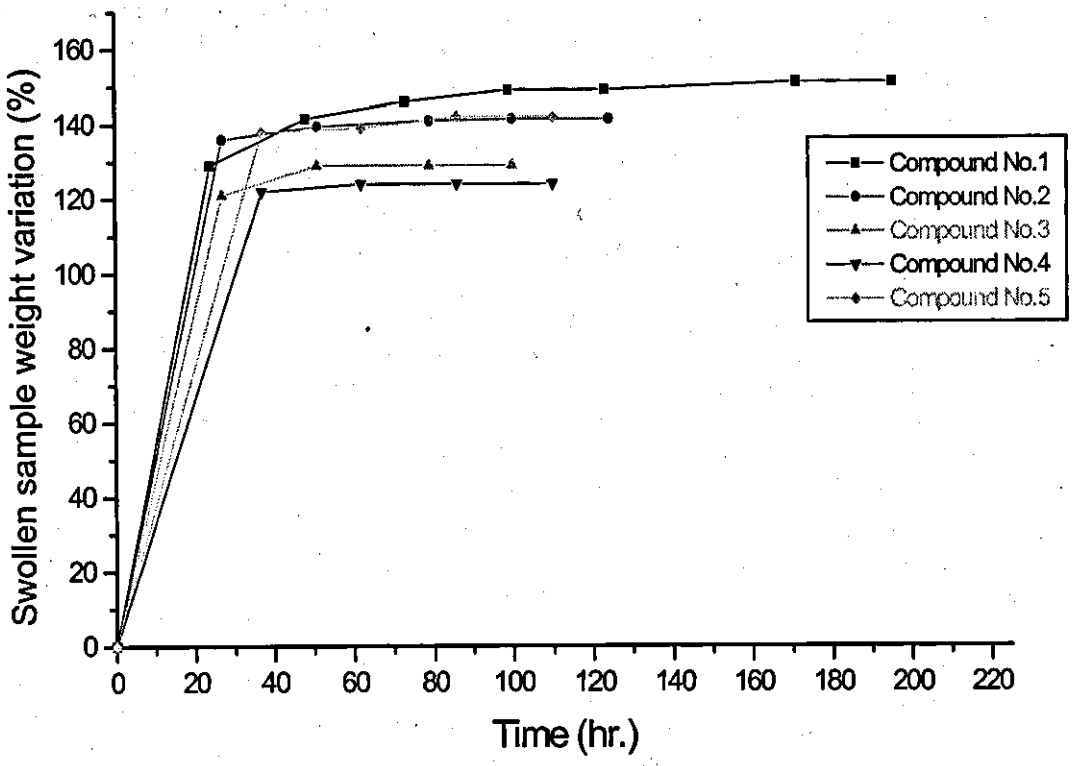

Figure 9-1 – Increase in weight in percentage versus time of immersion in toluene for compounds 1 and 2 and blends 3-5 (Table 9-4)

9.2.7 Hardness

For measuring the hardness of the rubbers, cylindrical samples 12 mm thick and 28 mm in diameter, were used. The samples were then placed in a Shore A Durometer hardness tester (The Shore Instrument & MFG, Co., New York), and the hardness of the rubber was measured at ambient temperature (25°C) over a 15-second interval after which a reading was taken. This was repeated at four different positions on the sample, and median of the four readings was calculated.[23].

9.2.8 Cohesive tear strength

Test pieces specification were explained in section 5.8.

The tear tests were performed at an angle of 180^0, at ambient temperature (23 °C) and at a constant cross-head speed of 50 mm/min [24] in a Hounsfield mechanical testing machine. The tears produced in the rubber after the test pieces were fractured were 15-57 mm in length. In each experiment, the tearing force was recorded as a function of crosshead separation to produce traces from which an average force was measured. In some cases, the test produced only one peak on the trace from which a tearing force was calculated (Fig. 9.2). Sometimes tearing produced several peaks on the trace which were used to calculate an average tearing force for the rubber (Fig. 9.3), or, a continuous trace where the peak force value was used for the rubber (Fig. 9.4). For each rubber, four test pieces were used. After these measurements were completed, and following the procedure described previously [25 and section 5.8], the tearing energies were calculated and the median values of the tearing energies were subsequently noted.

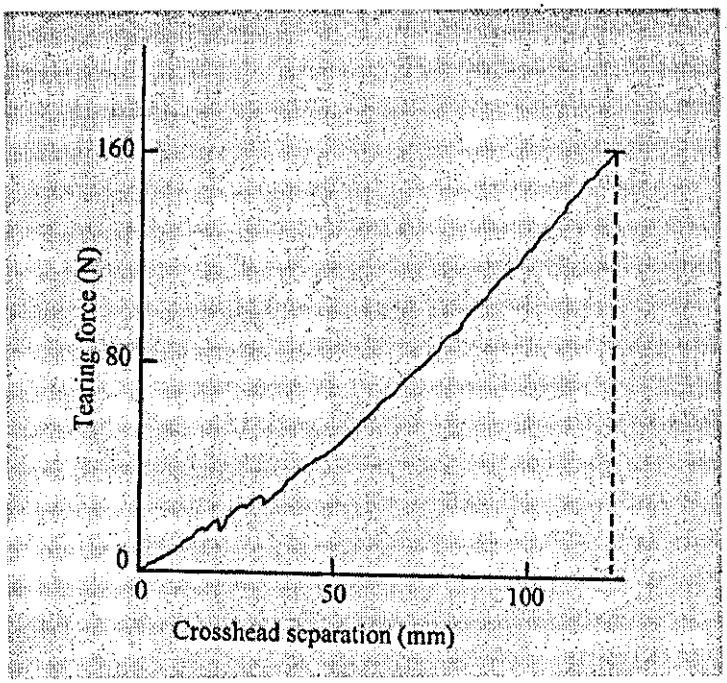

Figure 9-2 – Typical record of tearing force as a function of crosshead separation. Data for blend 4. T= 136 kJ/m^2

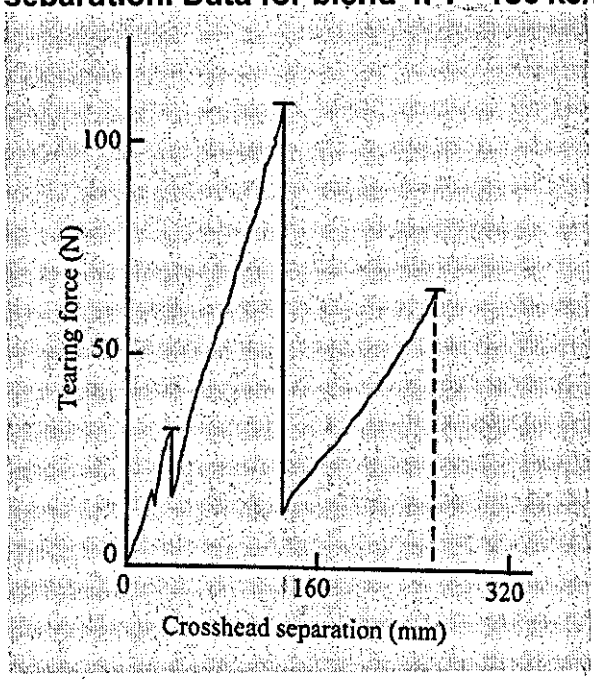

Figure 9-3 – Typical record of tearing force as a function of crosshead separation. Data for blend 5, T= 61 kJ/m^2

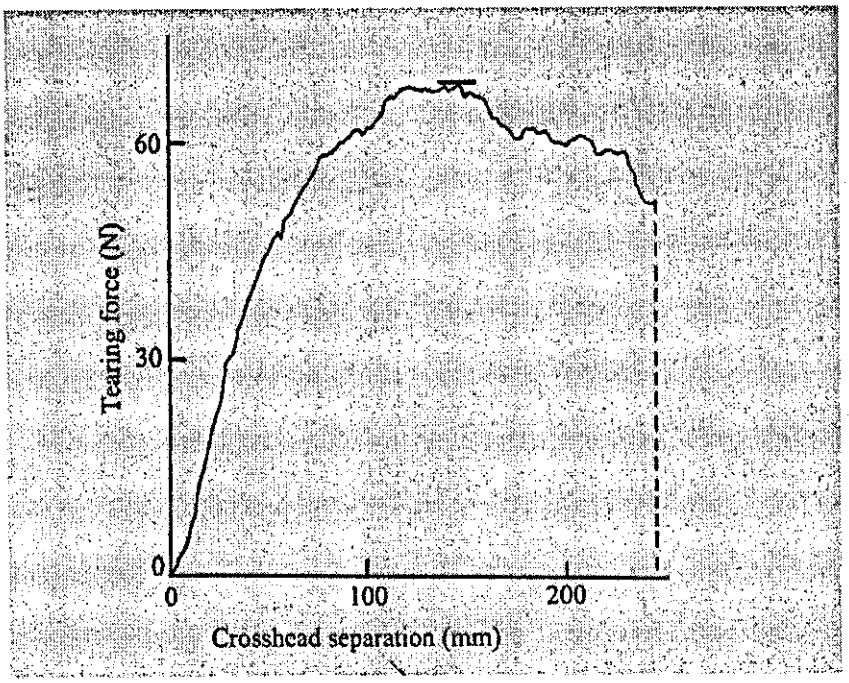

Figure 9-4 – Typical record of tearing force as a function of crosshead separation. Data for the SBR vulcanisates, T= 53 kJ/m^2

9.2.9 Tensile properties

The tensile stress, elongation at break, and stored energy density at break of the rubbers were determined in uniaxial tension in a Hounsfield mechanical testing machine in accordance with instructions in section 5.9. Hounsfield DAPMAT computer software was used for storing and processing the data.

9.2.10 Modulus at different strain amplitudes

The modulus of the vulcanisates at 50%, 100%, 200% and 300% strain amplitudes and Young's modulus were measured in uniaxial tension, using dumbbell test-pieces in accordance with instructions in section 5.10. QMAT-DONGLE version 2003 computer software was used to process the data.

9.2.11 Abrasion resistance

For determining the abrasion resistance of rubbers 1 and 2, molded cylindrical test pieces 8 mm thick and 16 mm in diameter were cured. The tests were performed at 23°C in accordance with BS 903: Part A9: 1995 with method A.1 (Zwick abrasion tester 6102, Croydon, UK and abrasion standard rubber S1). For each rubber, three samples were tested to calculate the relative volume loss (Δv) [26]. The abrasion resistance of the blends was measured by applying a similar procedure and using standard rubber S2, a typical tire compound formulation[27]. The abrasion resistance was expressed as an abrasion resistance index (ARI). An index value of greater than 100% indicated that the test compound was more resistance to abrasion than the standard rubber under the conditions of the test. The abrasion resistance index values recorded for the three rubbers were greater than 100% and therefore, they had a higher resistance to abrasion than the standard rubber against which they had been indexed.

9.2.12 Heat build up

The heat build up of the blends were determined in accordance with BS903 Part A50 as it was described in section 5.14.

9.3 Results and discussion

The differential of heat capacity with temperature, dCp/dT, vs. temperature data for the SBR/BR blend (blend 3 after 8 minutes pre-scorch) and for a physical mixture (samples of pure SBR and BR rubbers placed in physical contact) of the two samples of SBR and BR, baseline selection, global peaks resolution and interphase peaks resolution are shown in Figures 9-5 to 9-8.

Subsequently, the mass fraction of interphases and their composition were calculated as described in section 7.3.

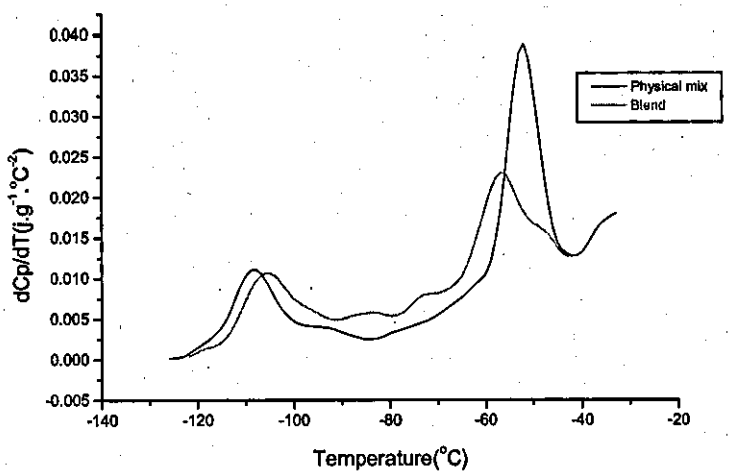

Figure 9-5: Typical dCp/dT versus temperature for SBR/BR blend and SBR/BR physical mixture. Samples were mixed at 34-54°C for 1 min.

9.3.1 Effect of the mixing time and mixing temperature on the composition and mass fraction of the interphase in the SBR/BR blend

The mass fraction of the interphase in the blend (Table 9-3) increased from 59 to 90% after the two compounds were mixed together for 20 min. The composition of the interphase also changed. As the mixing time was increased from 1 to 7 min, the mass fraction of BR to SBR in the interphase increased from 0.27 to 0.33. When the mixing time was raised to 20 min, the mass fraction of BR to SBR in the interphase decreased to 0.22. Evidently, mixing times longer than 7 min, replaced BR with SBR in the interphase. The properties of the interphase changed during a pre-scorch time of 8 min at 140°C.The blends had scorch times 9-10 min. The mass fraction of the interphase in the blend increased from 62 to 81% and the mass fraction of BR to SBR in the interphase decreased from 0.63

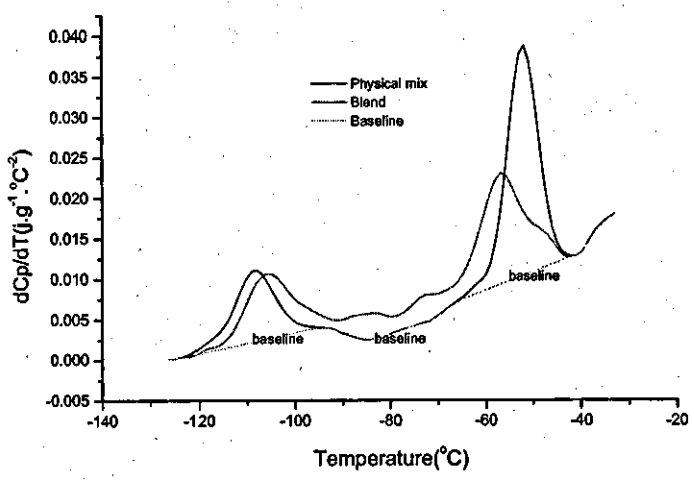

Figure 9-6: Typical dCp/dT versus temperature for SBR/BR blend and SBR/BR physical mixture and correspondent baseline. Samples were mixed at 34- 54°C for 1 min.

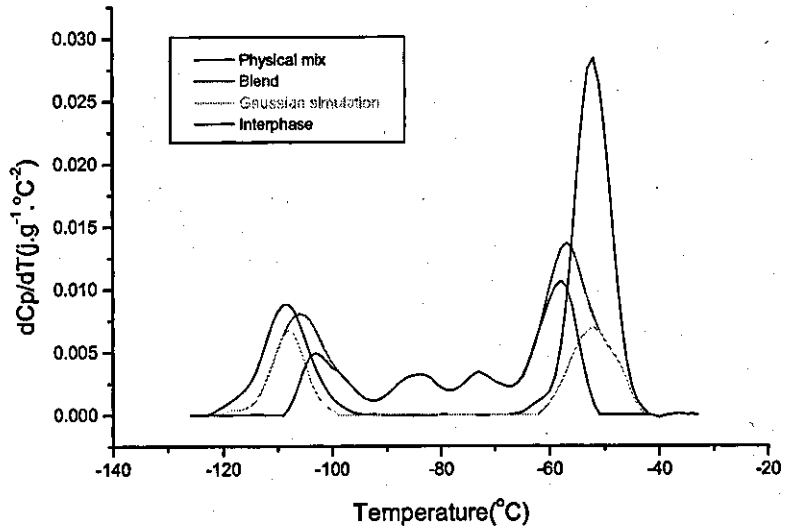

Figure 9-7 :Typical dCp/dT versus temperature for SBR/BR blend after peak resolution showing the interphase region

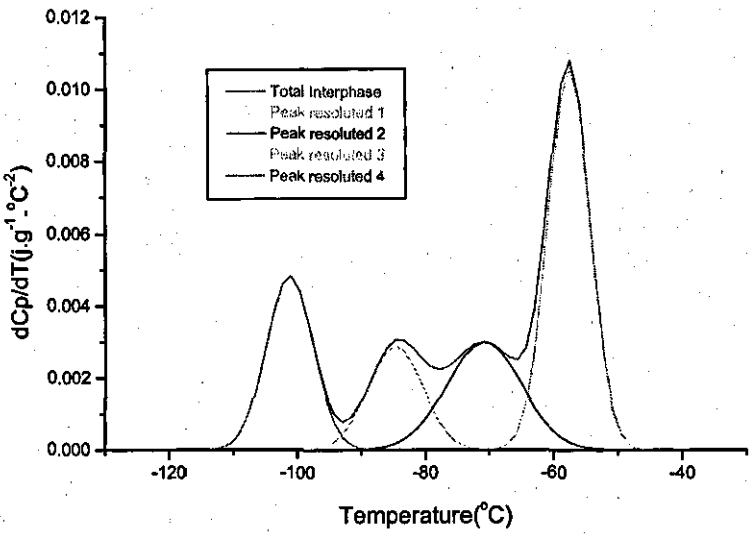

Figure 9-8: Typical dCp/dt versus temperature for SBR/BR blend showing typical interphase obtained by subtracting the blend curve from Gaussian simulation of the same curve. The area under the curve is a measure of the mass fraction of the interphase. Sample was prepared at 34-54 °C for 1 min.

to 0.37 when the mixing time was increased to 20 min (Table 9-3). A strong interphase was formed in the blend during the pre-scorch stage of the cure cycle at elevated temperature and the BR component of the interphase decreased.

When two samples of uncured rubbers are brought into intimate contact, the diffusion of polymer chains across the interface occurs, and this interdiffusion enhances the adhesion between the two rubbers [28]. In order to obtain adhesion by interdiffusion [29,30], the substrates must be mutually soluble or compatible, and, the macromolecules must be very mobile. The latter is temperature dependent. For pure SBR and BR rubbers, solubility parameters 8.30 and 8.41 $(cal/cc)^{1/2}$ have been reported, respectively [31,32]. The small difference in the solubility parameters of the rubbers suggested that they were, at least, partially miscible, and therefore adhesion by interdiffusion could have occurred. Note that the presence of a large amount of reinforcing filler did not change the solubility parameters of the rubbers[32]. The glass transition temperatures of the SBR and BR rubbers were -50 and -107°C, respectively (Table 9-1), which indicated a high

degree of mobility for the macromolecules at ambient temperature. However, temperature during the mixing of the SBR and BR compounds rose to 105°C, and this increased the mobility of the chain segments further, facilitating a more extensive interdiffusion between the rubbers. In addition, the mixing time of the two compounds was increased to 20 min, allowing sufficient time for the mutual diffusion of the SBR and BR macromolecules to take place [28]. This lead to the formation of a strong interphase in the blends.

The large mass fraction of the interphase in the blends, up to 90% (Tables 9-3) indicated that significant molecular diffusion had taken place between the BR and SBR rubbers, which improved the adhesion between the two. Properties related to fracture were more likely to have benefited from the formation of strong interphases in the blend.

9.3.2. Filler dispersion and filler effect on the viscosity of the SBR and BR rubbers and SBR/BR blends

To optimise the reinforcing effect of the filler on the mechanical properties of the vulcanisates, it was essential to disperse the filler particles well in the rubber [33]. The BR and SBR compounds were mixed for 16 and 10 min, respectively, to achieve good dispersion of the silica particles in the rubbers (Fig. 8-2).
However, long mixing time, e.g. 10 min, breaks down the rubber and causes reduction in its molecular weight [34] and viscosity [35]. The reduction is due to chain scission, or, the mechanical rupture of the primary carbon-carbon bonds that are present along the backbone of the rubber chains [36,37]. The reinforcing effect of filler often compensates for the adverse effects produced by the scission of the chains and mechanical degradation of the rubber during processing.
The addition of the filler increased the viscosity of the raw rubbers, which rose from 51 (raw SBR) to 109 and 49 (raw BR) to 162 MU, respectively (Table 9-1 and 9-2). The viscosity of the SBR/BR blends was also affected by the mixing time. As expected [34,35] a longer mixing time of 20 min reduced the viscosity of

the blend from 108 to 78 MU (Table 9-3). This was attributed to chain scission [36,37].

Fillers increase rubber viscosity because of the formation of bound rubber [38]. The bound rubber content of the BR and SBR rubber vulcanisates were 93 and 66 %, respectively (Table 9-4), which indicated a high level of rubber-filler interaction. Similarly, the bound rubber content of blends 3-5 were 69.5-73%, which showed a strong interaction between the filler and rubber (Table 9-4).

It is known that bound rubber forms during mixing while filler dispersion occurs [39] and increases as a function of mixing temperature[40], mixing time[41] and storage time [42]. Since the mixing time increased to 20 min and the compound temperature rose to 105°C during mixing, and the blends were stored at ambient temperature (~23°C) for a total of 36 h before they were tested, the bound rubber formation occurred.

9.3.3 Cure properties of the SBR and BR rubber compounds and SBR/BR rubber blends

The ODR test results of the two SBR and BR compounds and the SBR/BR blends are shown in Tables 9-2 and 9-3, respectively. The scorch time of the BR and SBR compounds were 5 and 12 min, respectively, and the SBR compound had a faster rate of cure with a cure rate index of 2.7 min^{-1}. The optimum cure time of the two compounds were almost the same, i.e. 49 min (Table 9-2). The cure properties of the SBR/BR blends were different from the two compounds (cf. compounds 1 and 2; Table 9-2 with blends 3-5; Table 9-3). The scorch time of the blends were similar at 9-10 min. However, the optimum cure time rose from 35 to 45 min as mixing time was increased to 20 min. Blend 3 had the highest rate of cure with a cure rate index of 4 min^{-1}. Δtorque increased from 69 to 72 dN m, which indicated a small rise in the crosslink density of the blend. It was also noted that Δtorque and the weight of toluene uptake per gram of the rubbers, Q, followed a similar trend (Table 9-4). For example, for blends 3-5, Δtorque were

69, 73, and 72 dN m, which corresponded to 2.10, 2.40 and 2.18 toluene up take per gram of rubber, respectively. Similarly, for the BR and SBR vulcanisates, Δtorque were 85 and 43 dN m, which corresponded to 2.55 and 2.40 toluene up take per gram of rubber, respectively.

9.3.4 Mechanical properties of the BR and SBR rubber vulcanisates and cured SBR/BR blends

The mechanical properties of the BR and SBR rubber vulcanisates and the three blends tested are summarized in Table 9-4. With the exception of the tearing energy, abrasion resistance, hardness and modulus, the remaining properties of the SBR vulcanisate were noticeably better than those of the BR. It was also interesting that the relative volume loss of the BR rubber was approximately 88% lower than that of the SBR rubber. The properties of the blends were influenced differently by changes in the mass fraction and composition of the interphase. For blends 3 and 5, properties related to fracture improved as the mass fraction of the interphase was increased from 59 to 90%. For example, elongation at break, stored energy density at break and tearing energy rose from 856 to 900%, 99 to 103 mJ/m^3, and 40 to 92 kJ/m^2, respectively. There was also improvement in the abrasion resistance with the abrasion resistance index (ARI) rising from 129 to 139 %, but the tensile strength remained unchanged at 26 MPa. Prolonged mixing reduces viscosity and mechanically damages the rubber.[34, 35]. On this basis, the properties related to fracture were expected to deteriorate as a function of mixing time. However, as the results show, these properties improved. Note that weak interfacial adhesion between the two rubbers, or, absence of interphase in the blend could have caused poor mechanical properties.[31,32] It was concluded that increases in the properties aforementioned were due to the development of a strong interphase in the blends. Rubber properties for example tensile strength and stored energy density at break increase as a function of crosslink density [43]. For the blends, Δtorque

rose from 69 to 72 dN m (Table 9-3), which indicated a small increase in the crosslink density of the rubber. However, this increase was too small to account for the large improvement recorded in the properties of the blends discussed above. Therefore, the improvement was due to the increase in the mass fraction of the interphase in the blends. The hardness and Young's modulus decreased from 74 to 71 Shore A and 6.3 to 5.4 MPa, respectively. Moreover, the modulus of the blend decreased by as much as 25% at 50% strain amplitude and by about 3% at 300% strain amplitude. These properties are often affected by the loading of filler and mixing time [44]. Since the blends had the same loading of silica, hence the reduction in the hardness and modulus was due to prolonged mixing which mechanically damaged the rubber [34-37]. Notably, these properties did not benefit from a strong interphase in the blend. It is worth mentioning that the tensile strength, elongation at break, and stored energy density at break of blend 4 were slightly inferior to those of blends 3 and 5 (Table 9-4). The heat build up tests showed no evidence of porosity in the blends on examining the internal structure of the test pieces. The permanent set was 6.1-6.2% and the blend temperature rose from 62.5 to 67°C. The fact that the blend became softer. i.e. the hardness decreased from 74 to 71 Shore A, and its temperature rose to 67°C in the heat build up tests, suggested that prolong mixing was detrimental to the blend, at least, as far as these properties were concerned.

Conclusions

From this study, it was concluded that:

1. Properties related to fracture such as elongation at break, stored energy density at break, tearing energy and resistance to abrasion benefited from increases in the mass fraction and changes in the composition of the interphase in the SBR/BR blend.

Table 9-4 - Bound rubber and mechanical properties of the SBR and BR rubber vulcanisates and the cured SBR/BR blends

	Compound		Blend		
	1	2	3	4	5
	Swelling test data				
Q^1	2.55	2.40	2.10	2.40	2.18
Bound rubber (%)	93	66	69.5	73	73
	Properties related to fracture				
Tensile strength (MPa)	12	23	26	23	26
Elongation at break (%)	516	1053	856	768	900
Stored energy density at break (mJ/m^3)	30	111	99	86	103
T (kJ/m^2)	71	59	40	92	92
Range of values	62-90	53-67	37-140	73-136	61-121
Δv(mm^3/mg)	15.5	126	-	-	-
ARI (%)	-	-	129	135	139
	Heat build up test results				
Initial static deflection (%)	-	-	15.5	14.5	14.1
Initial dynamic deflection (%)	-	-	18.6	18.7	19.0
Final dynamic deflection (%)	-	-	20.5	20.7	21.9
Temperature (°C)	-	-	62.5	64	67
Permanent set (%)	-	-	6.1	5.8	6.2
Test outcome[2]	-	-	No fail	No fail	No fail
Hardness (Shore A)	77	70	74	73	71
Young's modulus (MPa)	8.2	4.5	6.3	4.4	5.4

Table is continued on the next page

	Modulus at different strain amplitudes (MPa)				
Strain amplitude (%)					
50	2.5	1.6	2.5	2.1	2.0
100	1.9	1.8	2.5	2.2	2.0
200	2.2	2.2	3.1	2.9	2.8
300	2.5	2.4	3.5	3.5	3.4

Definitions:

[1] the weight of toluene uptake per gram of rubber. [2] There was no evidence of porosity in the rubber on examining the internal structure of the test pieces and this was reported as "No fail".

2. Other properties such as heat build up , hardness and modulus were influenced mainly by the filler loading, mixing time and rubber viscosity and did not benefit from increases in the mass fraction and changes in the composition of the interphase in the blend.

References

1) Lipatov S, Shumsky V F, Gorgatenko A N, Panov Yu N, Bolotnikova L S, *J. Appl. Polym. Sci.* **26**:499(1981).

2) Nelson C J., Avgeropoulous G N, Weissert F C, *Macromol Chem.* **60/61**:49 (1977).

3) Lemiex M A., Killogoar P C., *Rubber Chem.Thechnol.***57**:792 (1984).

4)Bauer R F, *Pol. Eng. Sci.* **22**:130 (1982), Mitchell J M., *Rubber Plast. News***14:**(23) 18(june 3, 1985).

5) Hamed G R., *Rubber Chem. Technol.* **55**:151(1982).

6) Buckler E J., Shakelton J, Walker J, *Elastomerics* **114**:(1)17(1982).

7) Phadke A A., Chakraborty S K., De S K., *Rubber Chem.Technol.***57**:19(1984).

8) Hess W M., Chirico V E., *Rubber Chem.Technol.***50**:301(1977).

9) Lee B L, Paper presented in *Thirteenth Akron Polymer Conference*,Akron, Oh (1982).

10) Llorente M A., Andrady A L., Mark J E, *J.Polym.Phys.***18**:621(1981).

11) Fujimoto K., Inomata I., et al., *J. Soc. Rubber Ind. Japan* **46**:216(1973),Nguyen M.N., *Unpublished Results* **2**:219 (1981).

12) Roger J E., Waddel W H., *Rubber World* (Feb.,1999).

13) Rattanasom N, Poonsuk A, Makmoon T, *Polymer Testing* **24**:728(2005).

14) Pham Thi Hao, Ismail H, Hashim A S, *Polymer Testing* **20**:539 (2001).

15) Rattanasom N, Saowapark T, Deeprassertkul C,*Polymer Testing* **26**:369 (2007).

16) Poh B T, Ismail H, Tan K S, *Polymer Testing* **21**:801(2002).

17) Ansarifar A, Wang L, Ellis R J, Kirtley S P,Riyazuddin N J, *Appl Polym Sci* **105**:322(2007).

18) Ansarifar A.,Wang L, Ellis R J, Haile-Meskel Y, *J Appl Polym Sci* **106**:1135(2007).

19) Evans, L. R.; Waddell, W. H. Rubber Chem Technol 1996, 69, 377.

20) Br Standards Institution. Methods of testing raw rubber and unvulcanized compounded rubber: Methods of physical testing. Br Standard 1673: London, UK, Part 3(1969).

21) Br Standards Institution. Methods of test for raw rubber and unvulcanized compounded rubber: Measurement of pre-vulcanizing and curing characteristics by means of curemeter. Br Standard 1673: London, UK, Part 10(1997).

22) Br Standards Institution. Methods of test for raw rubber and unvulcanized compounded rubber: Measurement of pre-vulcanizing and curing characteristics by means of curemeter. Br Standard 903: London, UK, Part A60, Section 60.1(1996).

23) Br Standards Institution. Physical testing of rubber: Method for determination of hardness. Br Standard 903: London, UK, Part A26(1995).

24) Br Standards Institution. Physical testing of rubber: Method for determination of tear strength trousers, angle and crescent test pieces. Br Standard 903: London, UK, Part A3(1995).

25) Greensmith H V, Thomas A G, *J Polym Sci* **43**:189(1955).

26) Br Standards Institution. Method of testing vulcanized rubber. Determination of resistance to abrasion. Br Standard 903: Part A9: Method A.1. London, UK, (1995).

27) Br Standards Institution. Rubber, vulcanized or thermoplastic – Determination of abrasion resistance using a rotating cylindrical drum device. ISO 4649: (2002).

28) Skewis J D, *Rubber Chem Technol* **39**: 217(1966).

29) Vasenin R M, In Adhesion: Fundamentals and Practices, Part 1, Ch. 4. *Ministry of Technology* (UK). Elsevier, New York (1970).

30) Fourche G, *Polym Eng Sci* **35**:957(1995).

31) Ansarifar A, Fuller K N G,Lake G J, *Int J Adhes Adhes* **13**:105(1993).

32) Ansarifar M A., Fuller K N G.,Lake G J, Raveendran B, *J Rubb Res* **3**:1(2003).

33) Polmanteer K E, Lentz C W, *Rubber Chem Technol* **48**:795(1975).

34) Fries H., Pandit R R, *Rubber Chem Technol* **55**:309(1982).

35) Harmon D J, Jacobs H L, *J Appl Polym Sci***10**:253(1966).

36) Pike M, Watson W F, *J Polym Sci* **9**:229(1952).

37) Ahagon A, *Rubber Chem Technol* **69**:742(1996)..

38) Wolff S, Wang M, Tan E H, *Rubber Chem Technol* **66**:163(1993).

39) Wang Meng-Jiao, *Rubber Chem Technol* **71**:520(1998).

40) Stickney P B, McSweeney E E, MuellerW J, *Rubber Chem Technol* **31**:31(1958).

41) Boonstra B B, *J Appl Polym Sci* **11**: 389(1967).

42) Leblanc L, Hardy P, *Kautsch Gummi Kunststs* **44**:1119(1991).

43) Bristow G M., Tiller R F, *Kautsch Gummi Kunststs* **23**: 55(1970).

44) Dannenberg E M, *Rubber Chem Technol* **25**:843 (1982)..

CHAPTER 10

Measuring the dynamic properties of NR, IR, SBR and BR rubbers filled with a high loading of silanized silica nanofiller

10.1 Introduction

Although measuring the static mechanical properties such as tensile strength, hardness, tear strength, and modulus helps to determine the suitability of elastomers for use in industrial applications, similar measurements should also be made of the dynamic properties for applications where the article may be exposed to repeated or cyclic stressing for example car tyres. In fact, wearing of tyre tread and tyre performance are directly related, and are two sides of the same coin. In tyre tread applications, SBR and BR provide high abrasion resistance and low rolling resistance, whereas, NR provides resilience and low heat build up [1].

Fillers, when added to polymers, are known to cause a considerable change in the dynamic properties of rubber vulcanisates, not only the dynamic modulus, which includes both the viscous and loss modulus and elastic and storage modulus. The loss modulus represents the viscous component of modulus and includes all the energy dissipation processes during dynamic strain. Tan δ is the ratio between viscous modulus (G") and elastic or storage modulus (G') [2].

In recent years, an enormous amount of work has been done on the application of conventional nanofillers in elastomers and the development of new products to improve the dynamic properties of rubber articles. While there is agreement that nanofillers are one of the main components of the filled rubber nanocomposites and have a very important role to play in improving the dynamic performance of rubber products, yet many new ideas, theories, practices, phenomena and observations about how and why nanofillers alter the dynamic stress-strain response of rubbers are being investigated. In fact filler networking, both it's

architecture and the strength it provides, are the main although not the only parameters to govern the behaviour of the filled rubber under dynamic strain. In practice, the energy losses in rubber products during dynamic strain is of great importance, as for example, in vibration mountings and automotive tyres where it affects the service performance of these products with regard to heat generation and fatigue life for the former, and rolling resistance, traction and skid resistance for the latter. In fact, with regard to tyre applications, it has been well established that repeated straining of the compound due to rotation and braking can be approximated as a process of constant energy input involving different temperatures and frequencies [3-5] .

Rolling resistance is related to the movement of the whole tyre corresponding to deformation at a frequency of 10-100Hz and a temperature ranging from 50-80°C [2]. In the case of skid- or wet-grip, the stress is generated by resistance from the road surface and movement of the rubber at the surface, or near the surface of the tyre tread. The frequency of this movement depends on the roughness of the road surface but should be very high, probably around 10^4 to 10^7 Hz at room temperature [4,5]. It is therefore obvious that any change in the dynamic hysteresis of the compounds at different frequencies and temperatures will alter the performance of the tyre. Since, certain tyre properties involve frequencies which are too high to be measured, these frequencies are reduced to a measurable level, e.g. 1Hz, at lower temperatures by applying the Time–Temperature Equivalence principle[6].

In this chapter, the tan δ, storage modulus and loss modulus of some SBR, BR, NR and IR rubbers filled with 60 phr silanized silica nanofiller will be investigated. These compounds will be mixed together to produce blends, which can be used in the manufacture of tyre tread. Therefore, understanding their dynamic properties is of significant importance to the tire industry.

10.2 Experimental

10.2.1 Mixing

The mixing procedures for preparing the NR, SBR, BR and IR compounds were fully described in section 6.2 of chapter 6, section 8.2.2 and 8.2.3 of chapter 8, and in reference 7 respectively. These formulations are shown in Table 10-1 below.

Table 10-1: Formulation of compounds 1-7

	Compound number						
	1	2	3	4	5	6	7
SBR	100	---	---	---	---	---	100
BR	---	100	---	---	---	---	---
NR	---	---	100	100	---	100	---
IR	---	---	---	---	100	----	---
Silica	60	60	60	60	60	----	60
TBBS	3	7.5	6	6	7	6	3
ZnO	0.5	---	0.3	0.3	1	0.3	0.5
Sulphur	---	0.3	---	1.5	---	1.5	0.2
Enterflex 74	5	---	---	---	---	----	5
Santoflex 13	1	1	1	1	1	1	1

Table 10-2 below summarises the ODR test results, Mooney viscosity, bound rubber content, and crosslink density of compounds 1-7 detailed in Table 10-1.

Table 10-2: ODR test results, Mooney viscosity, bound rubber content and crosskink density of the compounds shown in Table 10-1.

	Compound number						
	1	2	3	4	5	6	7
Minimum torque (dN.m)	23	45	26	27	26	12	21
Maximum torque (dN.m)	66	133	107	135	137	71	70
Δtorque (dN m)	43	88	81	108	111	59	49
t_{s1} (min)	12	5	8	6	8	21	11
t_{90}(min)	49	49	24	9	34	32.5	37
CRI (min^{-1})	2.7	2.3	6.5	28.3	3.9	8.7	3.8
Mooney viscosity (MU)	109	162	106	111	105	49	---
Bound rubber (%)	66	93	94	94	93	---	---
Crosslink density (mol/m^3)	124	220	153	168	211	85	---

10.2.2 Compound curing procedure

Compounds curing procedure were described in section 5.3.

10.2.3 Measurement of G', G"and tan δ of the rubbers

Measurement of G', G"and tan δ of the rubbers were performed by DMA as it was described in section 5.13.

10.3 Results and discussion

10.3.1 Determination of tan δ for the silica filled NR compound

Figure 10-1 shows tan δ versus temperature at 1 Hz frequency for compound 3 in Table 10-1. The regions were tan δ values correspond to ice-grip, wet-grip and rolling resistance of passenger car tyres are shown on the figure.

From the viscoelastic property point of view [2], an ideal material, which is able to meet the requirement of a high-performance tyre tread should give low tan δ values at a temperature range of 50-80°C in order to reduce rolling resistance and save energy. The ideal material should also have high tan δ values or high hysteresis at lower temperatures for example less than -20°C in order to obtain high skid resistance and wet grip. However, the factors involved in skid resistance are recognized to be more complex than a single compound property. It is therefore evident that compound 3 satisfies all the requirements mentioned above. As can be seen in Figure 10-1, at sufficiently low temperatures, i.e. less than the Tg of the rubber, the tan δ value is very low (here about 0.05). This is due to the fact that the viscosity of the rubber is so high and the free volume in the polymer is so small that the movement of the polymer chain segments and the adjustment of their relative positions can hardly take place in the time scale involved in these experiments. Therefore, this results in a low energy dissipation or absorption in the rubber and low loss modulus, hence low hysteresis or tan δ. Under this condition, the polymer falls in the glassy state with a very high storage modulus.

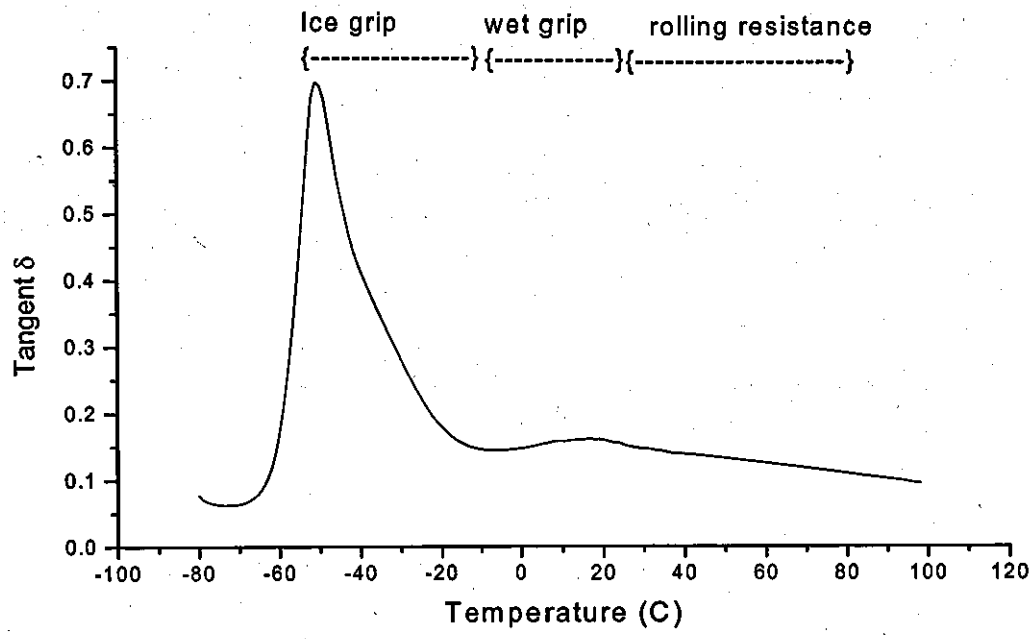

Figure 10-1: Tan δ versus temperature for compound 3 in Table 10-1

With increasing temperature, the movement of the polymer chain segments increase. When the temperature reaches a certain level, i.e. Tg, the free volume of the polymer increases more rapidly than the volume expansion of the molecules, facilitating the segmental motion.

Above Tg, the viscosity of the polymer decreases very rapidly and the molecular adjustment takes place more easily, so the storage or elastic modulus decreases. Simultaneously the energy dissipation within the polymer molecules increases with temperature, resulting in a high hysteresis or high tan δ values.

At temperatures high enough, i.e. greater than 50°C, the Brownian motion is so rapid and viscosity is so low in the polymeric solid that the thermal energy is comparable to the potential energy barriers to segmental rotation, the molecular adjustment is quick enough to be able to follow the dynamic strain. Hence, long range contour changes of polymer molecules may take place and low resistance

to strain. Now the material is in rubbery region with low energy dissipation or low loss modulus during dynamic deformation.

Figure 10-2 represent tan δ versus temperature at 1, 10 and 100 Hz test frequencies and 500 µm oscillation amplitude for the filled NR rubber (compound 3 in Table 10-1). With increasing the test frequency from 1 to 100 Hz, the curves shifted to the right hand side towards higher temperatures. In addition, as the test frequency increased from 1 to 100 Hz, the tan δ values were noticeably higher at a given temperature above the peak tan δ values. This was the case for temperatures greater than – 40°C and up to 0°C. For example, at -20°C, the tan δ values were 0.28, 0.42 and 0.58 at 1, 10 and 100 Hz, respectively. Evidently, an increase in the test frequency raised tan δ or energy dissipation in the rubber significantly, at least for temperatures up to 0°C. Thereafter, tan δ decreased sharply to approximately 0.02 at 100 Hz and very slowly to 0.12 at 1 and 10 Hz, respectively.

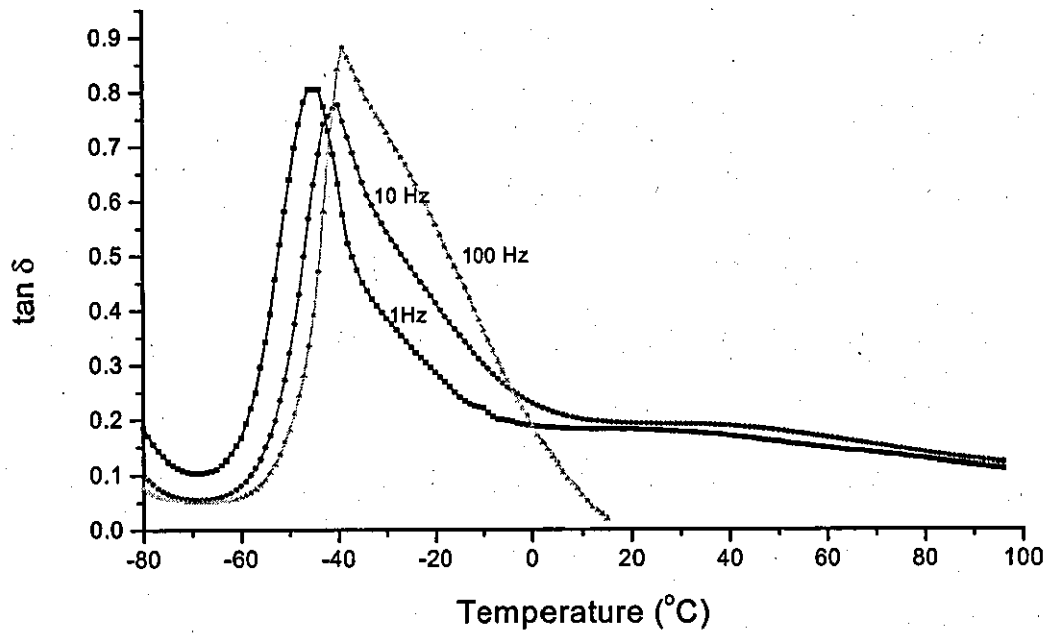

Figure 10.2: Tan δ versus temperature for compound 3 in Table 10-1 at different frequencies and an oscillation amplitude of 500 µm.

Figure 10-3 shows tan δ versus temperature for the filled NR compound (compound 3 in Table 10-1) at three different frequencies and an oscillation amplitude of 1000 µm. Before tan δ reached its peak, the tan δ values increased as a function of frequency. For instance, at -50°C, tan δ were 0.68, 0.34 and 0.21 at 1, 10 and 100 Hz, respectively. However, after tan δ reached its maximum value, the trend changed. For example, at -30°C tan δ were 0.58, 0.76, and 0.79 as the test frequency was increased from 1 to 100 Hz, respectively. It was also noted that at about -8°C tan δ at 100 Hz continued decreasing sharply to 0. At 1 and 10 Hz, tan δ reduced at a slower rate to 0.14 and 0.19, respectively as the temperature reached 100°C.

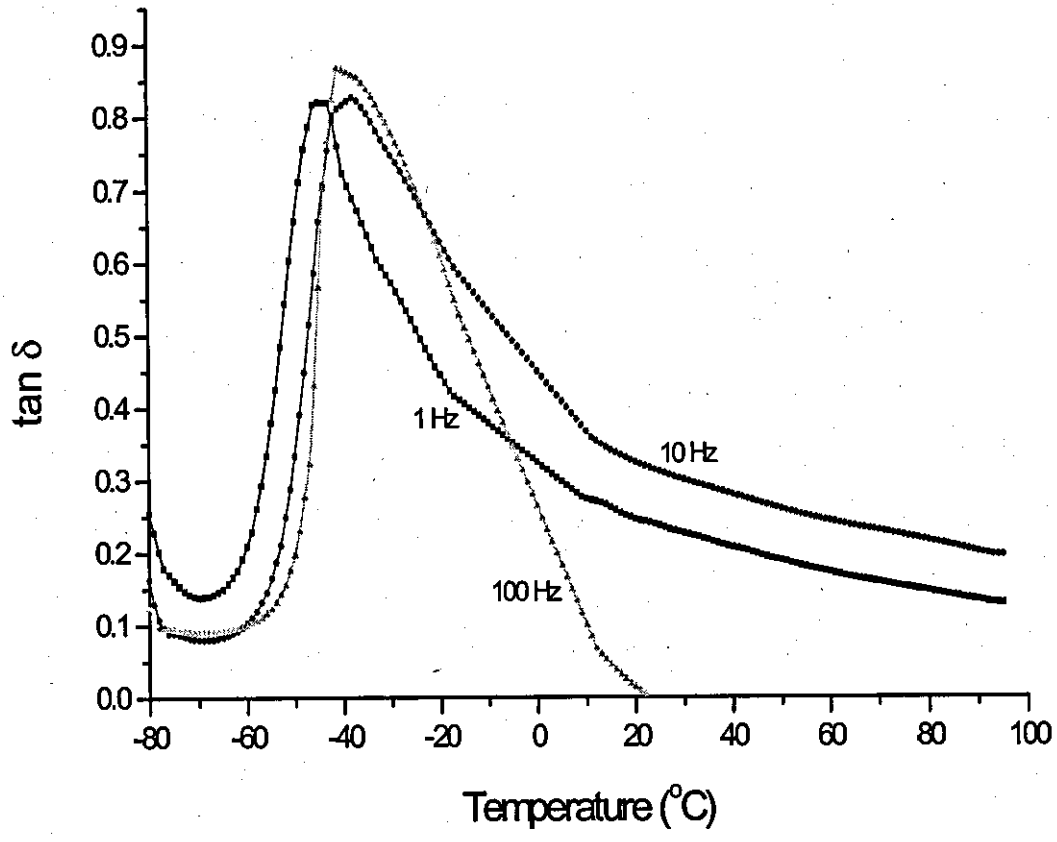

Figure 10-3: Tan δ versus temperature for compound 3 in Table 10-1 at different frequencies at an oscillation amplitude of 1000 µm.

The peak tan δ values as a function of test frequency for 500 and 1000 μm oscillation amplitudes are summarised in Table 10-3. At 500 μm oscillation amplitude, this property was frequency dependent and decreased from 0.85 to 0.76 as the frequency was increased from 1 to 10 Hz, and then rose to 0.87 at 100 Hz. At 1000 μm oscillation amplitude, this property was unchanged with test frequency and was at 0.82, and then increased to 0.86 when the frequency was increased to 100 Hz.

Table 10-3 Peak tan δ values as a function of test frequency. Data taken from Figures 10-2 and 10-3.

Test frequency	1 Hz	10 Hz	100 Hz
At 500 μm oscillation amplitude			
Peak tan δ value	0.85	0.76	0.87
At 1000 μm oscillation amplitude			
Peak tan δ value	0.82	0.82	0.86

It seemed that increasing the test frequency and oscillation amplitude in some cases raises tan δ or energy dissipation in the rubber as a function of temperature. For example, at 500 μm, the peak tan δ value increased from 0.85 to 0.87 when the test frequency was raised from 1 to 100 Hz. It was also noted that the results at 10 Hz did not follow the trend. Similarly, when the oscillation amplitude was increased from 500 to 1000 μm, the peak tan δ value reduced from 0.85 to 0.82 at 1 Hz, and from 0.87 to 0.86 at 100 Hz. The result at 10 Hz followed an opposite trend, and it increased from 0.76 to 0.82.This is explained in terms of filler-filler and polymer-filler network break down and re-formation, which causes heat dissipation in the rubber. It means that as the test frequency and oscillation amplitude increase, the filler-polymer network breaks down and reforms more rapidly, and consequently more energy is dissipated in the rubber,

giving rise to higher tan δ values. However, the exact reason for the unusual trend at 10 Hz is not immediately clear.

Note also that at sufficiently low temperatures for example at -50°C, the tan δ values at 1 Hz and oscillation amplitudes of 500 and 1000 μm were 0.65 and 0.69, respectively. At 10 Hz, these values were almost the same at 0.34-0.35, and at 100 Hz, they were 0.17 and 0.22, respectively. At the same temperature above approximately -30°C, the tan δ values were higher at higher frequencies and oscillation amplitudes. Clearly, the oscillation amplitude has a major effect on these measurements. This will be investigated further.

When the tanδ increments (Δtanδ) were measured at the same oscillation amplitude and at different frequencies, for example at 500 μm and at 1, 10 and 100 Hz, at high temperatures, e.g. -10°C, they were 0.09 and 0.17, and at low temperatures, e.g. -50°C, 0.13 and 0.46, respectively, which showed larger Δtanδ increases in the latter case. This is because at sufficiently low temperatures, in addition to heat dissipation produced by filler-filler and filler-polymer networks break down and reformation, polymer in situ, also has an important role in the processes causing heat dissipation. This can be further confirmed when we examine the tan δ results at 1Hz and an increasing oscillation amplitudes. Figure 10-4 represents tan δ versus temperature at 1 Hz and 15, 256, 500 and 1000 μm oscillation amplitudes for compound 3 in Table 10-1. It is clear that at higher temperatures, i.e. approximately above -50°C, tan δ increases as a function of the oscillation amplitude a lot more significantly than it does at lower temperatures, i.e. below -50°C. This confirms our previous findings namely that the oscillation amplitude as well as the test frequency affect the tan δ values.

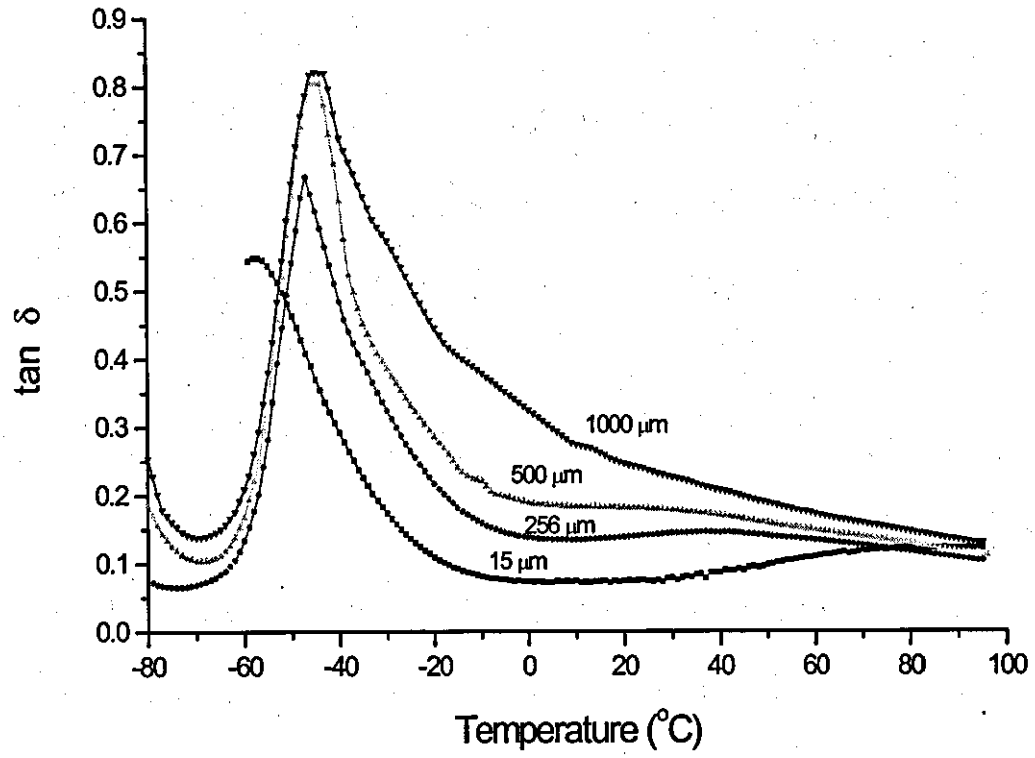

Figure 10-4: Tan δ versus temperature at 1 Hz and 15, 256, 500 and 1000 µm oscillation amplitudes. Data for compound 3 in Table 10-1.

Figure 10-5 represents tan δ versus oscillation amplitude at 1 Hz and at -50, -35, -20, 0, 25, 45, 65 and 85°C for compound 3 in Table 10-1.

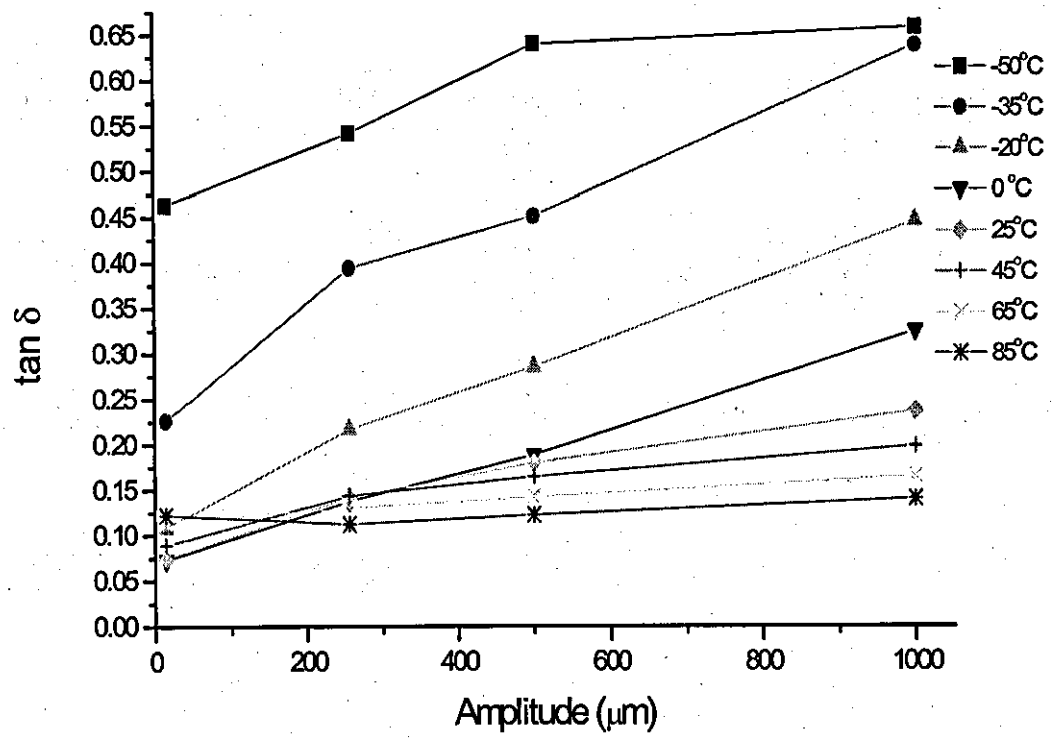

Figure 10-5 - Tan δ versus oscillation amplitude at 1 Hz at different temperatures for compound 3 in Table 10-1.

It is evident that the rate of increase of tan δ as a function of the oscillation amplitude depends on temperature. At low temperatures, i.e. 0 - -50°C, tan δ increases at a faster rate. The lowest rate of increase occurs at 65 and 85°C. At high temperatures the polymer matrix is too rubbery to resist imposed strains. Indeed, polymer chains move in the same direction of the applied strain with the least resistance and consequently the heat dissipation in the rubber will be minimum. Hence, increasing the oscillation amplitude has little or no effect on the tan δ measurements.

Figure 10-6 represents loss modulus, G" as a function of the oscillation amplitude at 1 Hz and -50, -35, -20, 0, 25, 45, 65 and 85°C temperatures for compound 3 in Table 10-1.

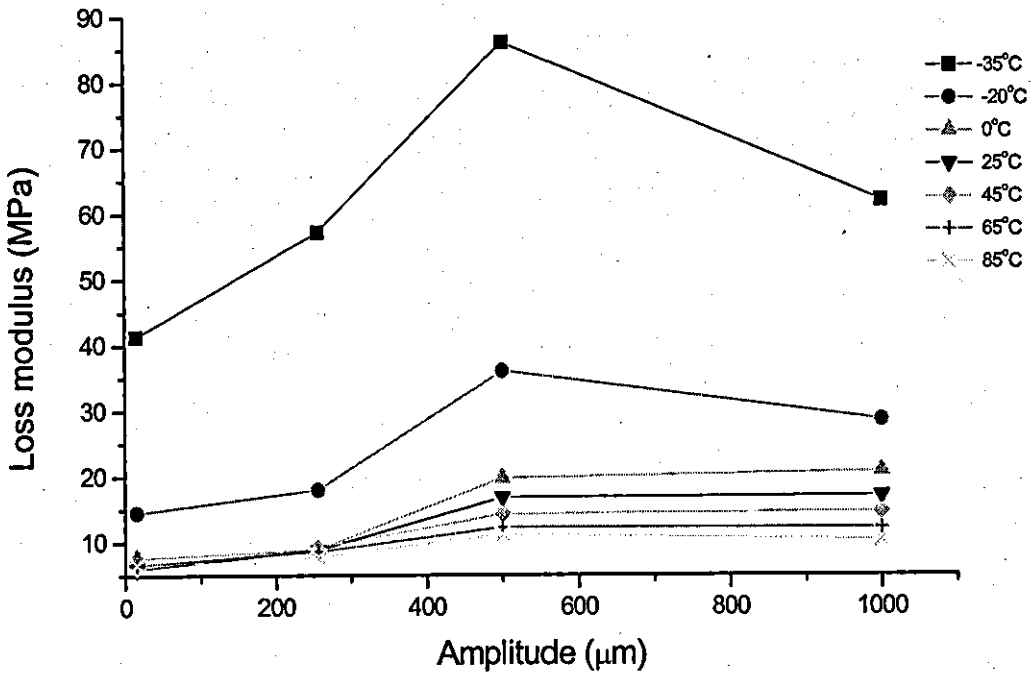

Figure 10-6 - Loss modulus versus oscillation amplitude for compound 3 in Table 10-1 at 1 Hz and different temperatures

As it is evident, the loss modulus of the rubber reaches a maximum value at 500 μm oscillation amplitude irrespective of the temperature value. The loss modulus has the highest values at -35°C, reaching a peak and then dropping to lower values. This trend was also present at -20°C. As the temperature increases to 85°C, the loss modulus decreases progressively. Note also that the lowest values were recorded at 85°C.

This bahaviour confirms that at high temperatures heat dissipation is minimum because of the rubbery state of the material.

Figure 10-7 shows storage modulus, G', versus oscillation amplitude at 1 Hz and -50, -35, -20, 0, 25, 45, 65 and 85°C temperatures for compound 3 in Table 10-1.

It is interesting that the storage modulus decreases as the oscillation amplitude reaches 256 μm and then, it increases when the oscillation amplitude reaches 500 μm. Thereafter, it continues decreasing at different rates depending on the temperature value. For example, the largest decrease is recorded at -35°C and the smallest at 45-65°C. The only exception is at 65 and 85°C, where the storage modulus keeps increasing until the oscillation amplitude reaches 500 μm. Clearly, both temperature and oscillation amplitude have a large effect on the storage modulus.

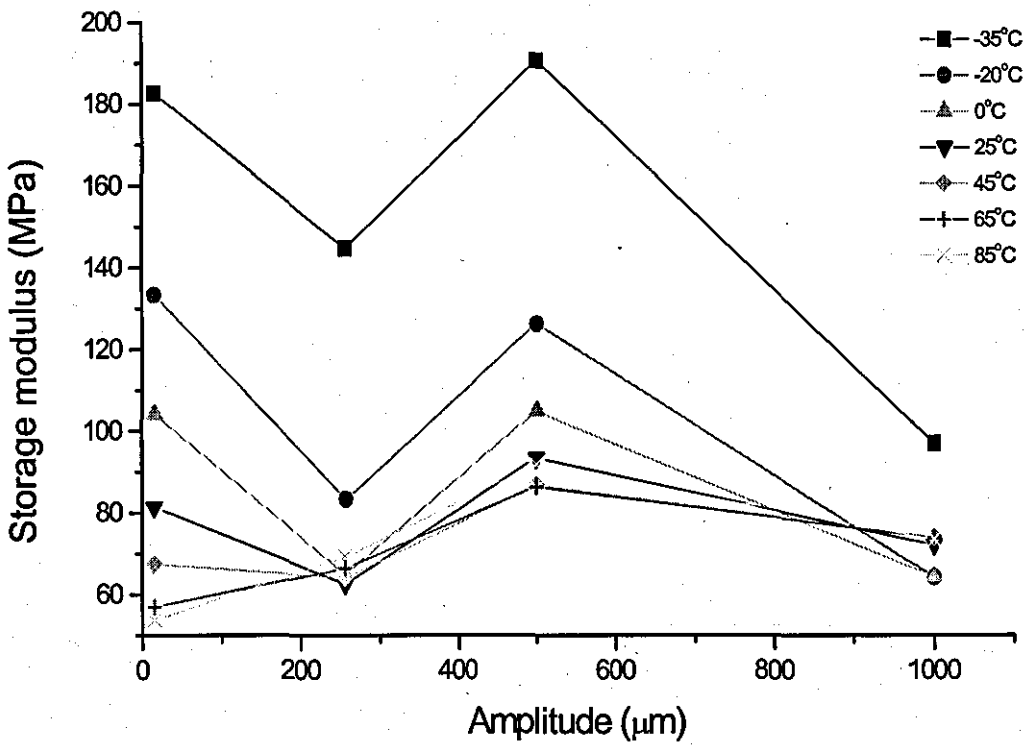

Figure10-7 - Storage modulus versus oscillation amplitude of compound 3 in Table 10-1 at 1 Hz frequency and different temperatures

Figures 10-8 and 10-9 represent loss and storage modulus (G'' and G') versus temperature at 1, 10 and 100 Hz and 500 μm oscillation amplitude for compound 3 in Table 10-1. Increases in test frequency shifts the storage and loss modulus to the right hand side or higher temperatures. The loss modulus decreases first

as temperature increases to about -70°C and then it rises sharply, reaching a peak at approximately -55 to -40°C. Thereafter, it drops to a much lower value at temperatures above -20°C where temperature differences no longer affect it. Note that the peak values of the loss modulus were test frequency and temperature dependent and the lowest and highest values were at 1 and 100 Hz, respectively. In different way, storage modulus rises up to reach to a peak at -65 °C and then drops sharply for all studied frequencies.

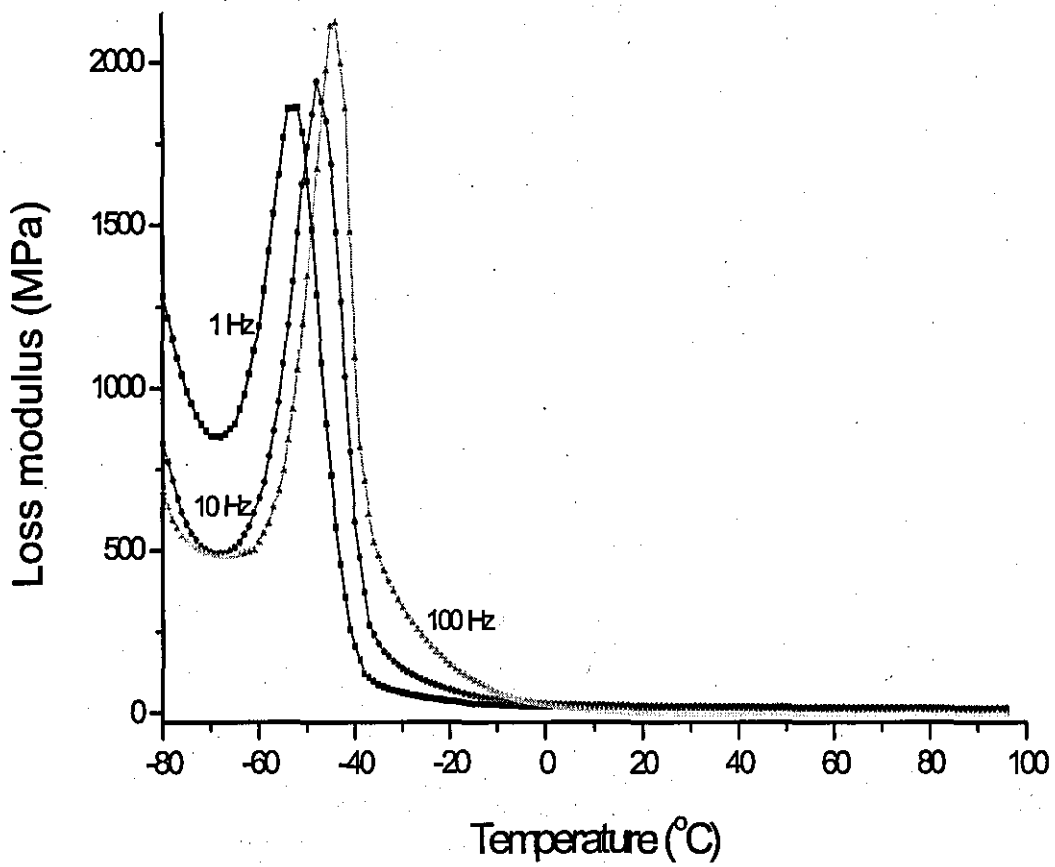

Figure 10-8 - Loss modulus versus temperature at different test frequencies. Data for compound 3 in Table 10-1 and oscillation amplitude of 500 µm

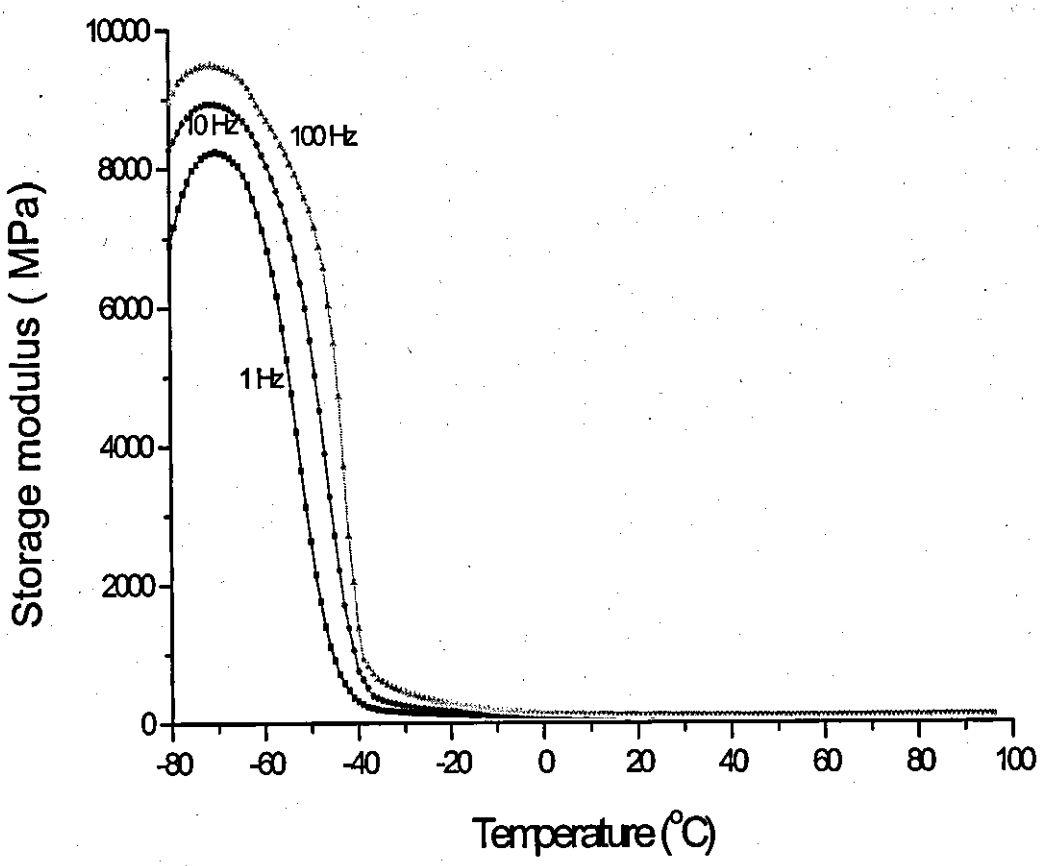

Figure 10-9 - Storage modulus versus temperature at different test frequencies and oscillation amplitude of 500 µm. Data for compound 3 in Table 10-1.

Figure 10-10 to 10-12 show tanδ, loss modulus and storage modulus as a function of oscillation amplitude at different temperatures for compounds 3 and 4 in Table 10-1. The data were produced at a test frequency of 1 Hz. At low temperatures, e.g. -35°C, tanδ rises for both compounds as the oscillation amplitude increases. For up to 350 µm oscillation amplitude, the tanδ value of compound 4 is higher than that of compound 3, however, above this amplitude, the trend reverses. Interestingly, for compound 4 tanδ remains constant as the oscillation amplitude increases to 1000 µm (Fig. 10-10).

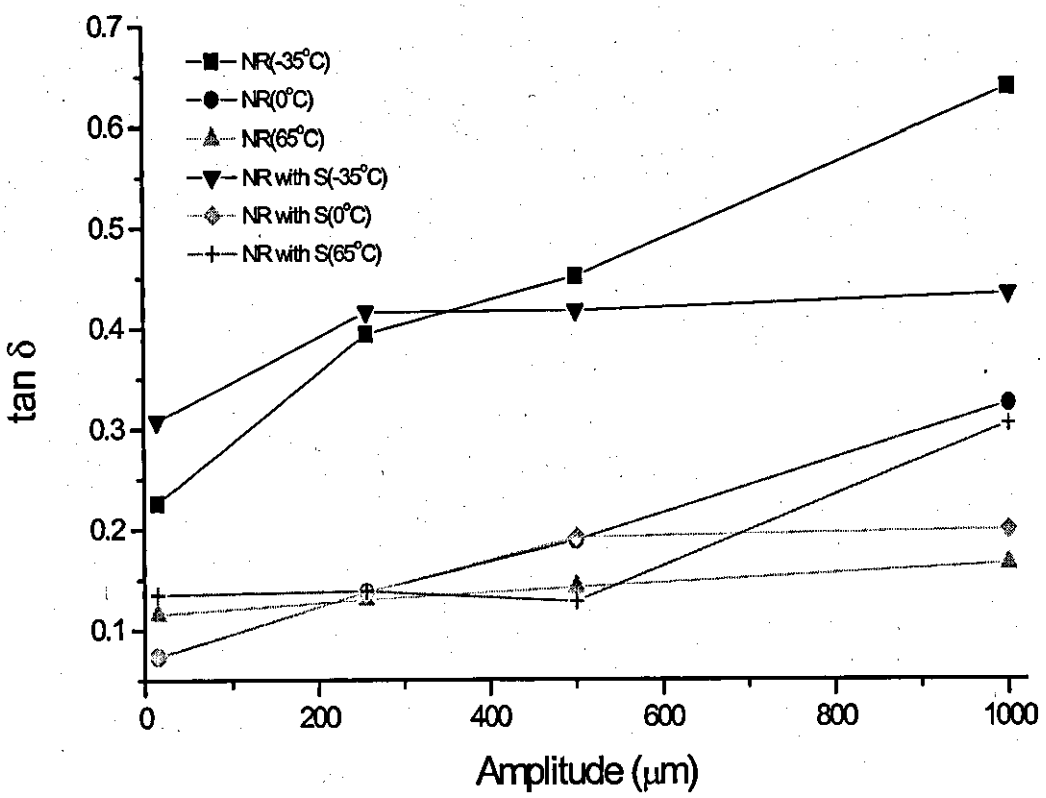

Figure 10-10 - Tan δ versus oscillation amplitude at different temperatures for compounds 3 and 4. The test frequency was 1 Hz.

Compound 4 was cured with elemental sulphur in addition to the sulphur crosslinks, which were formed between the rubber and filler via TESPT. Therefore, compound 4 had more crosslinks than compound 3 and consequently the polymer-filler interaction was stronger. This limited the polymer chains mobility and reduced the energy dissipation processes in compound 4, hence giving lower tan δ values. Beyond 256 μm oscillation amplitude, the network breaks down and re-forms under an increasing strain level but remained unchanged for compound 4. Therefore, the value of tan δ at this temperature may be used as a means of measuring the skid resistance of a tyre tread. It is worth mentioning that the higher the tan δ value is, the higher the skid resistance

of a tyre tread will be. On this basis, it seems that compound 3 has a better skid resistance than compound 4 because of a higher tan δ value.

At higher temperatures, e.g. 0 and 65°C, the tan δ values for these compounds are very similar for up to 500 µm and increase for compound 3 at 65°C and for compound 4 at ^{0}C as the oscillation amplitude increases. Tan δ for compound 3 at 0°C and for compound 4 at 65°C increases substantially above 500 µm. Therefore, 65°C is a good temperature for measuring the rolling resistance of a tyre tread, at least for these compounds. The lower the tan δ value of a compound is, the lower the rolling resistance of a tyre will be. Both compounds have more or less the same tan δ values for up to 500 µm oscillation amplitude, but above this, compound 3 at 65°C and compound 4 at 0°C have the lowest tan δ values. Therefore, compound 3 with the lowest tan δ values at 65°C offers the lowest rolling resistance. Note that to minimize the rolling resistance of tyres, it is essential to keep tan δ low over a temperature range of 50 to 100°C.

The behaviour of loss modulus at -35 $°C$ for compounds 3 and 4 are completely different (Fig. 10-11). Compound 4 has a higher loss modulus below 400 µm oscillation amplitude, and a lower one at higher amplitudes compared with compound 3. At 0 and 65°C, the loss modulus is significantly lower for both compounds. The loss modulus is almost the same for the two compounds for up to 250 µm oscillation amplitude irrespective of temperature. However, as the oscillation amplitude increases to 500 µm, the compounds have different loss modulus. The lowest loss modulus is recorded for compound 4 at 65°C and the highest for compound 3 at ^{0}C. The loss modulus for compound 4 at 0 and 65°C reaches a peak at 500 µm, whereas for compound 3, it remains constant at 0 and 65°C as the oscillation amplitude is raised to 1000 µm.

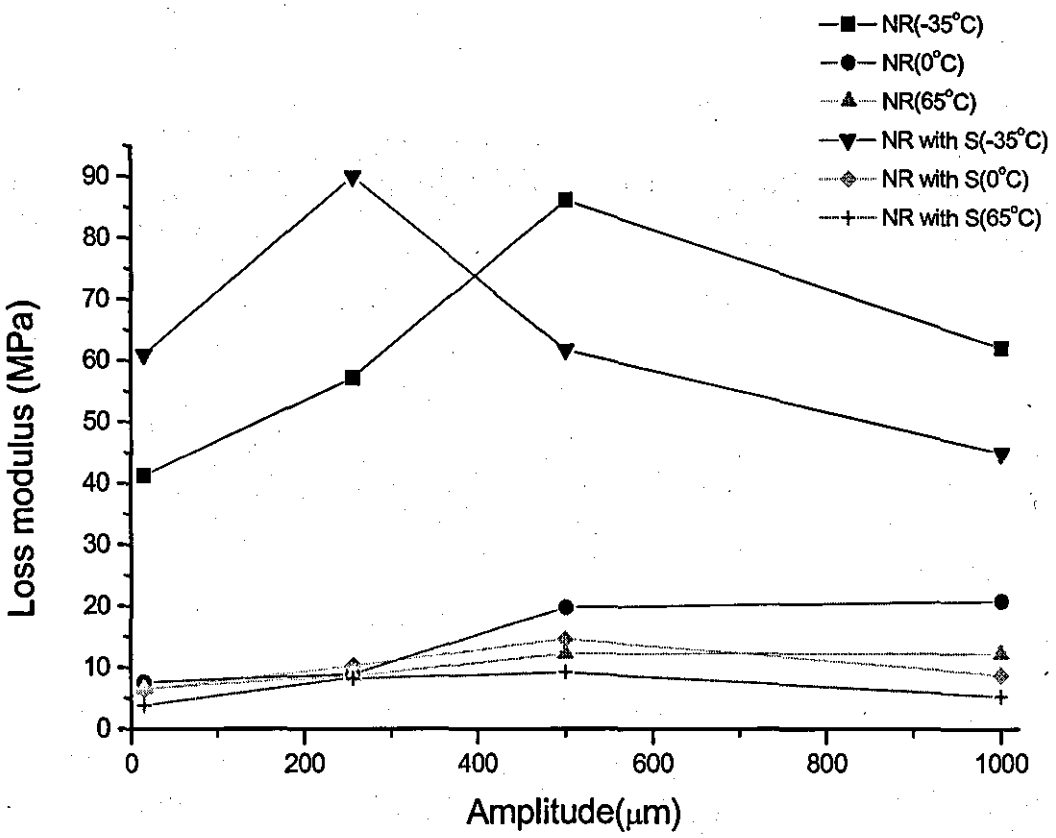

Figure 10-11: Loss modulus versus oscillation amplitude at different temperatures for compounds 3 and 4. The test frequency was 1 Hz.

The storage modulus of compound 4 was higher than that of compound 3 at -35°C for up to 400 μm oscillation amplitude (Fig. 10-12). Thereafter, compound 3 had a higher storage modulus but at 1000 μm oscillation amplitude, there was no difference in the storage modulus of the two compounds. At 0 and 65°C, the storage modulus of the compounds converged when the oscillation amplitude was increased to 250 μm. However, as the oscillation amplitude was raised to 500 μm, compound 3 at 0°C had the highest and compound 4 at 65°C the lowest storage modulus. This trend continued when the oscillation amplitude was increased progressively to 1000 μm. It should be mentioned that at this oscillation amplitude, compound 3 at 65°C had the highest storage modulus.

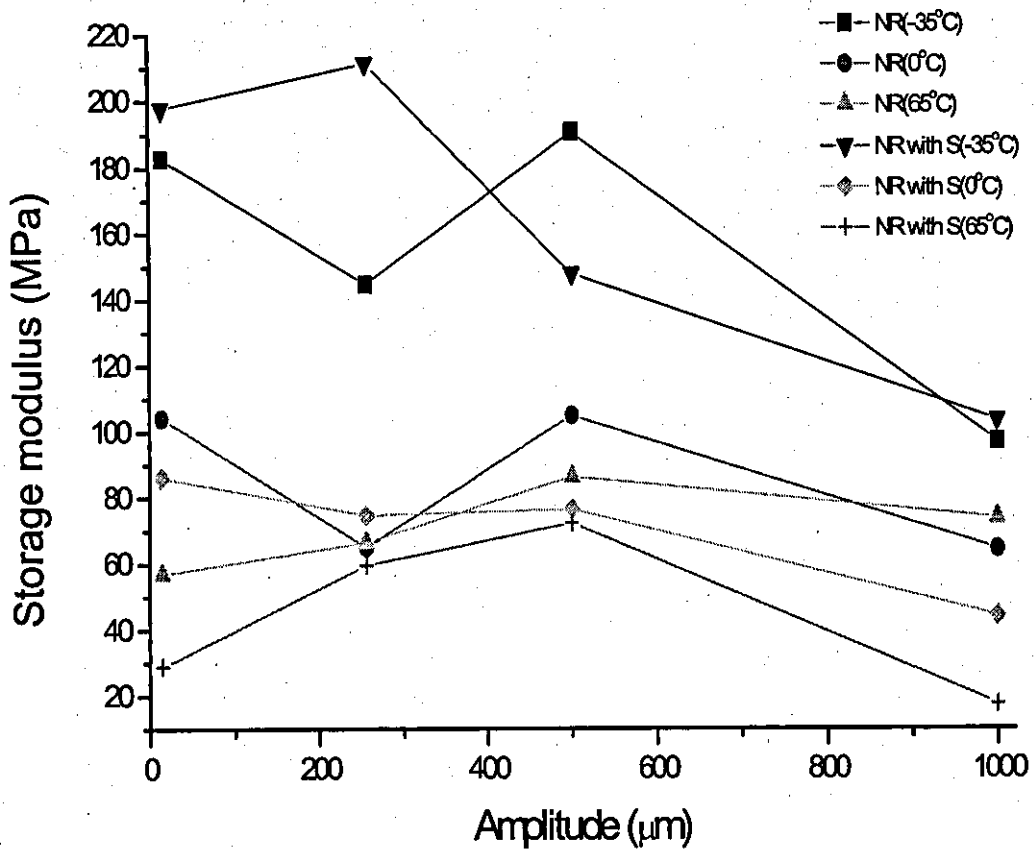

Figure 10-12: Storage modulus versus oscillation amplitude at different temperatures for compounds 3 and 4. The test frequency was 1Hz.

Figures 10-13 to 10-15 show tan δ, loss modulus and storage modulus as a function of temperature for compounds 3, 4 and 6 at 1 Hz and an oscillation amplitude of 256 μm. Compound 6 being the control compound (Table 10-1).

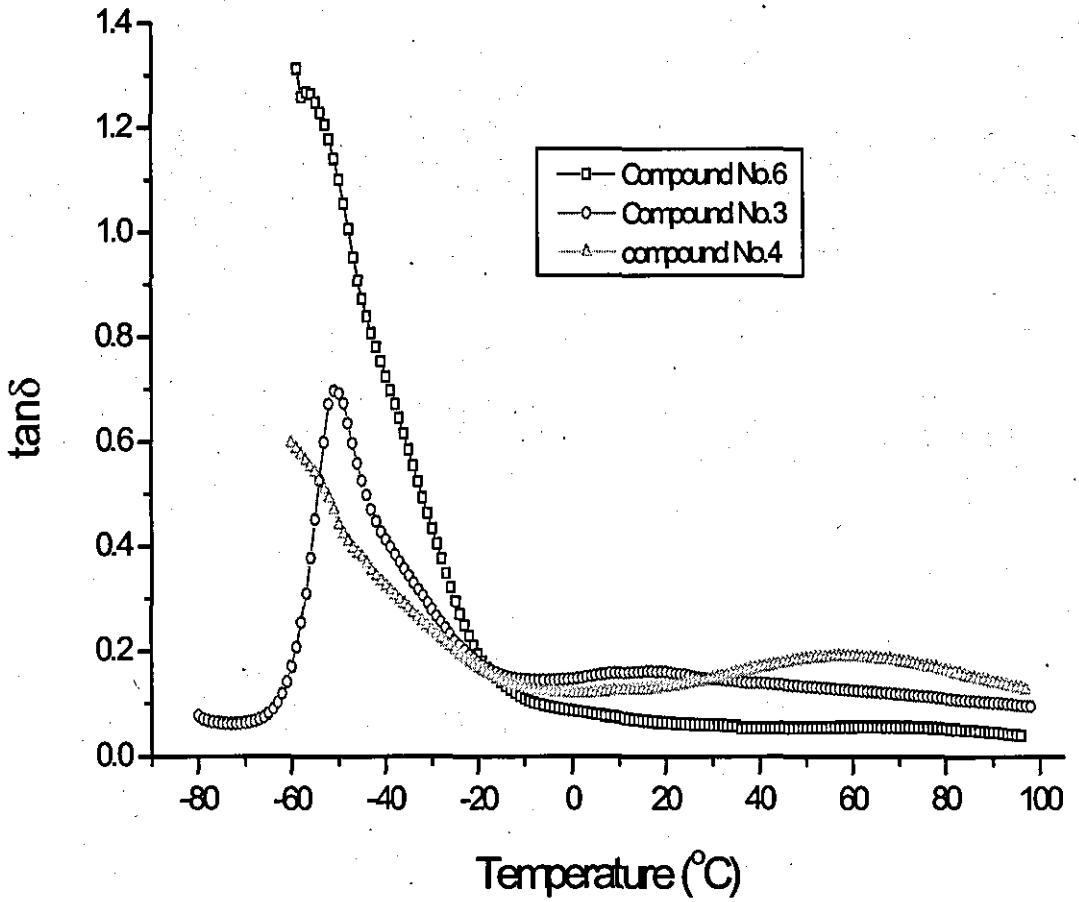

Figures 10-13: Tan δ versus temperature for compounds 3, 4 and 6 at 1 Hz and an oscillation amplitude of 256 µm.

As it is clear from this figure, compound 6 has the largest peak tan δ value followed by compound 3.It is also noted that the compounds have the same tan δ values at about -20°C and these values decrease slowly as the temperature was raised to 100°C. Over this temperature range, compound 6 has the lowest tan δ values.

Compound 4 had extra crosslinks by the addition of elemental sulphur, whereas, compound 3 was cured primarily by the tetrasulphane groups of TESPT. Hence,

the polymer chains were less mobile in compound 4 and this affected the tan δ of the compound at temperatures below and above -20°C. At low temperatures up to Tg, the bulk of polymer (polymer in situ) is the dominant factor in its dynamic bahaviour and responsible for most of the energy dissipation processes.

When polymer is replaced with solid filler in compounds 3 and 4, at low temperatures, the low energy dissipation is due to the polymer chains trapped in the polymer-filler and filler-filler networks. In fact, trapped rubber at low temperature acts as a rigid glass substance and therefore is not rubbery, and the individual solid filler particles in the filler-filler network in the polymer matrix do not absorb energy significantly.

In contrast, at high temperatures the polymer-filler and filler-filler networks have significant effect on the energy dissipation processes in the rubber. There are two mechanisms involved in the filler-filler network behaviour as discussed by Wolff and Wang [8]. They named it 'direct contact mode' and 'joint shell mechanism' or 'junction rubber mechanism'. In most cases, both of these mechanisms are responsible for the filler-filler network dynamic behaviour. In direct contact mode, the break down and reformation of the filler network dissipate energy and consequently increase tan δ.

For joint shell mechanism, at high temperatures the polymer matrix is in the rubbery state but the polymer in the rubber shell is in it's transition zone caused by the adsorption of the polymer molecules on the filler surfaces or the interaction between the polymer chains and filler. In this case, the joint shell rubber would absorb more energy, resulting in higher hysteresis or tan δ due to an increase in energy dissipation in the rubber shell as well as in polymer matrix.

Figure 10-13 shows tan δ as a function of temperature at 1 Hz and an oscillation amplitude of 256 μm for compounds 3, 4 and 6. At temperatures above 30°C, tan δ is higher for compound 4 and as temperature decreases to about -20°C,

compounds 3 and 4 have almost the same tan δ values. However, at temperatures lower than -20°C, compound 4 has much lower tan δ values than compound 3. We may therefore say that compound 4 has stronger filler-filler and filler-polymer networks due to extra crosslinks in its structure. The tanδ of compound 6 is significantly lower above -20°C and higher below this temperature when compared with those of compounds 3 and 4.

As seen in Figure 10-14, the loss modulus of compounds 3 and 4 are noticeably higher than that of compound 6. Above 20°C, compound 3 has a higher loss modulus than compound 4, otherwise at lower temperatures, they are almost the same. The storage modulus of compounds 3 and 4 are much higher than that of compound 6 over the entire range of temperature tested. Above 20°C, compound 3 has a significantly higher modulus than compound 4 but below this temperature, the trend reverses until both values converge at about -40°C. We may choose compound 3 for use in tyre tread because at high temperatures it has the lowest tanδ values.

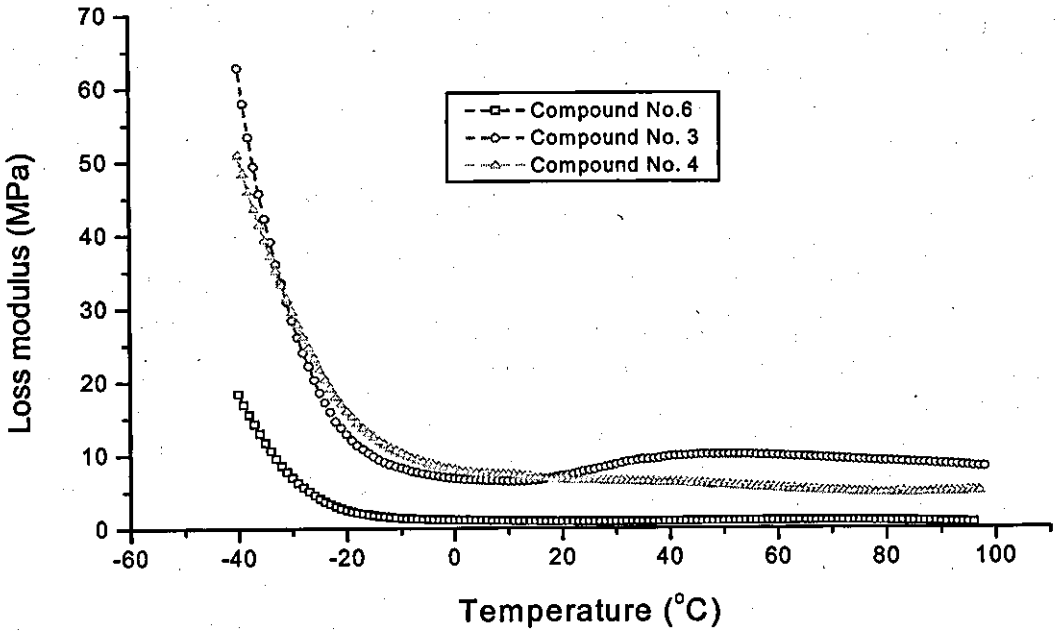

Figures 10-14: Loss modulus versus temperature for compounds 3, 4 and 6 at 1 Hz and an oscillation amplitude of 256 µm

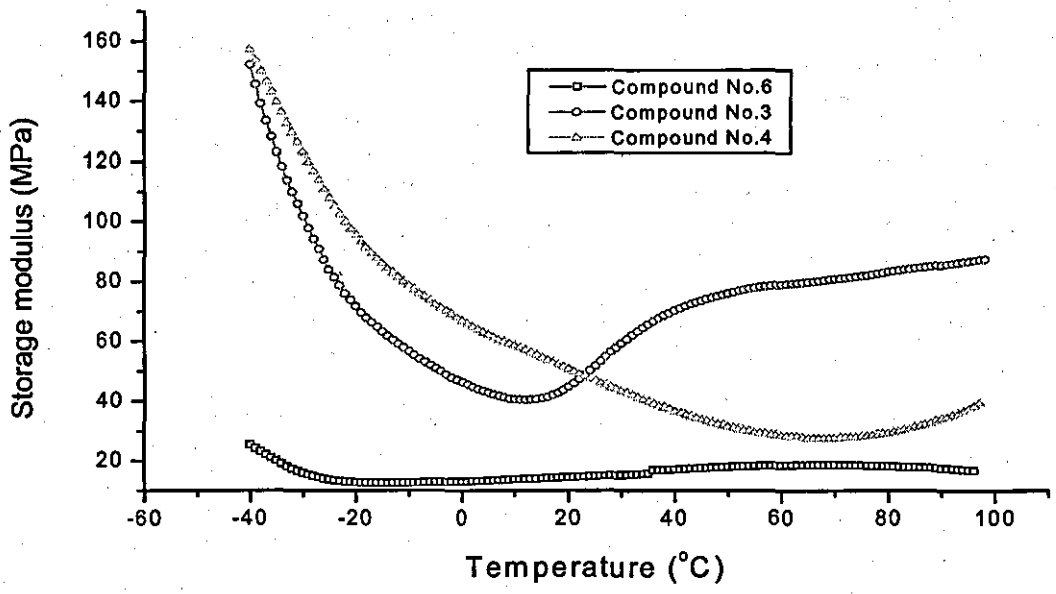

Figures 10-15: Storage modulus versus temperature for compounds 3, 4 and 6 at 1 Hz and an oscillation amplitude 256 µm

10.3.2 Comparing the dynamic properties of the silanized silica filled Compounds

Figures 10-16 to 10-18 show tanδ, loss modulus and storage modulus as a function of the oscillation amplitude at 1 Hz for compounds 1-5 from Table 10-1. The data were produced at -35°C. The tanδ values of compounds 3 and 4 (Fig. 10-16) increase and converge at 250 µm oscillation amplitude, and then diverge as the amplitude increases progressively to 1000 µm. Above 250 µm amplitude, the tanδ of compounds 1, 3 and 5 have the largest increases and that of compound 4 reaches a plateau. Note that compound 2 has the lowest tan δ values over the entire temperature range. This is because BR has the lowest Tg, -107°C, and therefore it is tested at a temperature well above it's Tg. Consequently, the polymer chain segments have a higher Brownian motion and lower viscosity, which cause less resistance to imposed strains, resulting in lower heat dissipation and tanδ values. In contrast, the test temperature is near to the

glass transition temperatures of the SBR, NR and IR rubbers, i.e. -50°C for the SBR and -61 and 64°C for the IR and NR rubbers respectively, and therefore these rubbers have higher viscosities and offer more resistance to imposed strains, resulting in higher heat dissipation and tan δ values.

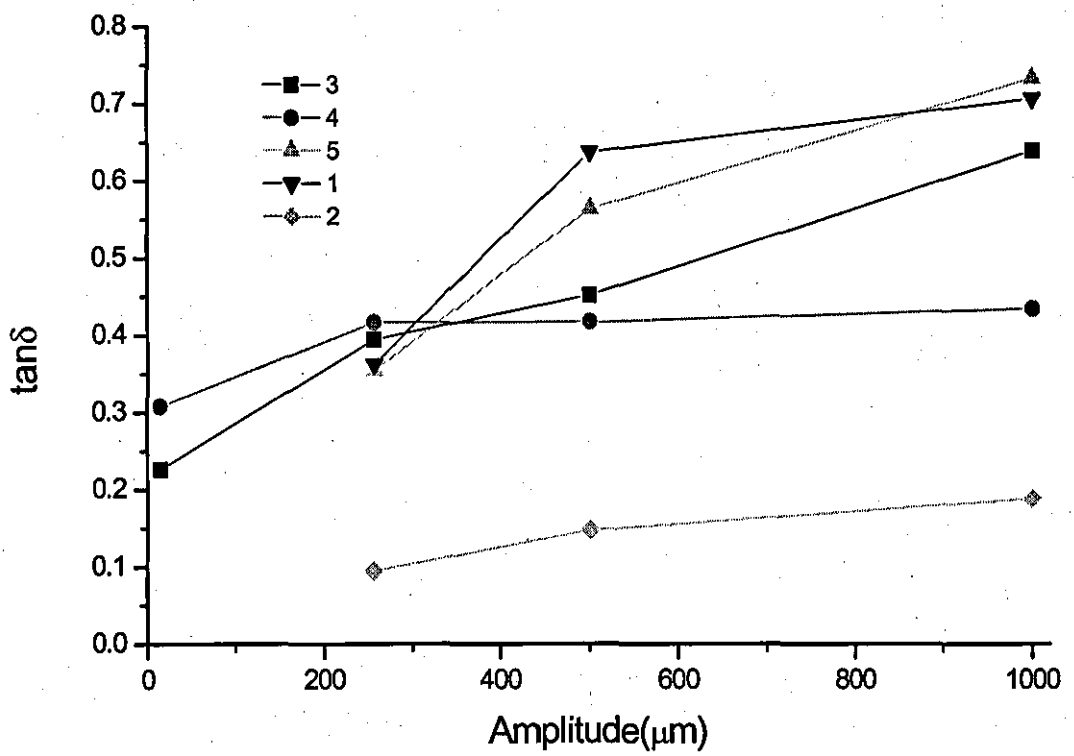

Figure 10-l6: Tan δ versus oscillation amplitude at 1 Hz and -35 ^{0}C for compounds 1-5.

At moderate oscillation amplitudes, e.g. 256-500 μm, the rate of tan δ increase for compounds 1 (the SBR rubber), 3 (the NR rubber) and 5 (the IR rubber) are the fastest. At low temperatures, the polymer in situ is more responsible for heat dissipation in the rubber than the polymer-filler and filler-filler networks break down and re-formation. Compound 1 has the least bound rubber content, i.e. 65.7%, and the lowest crosslink density, i.e.124 mol/m^3 among the compounds tested (Table 10-2). Hence, it has more free polymer chain segments in the rubber matrix, and this can generate more heat dissipation, giving rise to higher tan δ values and also a faster rate of tan δ increase when the oscillation

amplitude increases. A similar argument can not be applied to compounds 3 and 5 because these compounds have higher bound rubber content and crosslink densities.

This can be investigated further by examining the dependence of loss modulus and storage modulus on the oscillation amplitude. Figure 10-17 shows loss modulus as a function of the oscillation amplitude at 1 Hz and -35°C for compounds 1-5. Compound 1 has the highest loss modulus values over the entire amplitude range. This is because in this compound, the polymer chain segments have more freedom to respond to the applied strain due to lower bound rubber content and crosslink density. The loss modulus of the remaining compounds, show little or very modest increase as a function of the oscillation amplitude and are fairly similar. Note that compounds 2-5 have bound rubber contents 93-94% and crosslink densities 149-220 mol/m^3, which means that the polymer chain segmental mobility was minimum and this resulted in the polymer-filler and filler-filler networks break down and reformation, which are responsible for the heat dissipation in the rubber.

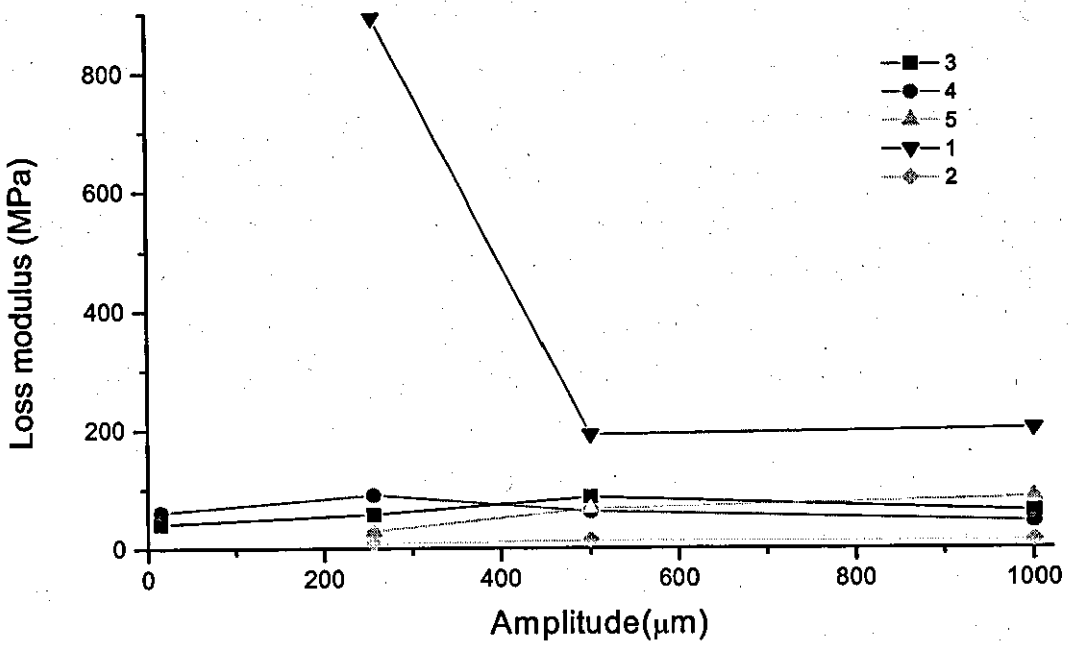

Figure 10-I7: Loss modulus versus oscillation amplitudes at 1 Hz and -35^{0}C for compounds 1-5.

Figure 10-18 shows storage modulus as a function of the oscillation amplitude at 1 Hz and -35°C for compounds 1-5. Here, compounds 1 and 2 have the highest and lowest storage modulus, respectively. The storage modulus of the compounds with the strongest polymer-filler networks, i.e. with the highest crosslink density, increases at the slowest rate when the oscillation amplitude is increased. This is because the break down and reformation of the networks is severe under different applied strains. Compound 5 is an exception. In spite of having a bound rubber content of 93% and a crosslink density of 211 mol/m^3, the storage modulus increases, though at a slow rate, when the oscillation amplitude is increased.

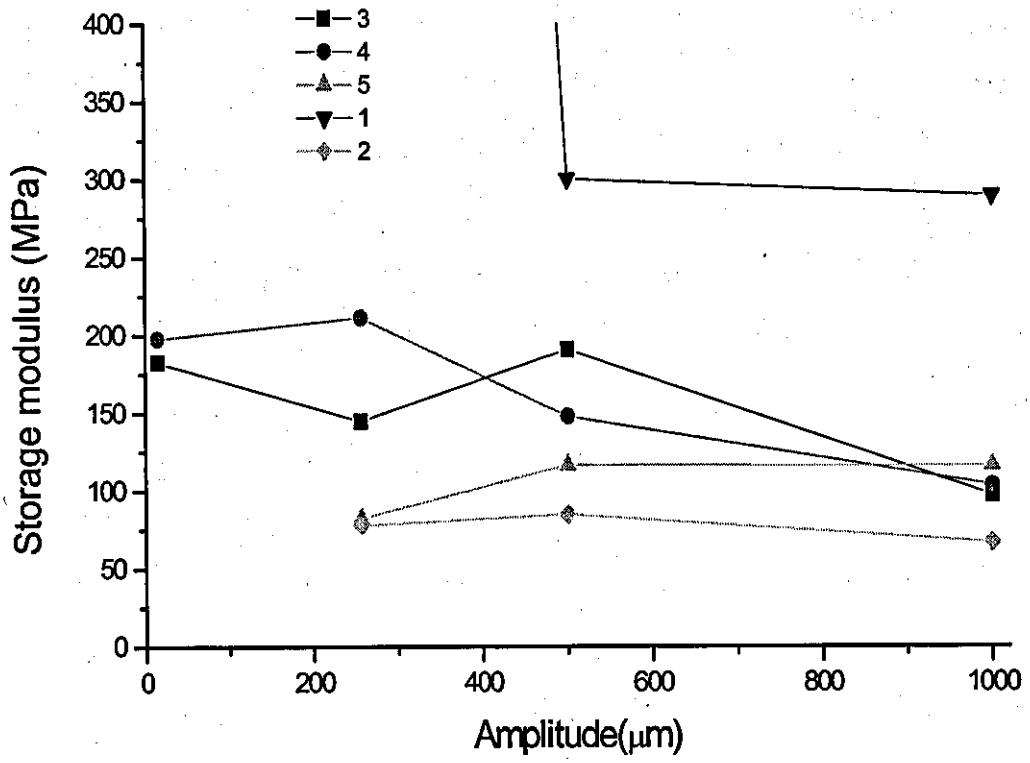

Figure 10-I8: Storage modulus versus oscillation amplitude at 1 Hz and -35°C for compounds 1-5.

Figures 10-19 to 10-21 represent tan δ, loss modulus and storage modulus as a function of the oscillation amplitude at 1 Hz and 25°C for compounds 1-5. At this temperature, tan δ increases as the oscillation amplitude is raised (Figure10-19), which is the result of the break down and reformation of the polymer-filler and filler-filler networks. The tan δ values at this temperature are less than half the values measured at -35°C. This is because at this temperature, the polymer matrix is more rubbery and polymer chain segments show less resistance to the imposed strains and move in the same direction of the applied strain. This consequently produces less heat dissipation in the rubber and lower tan δ values.

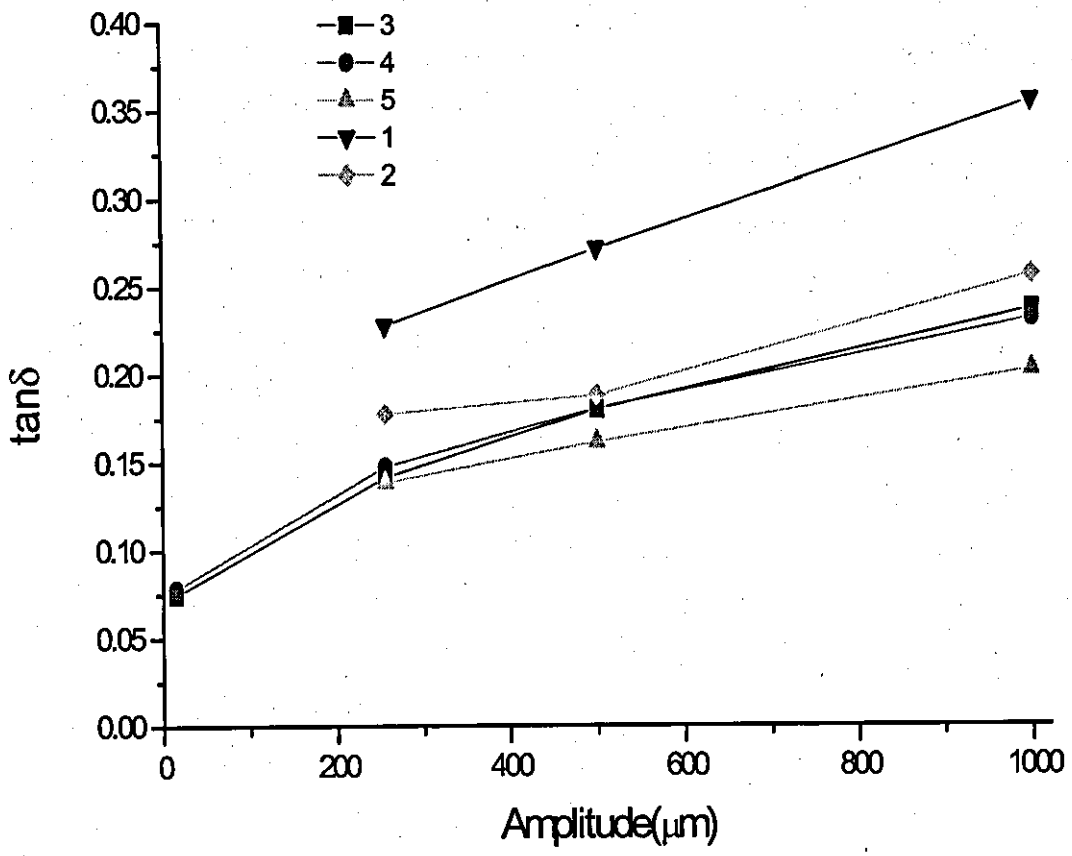

Figure 10-19: Tan δ versus oscillation amplitudes at 1 Hz and 25^{0}C for compounds 1-5.

The highest tan δ values are recorded for compound 1. At this temperature, the break down of the polymer-filler and filler-filler networks causes heat dissipation in the rubber. Hence, this compound with the smallest bound rubber content and crosslink density will have the largest heat dissipation and the highest tan δ values. The remaining compounds have much lower tan δ values because they have higher crosslink densities and bound rubber content (Table 10-2).

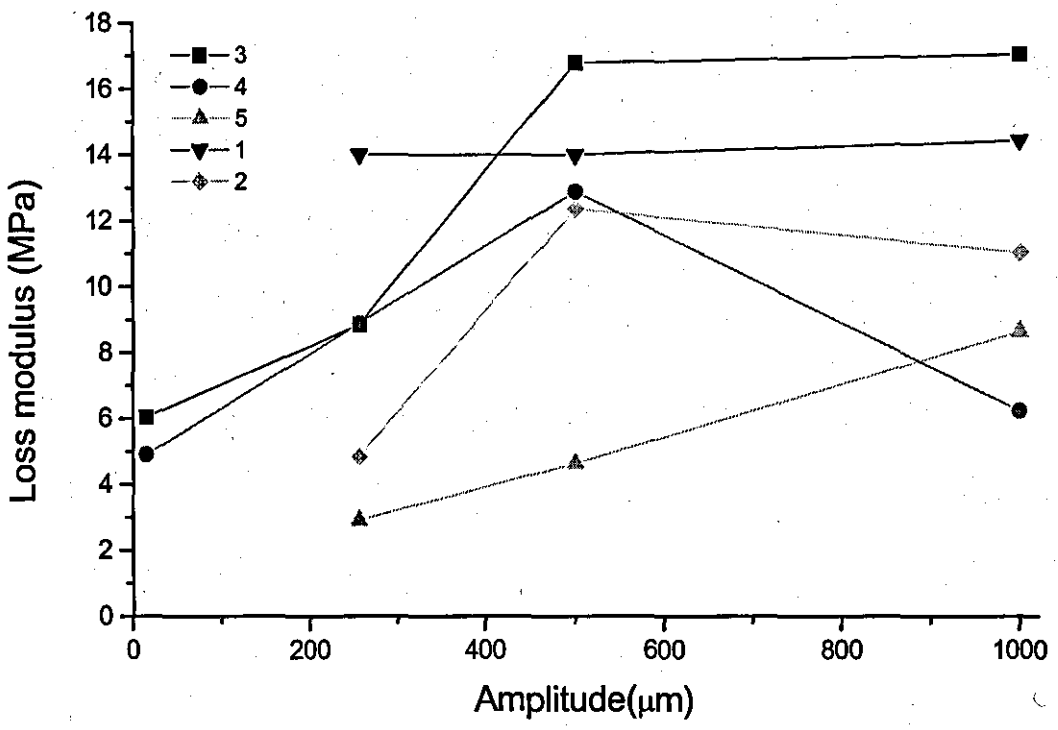

Figure 10-20: Loss modulus versus oscillation amplitudes at 1 Hz and 25^{0}C for compounds 1-5.

Figure 10-20 shows loss modulus as a function of the oscillation amplitude at 1 Hz and 25^{0}C for compounds 1-5. The loss modulus passes through a maximum for compounds 2, 3 and 4. For compound 1, the loss modulus remains almost constant, and for compound 5, it continues increasing as a function of the oscillation amplitude.

Figure 10-21 shows storage modulus as a function of the oscillation amplitude at 1 Hz and 25°C for the same compounds. Like the loss modulus, the storage modulus passes through a maximum for compounds 2, 3, and 4 but for compound 1, it decreases as a function of the oscillation amplitude. Interestingly, for compound 5, it continues rising when the oscillation amplitude is increased. The loss and storage modulus of all the filled compounds at 25°C are noticabely lower than the values measured at -35°C because the test temperature was

much higher that the Tg of the rubbers (Figures 10-17, 10-18, 10-20 and 10-21). Note that the storage modulus of compounds 1, 3 and 4 converge at about 250 μm oscillation amplitude.

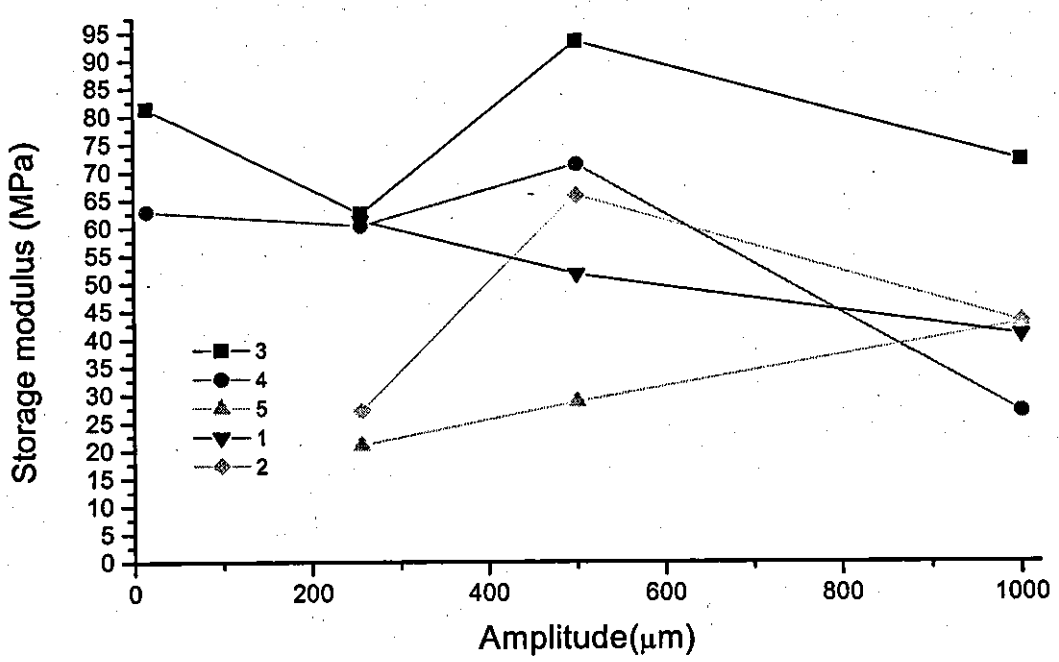

Figure 10-21: Storage modulus versus oscillation amplitudes at 1 Hz and 25 ^{0}C for compounds 1-5.

Figures 10-22 to 10-24 show tan δ, loss modulus and storage modulus as a function of the oscillation amplitude at 1 Hz and 65 $°C$ for compounds 1-5.

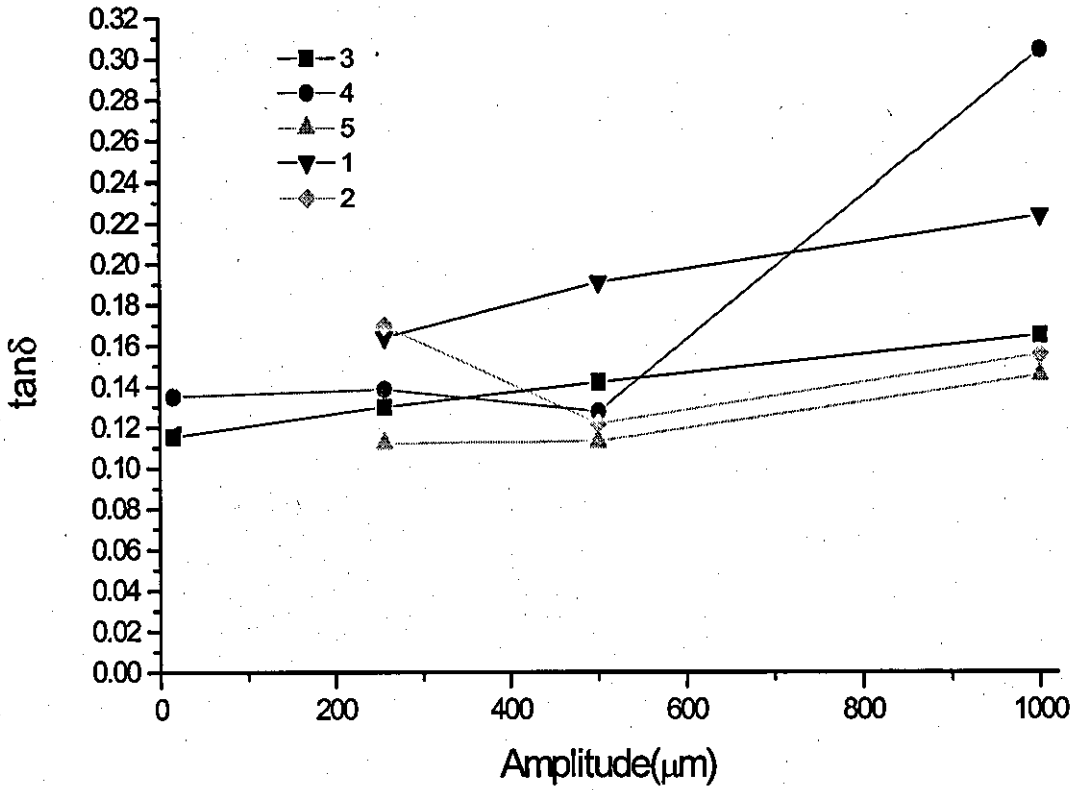

Figure 10-22: Tan δ versus oscillation amplitudes at 1 Hz and 65 ^{0}C for compounds 1-5.

This temperature is within the range of temperatures, which is used to measure the rolling resistance of car tyre treads. Low tan δ values correspond to low rolling resistance. Figure 10-22 shows slight increases in tan δ as a function of the oscillation amplitude for compounds 1, 3, 4 and 5. Note also that compounds 1 and 5 have the highest and lowest tan δ values, respectively. This suggests that these two compounds experienced the largest and the least break down and reformation of the filler-filler and polymer-filler networks during the imposed strain on the rubbers. The tan δ of compound 2 reduces sharply when the oscillation amplitude is raised to 500 μm and then increases at a slower rate as the amplitude approaches 1000 μm. The largest increases in tan δ as a function of the oscillation amplitude were measured for compound 4 above 500 μm

(Figure10-22). The highest and lowest tan δ values correspond to compounds 2 and 5 at 256 µm, compounds 1 and 5 at 500 µm and compounds 4 and 5 at 1000 µm oscillation amplitudes.

Generally, the tan δ values at this temperature are lower than those at 25 and -35°C due a to more rubbery behaviour of the rubbers as explained previously (see also Figures 10-16 and 10-19).

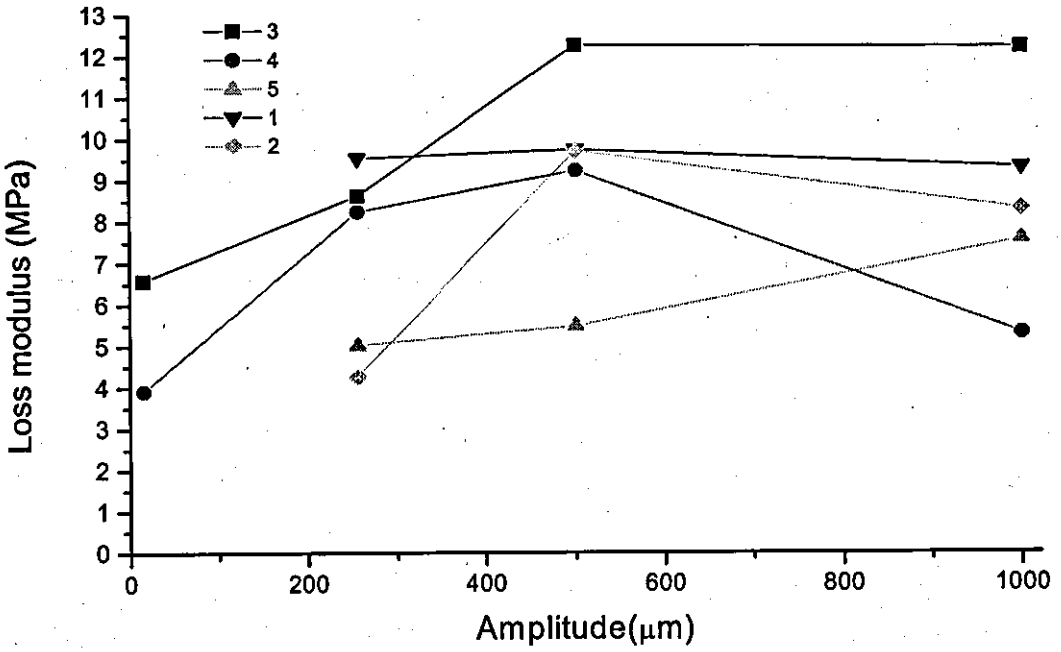

Figure 10-23: Loss modulus versus oscillation amplitudes at 1 Hz and 65 ^{0}C for compounds 1-5.

Figure 10-23 shows loss modulus versus the oscillation amplitude at 1 Hz and 65°C for compounds 1-5. The loss modulus of compounds 2, 3 and 4 increase, reaching a maximum when the oscillation amplitude is raised to 500 µm. Thereafter, the loss modulus of compound 3 remains constant and those of compounds 2 and 4 reduce with compound 4 reaching the lowest and compound 3 the highest values at 1000 µm. Note that the loss modulus of compound 1 decreases very slowly and that of compound 5 increases when the oscillation

amplitude is raised to 1000 μm. It is also interesting that at 256 μm, the loss modulus of compounds 2 and 5, and compounds 1, 3 and 4 are so similar. A similar bahaviour is also observed at 500 μm, where compounds 1, 2 and 4 have very close values. At high amplitudes, i.e. 1000 μm, the compounds have very distinct loss modulus.

The storage modulus as a function of the oscillation amplitude at 1 Hz and 65°C for compounds 1-5 is shown in Figure 10-24. The storage modulus of compounds 2, 3 and 4 increase progressively and peak at 500 μm and then decrease significantly as the amplitude reaches 1000 μm. The fastest and slowest rates of increases were measured for compounds 4 and 3, respectively. Note, the storage modulus of compound 1 decreases and that of compound 5 increases at very slow rates as the amplitude is raised to 1000 μm.

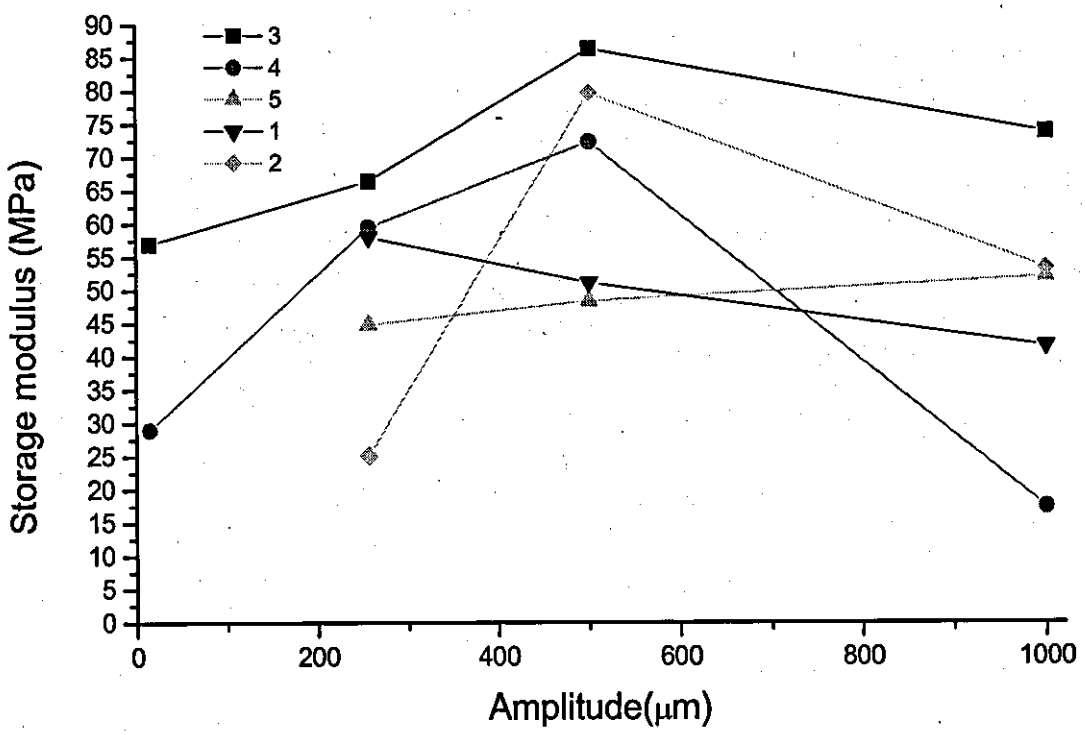

Figure 10-24: Storage modulus versus oscillation amplitudes at 1 Hz and 65 ^{0}C for compounds 1-5.

The loss and storage modulus of the compounds at 65 and 25°C are very similar but substantially lower than the values measured at -35°C (comparing Figures 10-17, 10-18, 10-20, 10-21, 10-23, and 10-24).

Figures 10-25 and 10-26 show tan δ versus temperature at 1 and 20 Hz for compounds 1-5. From the viscoelastic property point of view, an ideal material which is able to meet the requirements of a high performance tyre tread should have a low tan δ value at a temperature range of 50-80°C in order to reduce the rolling resistance and save energy [2]. The ideal material should also demonstrate high hysteresis at lower temperatures, e.g. -30-0°C in order to obtain high skid- or ice- and wet-grip resistance. We may therefore consider the tan δ variations at two temperature regions -30-0°C and 50-80°C. Figures 10-25 and 10-26 show tan δ as a function of temperature at 1 and 20 Hz and 256 μm oscillation amplitude. At -30-0°C temperature range, compound 1 has the highest and compound 2 the lowest tan δ values, respectively. There is hardly any difference in the values measured for compounds 3, 4 and 5. Note also that the tan δ values of compound 2 is at the far left hand side and those of compound 1at the far right hand side of figure 10-25. At temperatures above 0°C, compound 5 has the lowest and compounds 1 and 2 the highest tan δ values. Somewhere between 35 and 65°C, compound 1 has the highest tan δ values when compared with the other compounds. This suggest a higher heat dissipation in th compound at this range of temperature.

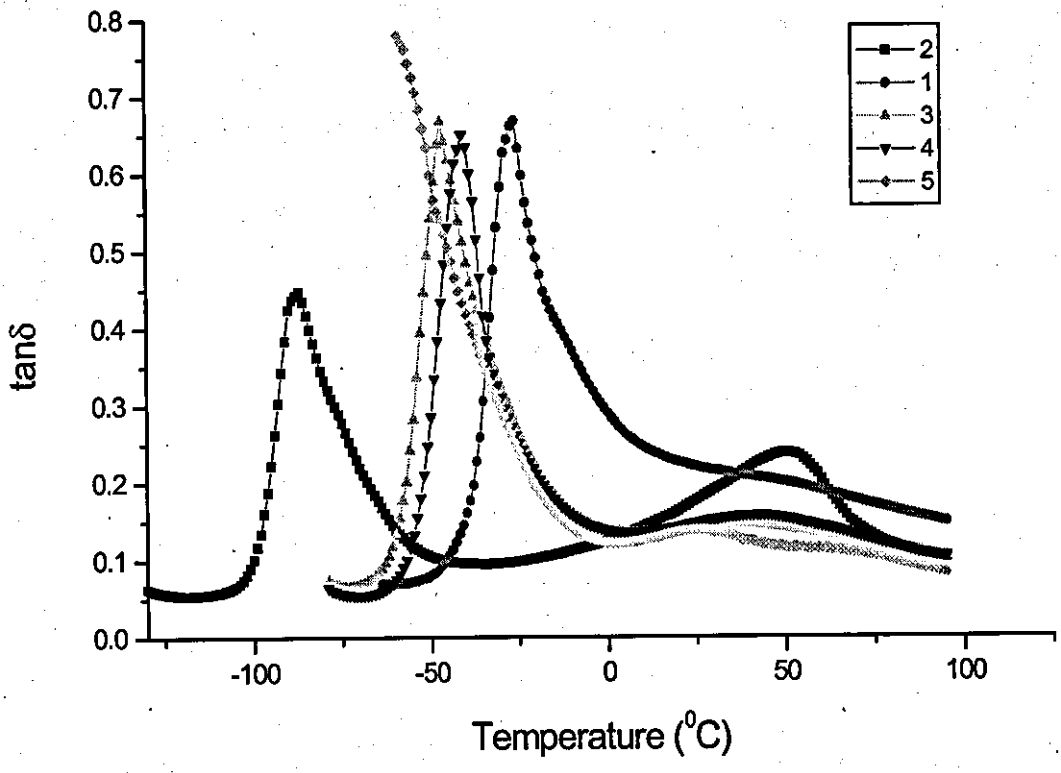

Figure 10-25: Tan δ versus temperature at 1 Hz and oscillation amplitude 256 µm for compounds 1-5.

We may therefore conclude that compound 1 has the highest and compound 2 the lowest skid-resistance, respectively. Moreover, the rolling resistance of compounds 1 and 2 is higher than that of the remaining compounds.

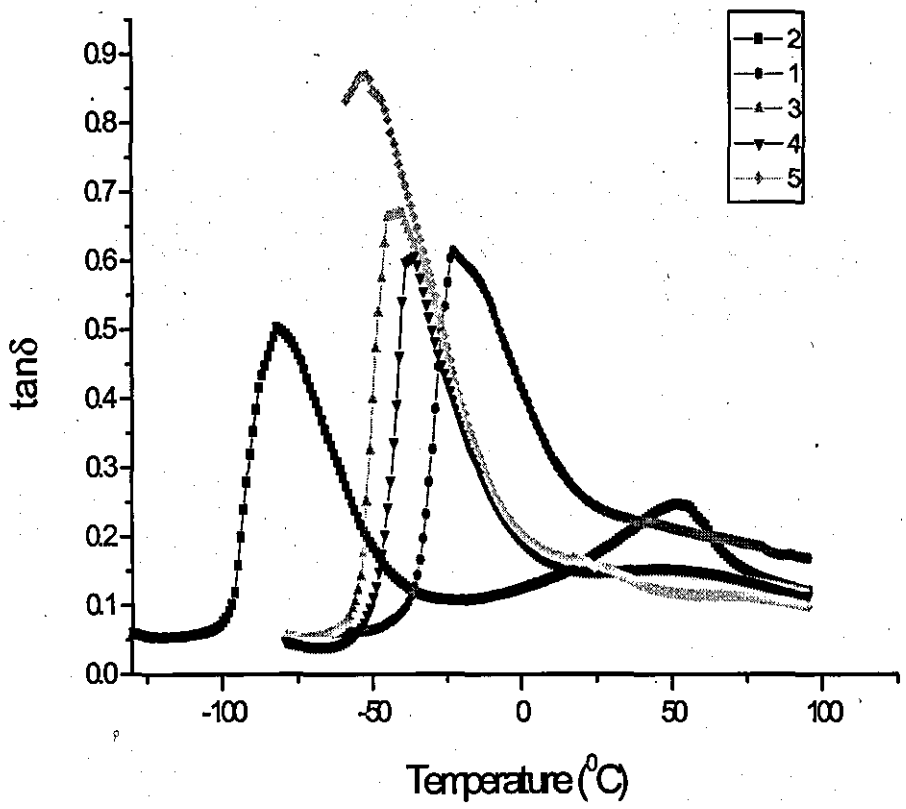

Figure 10-26: Tan δ versus temperature at 20 Hz and oscillation amplitude 256 µm for compounds 1-5.

When the peak tan δ values are measured from Figures 10-25 and 10-26, it is clear that they are affected by an increase in the test frequency (Table 10-4).

Table 10-4 – Peak tan δ values for compounds 1-5 at 1 and 20 Hz and an oscillation amplitude of 256 µm.

	Compound no				
	1	2	3	4	5
	1 Hz				
Peak tan δ value	0.68	0.45	0.68	0.66	0.79
	20 Hz				
Peak tan δ value	0.62	0.50	0.67	0.61	0.87

At both 1 and 20 Hz, compounds 5 has the largest and compound 2 the lowest $\tan\delta$ peak values. Clearly, the test frequency has had a major effect on the energy dissipation processes in the rubber.

In summary, comparison between Figures 10-25 and 10-26 shows that with frequency increasing from 1 to 20 Hz, the maximum $\tan\delta$ values of SBR, NR and NR with S filled rubbers decrease and those of BR and IR increase. The glass transition temperatures (Tg) of raw rubbers NR, SBR and BR are −64, −50 and −107 ^{0}C, respectively. Comparing these values with those of filled rubbers (−45, −24 and −85°C) shows a substantial shift of this parameter to higher temperatures owing to the reinforcing effect of the silanized pre-treated silica nanofiller. This is only qualitatively true, as the Tg values of the filled rubbers measured by the MTDSC technique are 1–5% different from those obtained from dynamic mechanical Analyser, DMA.

10.3.3 Effect of elemental sulphur on the cure and dynamic properties of the SBR compound filled with silanized silica nanofiller

As seen in Tables 10-1 and 10-2, the addition of 0.2 phr elemental sulphur to the SBR compound reduced both the scorch and optimum cure times and increased the rate of cure. For example, the scorch time, t_{s1}, decreased from 12 to 11 min and cure time, t_{90}, from 49 to 37 min. The cure rate index rose from 2.7 to 3.8 min^{-1}, which indicated a large improvement in the rate of cure. Evidently, the addition of a small amount of elemental sulphur was beneficial to the cure properties of the compound.

Figures 10-27 to 10-29 compare the $\tan\delta$ versus temperature data of compounds 1 and 7 at 1, 20 and 100 Hz test frequencies and 256 μm oscillation amplitude.

There is hardly any improvement in tanδ when elemental sulphur is added. However, it seems that for compound 1, the tanδ values are slightly lower above 40 and below -40°C. It may be that compound 1 may offer a lower rolling resistance because it has lower tanδ at higher temperatures, whereas, compound 7 may offer a better ice-grip properties because of higher tanδ values at lower temperatures. This is more clear in Figure 10.28 where the data at 20 Hz are presented. Again at above 40 and below -40°C, the tanδ values for compound 1 are lower, which indicate that this compound will have a lower rolling resistance.

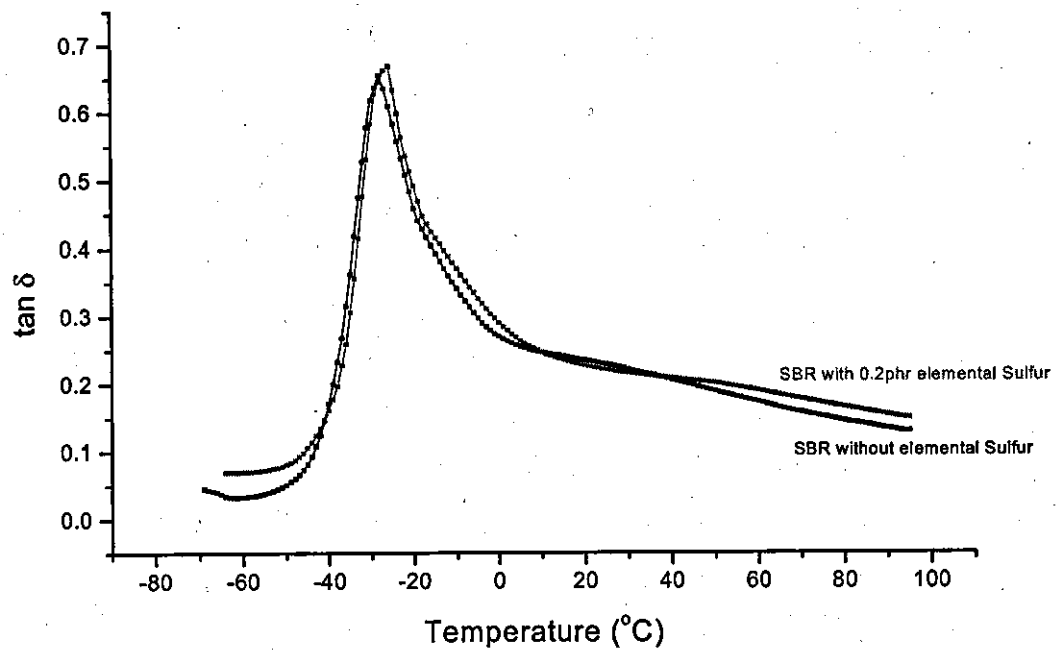

Figure 10-27: Tan δ versus temperature at 1 Hz and 256 µm oscillation amplitude for compounds 1 and 7.

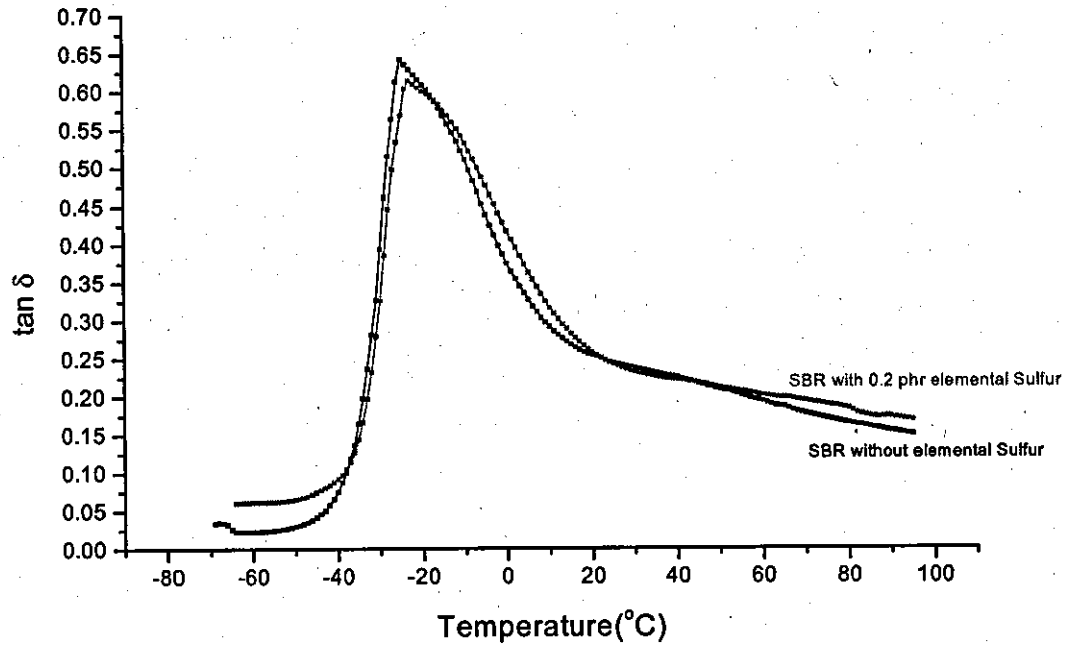

Figure 10-28: Tan δ versus temperature at 20 Hz and 256 µm oscillation amplitude for compounds 1 and 7.

When the tanδ versus temperature data at 100 Hz and oscillation amplitude 256 µm is examined for compounds 1 and 7 (Figure 10-29), there is significant differences between the two compounds. Tanδ peaks are at 0.80 for compound 7 and at 0.77 for compound 1. At temperatures above -10°C, compound 7 has a much higher tanδ values, whereas, at lower temperatures, i.e. below approximately -20°C, compound 7 has lower tanδ values. Note, compound 7 has higher tanδ values between -15 to 60°C. Thereafter, compound 1 shows higher values. Therefore at this frequency, compound 7 is less suitable for tyre tread applications because it has higher tanδ values at high temperatures and hence a higher rolling resistance. At low temperatures, it is more difficult to distinguish which compound has a better ice- or wet-grip properties.

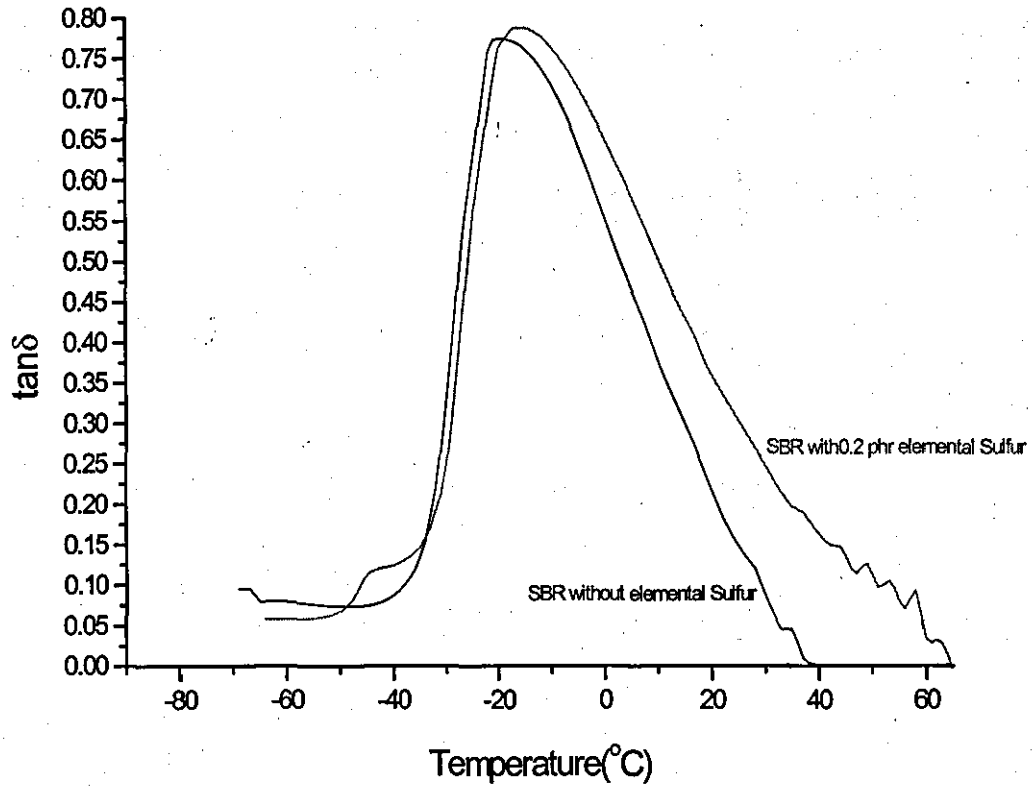

Figure 10-29: Tan δ versus temperature at 100 Hz and oscillation amplitude 256 µm for compounds 1-7.

As shown in Table 10-2, the addition of silanized silica nanofiller increased the viscosity of the NR, SBR, BR and IR rubbers from 97, 51, 49 and 69 to 106, 109, 162, and 105 Mooney units. Filler loading and subsequent viscosity increases may be considered an important indication of a substantial difference between the dynamic bahaviour of raw rubbers and filled ones. The differences between the dynamic properties of compounds 4 and 6 are understood in this light. Also as mentioned earlier, the dynamic bahaviour of the filled rubbers is governed by in situ polymer (i.e. polymer that is not bound to filler particles) in the glass transition zone, and by filler-filler and filler-polymer nertworks in the rubbery state.

At low temperatures, e.g. -35°C, polymer-polymer interactions are more responsible for heat generation than polymer-filler or filler-filler network breakdowns and reformation. At high temperatures, e.g. 25°C, the polymer matrix including polymer chains and polymer-filler networks are more rubbery and they resist less against imposed strains and move in the same direction as the strain, resulting in lower heat dissipation and $\tan\delta$ values. In the rubbery state, the SBR rubber shows the highest $\tan\delta$ values, followed by BR, NR, and NR with elemental sulphur and IR. In fact, at ambient temperature, the dominant mechanism of heat dissipation is filler-filler netweork break down and reformation. Hence, The SBR rubber with the lowest bound rubber and crosslink density (the highest filler-filler and lowest filler-polymer network) has the highest level of heat dissipation resulting in the highest $\tan\delta$ among the filled rubbers. The trend of $\tan\delta$ decrease with crosslink density increase holds true, except for the BR rubber, with the sequence SBR, NR, NR with elemental sulphur and IR.

10.3.4. Additional discussion of non-linear viscoelastic bahaviour of the filled rubbers

As has been observed, rubbers filled with silanized pre-treated silica nanofiller show a complicated oscillation amplitude dependency of dynamic characteristics compared with traditional silica and carbon black fillers [1]. A widely held view is that filler agglomeration and network formation are responsible for the high levels of reinforcement and that de-agglomeration and network breakdown are responsible for the nonlinearity with strain [9,10]. A normally defined Payne effect in filled elastomers refers to the reduction of dynamic storage modulus with increasing strain amplitude. This is attributed to the strain amplitude dependency of filler–filler linkages, which are broken down by strain [11,12]. Because the storage modulus of pure gum polymers is independent of strain amplitude [12] and the lower bound rubber of the SBR filled rubber results in higher filler–filler agglomeration, the Payne effect is clearly observed for this compound.

In contrast, more complicated behaviour was observed for the other filled rubbers. This means that, whereas in some strain ranges storage modulus increases with strain amplitude, in other ranges it decreases (Payne effect). Drawing attention to the high bound rubber (rubber bounded by filler particles) and covalent chemical bonds between the filler particles and polymer chains (via TESPT) in the filled rubbers, it may be concluded that there is a different predominant filler–filler interaction mechanism than simply de-agglomeration and filler–filler network breakdown, as was suggested by the Payne model [12].

Maier and Gortiz [13] have proposed an alternative mechanism to filler structure breakdown, suggesting that the Payne effect is due to the stress induced by de-bonding of polymer chains from the filler surface. Sternstein and Zhu [14] proposed a new mechanism underlying the reinforcement and nonlinear behaviour of storage modulus with strain in nanofilled polymers. They believed that filler–matrix interactions, and not filler agglomeration or de-agglomeration, are responsible for such nonlinearity. They also believed that the polymeric matrix (entanglements) and the manner in which the filler–matrix interface alters matrix behaviour in the presence of an applied stress share a fundamental mechanism regarding the origin of the nonlinear viscoelastic behaviour. We more or less agree with them and believe that the polymeric matrix (entanglements) along with structure and type of polymer (here rubber) in the interface of filler–filler networks (particles) alter the viscoelastic behaviour of the whole polymeric system. For example, it is observed in Figures 10-18, 10-21 and 10-24 that, whereas storage modulus versus strain amplitude for the IR filled rubber increases for all the applied strains, it passes through a maximum or a minimum for other rubbers. Alternatively, there is a tendency for fillers to form some sort of 'weak structure' when filler size becomes very small (nanoscale) [14]. In the systems studied here, the amount of filler loading is relatively high (60 phr) at the nanoscale. This high loading increases the chance of filler particles existing in the system without chemical interaction (bonds) with polymer chains

and simultaneously this may reduce filler particle distances. Incorporating strain with the above phenomena may facilitate the filler particles making aggregates and subsequently agglomerates, resulting in storage modulus increasing with strain. However, the nature of these new mechanisms is not well understood at this stage and will require further investigations.

Conclusions

From this work, it is concluded that:

• The dynamic properties of all the compounds were affected by the addition of silanized silica nanofiller. This fact was more evident when the glass transition temperatures of the gum (unfilled) SBR, BR and NR rubbers with values −50, −107 and −64°C were compared with those of the filled rubbers, which were −24, −85 and −45°C, respectively.

• The filled IR rubber showed the least rolling resistance with tan δ values 0.1–0.12 at 50–80°C and the SBR and BR filled rubbers the highest rolling resistance with tan δ values 0.12–0.24 and 0.17–0.20, respectively, in the same temperature range.

• The filled SBR rubber showed the best skid resistance with the tan δ values 0.58–0.29 at −30 to 0°C. The filled BR rubber showed the worst skid resistance with the tan δ values 0.1–0.13 in the same temperature range.

• A temperature of 65°C is considered to be a suitable temperature for measuring the rolling resistance of tyre tread. A slight increase of tan δ at all oscillation amplitudes for all the filled rubbers was a distinction of this temperature with the exception of NR with elemental sulphur filled rubber, which showed a sharp tan δ increase at higher oscillation amplitudes (greater than 500 μm).

Generally, the values of tan δ were lower than those at the two other temperatures studied −35 and 25°C. The loss modulus of the filled SBR rubber was constant, more or less, for all the oscillation amplitudes at this temperature.

- The addition of elemental sulphur to the SBR compound improved the curing properties, but simultaneously worsened the dynamic behaviour of this compound.
- Owing to high bound rubber content of the filled rubbers and formation of covalent chemical bonds between the filler particles and polymer chains, it is expected that there should be another mechanism predominant to explain the nonlinear viscoelastic behaviour of the filled rubbers rather than the one proposed by the Payne model based on the filler–filler interactions. In addition, the nanoscale properties of the filler may also be affecting this behaviour. This is because the filler particles were dispersed well and did not form aggregates, which could have been broken and reformed under high strains causing energy dissipation and high tan δ values.

References

1) "*The Vanderbilt rubber handbook*", 13th edition, The Vanderbilt Co. 650 (1990).

2) Wang M J, *Rubber Chem.Technol.* **71**:521(1998).

3) Medalia A L., *Rubber Chem. Technol.* **51**:437 (1978).

4) Buigin, Hubbard D G., Walters M H., *Proc. Rubber Technol. Conf.*, London,173 (1962).

5) Saito Y, *Kautsch, Gummi Kunstst* **39:**30(1986).

6) Duperray B, Leblanc J L., *Kautsch. Gummi. Kunstst* **35**:298(1982).

7) Ansarifar A, Ostad Movahed S, Ansar Y, *J Appl Polym Sci* **109**:(**2**)869(2008).

8) Wolff S , Wang M J., *Rubber Chem. Technol.* **65**:329(1992).

9) Kraus G., *J Appl Polym Sci, Apply Polym Symp.* **39**:75(1984).

10) Heinrich G ,Klupped M., *Adv polym Sci* **160**:1(2002).

11) Payne A R., *Reinforcement of Elastomers*, ed. By Kraus G. Wiley Interscience, New York, Chap. 3 (1965).

12) Byers J T., *Rubber Chem Technol* **75**:527(2002).

13) Maier P G , Gortiz D, *KautschGummi Kunstst* **49**:18(1996).

14) Sternstein S S,Zhu A J, *Macromolecues* **35**:7262 (2002).

CHAPTER 11

Measuring the dynamic properties of the SBR/BR rubber blends filled with silanized silica nanofiller

11.1 Introduction

Elastomers are often mixed together to produce blends to reduce hysteresis losses. This is because losses due to hysteresis for blends is often lower than those of their individual components. Hysteresis of rubber compounds can be reduced by increasing crosslink density [1].

Hess and Chirico have shown that hysteresis is reduced when the continuous phase contains high levels of filler [2]. Nguyen studied the effect of filler loading on the hysteresis of some elastomer blends and found a non linear relationship between it and the filler loading [3]. Keller found that the addition of a small amount of chlorobutyl rubber to NR/BR blend (tyre tread compound) reduced its rolling resistance [4]. Ahagon et al. have patented a blend composition of three rubbers containing chlorobutyl rubber, which reduces hysteresis without changing the wet traction [5].

Recently, Roger and Waddel [6] reviewed the past work on the use of blends of butyl, chlorobutyl, bromobutyl and brominated methyl styrene-isobutylene co-polymers with natural rubber (NR) and SBR in many tyre and non tyre applications. Addition of butyl and halo-butyl rubber to tyre tread compounds based on NR/SBR and NR/BR blends can lower resilience and improve skid resistance. In general, butyl rubber provides poor abrasion resistance but improves skid resistance, which is very important for tyre application. Typical rubber blends were used in the tyre tread investigation [7]. Wang and co-workers [8] studied the effect of different fillers, i.e. carbon black and silica included, and TESPT coupling agent, on the dynamic behaviour of some SBR-

BR blends. According to their findings, silica filled compounds had better rolling resistance in comparison with the carbon black ones. The strain dependence of storage modulus for NR and SBR vulcanisates filled polymeric fillers were also studied by Schuster [9] who showed that the storage modulus of filled NR was substantially higher than that of the filled SBR.

In this chapter, the dynamic behaviour of some SBR/BR rubber blends reinforced with silanized silica nanofiller will be measured at different oscillation amplitudes, temperatures and frequencies. The results will be compared and discussed subsequently.

11.2 Rubbers formulations and mixing procedure

The procedure for mixing the SBR and BR rubbers to produce the SBR/BR blends were described in section 8-2 of chapter 8 in detail. The blends used for this study were compounds 3-5 in Table 9-3 in chapter 9.

11.3 Results and discussion

Table 9-4 in chapter 9, shows the difference in the bound rubber content between the three blends to be in the range 0 - 5 %, which is very small. Hence the difference between the dynamic properties of the blends may not be related to the small differences between the bound rubber content, rather, it may be due to differences in the mass fraction of the interphase and the mass fraction of SBR to BR in the interphase.

11.3.1 Effect of changes in the oscillation amplitude on the dynamic properties of the SBR/BR blends tested at -50 and -35°C

Figures 11-1 to 11-3 show tanδ, loss modulus and storage modulus as a function of the oscillation amplitude at -50 and -35°C and 1Hz. The silanized silica-filled SBR and BR rubbers were mixed together for 1, 7 and 20 min to produce the blends. At these test temperatures, the blends were at or very near to the glass transition temperature of the SBR rubber (-50°C) and therefore, the free volume of the polymer increases very rapidly than the volume expansion of the polymer molecules as temperature goes up. This will facilitate segments motions and subsequently reduces the viscosity and storage modulus of the blend.

Figure 11-1 shows tanδ versus the oscillation amplitude for the blends. At -50°C, the rubber viscosity was high and this resulted in high energy dissipation in the rubber because of high frictional forces between the polymer chains. This in turn, produced the high tanδ values seen at this temperature. As the temperature was increased to -35°C, the tanδ values rose considerably. With the exception of the blends, which were mixed for 1 and 7 min, tanδ increases as a function of the oscillation amplitude for the other blend. It is also noted that the blends prepared for 20 min and tested at -35°C and for 1 min and tested at -50°C, had the highest and lowest tanδ values, respectively. Note that a longer mastication time, softens the rubber and reduces its viscosity. The viscosity of the blend reduced from 108 to 78 MU after the mixing time was increased to 20 min.[Table 9-3]. This explains the higher tanδ values recorded for the blends with longer mixing times and higher test temperatures. In general, blend with 20 min. mixing time shows higher tanδ values than those of blends with 1 and 7 min. mixing times, hence better skid resistance in tyre tread applications.

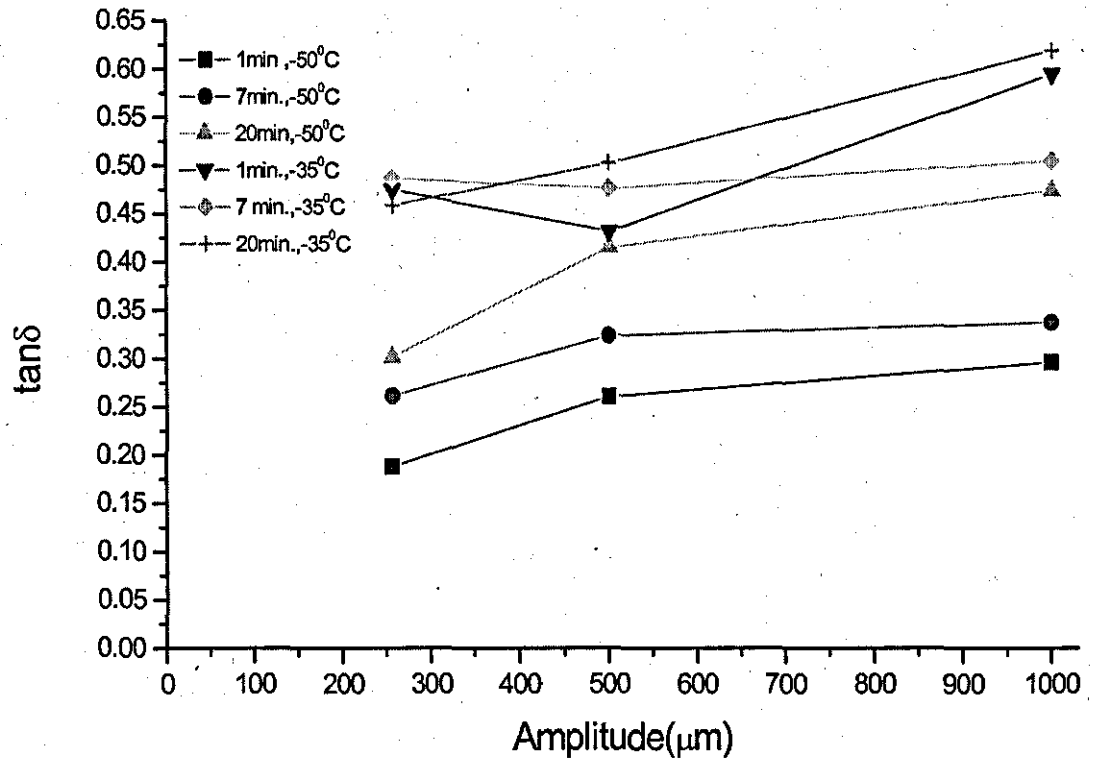

Figure 11-1: Tan δ versus oscillation amplitude for the SBR/BR blends at -50 and -35^{0}C and 1Hz. The silanized silica filled SBR and BR rubbers were mixed together for 1, 7 and 20 min to produce the blends.

The loss modulus of the blends mixed for 1 and 7 min at -50°C shows the large reduction and the ones prepared for 1 and 7 min at -35°C, the smallest reduction as the oscillation amplitude reaches 500 μm (Fig. 11-2). The loss modulus of the blends mixed for 20 min at -35 and -50°C, are almost independent of the oscillation amplitude over the range tested. It is interesting that as the oscillation amplitude increases above 500 μm, the loss modulus remains unaffected for all the blends. Above this amplitude, the blend mixed for 20 min at -50°C has the largest loss modulus values but the picture is less clear for the remaining blends.

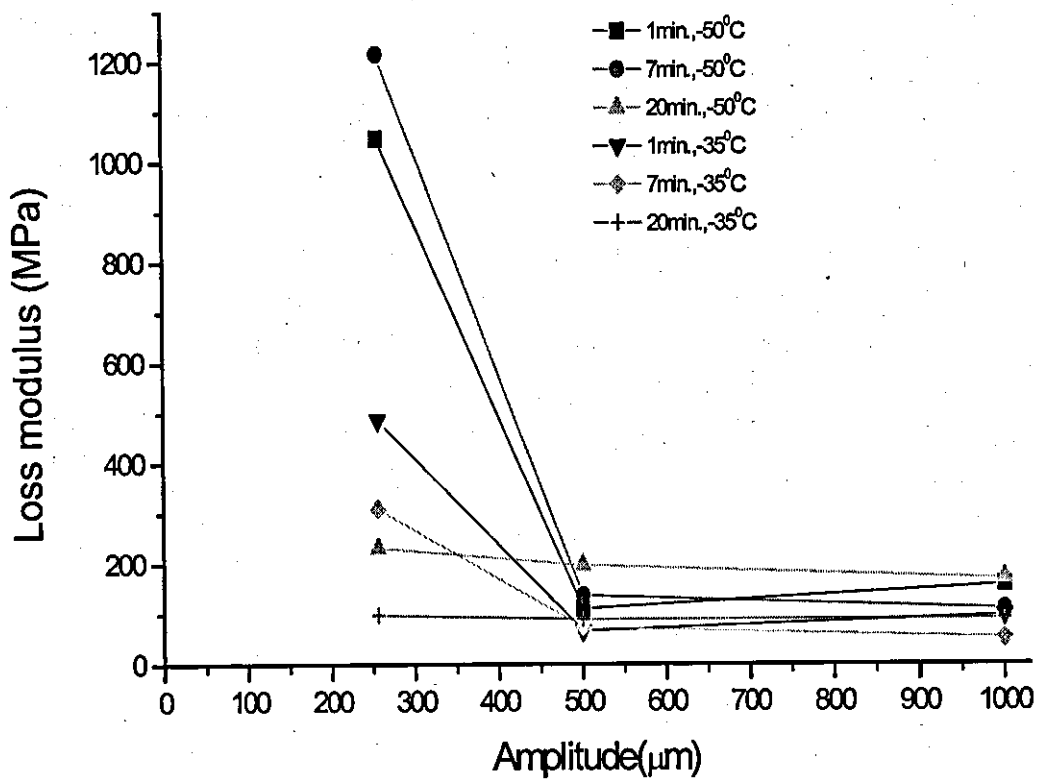

Figure 11-2: Loss modulus versus oscillation amplitude for the SBR/BR blend at -50 and -35oC and 1Hz.The silanized silica filled SBR and BR rubbers were mixed together for 1, 7 and 20 min to produce the blends

A similar picture also emerges when Figure 11-3 is examined. In this figure, storage modulus is plotted against the oscillation amplitude at 1 Hz and -50 and -35°C for the SBR/BR blends. The blends are as in Figure 11-2. For the blends mixed for 1 and 7 min and tested at -50°C, and mixed for 1 and 7 min and tested at -35°C, the storage modulus decreases as a function of the oscillation amplitude for up to 500 μm. The fastest reduction was recorded for the blend mixed for 1 min at -50°C and the slowest for the blends mixed for 7 min at -35°C, respectively. As the oscillation amplitude increases to 1000 μm, there is hardly any differences between the storage modulus of these blends, but that of the blend mixed for 1 min and tested at -50°C, remains higher, at least at amplitudes

greater than 700 -1000 μm, than the other blends over the same range of the amplitude.

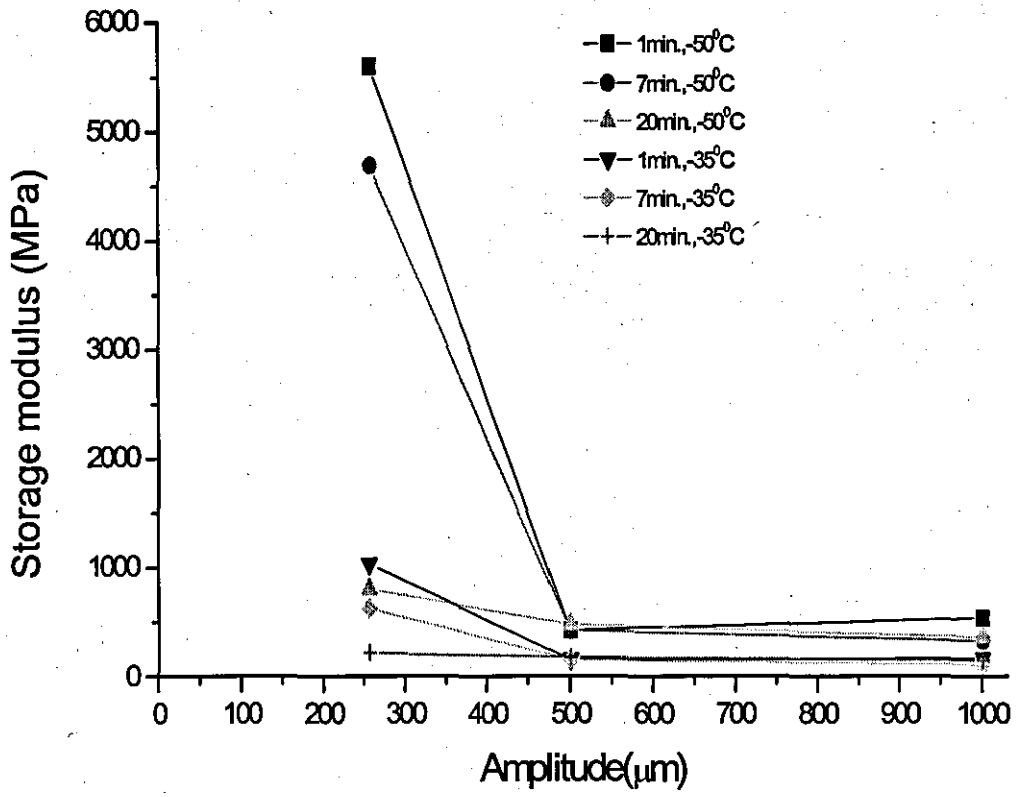

Figure 11-3: Storage modulus versus oscillation amplitude for the SBR/BR blend at 1 Hz and -50 and -35°C and 1Hz. The silanized silica filled SBR and BR rubbers were mixed together for 1, 7 and 20 min to produce the blends

11.3.2 Effect of changes in the oscillation amplitude on the dynamic properties of the SBR/BR blends tested at 0 and 25°C

To study the effect of temperature changes further, the tan δ, loss and storage modulus of the blends were measured at 1 Hz and 0 and 25°C. At these temperatures, the blends are softer and the rubber responses more readily to the imposed strains and therefore lower hysteresis and tan δ values are expected. As the amplitude increases to 500 μm, tan δ increases. The largest and lowest

rises are recorded for the blends mixed for min 7 min at 0°C and for 1 min at 25°C, respectively (Fig. 11-4). No increase is seen for the blend mixed for 1 min at 0°C. Thereafter, the tanδ of the blend mixed for 7 min and tested at 0°C shows a rapid decrease, that of the blend mixed for 7 min and tested at 25°C, no increase at all. Those of the remaining blends show some modest rises as the oscillation amplitude reaches 1000 μm. Evidently, the blend mixed for 7 min and tested at 25°C has the lowest tanδ values in range 620-1000 μm.

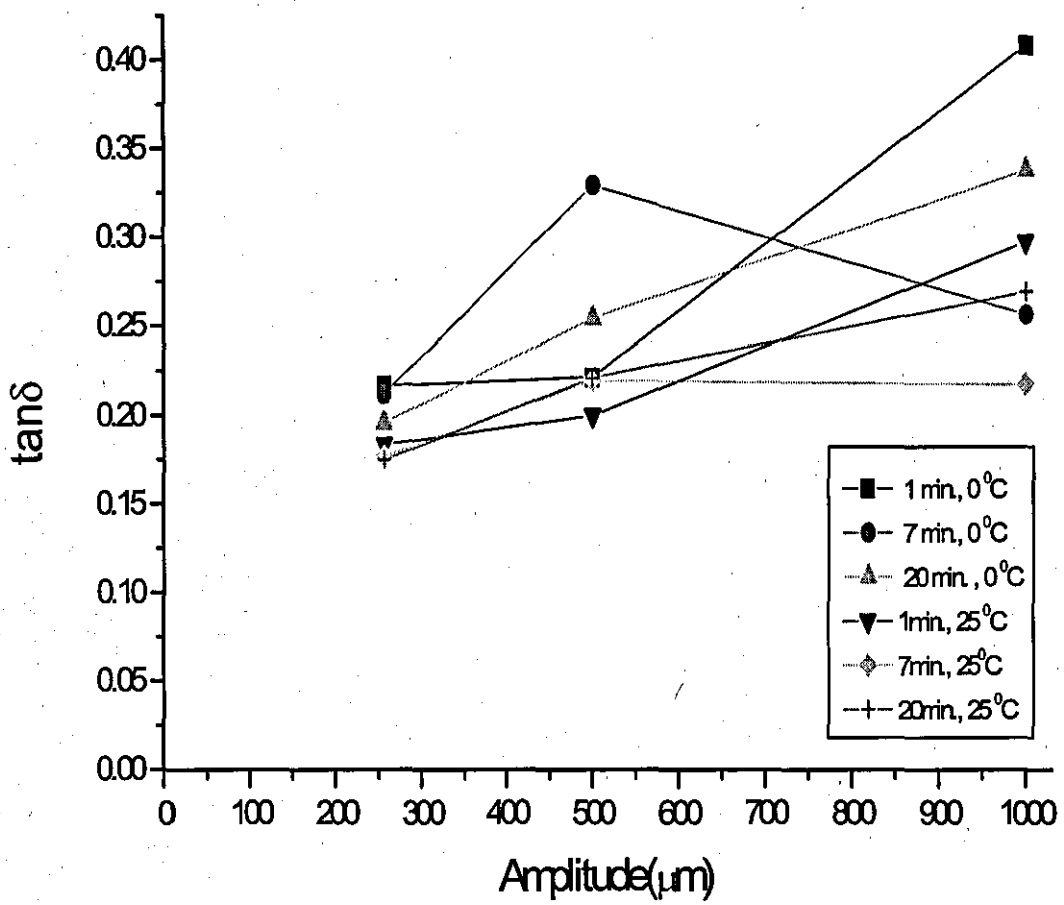

Figure 11-4: Tan δ versus oscillation amplitude for the SBR/BR blends at 1 Hz and 0 and 25^{0}C. The silanized silica filled SBR and BR rubbers were mixed together for 1, 7 and 20 min to produce the blends

Figure 11-5 shows loss modulus versus oscillation amplitude for the three blends at 1 Hz and 0 and 25°C. This property drops quite sharply for the blends mixed

for 1and 7 min and tested at 0 and 25°C as the oscillation amplitude increases from 256 to 500 μm. Thereafter, the loss modulus increases rapidly as the oscillation amplitude reaches its maximum value for the former. The loss modulus of the blends mixed for 7 min and tested at 0 and 25°C, decrease continuously above 500 μm. For the blends mixed for 20 min and tested at 0 and 25°C, the loss modulus rises when the oscillation amplitude reaches 1000 μm, with the former showing a much larger increase.

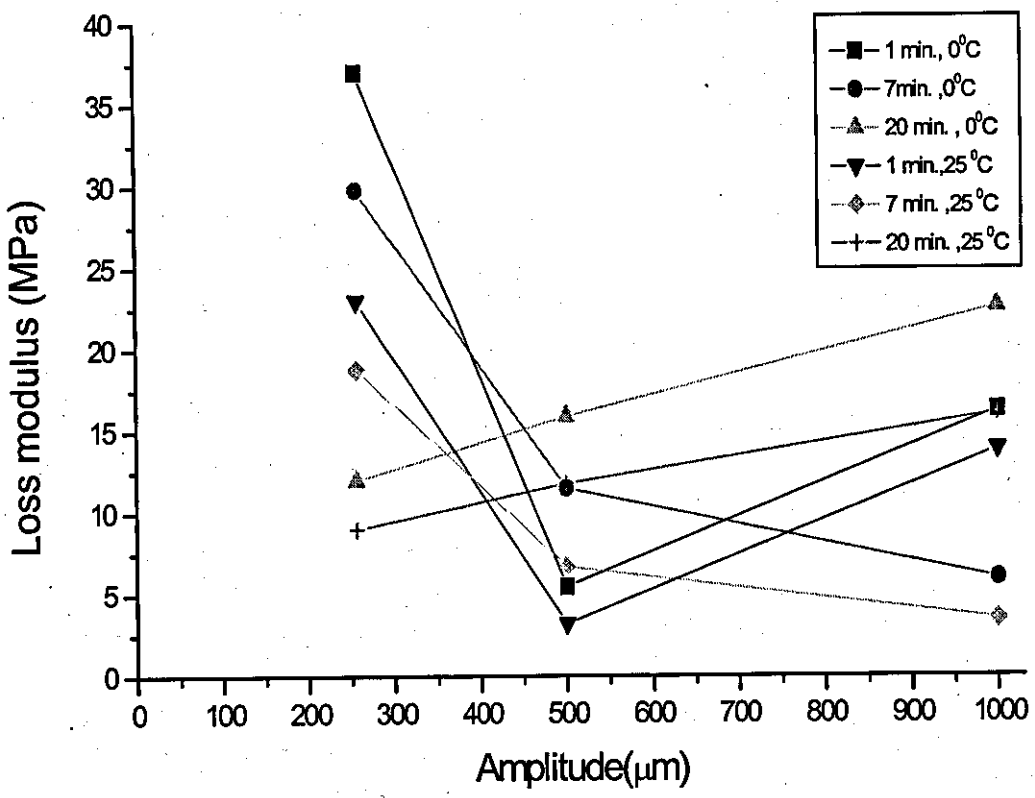

Figure 11-5: Loss modulus versus oscillation amplitude for the SBR/BR blends at 1 Hz at 0 and 25°C. The silanized silica filled SBR and BR rubbers were mixed together for 1, 7 and 20 min to produce the blends.

Finally, storage modulus versus the oscillation amplitude for the three blends at 1 Hz and 0 and 25°C is shown in Figure 11-6. The picture is very similar to Figure 11-5. The storage modulus of the blends mixed for 1 and 7 min and tested at 0

and 25°C decrease sharply and converge, when the oscillation amplitude reaches 500 μm. Thereafter, the modulus of the blends mixed for 1 min and tested at 0 and 25°C rise, whereas, those of the blends mixed for 7 min at tested at 0 and 25°C, decreases as a function of the oscillation amplitude. The storage modulus of the blends mixed for 20 min and tested at 0 and 25°C continue rising over the entire range of the oscillation amplitude slowly.

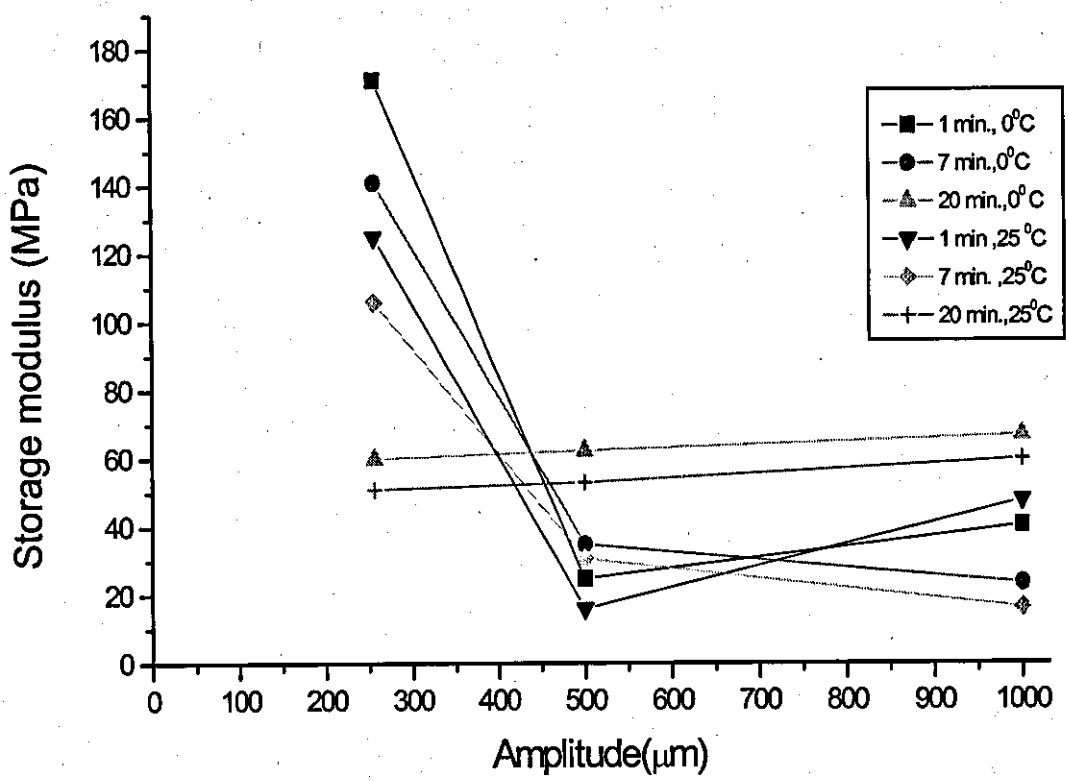

Figure 11-6: Storage modulus versus oscillation amplitude for the SBR/BR at 1 Hz and 0 and 25 ^{0}C. The silanized silica filled SBR and BR rubbers were mixed together for 1, 7 and 20 min to produce the blends.

11.3.3 Effect of changes in the oscillation amplitude on the dynamic properties of the SBR/BR blends tested at 65 and 85°C

Figures 11-7 to 11-9 show tan δ, loss and storage modulus and storage modulus as a function of the oscillation amplitude at 1 Hz and 65 and 85°C for

the three blends. As shown in Figure 10-1, tyre tread compounds must have low tanδ at temperatures greater than ambient. Therefore, 65 and 85°C are good temperatures at which the suitability of the blends for use in tyre tread applications can be assessed. The lower the tanδ values, the lower the rolling resistance of a tyre will be. At the lowest oscillation amplitude, i.e. 256 µm, the blends mixed for 1 and 20 min and tested at 85 and 65 °C have the lowest and highest tanδ values, respectively. As the amplitude increases to 500 µm, the tanδ of the blends mixed for 1, 7 and 20 min and tested at 65 and 85°C converge. However, as the oscillation amplitude increase to 1000 µm, the tanδ values of the blends mixed for 1 min and tested at 65 and 85°C drop, whereas, those of the other blends continue rising. The blend mixed for 20 min and tested at 85°C, has the lowest tanδ, and hence offers the lowest rolling resistance and may be used in tyre tread applications.

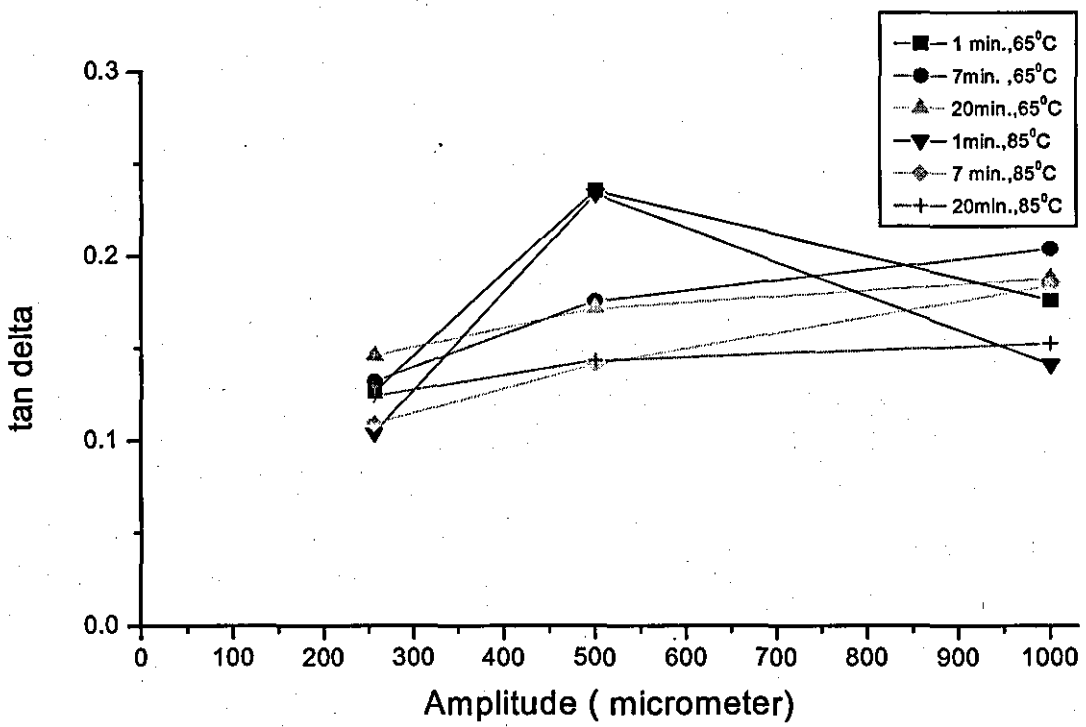

Figure 11-7: Tan δ versus oscillation amplitude for the SBR/BR blends at 1 Hz and 65 and 85 ^{0}C. The silanized silica filled SBR and BR rubbers were mixed together for 1, 7 and 20 min to produce the blends.

Figure 11-8 shows loss modulus as a function of the oscillation amplitude at 1 Hz and 65 and 85°C for the three blends. The loss modulus of the blends mixed for 1 and 7 min and tested at 65 and 85°C decreased very substantially and converged when the amplitude increased from 256 to 500 μm. Thereafter, the loss modulus increased rapidly when the amplitude reached 1000 μm. A similar trend was also seen for the blends mixed for 7 min and tested at 65 and 85°C, but these values declined as the amplitude was raised to its maximum. It was interesting that the loss modulus of the blends mixed for 20 min and tested at 65 and 85°C continued rising with the oscillation amplitude.

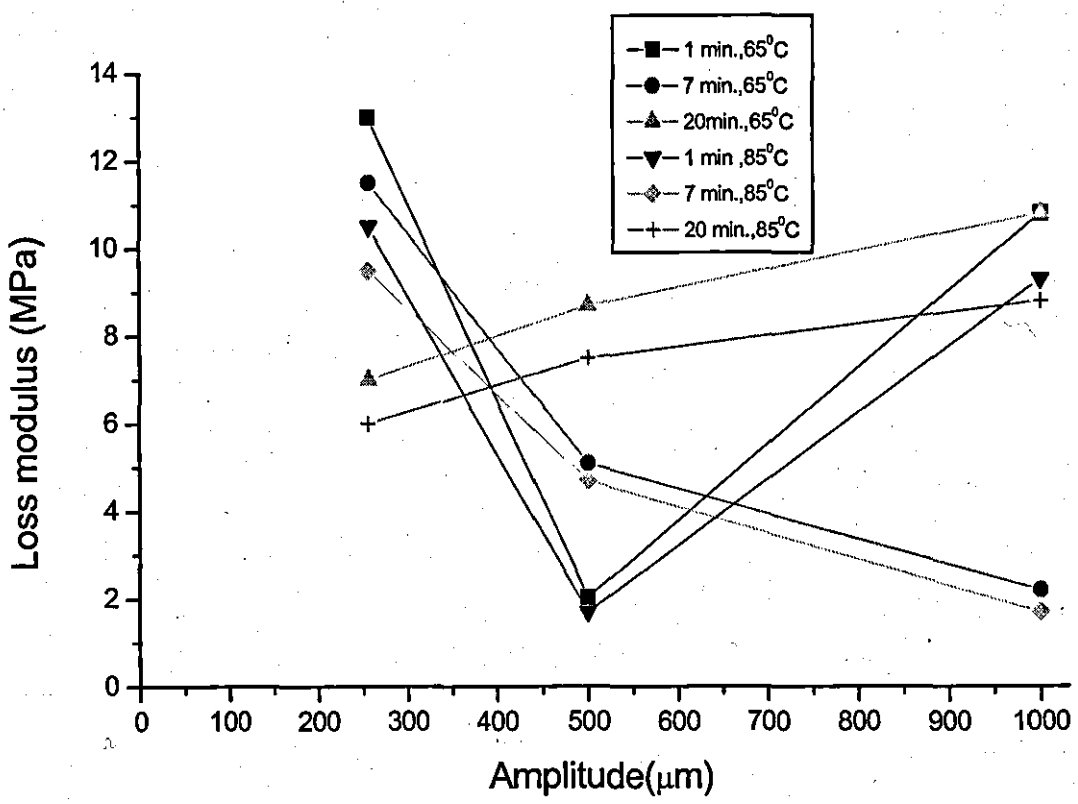

Figure 11-8: Loss modulus versus oscillation amplitude for the SBR/BR blends at 1 Hz and 65 and 85 ^{0}C. The silanized silica filled SBR and BR rubbers were mixed together for 1, 7 and 20 min to produce the blends.

A similar trend was also seen in Figure 11-9 where storage modulus is plotted as a function of the oscillation amplitude at 1 Hz and 65 and 85°C. In this figure, the storage modulus of the blends mixed for 1 min and tested at 65 and 85°C decreases as the oscillation amplitude is increased from 256 to 500 μm and then rise rapidly when the amplitude reaches 1000 μm. The results are almost the same. Similarly, for the blends mixed for 7 min and tested at 65 and 85°C, the storage modulus decreases when the oscillation amplitude reaches 500 μm, and then it continues dropping further as the amplitude is raised to 1000 μm. For the blends mixed for 20 min and tested at 65 and 85°C, the storage modulus keeps going up with increases in the oscillation amplitude. It is also noted that these values are almost similar for these two blends.

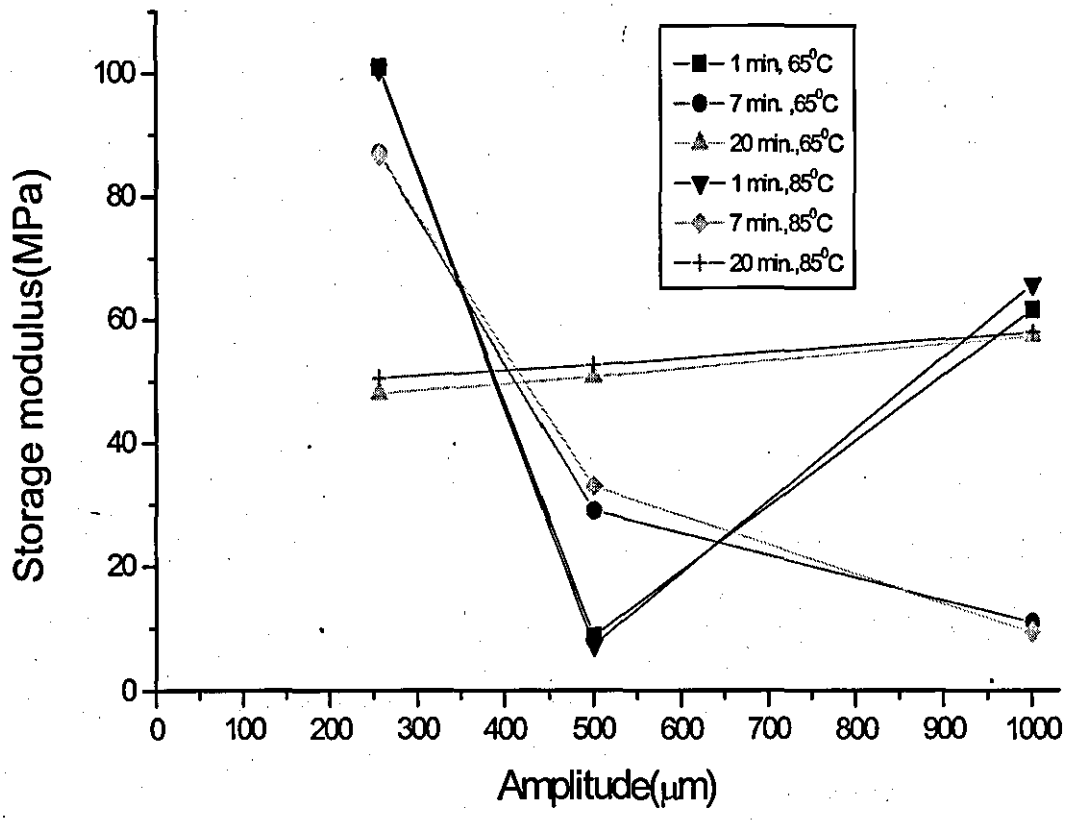

Figure 11-9: Storage modulus versus oscillation amplitude for the SBR/BR blends at 1 Hz and 65 and 85 ^{0}C. The silanized silica filled SBR and BR rubbers were mixed together for 1, 7 and 20 min to produce the blends.

11.3.4. Effect of temperature variation on the tan δ of the SBR/BR blends at different test frequencies and constant oscillation amplitude

Figure 11-10 shows tan δ versus temperature at 20 Hz and an oscillation amplitude of 256 μm for the three blends.

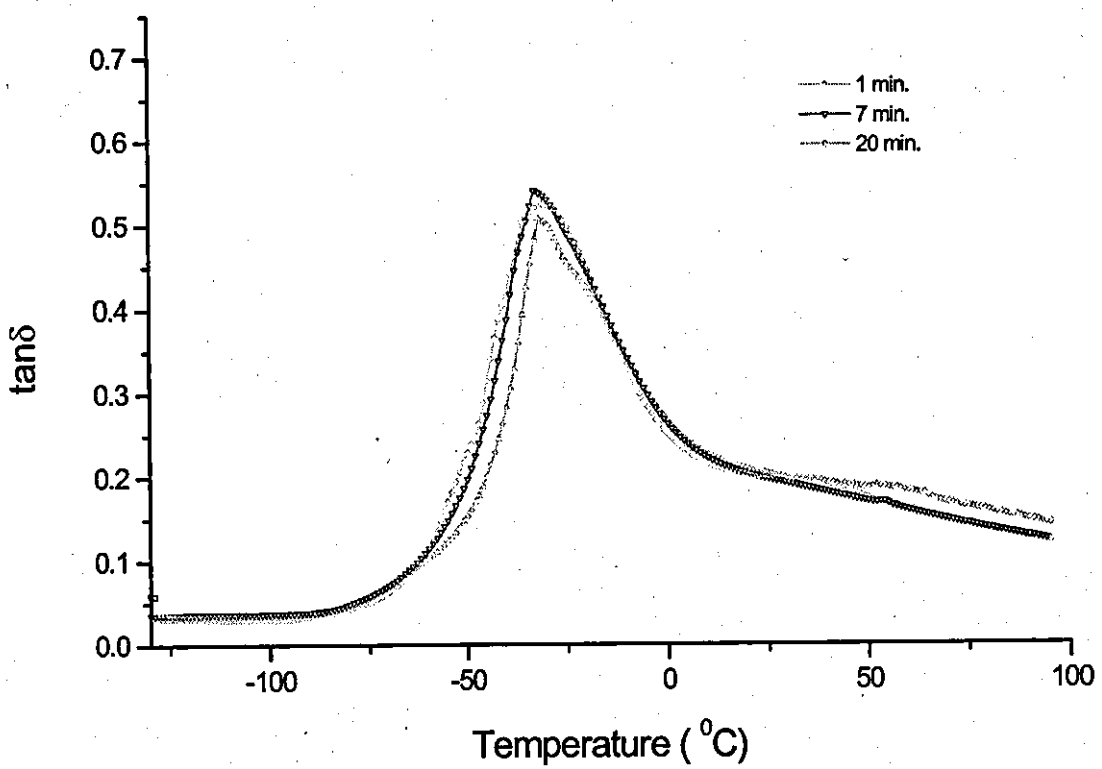

Figure11-10: Tan δ versus temperature for the SBR/BR blends at 20 Hz and an oscillation amplitude of 256 μm. The silanized silica filled SBR and BR rubbers were mixed together for 1, 7 and 20 min to produce the blends.

The tan δ values of the blends mixed for 7 and 20 min are almost the same, whereas, the ones for the blend mixed for 1 min are noticeably lower, at least for temperatures up to -15°C. Thereafter, there is little difference between these

blends for up to 20°C. It appears that the blend mixed for 7 min has the highest peak tan δ value and hence offers the best ice-grip or skid resistance and it also has the lowest tan δ values, at least for temperatures above 20°C, and therefore it offers the minimum rolling resistance. The blend mixed for 1 min has the same tan δ values as the one mixed for 7 min, and therefore offers the same rolling resistance.

Figure 11-11 compares the tan δ versus temperature data at 1 Hz and an oscillation amplitude of 256 μm for the silanized silica-filled SBR and BR rubbers and the three blends. Table 11-1 shows the peak tan δ values for these rubbers.

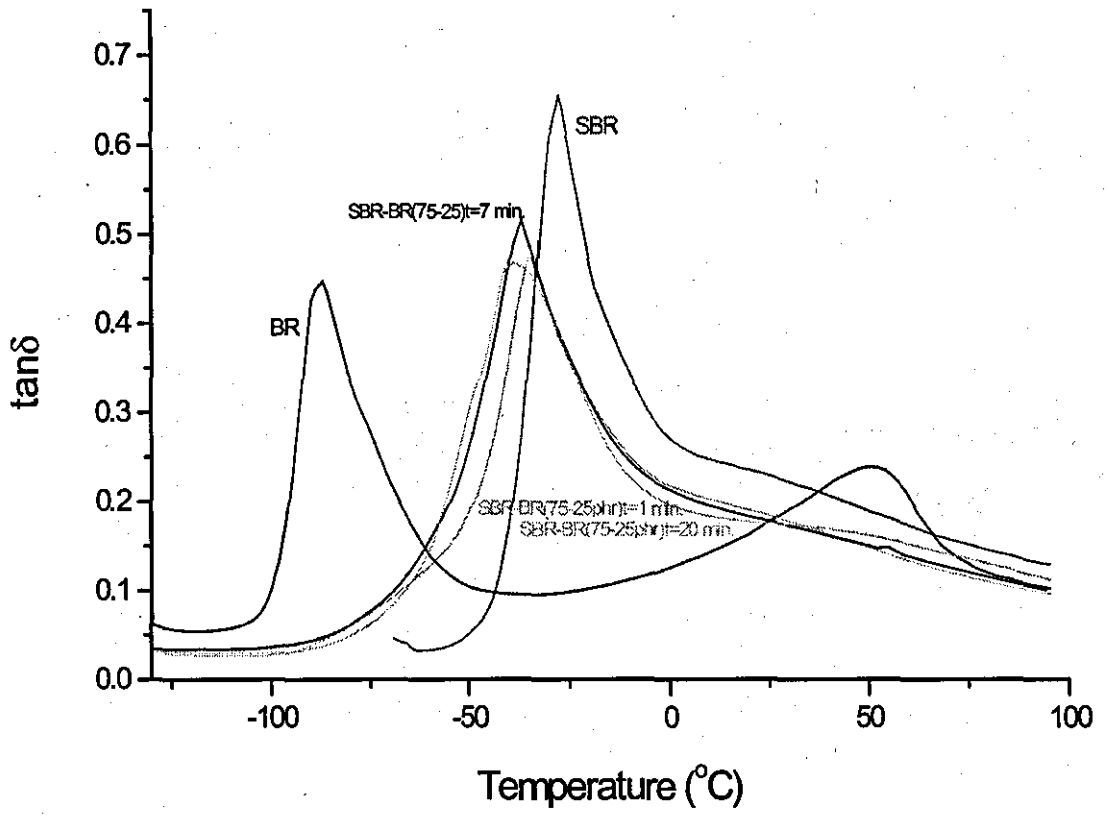

Figure 11-11: Tan δ versus temperature for the silanized silica-filled SBR and BR rubbers and the SBR/BR blends at 1 Hz and an oscillation amplitude of 256 μm.

Table 11-1:Peak tan δ values for the rubbers in Figure 11-11.

	BR rubber	SBR rubber	SBR/BR blend (1 min)	SBR/BR blend (7 min)	SBR/BR blend (20 min)
Peak tan δ	0.44	0.66	0.48	0.51	0.47

The SBR and BR rubbers have the highest and lowest peak tan δ values. For the blends, the peak values lie somewhere between these two, and the blend mixed for 7 min has the highest and the one mixed for 20 min the lowest values. The tan δ trace for the SBR rubber is to the right hand side of the figure, whereas, the one for the BR rubber is to the left hand side. Clearly, the two rubbers have very different dynamic properties over the range of temperature studied.

The tan δ traces for the blends mixed for 7 and 20 min coincide, though the peak values are clearly different. The tan δ values for the blend mixed for 1 min are lower for up to approximately -30°C, but equal those of the two other blends above this temperature. Note that above 35°C, the blend mixed for 20 min has the highest tan δ values. It is concluded that the blends mixed for 7 and 20 min offer the highest ice- and wet-grip and the ones mixed for 1 and 7min the lowest rolling resistance. Therefore, the blend mixed for 7 min may be considered for tyre tread applications.

Figure 11-12 shows tan δ versus temperature for the SBR and BR rubbers and the three blends at 20 Hz and an oscillation amplitude of 256 μm. Table 11-2 shows the peak tan δ values for these rubbers.

Table 11-2 : Peak tan δ values for the rubbers in Figure 11-12

	BR rubber	SBR rubber	SBR/BR blend (1 min)	SBR/BR blend (7 min)	SBR/BR blend (20 min)
Peak tan δ	0.50	0.64	0.50	0.54	0.53

It is obvious that the peak tan δ values are now different. For example, for the BR rubber it is increased and for the SBR, it is reduced as the test frequency is raised from 1 to 20 Hz. For the blends, the trend is not changed and the blend mixed for 7 min is still a suitable one for tyre tread applications.

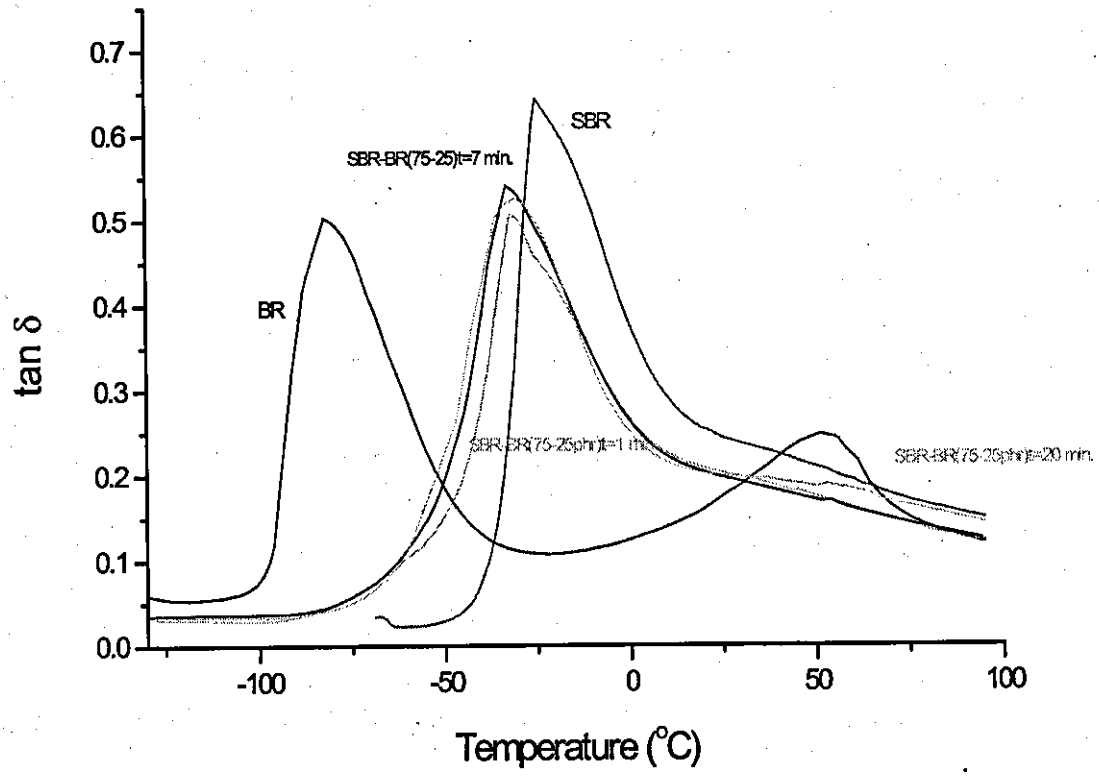

Figure 11-12: Tan δ versus temperature for the silanized silica-filled SBR and BR rubbers and the SBR/BR blends. The results were produced at 20 Hz and an oscillation amplitude of 256 μm.

Conclusions

We may conclude the gains of this study as follows:

- The dynamic properties of all the rubbers are highly affected by the addition of silanized silica nanofiller.

• In the glass transition zone (-50°C and -35°C), the storage modulus reduction as a function of the oscillation amplitude applied (strain) was observed. This was attributed to the Payne effect.

• At -50 and -35°C temperatures, the $\tan\delta$ values increased as a function of the oscillation amplitude. It seemed that compound 5 had the best skid resistance among the compounds tested. Moreover, the loss and storage modulus of this compound were independent of the oscillation amplitude.

• At temperatures 0 and 25°C temperatures, the $\tan\delta$ versus oscillation amplitude data of all the blends were incremental with the exception of that for compound 4.

• In the rubbery state where the temperatures are typically high, e.g. greater than ambient and are suitable for measuring the rolling resistance of tyre treads, the average $\tan\delta$ values of compounds 4 and 5 were less than that of compound 3. It was also concluded that blends with interphase characteristics, e.g. higher mass fraction of the interphase, had less rolling resistance.

• Owing to very high bound rubber content for all the blends, and the formation of covalent chemical bonds between the filler particles and polymer chains via TESPT, we may expect that new mechanisms other than the one proposed by the Payne model for the filler–filler interaction to explain the nonlinear viscoealstic bahaviour of the blends in this study. In addition, the good dispersion and nanoscale properties of the filler used may also have had an effect of the deformation bahaviour of the blends studied.

References

1) Hirshfield S M., *U.S.3*, **280**:876(1966).

2) Hess W M., Chirico V E., *Rubber Chem.Technol.***50**:301(1977).

3) Nguyen M N., *Unpublished Results*, Ref.2, p.215.

4) Keller R C., *Tyre Sci.Technol.* **1**:190(1973).

5) Ahagon A., Misawa M., et al., *Brit. Pat., Appl.G.B.2*, 046, 276(Yakahama Rubber Co.)

6) Roger J E., Waddel W H., *Rubber World*, (Feb.,1999).

7) "The Vanderbilt Rubber Handbook",13 th edition, *The Vanderbilt Co.*, 686(1990).

8) Wang M J, Patterson W J, Brown T A, Paper No. 25 Presented at a *meeting of rubber division, ACS*, Anaheim, California (May 6-9 ,1997).

9) Schuster R H, Educ. Symp., Paper F., Presented at a *meeting of rubber division, ACS,* Montreal, Canada (May 5-8 ,1996).

CHAPTER 12

Effect of silanized silica nanofiller on the tack and green strength of NR, SBR and BR rubbers and SBR/BR blend filled with silanized silica nanofiller

12.1 Introduction

The ability of two uncured rubber surfaces to resist separation after they are brought into intimate contact for a short period of time under a light pressure is called tack. Two types of tack may be defined, autohesive tack in which both materials are of the same chemical composition and heterohesive (adhesive) tack where the materials have different compositions. A factor inherent in tack is compound green strength, the resistance to deformation and fracture of a rubber stock in the uncured state. The tack or autohesion and green strength of the unvulcanised rubber compounds are of considerable importance in tyre manufacture. Tack properties must be optimised, however, when tack is too high it will cause difficulties in positioning rubber layers into intimate contact during the building or assemblying of rubber articles such as tyres and may lead to trapped air between rubber layers and producing after-cure defects. Simultaneously, sufficient tack must be present to enable the components of the green tyre to hold together until the curing process is completed. In addition, to prevent creep from occurring when component is distorted during processing and manufacture and tear during moulding in the curing press good green strength is required .

The principal theories that have been proposed to explain the mechanism of autohesion have been reviewed by Wake [1, 2] and Allen [3]. The diffusion theory associated mainly with Voyutskii [4] and Vasenin [5] states that autohesive bonding takes place as a result of self-diffusion of the polymer chains or molecules across the interface between two similar polymer surfaces. The

strength of the autohesive bond is controlled by the self-diffusion due to the ability of the polymer chains to undergo micro-Brownian motion of the surface polymer molecules across the interface. Rhee and Andries [6] when investigating the factors influencing the autohesion of NR and SBR rubbers considered that a combined diffusion-adsorption process was operative. It has been reported [4, 7-9] that the conditions must be met by a rubber compound for exhibiting high tack are: (a) the two surfaces must come into intimate molecular contact (b) diffusion of polymer chains across the interface must take place and (c) the bond thus formed should be capable of resisting high stresses before rupture. The first two conditions describe the bond formation and take place in series. The molecular contact must always precede inter diffusion of chain segments. When two surfaces are brought into contact, only a fraction of total surface area comes in intimate contact due to surface asperities.

The viscous flow of polymer due to contact load generally referred to as contact flow, results in an increase of the contact area between the two surfaces with contact time. The interdiffusion of polymer chains is facilitated upon achieving molecular contact. The third condition for high tack describes the bond breaking resistance and is dependent on both green strength and tear strength of the polymer. It has been reported that [8-13] diffusion of polymer chains across the interface is the major factor for bond formation. However, it has also been reported that [14-19] an intimate molecular contact precedes the interfacial diffusion of polymer chains and thus it should be an important factor for bond formation. Hence, the bond formation kinetics is influenced by both contact flow and interdiffusion of polymer chains [20]. Although the autohesion of NR and SBR rubbers have been measured and studied by several authors at different conditions earlier [6, 21, 22], however, so far there is not any report on the effect of silanized precipitated silica nanofiller on the autohesion and adhesion of these rubbers particularly with respect to tyre tread applications.

In the current work, autohesion and green strength of several samples of uncured NR, SBR and BR rubbers and SBR/BR blends filled with different loading of silanized silica nanofiller were measured by means of the peel test and tensile tension test , respectively, and the results were compared and discussed.

12.2 Sample preparation

12.2.1. Mixing

The compounds were prepared in a Haake Rheocord 90 (Berlin, Germany), a small laboratory mixer with counter rotating rotors. In these experiments, the Banbury rotors and the mixing chamber were maintained at ambient temperature ($23\,^{\circ}C$) for SBR and $50\,^{\circ}C$ for NR and BR. In all cases, the rotor speed was 45 rpm. Mixing time for all the rubber compounds was 13 minutes and both the rubber and filler were loaded in mixing chamber in one stage.

For preparing the unfilled rubbers, a maximum mixing time of 13 minutes (mastication time) was considered. For preparing the SBR/BR blends, filled SBR and BR rubbers were mixed together (SBR/BR 75/25 by weight ratio). The two rubbers were placed in the mixer at the same time and mixed for 7 minutes with mixing temperature ranging from 90-105°C.

12.2.2. Test pieces and test procedure

For measuring the tack strength, rubber sheets, 10cm by 10cm in dimensions and 2 mm thick, were prepared in a hydraulic press with a nominal pressure of 110 atmosphere for 5 minutes at 100°C. To prevent the mould surfaces from contaminating the rubber surfaces, aluminium foil was used. To prepare suitable test pieces for the peel experiments, the aluminum cover of one side was

removed and replaced with a latex-treated backing fabric (Henkel Consumer Adhesives, Winsford, Cheshire, UK). Without using this fabric support, the rubber would have fractured during peeling because the legs were too weak and the tests would not have been completed. The test pieces for the peel experiments were prepared by cutting samples 2cm by 9 cm in dimensions from the moulded sheets. Aluminum foil was removed to allow the fresh surfaces to be brought into intimate contact under a constant pressure of 2 kg and at ambient temperature ($23\,^{\circ}C$) for NR, and $50\,^{\circ}C$ for SBR and BR. A similar procedure was used to make test pieces for the rubber blends. The total area of contact between the rubber surfaces for each test piece was approximately 16 cm^2 (Scheme 12-1). The rubber surfaces were kept in intimate contact under pressure for up to 30 min.

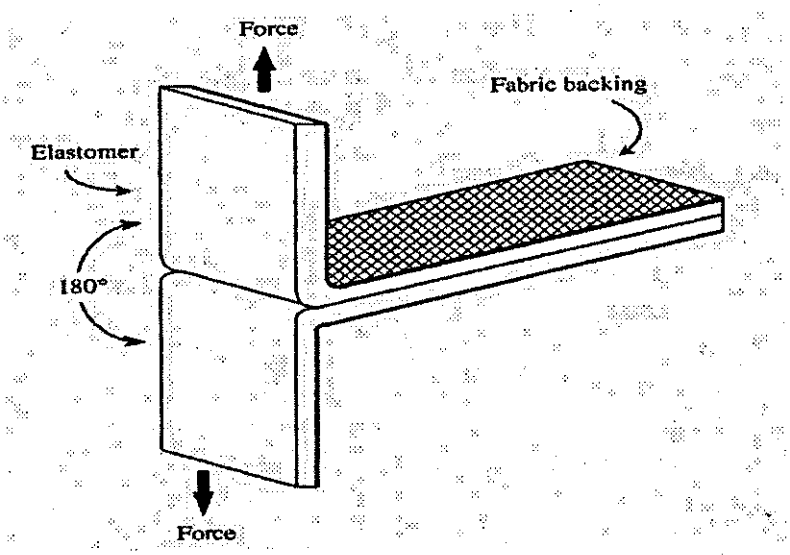

Scheme 12-1: Test piece for the peel experiment

Peel tests were carried out at 180° (scheme 1) in a Lloyd mechanical testing machine at ambient temperature ($23\,^{\circ}C$) and at a crosshead speed of 50 mm/min. Lloyd DAPMAT computer software was used to store and process the

data. A 500 N load cell was used on the machine. Figure 12-1 represents a typical force versus extension trace from the peel tests. The peak force values were averaged and placed in equation 12.1 to calculate a peeling energy for the test piece. The result was then expressed in N/m.

Peeling energy or tack = 2F/w (12.1)

where F = Average peeling test force (N) and w is the width of sample (m).

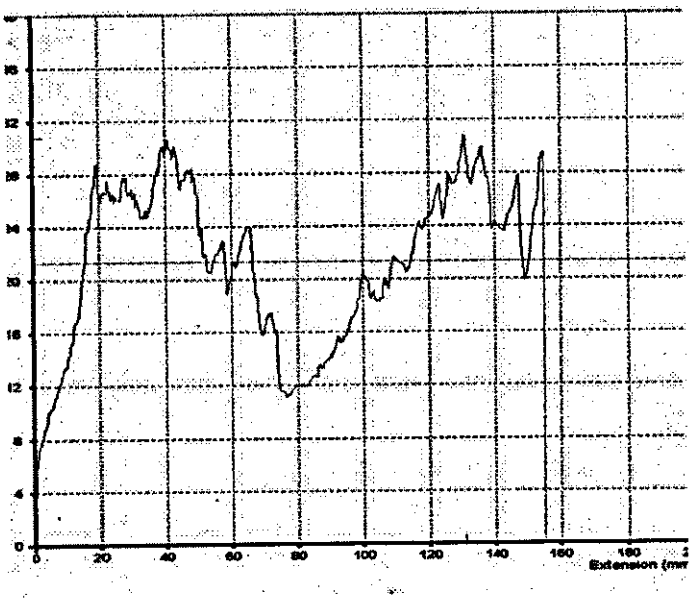

Figure 12-1: Typical force versus extension trace from the peel tests

To measure the green strength of the rubbers, dumb-bell shaped test pieces, 3.6 mm wide, 25mm gauge length, 75mm long, and 2 mm thick were cut from the moulded sheets. The test pieces were fractured in a Lloyd mechanical testing machine at ambient temperature ($23\,°C$) to produce force versus extension traces from which the maximum stress was noted (Figure 12-2). For each rubber, three samples were tested and median values were considered.

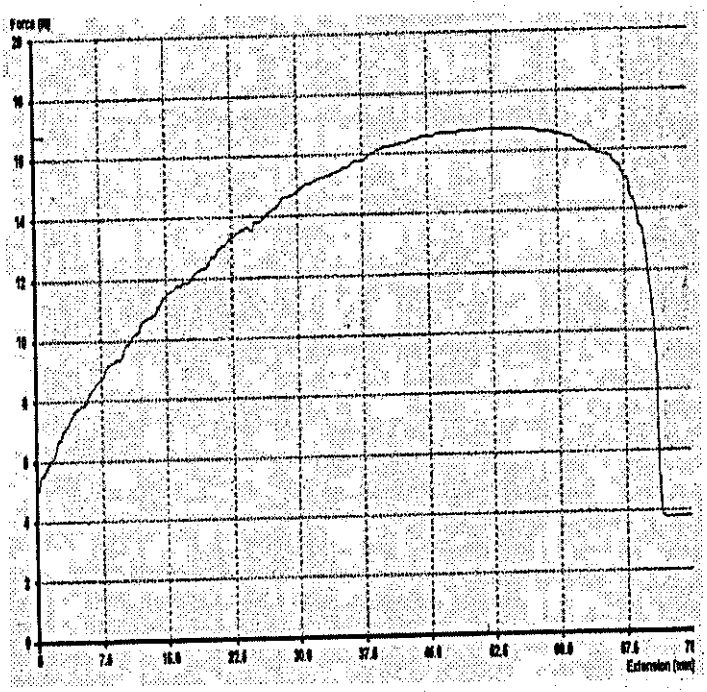

Figure 12-2: Typical force versus extension trace from the tension tests on a dumbbell test piece.

12.3 Results and Discussion

As mentioned earlier [1-6], when two pieces of rubber are brought into intimate contact, polymer chains diffuse through the interface (contact flow) to form new polymer-polymer and/or polymer-filler bonds (bond formation).
High tack strength is often produced by strong bond formation between two rubbers. The latter is dependent on the green strength of the two rubbers in contact. The nature of rubber and filler and their ability to form strong bonds are key factors in the determination of tack strength [7] .

If rubbers can form strong bonds regardless of poor contact flow due to the presence of filler particles in rubber matrix and consequent restriction of polymer chains mobility, then tack strength will increase. Enhancement of tack strength of NR with 40phr carbon black filler is an example of this mechanism [21] .On the

other hand, if rubbers do not form strong bonds and at the same time, the contact flow is poor, then tack strength will be low too. As an illustration of this mechanism, the tack strength of SBR reduced after 40phr carbon black filler was added [6]. In some cases, depending on the amount of filler, both of the above mechanisms may be applicable in the same system for tack strength estimation. Here an optimum filler loading exists for the maximum tack strength to occur [22]. The results and findings from this study will be examined and interpreted in the light of the mechanisms discussed above.
In addition, author draws attention of reader to peel tests protocols [23].

12.3.1 Effect of different amounts of silanized silica nanofiller on the green strength and Mooney viscosity of the SBR, BR and NR rubbers and SBR/BR blend

When the green strength of a filled rubber is measured, it is also useful to determine its viscosity because the addition of filler increases both of these properties. Generally, when the loading of filler such as silanized silica increases green strength, the elongation at break reduces. Figure 12-3 shows stress versus elongation for some unfilled and silica filled SBR/BR blends. As can be seen, elongation at break decreased from 523 % for the unfilled blend to 207% for the blend filled with 75 phr silica.
The green strength of the blend increased from 0.08 MPa to 1.22 MPa as the loading of the filler was raised from 0 to 75 phr.

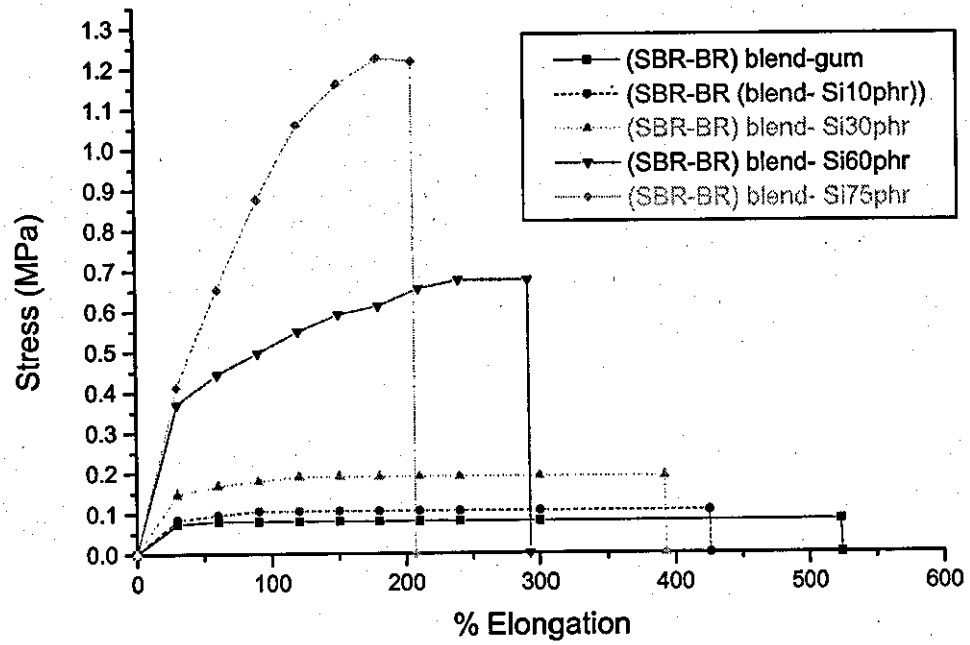

Figure12-3: Stress versus % elongation of SBR-BR blend (75/25 weight ratio) for different loading of silanized silica nanofiller

Figure 12-4 shows the green strength of different rubbers as a function of filler loading. The green strength of the NR rubbers is higher (0.235-3.56 MPa) than the others over the entire range of the filler loading. However, at filler loading less than 30 phr, the BR rubber has the lowest green strength and over 30 phr loading, the SBR-BR blend has the lowest green strength.

Unlike the NR and BR rubbers for which the green strength increases rapidly as a function of the filler loading, the rate of increase for the SBR rubber and SBR/BR blend filled with silica is noticeably slower.

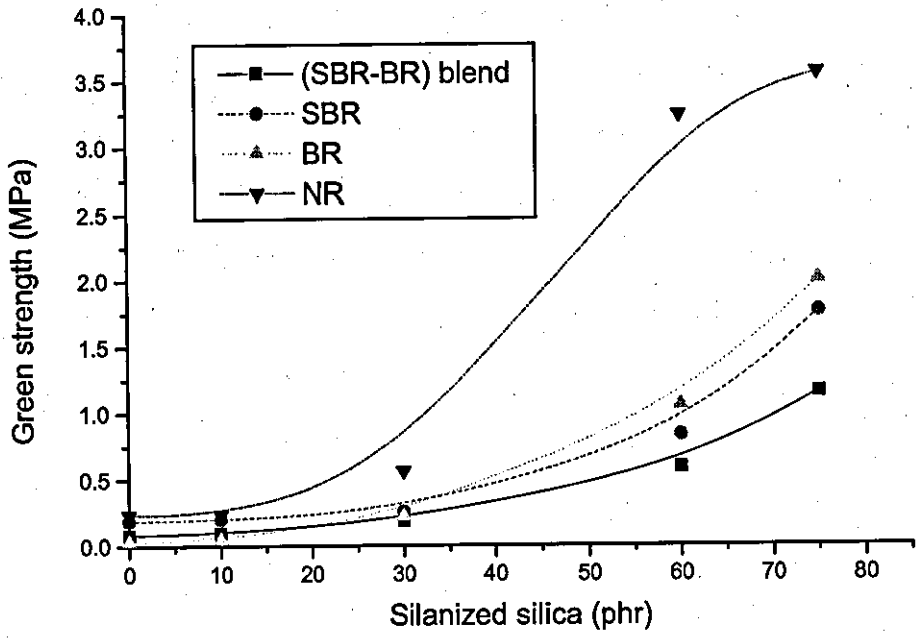

Figure12-4: Green strength versus silica loading of different rubbers and blends. Test temperature 23°C.

Figure 12-5 shows the Mooney viscosity (MU) of different rubbers as a function of filler loading. As expected, the Mooney viscosity of all the rubbers increases with the filler loading but at different rates. For filler loading up to approximately 30 phr, the viscosity of the NR rubber is higher and beyond this point, it is lower than the values measured for the other rubbers. This means that the viscosity of the NR rubber is more affected at a lower loading of the filler, whereas as the loading of the filler was increased, it raises the viscosity of the SBR and BR rubber and SBR/BR blend. The viscosity of the SBR/BR blend is 40-197 MU, BR rubber 42-191 MU, and SBR rubber 43-197 MU over the entire range of the filler loading.

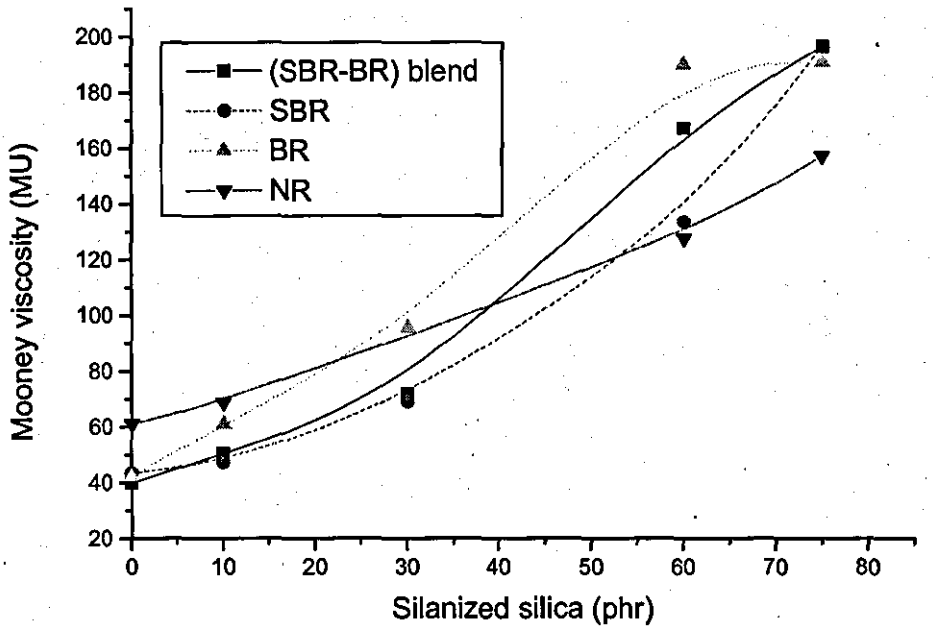

Figure12-5: Mooney viscosity as a function of silica loading for different rubbers and SBR/BR blend

12.3.2 Effect of different loadings of silanized silica nanofiller on the tack strength of the SBR/BR blend

Figure 12-6 shows tack strength versus intimate contact time for the SBR/BR blends filled with 0, 10, 30, 60 and 75 phr silanized silica nanofiller. It is clear that the tack strength of the unfilled blend and blends with low filler loading, i.e. 10 and 30 phr are higher than that of the blends filled with 60 and 75 phr filler. With the exception of the blend filled with 10 phr silica, the tack strength of the other blends are lower than that of the unfilled one. This is due to the inability of the polymer chains to form strong polymer-polymer and polymer-filler bonds because the polymer chains mobility was restricted by the presence of the filler particles in the polymer matrix. As the loading of the filler reached 75 phr, the polymer chains mobility was restricted even further, adversely affecting the tack strength of the

blend. It seems that to achieve an optimum tack strength, a maximum of 10 phr silica should be added to the blend and not more.

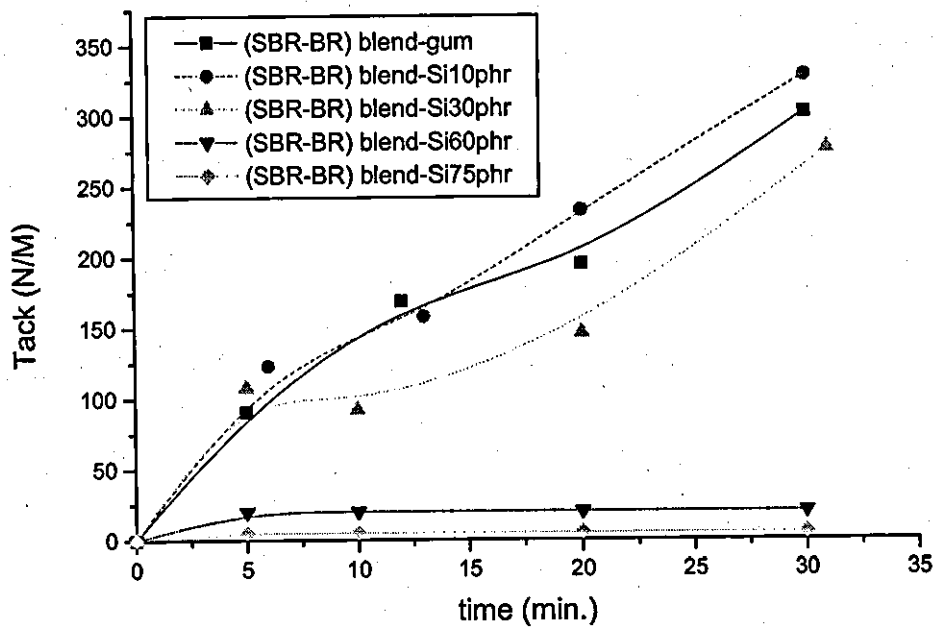

Figure 12-6: Tack versus intimate contact time for the SBR-BR blend (75/25 weight ratio) filled with different amounts of silanized silica nanofiller. Test temperature was 50°C.

12.3.3 Effect of different loadings of silanized silica nanofiller on the tack strength of the SBR rubber

Figure 12-7 shows tack strength versus intimate contact time for the SBR rubber filled with 0, 10, 30, 60 and 75 phr silica. It seems that the tack strength of all the filled rubbers is considerably less than that of the unfilled one. Possibly, as the loading of the filler increases, the chain mobility decreases and it becomes more difficult for the polymer chains to diffuse through the interface and form new bonds with other polymer chains or the filler particles. In addition, because the

polymer chains mobility is restricted by the filler presence, the polymer finds more difficult to flow and form polymer-polymer bonds.

Practically, rubbers loaded with 60 and 75 phr silica do not have enough tack in the current testing condition. Interestingly, the rubber filled with 30 phr filler, shows a higher tack strength when compared with the other filled ones and therefore, 30 phr silica can be considered to produce the optimum effect on the tack strength. However, it must be noted that the tack strength of the rubber filled with 30 phr silica is still much lower than that of the unfilled one. These results are in conformity with earlier findings [6] for tack reduction in SBR rubber filled with 40 phr carbon black.

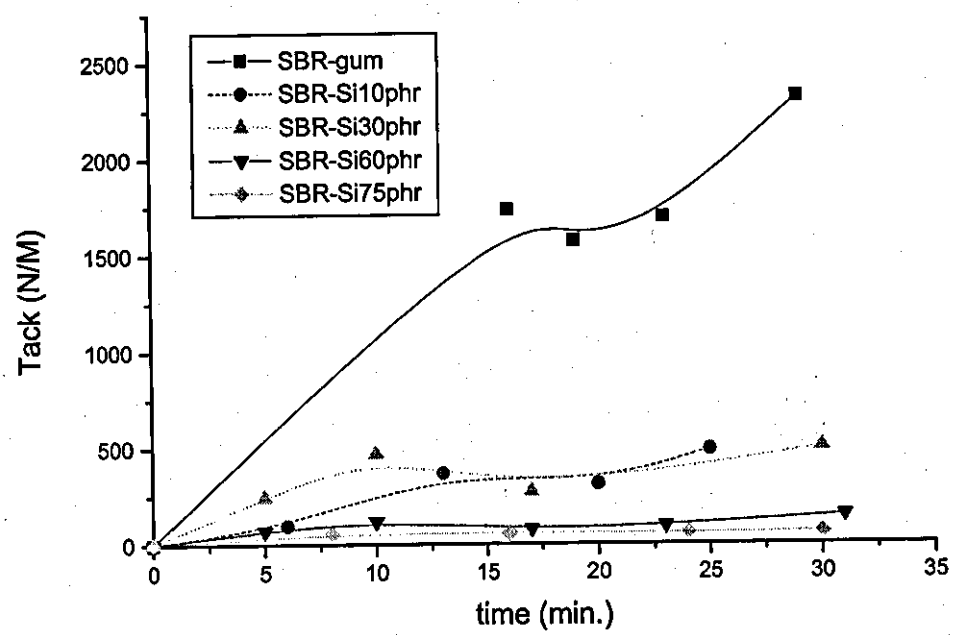

Figure 12-7: Tack versus intimate contact time for the SBR rubber filled with different loadings of silanized silica nanofiller . Test temperature was 50°C.

12.3.4 Effect of different loadings of silanized silica nanofiller on the tack strength of the BR rubber

Figure 12-8 shows tack strength versus intimate contact time for the BR rubber filled with 0, 10, 30, 60 and 75 phr silanized silica nanofiller. For this rubber, the tack strength reduces when the filler is added. This means that the inclusion of the filler reduces the polymer chains mobility and prevents the chains from diffusing through the interface into the opposite matrix to form strong polymer-polymer and polymer-filler bonds. It is also evident that the tack strength decreases progressively as a function of the filler loading reaching almost a negligible strength.

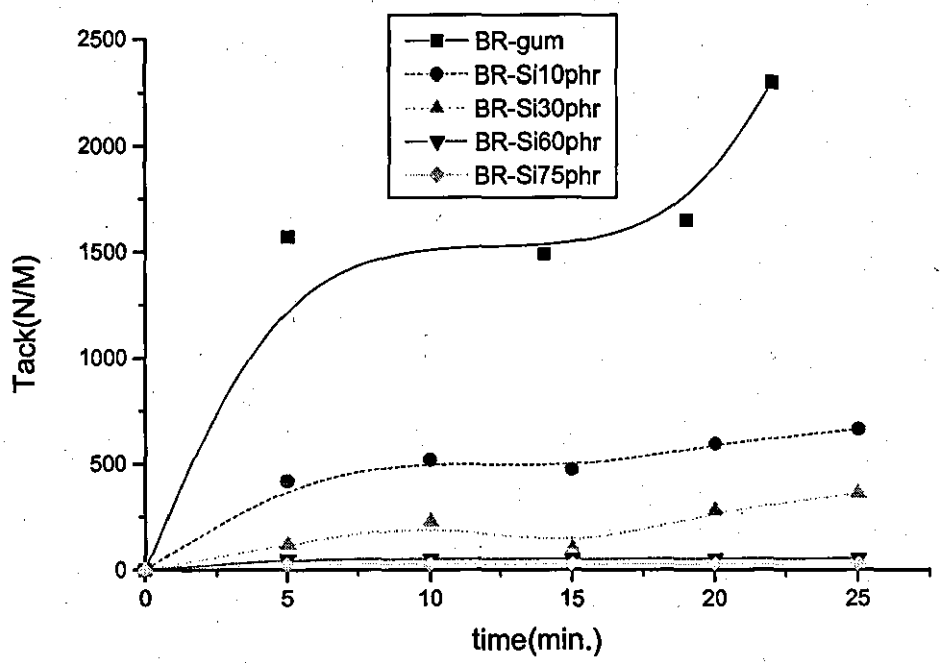

Figure 12-8: Tack versus intimate contact time for the BR rubber filled with different loadings of silanized silica nanofiller. Test temperature was 50°C.

12.3.5 Effect of different loadings of silanized silica nanofiller on the tack strength of the NR rubber

Figure 12-9 shows tack strength versus intimate contact time for the NR rubber filled with 0, 10, 30, 60 and 75 phr silanized silica nanofiller. For this rubber, the results are very interesting. With the exception of the rubber filled with 30 phr, where the tack strength is well above that of the unfilled rubber, the increase in the loading of the filler has had an adverse effect on the tack strength of the rubber, reducing it well below that of the unfilled rubber. It is also noted that the rubber filled with 10 and 60 phr silica had the lowest tack strength, whereas the rubber filled with 75 phr silica had a much higher tack strength though it still remained lower than that of the unfilled one. It was therefore concluded that to get an optimum tack strength, 30 phr silica was sufficient. These findings are in line with the previous results [21] for an NR rubber filled with 40 phr carbon black. It is not immediately clear why different loadings of silica are affecting the tack strength this way but it can be assumed that the two mechanisms described previously may be at work though at different extent.

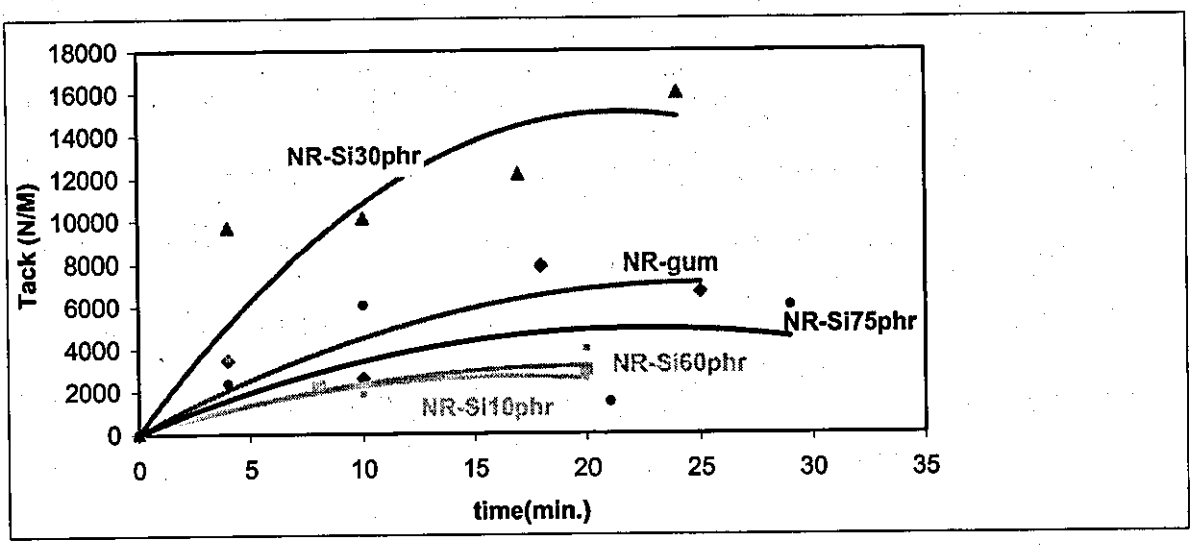

Figure12-9: Tack versus intimate contact time for the NR rubber filled with different loadings of silanized silica nanofiller. Test temperature was 23°C.

12.3.6 Comparison of the tack strength of different rubbers filled with 10 phr silica loading

Figure 12-10 shows tack strength versus intimate contact time for the NR, SBR, BR rubbers and SBR/BR blend filled with 10 phr silica. This figure shows that tack strength of the filled NR rubber is much higher than those of the BR, SBR abd SBR/BR rubbers. The lowest tack strength was measured for the SBR/BR blend. This may be due to the fact that the SBR and BR rubbers are partially miscible and therefore are not expected to mix at the interface by chain diffusion. In addition to the poor miscibility of the two polymers, the inclusion of the filler has also restricted the polymer chains mobility and made the process even more difficult, resulting in a poor tack strength.

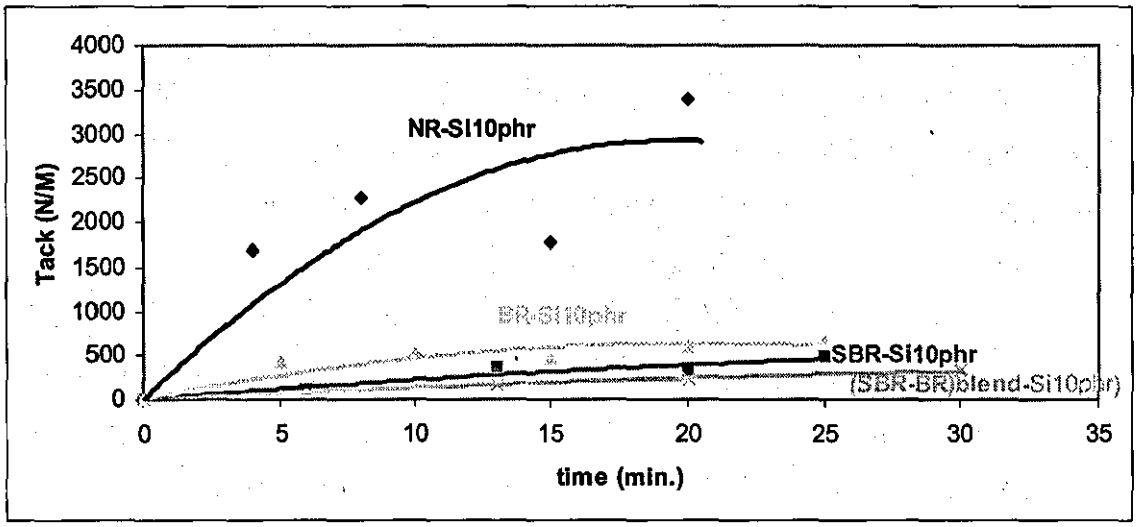

Figure 12-10: Tack versus intimate contact time for different rubbers filled with silanized silica nanofiller. Test temperature was 50°C for the SBR, BR and SBR/BR blend and 23°C for the NR rubber.

Conclusions

From this study, it is concluded that silanized silica nanofiller had a significant effect on the viscosity, green strength and tack strength of the NR, SBR and BR rubbers and SBR/BR blend. The following conclusions can be drawn:

- The Mooney viscosity of the rubbers increased as the loading of the filler was raised to 75 phr. For up to 30 phr silica, the NR and BR had the highest viscosity, and as the loading of the filler was raised above 55 phr, the SBR/BR blend and the SBR and BR rubbers had a higher viscosity than the NR rubber.

- The green strength of the SBR, NR and BR rubbers and the SBR/BR blend when the amount of the filler was increased to 75 phr, improved. The improvement was more substantial for the NR and BR rubbers as the loading of the filler was raised to above 30 phr. The SBR/BR blend showed the smallest improvement.

• The tack strength of the SBR/BR blend increased as a function of the intimate contact time. The blend with 10 phr silica had the highest tack strength. However, as the loading of the filler was increased to 75 phr, the tack strength dropped very substantially.

• The tack strength of the SBR rubber improved as the intimate contact time was increased. It was noted that the unfilled SBR showed the largest improvement with contact time and as the loading of the filler was increased to 75 phr, the tack strength dropped progressively.

• The tack strength of the BR rubber increased with contact time. The largest increase was recorded for the unfilled rubber and as the loading of the filler was increased to 75 phr, the tack strength decreased very substantially.

• The tack strength of the NR rubber improved significantly when 30 phr silica was added. The tack strength of the rubber continued decreasing as the loading of the filler was raised to 75 phr and remained below that of the unfilled rubber over the time scale which the tests were performed.

• At the given loading of the filler, i.e. 10 phr, the tack strength of NR was found to be substantially superior to that of the SBR and BR rubbers and SBR/BR blend as a function of the intimate contact time. The SBR/BR blend showed the poorest tack strength over the time scale of the test.

In summary, the addition of up to 75 phr silanized silica nanofiller to the NR, SBR and BR rubbers and SBR/BR blend increased the Mooney viscosity and improved the green strength. However, in most cases, the tack strength was adversely affected and the gum rubbers showed the largest improvement in tack as a function of intimate contact time. When the loading of the filler was kept constant, the NR rubber had the highest tack strength.

References

1) Wake W C, ``Adhesion and the formulation of adhesives ``, *2nd edition, Appl. Sci. Publishers London* 21(1982).

2) Wake W C, "Adhesion and Adhesives", Hollwink R, Salomom G , *Elsevier publishing co., Amsterdam, New York* **2:** 409(1965).

3) Allen K W, "In Aspects of Adhesion", Alner D J, CRCP press, *International Scientific series, Cleveland 5-edition*,11 (1969).

4) Voyutskii S S, "Autohesion and Adhesion of high polymers", *Interscience-Wiley, New York* (1963).

5) Vasenin R M, "Adhesion: Fundamentals & practice", *Ministry of technology, McLaren, London* (1969).

6) Rhee C K, Andries J C., *Rubber Chem. Technol.* **54**:101(1981).

7) Hamed G R, *Rubber Chem. Technol.* **54**:576(1981).

8) Voyutskii S S, Vakula V L, *J. Appl. Polym. Sci.***7**:(**2**) 475(1963).

9) Voyutskii S S ,Mcleod LA, *Rubber Chem. Technol.* **37**:1153(1964).

10) Skewis J D, *Rubber Chem. Technol.* **38**: 689(1965).

11) De Gennes P G, *J. Chem. Phys.* **55** : 572(1971).

12) Prager S, Tirrell M, *J. Chem. Phys.* **75**:5194(1981).

13)Wool R P, *Rubber Chem. Technol.* **57**:307(1984).

14) Anand J N, Karam H J, *J. Adhesion* **1**:16(1969).

15) Anand J N, Balwinsky R Z, *J. Adhesion* **1**:24(1969).

16) Anand J N, *J. Adhesion* **5**:265(1973).

17) Jabbari E, Peppas N A, *J. Macromol. Sci. Rev. Macromol. Chem. Phys. C34* ,205(1994).

18) Brown H R, *IBM J. Rers. Develop.* **38**:379 (1994).

19) Roland C M, Bohm G G A, *Macromolecules* **8**:1310(1985).

20) Roe R J, Davis D D, Kwei T K, *Bull. Am. Phys. Soc.* **15**:(**11**) 308(1970).

21) Beatty J R, *Rubber Chem. Technol.* **42**: 1040(1969).

22) Bussemarker O K F, Van Beek W V C, *Rubber Chem. Technol.* **37**:28(1964).

23) http:www3.imperial.ac.uk/meadhesion/testprotocol/peel

CHAPTER 13

Final conclusions and Suggestions for further work

13.1 Final conclusions

To finalise the gains and claims of this thesis, it is useful to examine some typical rubber formulations used in the manufacture of tyre treads and compare their mechanical and dynamic properties with the those of the rubbers developed and tested in this project.

Tables 13-1 and 13-2 show some SBR/BR blend formulations used in the manufacture of tyre tread and their mechanical and dynamic properties, respectively. Compounds 1, 2 and 3 are from reference 1, compounds 4, 5 and 7 were prepared and tested in this study (see chapter 9 for blends 3, 4 and 5), and compound 6 is for green tyres [2].

As it is evident from these tables, there are various chemicals present in the rubber formulations. They include carbon black, silica, coupling agent, antioxidant, processing oil, primary and secondary accelerators, primary and secondary activators and elemental sulphur. Compounds 1 and 2 (Table 13-1) have 71.5 phr silica/carbon black and 6.5 phr coupling agent adding up to 78 phr, and 78 phr silica/carbon black and 6.5 phr coupling agent adding up to 84.5 phr, respectively. The cure systems in these compounds consists of 9.6 phr chemicals. The green tyre compound (compound 6; Table 13-1), has 80 phr silica and 6.4 phr silane coupling agent adding up to 86.4. The curing chemicals add up to 10 phr. The compound with carbon black filler (compound 3; Table 13-1), has 71.5 phr black and 9.6 phr curing chemicals.

When compounds 4, 5 and 7 (Table 13-1) are compared with compounds 1, 2, 3 and 6, it is clear that there is a large reduction in the use of the filler, silane and curing chemicals. For example compounds 4, 5 and 7 have 60 phr silanized silica (53.2 phr silica and 6.8 phr silane coupling agent) and one accelerator, one activator and elemental sulphur adding up to 4.58 phr. This represents a substantial reduction in the use of filler, coupling agent and curing chemicals. For example, when compound 4 is compared with compound 6, it has 44% less silica and silane, and more than 100% less curing chemicals. This has greatly simplified rubber formulation for green tyres.

Table 13-1: Recipes of some standard tyre tread compounds (compounds 1, 2, 3, and 6) and compounds prepared and tested in this study (compounds 4,5 and 7)

Compound No.	1	2	3	4	5	6	7
SBR (phr)	75	75	75	75	75	75	75
BR (phr)	25	25	25	25	25	25	25
Precipitated silica (phr)	65	65	---	53.5	53.5	80	53.4
Coupling agent (TESPT) (phr)	6.5	6.5	---	6.8	6.8	6.4	6.8
Carbon black	6.5	13	71.5	---	---	---	---
Processing oil	25	25	25	3.8	3.8	34	3.8
Stearic acid	2	2	2	---	---	2	---
Wax	1.5	1.5	1.5	---	---	3	---
Antioxidant	2	2	2	0.75	0.75	2	0.75
Sulphur	1.4	1.4	1.4	0.08	0.08	2	0.08
zinc oxide	2.5	2.5	2.5	0.4	0.4	3	0.4
Accelerator I	2	2	2	4.1	4.1	2	4.1
Accelerator II	1.7	1.7	1.7	---	---	1	---
Total filler (silica + carbon) (phr)	71.5	78	71.5	53.2	53.2	80	53.2
Total silane loading (phr)	6.5	6.5	0	6.8	6.8	6.4	6.8
Total curing chemicals (phr)	9.6	9.6	9.6	4.58	4.58	10	4.58

To assess whether the reduction in the filler, silane and curing chemicals has had an adverse effect on the mechanical and dynamic properties of the cured rubbers, Table 13-2 was formed. In this Table, the hardness, tensile properties

tan δ, tear strength, abrasion resistance, heat build up, and cure properties of the compounds shown in Table 13-1 were summarised.

Table 13-2: Mechanical and dynamic properties of the compounds listed in Table 13-1.

Compound No.	1	2	3	4	5	6	7
Hardness	63	58	66	75	72	---	76
Tensile strength (MPa)	17.8	22.6	18.4	23	26	16	25
Elongation at break (%)	525	580	528	755	869	310	865
Modulus at 100%(MP	2.29	1.61	1.83	2.5	2.13	4.0	2.57
tan δ at -30 °C	0.546	0.609	0.554	0.48	0.62	---	0.50
tan δ at 0 °C	0.202	0.174	0.256	0.21	0.2	0.165	0.22
tan δ at 60 °C	0.12	0.09	0.224	0.12	0.14	0.11	0.12
Tear strength (N/mm)	---	---	---	98	107	60	64
Abrasion loss (mm^3)	---	---	---			98	
Heat built up							
Curing time (t_{90})*					8.32	21.3	
$\Delta Torque$ (dN.M)					72.21	22.9	

* Cure temperature= 170 °C

Of major interest, are the results for compounds 4, 5, 6, and 7, the so called green tyre compounds. The tensile strength elongation at break and tearing energy of compounds 4, 5 and 7 are superior to those of compound 6. It is also noted that compound 5 has a much shorter curing time and a higher Δtorque value. Δtorque is an indication of crosslink density changes in the rubber. The modulus at 100 % is lower for compounds 4, 5 and 7. However, tan δ at 60°C is almost the same for compounds 4, 6 and 7 which indicates the same rolling resistance. Therefore is seems that reducing the amounts of silica, silane and curing chemicals has had no adverse effect on the mechanical properties of the cured rubbers which are essential for good performance, durability and long lifer in service.

To show further the advantages of these newly developed compounds and the benefits of the new method for crosslinking and reinforcing rubbers, the curing

and mechanical properties of the SBR compound developed in this study were compared with those of a common silica/carbon black filled sulphur-cured SBR compound (Tables 13-3). Compound 8 was taken from reference 3 and compound 9 was prepared in this study (see chapter 9 for compound 2). As can be seen, compound 8 has 64.8 phr filler, 4.8 phr silane and 9.25 phr curing chemicals, whereas, compound 9 has 53.2 phr filler, 6.8 phr silane and 3.5 phr curing chemicals. Clearly, a significant reduction in the use of the additives in the rubber compound has been achieved. It is interesting that compound 9 has a shorter curing time in spite of a decrease in the use of the curing chemicals and much higher elongation at break and tensile strength.

Table 13-3: Recipe of a common SBR rubber compound (compound 8) compared with the SBR compound developed and tested in this study (compound 9).

Compound No.	8	9
SBR (phr)	100	100
silica(phr)	60	53.2
carbon black(phr)	4.8	---
zinc oxide (phr)	2	0.5
Stearic acid (phr)	3	---
Antidegradant(phr)	1.5	1
Wax(phr)	1	---
Oil(phr)	12	5
sulphur (phr)	1.2	---
Accelerator (phr)	3.05	3
TESPT (phr)	4.8	6.8
Total fillers (phr)	64.8	53.2
Total silane (phr)	4.8	6.8
Total curing chemicals	9.25	3.5
Cure time (t_{90}) (min.)	65	49
Elongation at break (%)	364	1027
Tensile strength (MPa)	9.25	23

Table 13-4 shows recipes and mechanical properties of typical truck tyre treads (compound 10 from reference 4 and compound 12 from reference 5). Compound 11 was developed and tested in this study (see chapter 6 for compound 37). As it

can be seen, compound 10 has 60 phr filler and 10.1 phr curing chemicals. Similarly, compound 12, has 56 phr filler, 6 phr silane and 11.6 phr curing chemicals. Compound 11 has 53.2 phr silica, 6.8 phr silane and only 6.3 phr curing chemicals. Obviously, compound 11 is a simpler and easier compound to make. The mechanical properties of compound 11, excluding modulus at 100%, are superior to those of compounds 10 and 12. For instance, compound 11 has a tensile strength of 37 MPa, whereas, compound 12 has 28 MPa. Compound 11 is harder and has higher tearing energy and elongation at break.

Table 13-4: Recipes and mechanical properties of some truck tyre compounds (compounds 10 and 12) compared with compound 11 developed in this study.

Compound No.	10	11	12
NR (phr)	100	100	100
silica(phr)	15	53.2	56
carbon black(phr)	45	---	---
zinc oxide (phr)	5	0.3	5
Stearic acid (phr)	2	---	3
Antidegradant(phr)	1.5	1	---
Wax(phr)	0.3	---	1.5
Oil(phr)	3	---	2.5
sulphur (phr)	2	---	1.6
Accelerator (phr)	1.1	6	2
TESPT (phr)	---	6.8	6
Resin	3	---	---
Antioxidant	1.5	---	3
Total fillers (phr)	60	53.2	56
Total silane (phr)	--	6.8	6
Total curing chemicals	10.1	6.3	11.6
Tensile strength(MPa)	---	37	28
Hardness	68	75	66
Elongation at break (%)	531	834	583
Tear strength (N/mm)	29.7	62.4	----
Modulus at 100% (MPa)	2.52	2.20	3.19

To see the commercial advantages of simpler rubber formulations, Table 13-5 [6,7] represents average prices of different curing chemicals.

Table 13-5: Average prices of some most widely used rubber chemicals

Curing agent	TBBS	ZnO	Stearic acid	Antioxidant	Process oil	Wax	sulphur	Resin
Price (USD/lbm)	3.19	0.85	0.72	4.18	1	1.21	0.8	0.86

It is also useful to compare the prices of common chemicals used in tyre tread compounds based upon data of Table 13-5 for 100 lbm raw rubber.

Table 13-6: Prices (USD) of different curing chemicals used in the manufacture of tyre tread rubber compounds based upon 100 lbm raw rubber

Compound No.	1	2	3	4	5	6	7	8	9	10	11	12
Total curing Agents price	16.5	16.5	16.5	13.5	13.5	15.2	13.5	14.5	10.0	10.8	19.4	14.1

The data in Tables 13-5 and 13-6 show that significant costs saving can be made when the number and amounts of the curing chemicals are reduced. Therefore, the rubber formulations developed and tested in this study will help to achieve these savings.

The work reported in this thesis, has provided ample evidence that the new method for crosslinking and reinforcing rubbers with silanized silica nanofiller is indeed a revolutionary approach to preparing rubber formulations for industrial articles such a tyres. This also offers the following benefits:

- Major benefits to health and safety at work place

- A significant reduction in costs

- Major improvements in the mechanical properties of rubber compounds which will enhance the quality of industrial rubber articles

- Less damage to the environment due to a lesser use of the harmful curing chemicals. For example, ZnO leaches out of discarded old tyres into landfill and causes extensive pollution in the ground water sources. A reduction in the use of ZnO in rubber compounds will help to remedy this problem.

13.2 Recommendation for future work

The ultimate aim of this project was to develop new blends of SBR/BR and SBR/NR for use in passenger car tyre tread. The preliminary work carried out in this project has shown that it is fully feasible to develop a safer, more efficient and cheaper rubber compounds for use in tyre tread. Therefore the following recommendations are made:

- The work should continue to measure the fatigue crack growth of the SBR/BR rubber blends at different frequencies and temperatures. This will be relevant to tyre applications, where rubber is repeatedly flexed in service and small flaws or cracks can growth under repeated stressing. An understanding of how crack growth rate under repeated stressing correlates with the strain energy release rate, will be useful.

- Also, to increase the efficiency of cure, it is essential to reduce the optimum cure times of the SBR, NR and BR compounds before they are mixed to produce blends. The cure times of the rubber compounds prepared and tested in this study were too long and therefore, industrially were not favourable. Perhaps

some fast curing accelerators can be tested to speed up the rate of cure and shorten the cure time of the blends.

- It will also be necessary to measure the abrasion resistance, tan δ and heat build up of the SBR/BR and SBR/NR blends, once their cure cycles are shortened. These properties are particularly important with respect to tyres.

In summary, it is highly recommended that this new concept in crosslinkng and reinforcing rubber compounds with a silanized silica nanofiller should be refined further and taken forward to develop compounds for industrial articles such as tyres. The results and findings from this project seem to point to a promising future development in this area.

References

1) Waddell W H, Beauregard P A, Evans R, *Tyre Tech. Int.* **95**: 14 (1995).

2) Datta R.N, Hondeveld M. G, *Kautschuk Gummi Kunststoffe* **6**:54(2001).

3) Schaal S, Coran A Y, Mowdeed S, *US patent 6737466, Pirelli S.p.A, Millan, Italy* (2004).

4) Waddell W H, Parker J R, *Rubber World* **207**:(**1**)29 (1992).

5) Meng Jiao Wang, Ing Zhang, Khaleed Mahmud, *Rubber Chem. Technol.***74**:124 (2001).

6) *Rubber World*, (September 1, 1999).

7) http://goliath.ecnext.com/coms2/summary_0199-1493883_ITM

Publications

ISI Journal papers

1) Comparing Effects of Silanized Silica Nanofiller on the Crosslinking and Mechanical Properties of Natural Rubber and Synthetic Polyisoprene, *Journal of applied polymer science* **109**:(**2**)869(2008).

2) Assessing Effects of Different Processing Parameters on the Interphases Between Dissimilar Rubbers Using Modulated-Temperature Differential Scanning Calorimetry , *Journal of rubber research* **11**:(1) 13(2008).

3) Using modulated-temperature differential scanning calorimetry to study interphases in blends of SBR and BR rubbers filled with silanized silica nanofiller , *Journal of applied polymer science* **111**:(**3**)1644(2009).

4) Comparing dynamic bahaviour of several rubbers filled with silanized silica nanofiller , *Polymer International* **58:**(**2**)209(2009)..

5) Effect of silanized silica nanofiller on tack and green strength of filled Rubbers, *Polymer International 58(2009).*

6) Effect of different interphases on the mechanical properties of cured silanized silica-filled SBR/BR rubber blends for use in passenger car tyre tread, *Journal of applied polymer science* (Accepted and in press).

Invited paper

1) Measuring the dynamic behavior of several rubbers filled with silanized silica nanofiller. *Rubber World* (March *2009).*

Referred conference papers

1) Comparing dynamic bahaviour of several rubbers filled with silanized silica nanofiller , A paper presented at the *174th technical meeting, Rubber division, ACS*, Kentucky, **USA** (Oct. 14-16, 2008).

2) Development a new tyre tread, A paper presented in *9th Iran national rubber (IRNC) congress*, **Kish island** (Nov. 18-19,2008).

3) Increasing efficiency of cure and optimising mechanical properties of rubber vulcanisates using a silanized silica nanofiller – a major advance in the use of high performance fillers, *High Performance Fillers for Polymer Composites, Fourth International Conference* 4-5 March 2009,Barcelona, **Spain.**

4) Tire Fillers: Is it all just black or white?, Tire Technology Expo. Hamburg, **Germany** (16-18 February 2009).

Poster presentations at international conferences

1) Reduction harmful chemicals in NR, NBR, SBR and BR compounds filled with silanized silica nanofiller, *Materials Congress*, Institute of Materials, Minerals and Mining's new regional centre, Grantham,**UK** (13-15 May 2008).